An Investigation into Sandy Beach Stabilisation through Controlled Drainage

by Heidi Sarah Mulvaney

Doctor of Philosophy Thesis

January 2001

Generations come and generations go,
but the earth remains for ever.
The sun rises and the sun sets, and hurries back to where it rises.
The wind blows to the south and turns to the north;
round and round it goes, ever returning on its course.
All streams flow to the sea, yet the sea is never full.
To the place the stream comes from there they return again...

The eye never has enough of seeing,
nor the ear its fill of hearing.
What has been will be again,
what has been done will be done again;
There is nothing new under the sun.
Is there anything of which one can say, "Look! This is something new"?

It was here already, long ago;
it was here before our time.

Ecclesiasties, Chapter 1, Verses 4 to 7, 9 and 10.

UNIVERSITY OF SOUTHAMPTON

ABSTRACT

FACULTY OF ENGINEERING
CIVIL AND ENVIRONMENTAL ENGINEERING

Doctor of Philosophy

AN INVESTIGATION INTO SANDY BEACH STABILISATION THROUGH CONTROLLED DRAINAGE

By Heidi Sarah Mulvaney

Previous studies have demonstrated the potential for improving beach stability through controlled drainage. However, the results of full scale trials are varied, and the application of the technique has been hindered by a shortage of practical information on the performance of beach drainage systems in conditions relevant to the UK shoreline.

This report describes an investigation into the mechanisms of beach drainage and the factors affecting system performance.

A beach drainage model was developed using a 1:20 linear scale and Bakelite sediment. Test results support the theories that beach stabilisation through drainage occurs due to surge volume reduction (leading to laminar flow phase extension) and pore water pressure reduction (resulting in reduced liquefaction in the swash zone). The results also show that drainage system effectiveness is proportional to discharge. Data support the theory that for non-tidal conditions and a monochromatic wave climate, the optimum performance occurs when the upper part of the swash is located over the zone of maximum influence of the drain. Scaling considerations suggest that in terms of the magnitude of beach volume change the model results are an overestimate, although qualitatively the results are likely to apply to the field.

As part of the study, a field trial was carried out at Branksome Chine, Dorset. This report describes the installation and first 6 months of operation during which time the system yield, local weather patterns and beach levels were recorded.

Field observations and survey data show that the drainage system successfully stabilised the beach at Branksome Chine during the first two months of the trial. However, spring tides and storms caused sufficient damage to render the system inoperative during a crucial period of further storms enabling erosion to occur. The system was reinstated soon afterwards, but with a considerably reduced yield, and the effect of the repaired system was limited. The trial demonstrated that beach drainage can be an effective stabilisation option, but robust design, prompt maintenance and high yield are vital to its success.

Model experiments show that during prolonged storms, some beach material loss is inevitable, and the stabilisation effect of the drainage system is not instantaneous. However, provided the system remains in operation beach levels will begin to recover and accretion will occur during otherwise erosive conditions.

Alternative drainage system designs comprising geo-composite permeable layers and a shore normal collector pipe have been proposed. Preliminary experiments demonstrate that geo-composite beach drainage may be a feasible method of shoreline stabilisation, however further study is recommended.

CONTENTS

List of Figures

List of Tables

Acknowledgements

Firstly, I am grateful to David Robson and Stuart Terry from the Borough of Poole Construction Related Services for their support and collaboration during this project, and to Jim Ross and his team of Beach Inspectors (Borough of Poole) who were kind enough to record weather data for the Branksome Chine beach drainage trial.

I am also very grateful to Harvey Skinner, Experimental Officer for the Department of Civil and Environmental Engineering (University of Southampton) who was able to, against the odds, conjure up a set of pore water pressure transducers that have provided data crucial to this investigation.

Dr Rycroft has been a valued source of encouragement throughout my time at Southampton, and I am grateful for the opportunities he has given me over the past few years.

I would like to acknowledge the help of Dr. Paul Tosswell for his technical advice and recommendations, Steve Wake for his practical assistance in surveying, and Ken Yeates and the team of technicians in the Department of Civil and Environmental Engineering at the University of Southampton.

The geotextile material for the model experiments were supplied by Polyfelt Geosynthetics and Hope and Clay Construction Ltd.

The following parties are acknowledged for their encouragement and support:
David Ayres, Regional Director, MAFF
Keith Belfield, who developed the Belfield tide plotter software
Steve Burstow, Restormel Borough Council, Cornwall
William N. Seelig, who granted permission for reproduction of part of his work for the purpose of this project (Seelig, 1983)
Tim Parsons and Mel Brash from MMG Ltd (MMG is the UK Beach Management Systems licensees)
Hans Vesterby, Geo (formerly the Danish Geotechnical Institute), Lyngby, Denmark
David Wheeler, PhD Colleague (University of Southampton)
All the team at the CBI, TAMU-CC, Texas.

My warmest thanks goes to my fiancé Reuben Shaw and my mum Farah Diggens, without whom I would have given up the ghost long ago. Thank you Dad for instilling in me an interest in how and why the world works.

Thank you finally to Professor William Powrie who made the completion of this project possible.

Nomenclature

a_o = wave amplitude
A_S = dimensional shape parameter
A = cross sectional area
α = proportional
C_u = coefficient of uniformity
C_z = coefficient of curvature
Dn = Dean number
d = depth below still water level
D = sediment diameter
Δ = delta
F = Froude number
F' = adapted Froude number
g = acceleration due to gravity
G_s = specific gravity
G = geometric scale number
γ = sediment bulk unit weight
H = wave height
H = head difference
i = hydraulic gradient
k = permeability
kg = kilograms
l = litres
L = linear scale factor
L = wave length
L = flow path length
m = metres
min = minute
mm = millimetres
M = mass
N_f = number of flow tubes
N_h = number of head drops
Pa = Pascals
PSD = particle size distribution
PPT = pore water pressure transducer
PWP = pore water pressure
Π = dimensionless group
q = system discharge
θ = beach slope angle
R = wave scaling number
Re = Reynolds number
ρ_s = density of sediment
ρ_w = density of water
s = seconds
S_o = beach slope
SWL = still water level
σ_v = vertical stress
σ'_v = vertical effective stress
t = time
T = wave period
τ = shear stress
u = pore water pressure
υ = kinematic viscosity
V = volume of sand grain
v = velocity
w = sediment fall velocity
W_s = weight of sand particle
W = beach face wetness number
x = survey grid co-ordinate
y = survey grid co-ordinate
y_o = overlap
y = distance between still water level location and beach drain in the horizontal plane
z = depth below beach surface

1. INTRODUCTION

1.1 Aim

The main aims of this PhD research project were to

- gain an understanding of the application of beach drainage and the practical limitations,
- investigate the mechanisms of beach stabilisation through drainage, and
- investigate the factors affecting beach drainage system performance.

1.2 Context

While the timescale for beach morphology is relatively rapid in geological terms, beach change may appear slow in human terms, and regions of apparent stability may be perceived. Some areas may take several hundred years for a noticeable change in the shoreline to occur, during which time settlements have arisen and an economy has developed.

Recent changes in coastal erosion and deposition through climate change and anthropogenic disturbance have been well documented (e.g. Morton, *et al*, 1983; Barratt; 1992, Summerfield, 1993), and articles describing and warning of the effects of climate change now feature frequently in the media. A selection of articles of interest are presented in Appendix A (The Independent, 1999; The Daily Telegraph, 1999; the Guardian, 2000). Global warming has been the subject of recent international summits because the issue is no longer a future threat, but a real problem that is affecting our lives today.

Coastal erosion is now an increasing problem due to five principal factors:

1) global warming resulting in sea level rise and increased storminess (Morton, *et al.*, 1983; Summerfield, 1993)
2) reduced sediment supply due to the end of the Pleistocene era, and the ensuing reduced rates of erosion from land (Summerfield, 1993),
3) changes in land level for various geological and historical reasons, for example post-Pleistocene rejuvenation (Summerfield, 1993),

4) reduction in sediment supply due to anthropogenic disturbance (Barratt, 1992), and
5) changing human perceptions of coastal erosion (Smith *et al.*, 1989): modern society has come to take it for granted that problem solvers can overcome anything. This attitude is particularly stark in the context of fossil fuel consumption – people fail to take the problem of finite energy resources and global warming seriously because it is easier to assume that 'they' will find a solution. Particularly in the western world, there is a feeling that when a problem arises we can and should do something about it, but, there is a tendency to deal with the symptoms rather than the cause.

Historically, coastal erosion is essentially a natural process, and it has only become a problem in recent years because it is perceived to interfere with human needs. However, accelerated erosion rates due to anthropogenic disturbance and climate change mean that shoreline retreat is beginning to pose a real and significant threat to coastal communities. Rates of retreat in the UK frequently exceed 5m per year, resulting in a considerable loss of agricultural land (e.g. Holderness, East England), conservation areas (e.g. Holme freshwater wetlands, Norfolk), and posing an increasing threat to recreational attractions and economies dependent on local tourism. In Bournemouth, for example, 16 000 people depend on tourism for their jobs, with the main tourist attraction being the sandy beaches (BBC 1 'South Today' programme, 28/8/00). Well established economic centres are under serious threat, either by direct physical land and property loss, or due to the loss of their beaches. Sandy beach preservation is an important part of coastline management, since the beach is both a valuable recreational asset, and also an effective defence against wave attack. In the current economic climate well planned integrated shoreline management is justified.

Past practice has tended to involve large scale hard engineering works: unfortunately these types of measures have come to define the term 'coastal defence' - a large, visible, physical barrier to the sea. However, if hard engineering works are misapplied, the consequences can be devastating. Obstructions to longshore drift may starve downshore beaches of sediment, while hard structures can cause changes in local energy patterns, and sometimes result in alterations in the coastline for many

miles downshore. In addition to this, it would require further financial resources to rectify or remove the man-made obstruction altogether in order to prevent the undesirable effects. For this reason, today's engineers have inherited a legacy of problematic or failing hard engineering works that are either too expensive to remove, or on which the local area has come to depend for mitigating the effects of similar upshore works. Many coastal zones have entered in to what is effectively a coastal arms race, and are trapped in a vicious circle of constructing works to counter the effects of upshore schemes or human activity, while creating further problems for their downshore neighbours to rectify.

Most traditional coastal protection measures seek to reflect wave energy or entrap sediment, often with negative impacts for downshore beaches. Hard engineering works, in particular seas walls, often result in a loss of the local beach, while shore normal structures such as groynes or breakwaters often result in downshore sediment starvation. Some traditional measures such as rip rap are designed to absorb wave energy, but these are often unsightly and relatively expensive, and frequently result in the loss of any remaining natural beach material. An ineffective structure may stand derelict creating an eyesore and presenting today's engineers with an expensive remediation problem.

These problems have now been recognised, and coastline management in the UK aims to provide integrated solutions to coastal erosion. When hard engineering works are misapplied, effects are rarely felt locally, and it is downshore beaches that will often suffer the consequences. This has been problematic in the past, particularly due to the division of sections of coastline according to local authority boundaries. For this reason, the UK shoreline is now divided into large units, or coastal zones, and these are covered by what are termed Shoreline Management Plans (SMPs), (Hamer *et al.*, 1999). The boundaries for the SMPs are divided according to natural factors, and the zones may cover several local authority areas. Consideration is now given to the wider impacts of proposed schemes, and an altogether more holistic approach has been adopted.

To implement the new planning approach, decision makers must be provided with practical alternatives to hard engineering works for shoreline management. Research and development into new techniques is vital if coastal engineering is to see a move away from traditional hard engineering works and their associated problems.

This thesis details an investigation into beach stabilisation through controlled drainage, a relatively new soft engineering method of coastal protection. This technique has been commercially available for approximately 15 years, but its application in this country has remained largely unexplored. The aim of this study is to gain an understanding of the process of beach stabilisation through drainage, investigate the principal factors affecting performance, and gain first hand practical experience of the installation and operation of a beach drainage system. The research consists primarily of an experimental investigation which aims to explore the effects of wave climate, drain location, sediment properties, discharge, and pore water pressure within the beach. The project also comprises the monitoring of a full scale trial over a six month period.

1.3 Introduction to beach drainage

The origins of beach drainage lie in several early studies which showed a relationship between the beach water table elevation and the rate of erosion (e.g. Emery and Foster, 1948; Grant, 1946 and 1948). It was later demonstrated that artificially lowering the water table can lead to increased beach stability and in some cases accretion (Chappel *et al.*, 1979; Vesterby, 1997).

The most commonly used drainage system consists of collector pipes running parallel to the shoreline, buried at a depth of approximately two metres below the beach surface. Water is fed by gravity to a sump whence it is removed using a submersible pump. The outlet is directed either back to the sea, a lagoon or recreational pool. The result is a stabilisation of the existing beach, and an increase in the upper sweep zone profile.

Previous work (e.g. Vesterby, 1996; Turner and Leatherman, 1997) has shown that beach drainage has the potential to become a viable coastal protection option. It acts

across the length of the beach, promoting an even distribution of sand and providing a natural means of defence. However, beach drainage is not the solution to generic 'coastal erosion'. Clearly where the forces of nature give rise to dramatic erosion such as cliff undercutting or headland erosion, or at other high energy focus points, soft engineering works are unlikely to be effective, and indeed one may debate the use of any engineering structures in such circumstances. Beach drainage is applicable to lower energy environments such as bays and other sheltered areas, of which a sandy beach is often an intrinsic part. In some such areas the natural beach may have been lost due to changes in sediment supply, while the energy dynamics of the location have remained constant. In this case a beach drainage system may be appropriate for the stabilisation of an imported or nourished beach.

The purpose of beach drainage is therefore to preserve a sandy beach environment for recreation or conservation, and in some cases coastal protection, in an area that would otherwise experience material loss due to reduced sediment supply for natural or more commonly anthropogenic reasons. Beach drainage may be applied in order to retain imported sand in areas where a sandy beach is considered desirable. The protection of such resources often has positive secondary impacts on the local economy and dependent community. Beach drainage is particularly appropriate for areas where tourism contributes to the local economy because the installed system is predominantly subsurface and visual impact is minimal. Beach drainage may be termed a coastal protection measure, since it promotes a sandy beach, which is intrinsically an effective means of wave energy absorption.

Another advantage of the beach drainage system is that it may be shut down if it is found to be ineffective, or over-effective, and if necessary pipes may be removed for relatively little cost (in contrast to hard engineering works).

The commercial use of beach drainage systems (particularly in the UK) has been hindered by ineffective pilot schemes and limited available information about the application of this technique. Site characteristics for which beach drainage would be appropriate are yet to be clearly defined, and potential clients are reluctant to invest money in a scheme for which the success is uncertain: most current design

information is based on full scale observations, and full scale trials have been subject to varying degrees of success.

Further study is necessary to improve confidence in the use of soft engineering measures such as beach drainage, and potential users need guidance in the application of beach drainage systems, in particular site selection and performance prediction.

1.4 Summary of contents

This project encompasses three main areas of study:

1) theory and background,
2) field investigation, and
3) model investigation.

These areas are summarised in Figure 1.1 at the end of this chapter. The purpose of this figure is to provide a schematic representation of the structure of this thesis.

Chapter 2 summarises previous work and some prominent case studies. A brief overview is given of the origin of beach drainage, the first field trials, and model experiments. The purpose of this chapter is to provide a summary of previous work, which will be discussed further throughout the thesis.

Chapter 3 describes the design, installation, monitoring, and results of a full scale trial carried out at Branksome Chine in Dorset. The aim of this section is to provide a detailed coverage of a full scale trial in the UK. This trial has been monitored for approximately 18 months, and is the third beach drainage system to be installed in the UK . This work provides first hand observations, survey data, weather records and prototype discharge information for the first 6 months of the trial (after the first 6 months the system was rendered ineffective and results were limited). Technical issues, monitoring methods, and system performance are discussed, and a practical knowledge base is developed.

Due to unanticipated problems with the full scale experiment at Branksome Chine beach, it was decided that further investigation must take place using a model beach drainage system. A model beach drainage system was developed using a wave tank

and monochromatic wave generator. Chapter 4 gives an introduction to physical modelling, and provides a summary of the variables to be investigated. Beach drainage theories identified in Chapter 2 are discussed in greater detail, and the understanding of the mechanism of beach drainage is developed further.

Chapter 5 details the model design phase, and describes the development of the beach drainage model and the methods and apparatus used. This chapter also describes the preliminary experiments which were necessary in order to determine the test procedures, sediment characteristics, and model drainage system design. Model scaling is also addressed in some detail and dimensionless groups are used to understand the relationship between the model and prototype.

In Chapter 6 the model and prototype flowrates are compared and discussed, and the measured discharge values are also compared to the calculated values.

The aim of Chapter 7 is to investigate the effect of beach drainage on sediment pore water pressure in the swash zone and to link these observations to system discharge and the effect on profile formation.

Factors controlling system performance are investigated in Chapter 8. These are namely:

1) discharge (as a controlling variable),
2) drain location relative to still water level, and
3) wave climate.

Alternative drainage system designs are described in Chapter 9. Although some preliminary experiments are discussed, further work in this area is recommended.

All chapters contain discussion and conclusions, however Chapter 10 aims to draw together the key comments from the previous chapters, and provide recommendations for further work.

Figure 1.1: Project Plan

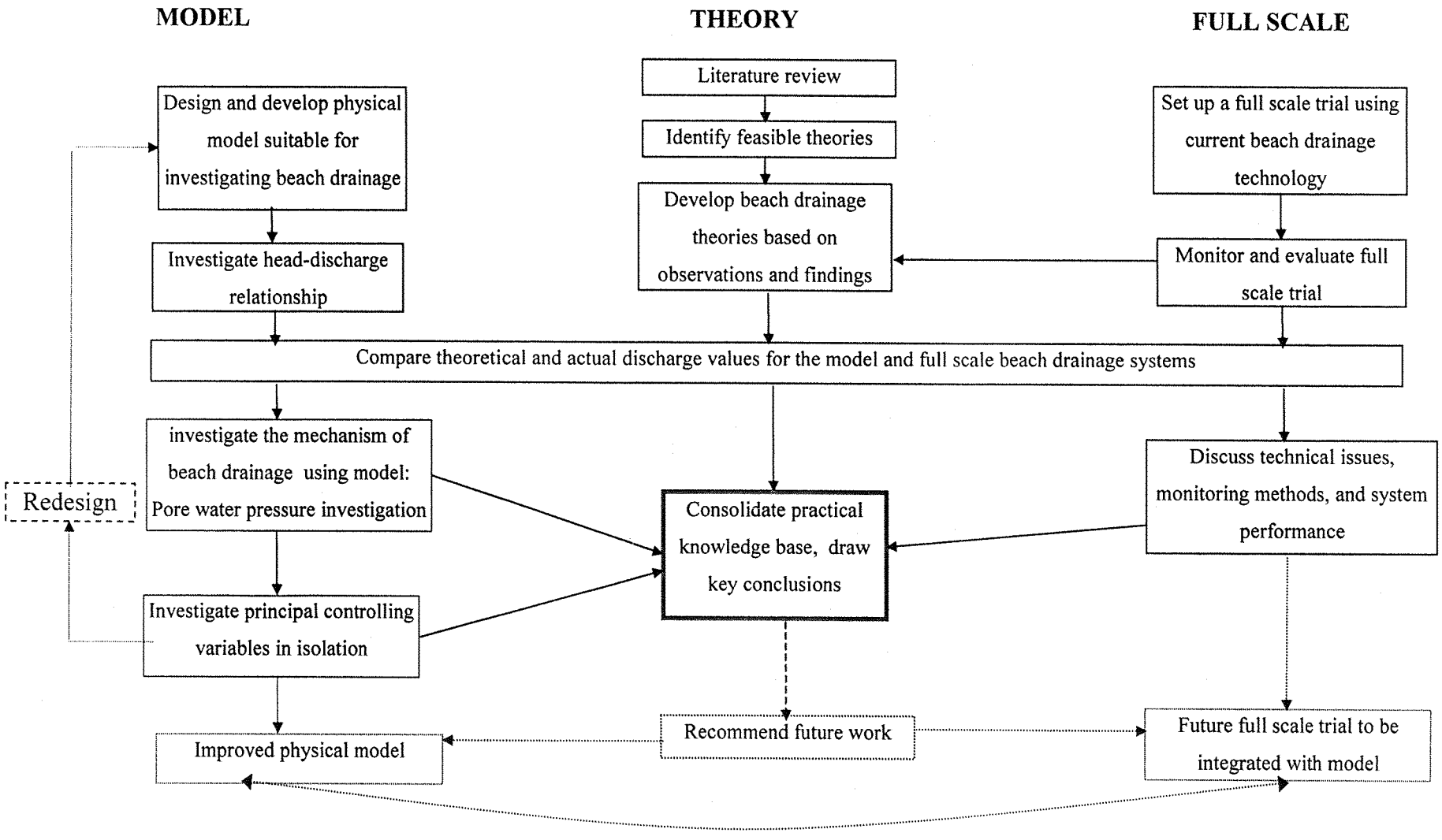

2. PREVIOUS WORK

2.1 Introduction

Previous studies have provided evidence of the advantages of effective beach drainage (e.g. Vesterby, 1997; Turner and Leatherman, 1997). However, results from full scale trials have been varied and it is clear that this new technique is only effective with certain boundary conditions. While beach drainage can offer an option for coastal stabilisation, its application should be approached with caution. Drainage system design is site specific, and performance is dependent on local characteristics. Performance prediction is complex due to the number of influencing factors, and in some cases the effectiveness has been found to be unpredictable.

Practical information detailing the application of beach drainage systems is relatively limited, and only three full scale systems have been installed in the UK to date. Several international pilot and commercial beach drainage projects have been summarised by Vesterby (1996), and additional material has been obtained through site visits and international collaboration.

Previous studies into swash zone theory (e.g. Bagnold, 1940; Grant, 1948; Duncan, 1964; Baird and Horn, 1996) have provided a foundation for this investigation, but a full understanding of the process of beach stabilisation through drainage is yet to be developed. One of the main aims of this project is to expand the current basic understanding the mechanisms of beach drainage.

The objective of this chapter is to provide an overview of previous work in four areas:

- theory and concepts,
- drainage system designs,
- case studies,
- model studies and concurrent work.

2.2 Theory

Two of the first studies of the relationship between beach characteristics and water tables were carried out concurrently by Emery and Foster (1948) and Grant (1948). Grant (1948) stated that 'a high water table accelerates beach erosion, and conversely a low water table may result in pronounced aggredation of the foreshore'.

2.2.1 Backwash energy reduction

Analysis of the mechanism of beach drainage is traditionally based on swash zone energy considerations, and one of the fundamental papers central to this project is by Bagnold (1940).

According to Bagnold (1940), with no losses the surge cycle is reversible and an equal quantity of sediment is transported in the swash and backwash. In the field, additional losses occur, and Bagnold (1940) divides these into two categories:

1) kinetic energy losses due to
    i) friction against the bed and
    ii) internal fluid friction (turbulence), and
2) potential energy loss due to infiltration: water that soaks into the beach does not take part in the backwash, hence backwash energy is lost due to percolation.

A beach drainage system is designed to remove water from the beach face resulting in a reduction in pore water pressure. This increases the opportunity for infiltration and promotes energy loss by mechanism (2) above, resulting in a change in the ratio of the swash and backwash energies. Chappell *et al.* (1979) carried out a full scale beach dewatering trial and demonstrated that beach accretion can be induced by maintaining a low water table. It was concluded that '...the mechanism is simply that by inducing greater infiltration in mid- and upper swash zone, sediment entrainment during backwash becomes less'. This may be summarised by the term backwash volume reduction.

2.2.2 Deposition phase extension

As the surge moves up the beach, the velocity decreases, and below a given critical limit the flow conditions will change from turbulent to laminar flow (Grant, 1948). During this short laminar flow phase, sediment is rapidly deposited, leaving a thin deposit of sediment on the upper foreshore. According to Grant (1948) water table lowering through beach drainage increases the opportunity for percolation, thus reducing backwash flow velocity and prolonging the laminar flow phase.

Although rapid sediment deposition is observed during laminar flow conditions, it is noted that deposition may also occur outside the laminar flow limit. According to Shields (1936) the threshold of movement is a function of the Reynolds number, where the Reynolds number relates to the grain conditions (see e.g. Chadwick and Morfett, 1993). Although rapid deposition occurs during laminar flow, sediment deposition is not *limited* to the laminar flow phase. Expanding Grant's (1948) theory, it may be possible that drainage results in deposition phase extension, rather than laminar flow phase extension.

2.2.3 Seepage cut-off

According to Grant (1948), seepage out of a saturated beach will contribute to backwash volume, resulting in backwash acceleration and increased erosion. Beach drainage removes water that is infiltrating into the beach, preventing it from rejoining the backwashed further down the beach face. This reduces the surge backwash volume, and therefore alters the balance between the swash and backwash energies.

Emery and Foster (1948) found that the elevation of a water table 20 to 40 feet behind the water line in a sandy beach may lag behind the tide level by between 1 and 3 hours. Hence during ebb tide, the water table level within the beach may be higher than the tide level. During this phase, water escapes from the beach face (the effluent zone) , and may collect into small rill channels as shown in Figure 2.1. Depending on the head difference, seepage velocities may be sufficient to entrain sediment particles, and these are carried along more efficiently once rill channels have formed.

Water removal via a drainage system would lower the elevation of the water table, reducing both the size of the effluent zone and the rate of seepage from the beach face.

Figure 2.1: Rill channels (Tresco, Isles of Scilly)

2.2.4 Seepage rate

The volumetric flowrate, q, through a porous material may be calculated using Darcy's Law (Darcy, 1856), which states that

$q = Aki$

where i is the hydraulic gradient, k is the coefficient of permeability, and A is the cross sectional area.

The coefficient of permeability, k, may be evaluated through laboratory testing (discussed in Chapters 3 and 5), or by applying the Hazen formula (Hazen, 1892) where $k = 0.01D_{10}^2$ ms^{-1} (D_{10} = 10% passing particle size)

2.2.5 Effective stress

The previous work discussed above may be useful in understanding the mechanism of beach stabilisation through drainage in terms of wave energy reduction and seepage cut-off. These two mechanisms concern the ability of the water to transport and deposit sediment.

The beach material has the ability to resist the shear force exerted by the wave, since the grains are held in contact by an effective stress and therefore there is friction between them. The shear stress, τ, is given by the equation $\tau = \sigma'_v \tan \varnothing'$ (σ'_v = vertical direct shear stress, and $\varnothing'$ is the angle of shearing resistance. The prime (') indicates that the parameters relate to effective stress).The effective stress is the proportion of the applied load that is taken by the soil skeleton, and according to Terzaghi (1936) effective stress, σ', is the difference between the vertical stress, σ, and the pore water pressure, u.

$\rightarrow \sigma' = \sigma - u$

According to this theory, beach drainage will result in an increase in the effective stress in the beach material, and hence an ability to resist shear.

2.2.6 Summary

From the above discussion it can be seen that beach drainage promotes beach stabilisation through several mechanisms. These mechanisms may be summarised as:

1) backwash energy reduction due to increased infiltration
2) seepage cut-off:
   i) backwash energy reduction
   ii) prevention of loss of material from the beach face during low water
3) increase in beach material shear resistance

All of these mechanisms arise from the fact that drainage causes a reduction in pore water pressure. Little previous work has been carried out into the effect of beach drainage on pore water pressure and material strength.

The study by Chappell *et al.* (1979) was the first to summarise the possible mechanisms of beach stabilisation and aggredation through drainage. Turner and Leatherman (1996) published a history and critical review of beach drainage as a means of coastal protection, which reiterates the mechanisms proposed by Chappell *et*

(e.g. Nielsen, 1992; Turcotte, 1960). However, from the literature review it is apparent that few studies have taken these concepts further, and there is little quantitative data to support the theories proposed by Chappell *et al.* (1979).

There have been numerous studies aiming to model beach ground water behaviour (e.g. Turner, 1995; Baird and Horn, 1995). However, there are few studies that specifically investigate the mechanism of beach drainage.

One of the main advantages of a physical model is that it can be designed specifically for the purpose of beach drainage system simulation and both qualitative and quantitative physical observations may be recorded during testing. However, most of the physical model studies of beach drainage systems have tended to focus on the effect of beach drainage on the beach profile (Weisman, 1995; Briere, 1999), and involved a qualitative comparison of profile data.

The aim of this PhD study is to use a physical model to investigate the relationship between individual controlling variables and beach profile formation, and examine the implications for the mechanism of beach drainage. One of the principal innovations in this project is the quantification of the impact of drainage on the potential for beach face liquefaction under wave action. This study examines the effective stress of the beach material, and cross sections of the beach profile showing the measured liquefaction boundary under wave action, with and without drainage, have been developed.

2.3 Beach drainage methods

1) **Pump assisted drainage:**

Although the studies by Grant (1948) and Emery and Foster (1948) identified that a relationship exists between water table level and rate of erosion, the first full scale beach drainage experiment was not carried out until thirty years later (Chappell *et al.*, 1979). Two full scale tests were carried out by Chappell *et al.* (1979) using a line of pumping wells parallel to the shoreline. This trial demonstrated that beach aggredation may be promoted by beach dewatering using a line of pumped wells, although horizontal pipes were recommended for future studies.

2) **Gravity drainage:**

Model experiments carried out by Machemehl in 1975 demonstrated that water table lowering using drainpipes perpendicular to the shoreline can have a positive effect on foreshore accretion. A full scale trial was conducted by Davis *et al.* (1992) using a similar configuration. The trial showed that full scale water table lowering was possible with this method, although results were limited and the lower ends of the pipes were subject to scour.

3) **The Beach Management System (BMS):**

It was only by accident in 1981 that the effectiveness of linear beach drains became apparent through a surprise discovery at Hirtshals West in Denmark (Vesterby 1996): The Danish Geotechnical Institute (DGI) was commissioned to design a clean (from debris) salt water supply system for a Sealife Centre at Hirtshals in the north of Jutland, Denmark. To obtain a supply of filtered sea water a perforated pipe surrounded in a geotextile filter was installed in the beach face, and the collected water was pumped to the aquarium. Within approximately 6 months of operation the flow rates from the beach drain had reduced by 60%. Upon further investigation it was found that a considerable amount of material had accreted over the drain, and the beach had widened by approximately 20 to 30m seaward of the drain (Vesterby, 1996).

Subsequent full scale testing at an adjacent beach verified the findings at Hirtshals West and it was soon realised that this method of beach dewatering could offer many

benefits as a method of coastal stabilisation. The system has been proven to be capable of significantly widening a beach, improving its recreational value, and has a relatively low environmental impact. The Danish design was named the 'Beach Management System' (BMS) and is now protected by international patents. A typical BMS layout is shown in Figure 2.2.

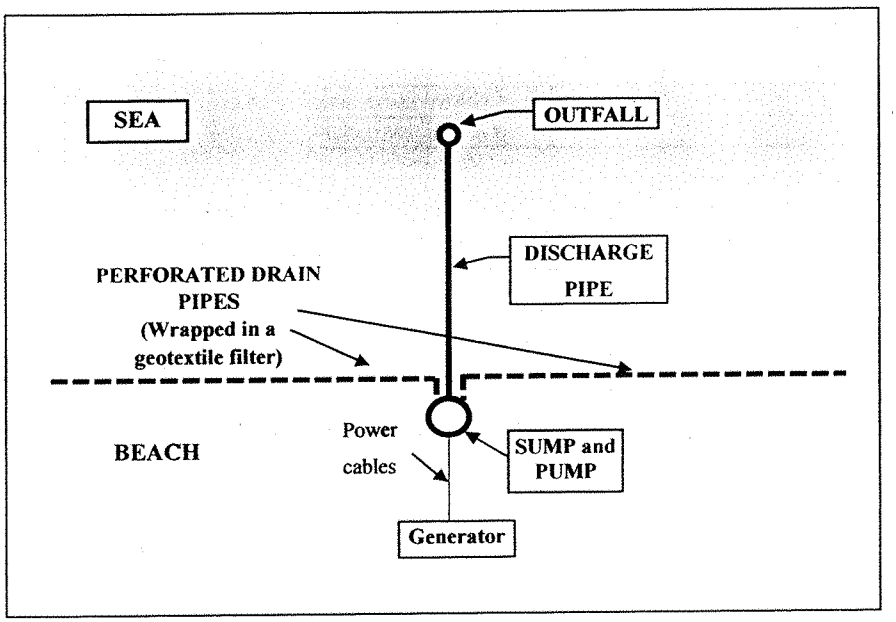

Figure 2.2: Schematic diagram of BMS (plan).

The first commercial system was installed at Sailfish Point, Florida (US) in 1988. This system also resulted in a significant widening of the beach in front of the drainage system.

Approximately 20 full scale systems have been installed since 1981 (including trial systems). These are summarised in Appendix, A which gives an overview, prepared by the Danish Geotechnical Institute, of Beach Management System projects to date. These data are summarised in Table 2.1 which gives the pump capacity per unit length of system and a qualitative success rating for each project. The success rating is allocated according to the comments supplied by the DGI in Appendix A.

System	D_{50}	Initial flow	Pump capacity	Success	System length
	mm	cubic m/hr/m	per m of system	Rating (1 - poor,	
			cubic m/hr per m	5 - good)	
Hirtshals W (Denmark)	0.26	2	2	5	200
Hirtshals E (Denmark)	0.2	0.4	0.5	2	200
Thorsminde (DK)	0.35	1.7	0.7	4	500
Sailfish point (USA)	0.3	1.5	1.7	4	177
Enoe Strand (DK)	0.25	0.4	0.5	3	600
Towan Beach (UK)	0.2	1.27	1.1	3	180
Codfish Park (USA)	1.5	1.7	2	2	357
LighthouseS (USA)	0.8	1.8	4.5	2	309
Chigasaki-Naka Beach (Japan)	0.4	3.2	3.5	3	405
Riumar, Ebro Dleta (Spain)	0.5	2.8	2.8	2	180
Lighthouse N (USA)	0.2	0.5	1.0	2	300
Hornbaek W (DK)	0.3	0.1	0.4	4	450
Hornbaek E (DK)	0.3	0.3	0.6	4	530
Ystad (Sweden)	0.3	0.8	1.2	3	200
Hitotsumatsu (Japan)	0.25	n/a	0.8	3	800
Les Sables d'Olonne (France)	0.25	n/a	0.8	3	300
Branksome Chine (UK)	0.25	0.36	0.65	3	100

Success rating key

Accretion and harvesting = 5
Large width increase = 4
Modest width increase 'accretionary trend' = 3
Maintained width = 2
Ineffective = 1

Table 2.1: Summary of case study data (for comparison purposes)

In all cases the width of the beach was maintained, and for 70% of the projects an increase in beach width was noted. There appears to be no direct correlation between pump rate and system success, therefore the system performance must be influenced by other forcing factors (e.g. drain location, local site characteristics, wave climate, sediment supply). It may be that system yield is important, but the relationship is occluded by other factors. In fact, this has been determined in the research described in this dissertation, in which the effects of individual variables have been investigated in isolation using a physical model.

The data suggest that there is a correlation between beach sediment size and flowrate, and this is used later in Chapter 3 to estimate the design pump capacity for the Branksome Chine beach drainage trial.

4) **Multiple pipes or a geotextile permeable layer**

Chapter 8 details an investigation into the effectiveness of a linear beach drainage system under different still water level positions relative to the drain. Results suggest that the performance depends on the position of the wave run-up relative to the zone of influence of the drain. With a single linear drain the zone of influence may be relatively limited, and optimum performance may only occur for limited periods during the tide cycle. For a large tidal range and linear drainage system, the proportion of time during which the run-up zone is over the zone of influence of the drain is relatively short. Performance may be optimised by designing a drainage system that extends to the limits of the tidal range. This will be discussed in Chapters 8 and 9.

2.4 Case studies

Three beach drainage systems have been installed in the UK (Burstow, 1996; Vesterby, 1996). Of these, the only commercial installation was installed in an area with unusual site characteristics; hence results are not comparable with those of the Danish trials.

1) Holme Beach, Norfolk (trial system)

Installed: 1996

Participants: MMG Beach management Systems (UK) Ltd. and the Environment Agency

Holme-next-the-Sea in Norfolk, England lies in an area prone to coastal flooding and high rates of erosion. This beach is part of Holme Nature Reserve, which is a protected area. The nature reserve is a rare wetland habitat and is a designated Site of Special Scientific Interest. The site is also protected under the EC Wild Birds Directive. The habitat includes freshwater ponds harbouring several protected species, in particular, the Natterjack Toad, an officially endangered species which is native to this area.

Since this is a freshwater habitat, Holme is sensitive to saltwater flooding from the sea. The beach is gently sloping and consists of fine to medium sand backed by steep dunes which protect the reserve from flooding during high tides and storms (Figure 2.3). The tidal range is approximately 3.5 metres and under normal conditions the high tide does not reach the back of the beach. Erosion problems are mainly caused by wave run-up reaching the back of the beach during spring tides and storms - a low tide the wet front of the dunes is exposed and slumping occurs.

Figure 2.3: Holme beach, Norfolk

The dunes are currently under threat of being breached, however, hard engineering works in this protected area would be unacceptable. If successful, beach drainage would be a suitable solution for this region, since the system is subsurface and would therefore not be an intrusion on the Holme nature reserve. A beach drainage trial was undertaken by the UK Beach Management System (BMS) licensees in order to determine whether beach drainage would be an effective coastal stabilisation alternative for this area.

The system consisted of two 200mm diameter uPVC perforated drain pipes wrapped in a geotextile sock, each 100m long and draining by gravity to a central sump. The drainage system is shown in Figure 2.4. The pump was activated by a depth gauge, and water was discharged through a solid uPVC discharge pipe as shown in Figure 2.5.

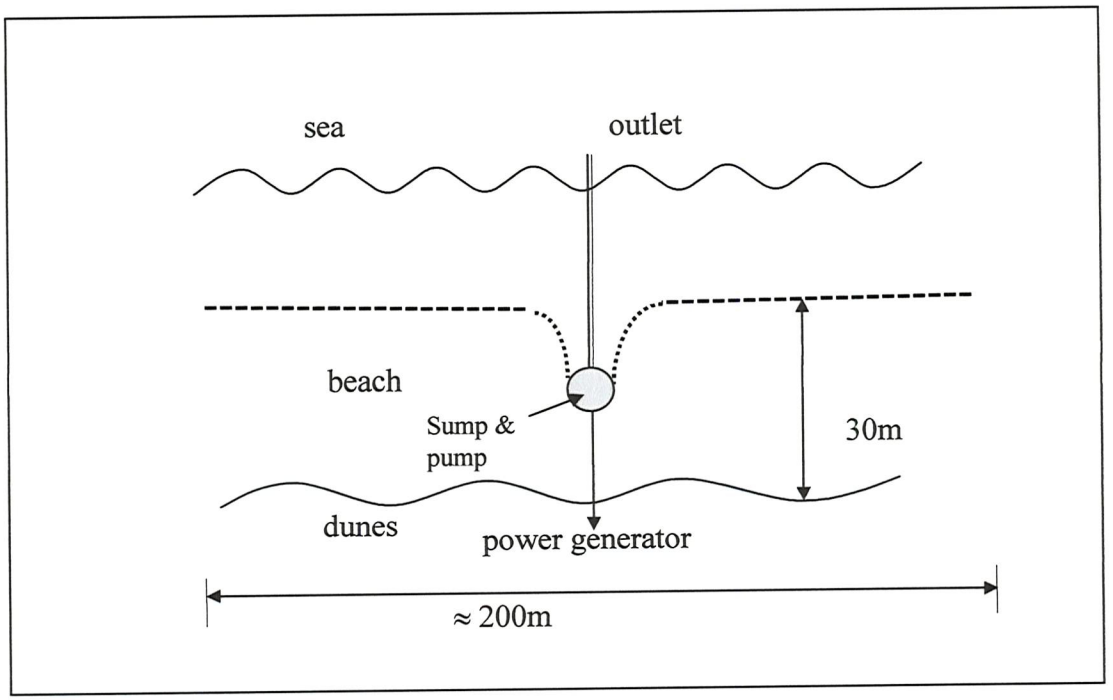

Figure 2.4: Schematic diagram of Holme beach drainage system

Figure 2.5: Drainage system outfall, Holme Beach, Norfolk

The aim of the drainage system was to lower the water table and allow the swash water to percolate more quickly into the beach. The objectives were to prevent dune slumping, increase beach stability and promote the accumulation of wind blown sand to protect the nature reserve.

The future use of a commercial beach drainage system at Holme would have the disadvantage of causing a drawdown in the beach adjacent to a freshwater wetland habitat. Although possibly preventing flooding of the freshwater ponds by sea water, there is a danger that the BMS might drain the wetland. Drainage would alter the ecosystem and destroy the natural site characteristics. However, if no action is taken, the dunes are likely to be breached in the near future and the nature reserve will become inundated with seawater.

Survey data indicate that during the period around 28/4/97 the drainage system was having a positive effect on the beach, in comparison to the undrained control beaches (Marin *et al.,* 1998). However, outside this period results are inconclusive. This may be due to weather conditions, since during the trial period the beach was subject to numerous storm events.

As part of this PhD project, a full scale experiment was monitored at Branksome Chine in Dorset (Chapter 3). Local weather data were recorded during the first 6 months, and it was evident that prolonged periods of erosive conditions resulted in system damage, reduced efficiency and poor performance.

The Holme beach experimental system was the first beach drainage system to be installed in the UK. Although the trial did not lead to a full scale commercial system at Holme, a commercial system is currently in operation at Towan Beach in Newquay, Cornwall.

2) Towan Beach, Newquay, Cornwall (commercial installation)

Installed: April 1994

Participants: Restormel Borough Council Technical Department, St. Austell in collaboration with MMG Beach Management Systems UK Ltd.

Towan is a gently sloping intertidal beach, approximately 300m wide, in a bay surrounded by cliffs, and is exposed to swell from the Atlantic Ocean. Towan beach is shown in Figure 2.6. At the base of the cliffs lies a Victorian sea wall, which forms a promenade and protects a number of properties. The wall is deteriorating and prior to the installation of the BMS the foundations had been exposed by storm damage. Figure 2.7 shows the upper part of Towan beach and the Victorian sea wall at high water.

Alternative schemes

An alternative option was to renovate and develop the promenade area at the back of the beach (Figures 2.6 and 2.7) with the intention of encouraging tourists to the area and promoting indirect benefits for the local economy. Unfortunately, the properties on the promenade are of low value and any likely increase in tourist revenue would be relatively small. Strengthening the sea wall would cost an estimated £2.5 million which could not be justified, hence the scheme was abandoned. A second option considered for Towan was a rock bund over the lower foreshore at a reduced cost of £1.2 million. A cost benefit analysis showed that even with grant aid both proposals were beyond any realistic future council budget.

Figure 2.6: Towan Beach during low water

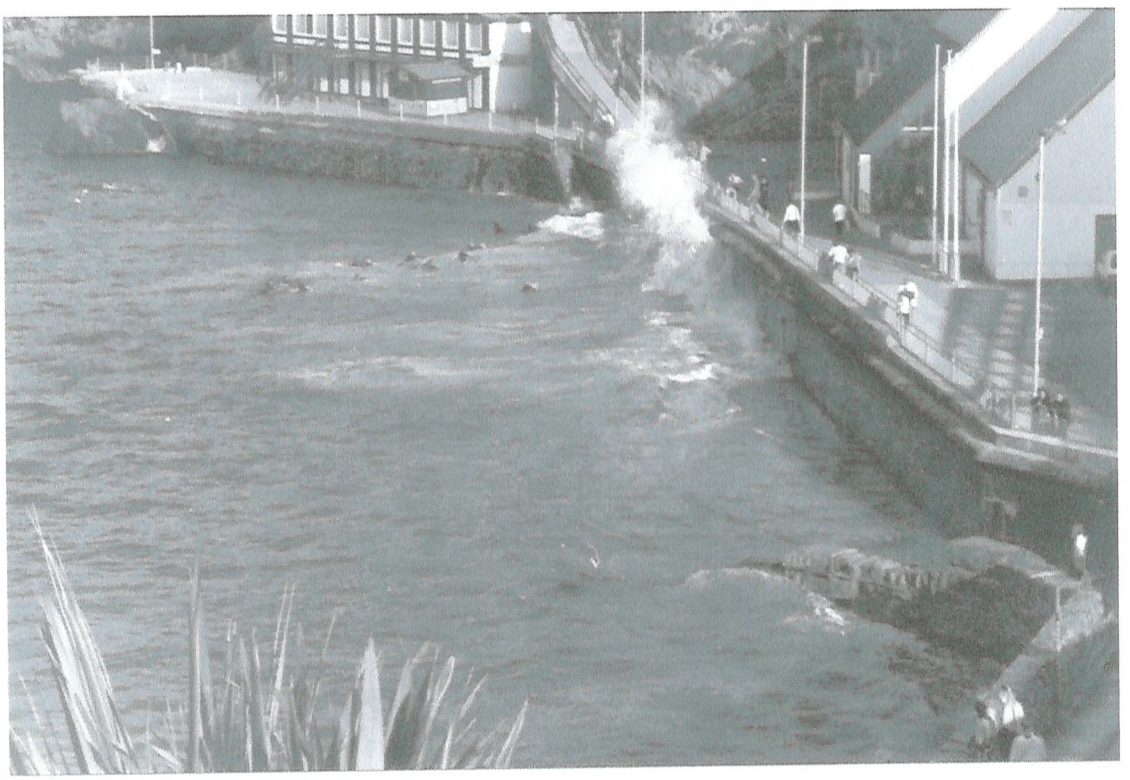

Figure 2.7: Towan Beach during high water

To establish the best way of protecting the wall at Towan, the local authority proceeded with a Coastal Study (a feasibility study), during which a beach drainage system was suggested.

In 1993 the feasibility study concluded that a Beach Management System would be suitable for this beach, and a study was carried out to establish water table level and local tidal patterns. The central issue with this BMS application was the high 7m tidal range compared to other BMS locations which have tidal ranges of approximately 2m or less. Due to limited research available at the time, the influence of the tidal range on the efficiency of the BMS could not be anticipated, and the project proceeded as a 'trial' installation.

The aim of the scheme was to protect the sea wall by replenishing and retaining beach sand, hence increasing the beach volume and improving wave energy dissipation. The project received grant aid from the Ministry of Agriculture Fisheries and Food for the monitoring of Towan and surrounding beaches for a six year period.

The scheme was designed to specifications provided by the Danish Geotechnical Institute (DGI), and a plan showing the location of the beach drains is shown in Figure 2.8. A land drain was included in the design to intercept land run-off which was contributing to the elevation of the beach water table.

The positions of the drains can be seen in Figure 2.6, since there is a dry mark on the beach above each of the two drains. The beach drain can be seen emerging from the bottom left of the photograph, while the land cut off drain is a few metres to the left of the sea wall on the right hand side of the photograph.

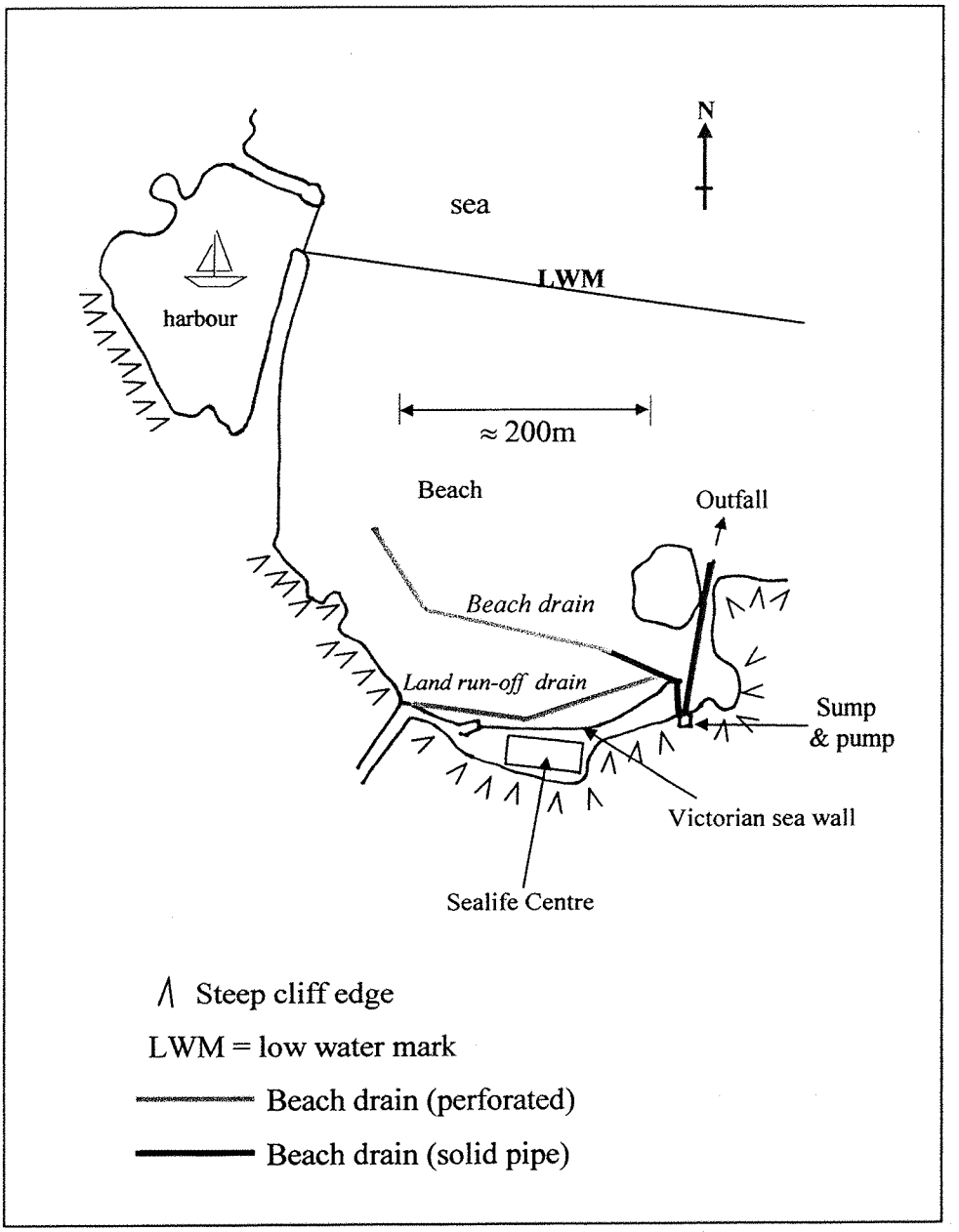

Figure 2.8: Schematic diagram of Towan Beach drainage system

The pumping station consists of a sump constructed of pre-cast concrete containing two submersible pumps. This was constructed in a cove at the eastern end of the beach (Figure 2.8) and was connected to power supplies and controls located behind the end of the promenade.

The beach profile was monitored for a total of 6 years, beginning nine months before the start of the scheme. The beach was initially surveyed along six profile lines and in

1994 the DGI added two control lines on adjacent beaches. Levels were taken during low spring tides once a month for the first three years, then less frequently for the remaining time.

During the monitoring period the beach displayed a trend of accretion on the foreshore which began almost immediately after pumping began. Consistent with the results of previous Danish trials, the system was able to withstand the effects of storms which in this case were magnified due to reflection from the sea wall. By January 1995 approximately one metre of sand had built up at the toe of the sea wall.

This study has demonstrated that beach drainage, originally chosen as a last resort due to financial constraints, has provided a cost effective solution for Towan beach. Being the first BMS installation in Britain, the success of this scheme has significant implications for the use of the beach drainage in the UK. The positive results of this trial, in particular proving that the BMS can be effective in a macrotidal tidal regime, may encourage other local authorities to consider the option of beach drainage.

An additional advantage of the beach drainage system at Towan is that the beach is dried out between successive high waters, where previously the beach surface remained extremely wet. This has improved the amenity value of the beach. The same advantage applies to a recent commercial installation at Les Sables d'Olonne (France).

Since this time, a third trial has been carried out at Branksome Chine in Poole, Dorset. This system was installed in June 1998, and is discussed in Chapter 3.

Summary of UK trials

A summary of the three UK case studies is given in Table 2.2.

Scheme	**Purpose**	**Date Installed**	**Capital Cost**	**Running cost**	**Dimensions**
Holme Beach, Norfolk	Trial system	1996	£13,000	£450 per week	200m long (100m x 2) Pipe diameter = 200mm
Towan Beach, Newquay	Commercial installation	April 1994	Feasibility study: £10,000 Total Cost: £200,000	£18,000 - £20,000 per year	Pipe diameter: 9 inches (approx 225mm). Length = 200m
Branksome Chine, Poole	Full scale experiment	June 1998	£20,000 approx	n/a	Four pipes in parallel, 100m long. Diameter = 200mm

Table 2.2: Summary of UK full scale beach drainage systems

2.5 Model studies and concurrent work

Wave tank models

One of the major advances in beach modelling using wave tanks was made by Bagnold (1940). This paper highlights the problems associated with full scale trials, namely the large number of uncontrollable variables that rarely remain constant for any length of time. The principal advantages of a physical model are that variables may be easily isolated and controlled, and observations may be made during the tests.

Bagnold (1940) also highlighted several limitations associated with wave tank modelling: The movement of both water and beach material is restricted to two dimensions, while on the prototype beach movement in the horizontal plane may also take place alongshore. Secondly, reliable model rules must be formulated so that the model data can be applied to full scale conditions. These rules are either mathematical (if theoretical relationships are available) or empirical. Model scaling will be discussed in Chapter 5.

Beach drainage modelling

Weisman *et al.* (1995) carried out an investigation into beach drainage using a physical model. Experiments were conducted using an irregular wave generator and 32.7m long channel. This study identified an important scale effect concerning the infiltration characteristics of the model beach face. Weisman *et al.* (1995) used the Froude number to scale the wave properties, and the sediment fall time parameter to scale the sediment. The scale problem arises due to the reduced periodicity of the model wave, coupled with the reduced sediment size. The combination of these factors results in a higher frequency of foreshore wetting, but a reduced rate of soaking away in comparison to the prototype. The surge water delivered to the beach face during each run-up has less time to soak away, and the ultimate result is a wetter beach face in the model than in the prototype.

It was concluded that this effect resulted in an underestimate of drainage system performance in the model and that a '....beach drain may be dramatically more effective on a prototype beach than in the model tested.' While the tests provided valuable model data, it is apparent that further work is necessary before the implications for the prototype system can be fully understood.

Concurrent Work

Modelling is currently being carried out at the University of Caen, France (Briere, 1999). The Caen model apparatus is similar to the arrangement used for the physical modelling carried out in this research.

The Caen model was intended to simulate a field environment, and tests have involved the use of tide cycles and land flux. The physical modelling in the research project described in this thesis differs from that of the University of Caen, in that the aim was to isolate controlling variables and identify the individual relationships between them and drainage system performance.

The Caen model encountered similar scale problems to those identified by Weisman *et al.* (1995) because the same sediment was used. A Bakelite sediment was used for the model described in this thesis. Despite this, scale effects were unavoidable, however these were of a different nature, and the effects have been investigated further through the use of dimensional analysis. Scaling issues are discussed in Chapter 5.

2.6 Factors affecting beach morphology

There are a large number of local factors and design parameters that influence beach morphology and drainage system performance. These have been drawn from literature review and previous University of Southampton research into beach drainage, and are listed in Table 2.3 below (e.g. Bagnold, 1940; Vesterby 1996; Marin *et al.*, 1998). The factors have been divided into two categories: A: Site characteristics (natural forcing conditions that influence beach change), and B: Design parameters (human influence).

A) NATURAL SITE CHARACTERISTICS		**B) DESIGN PARAMETERS (HUMAN INFLUENCE)**	
Variable	**Note**	**Variable**	**Note**
i) Beach Material	Grading, sorting, quantity, permeability, beach foundation material	i) Drain Design	Distance from shoreline, length, depth, number of pipes, diameter, filter medium, pipe permeability, position of outlet
ii) Wave Regime	Wavelength, period, velocity, height, steepness, form, energy, angle of incidence, shallow water effects	ii) Flow rate through pipes	Affected by other listed factors: Drain design, pump capacity, beach material, tide, wave regime, local beach conditions. Controlled by pump schedule, or vice versa
iii) Tides	Tidal range Tidal curve e.g. double high tides etc.	iii) Pump schedule	Frequency of pumping, length of run time, when pump is used, mechanism of cut-in/out
iv) Local Beach Conditions	Downshore, offshore, upshore, longshore drift, land backing beach e.g. cliffs, land run-off conditions Windblown sand	iv) Other coastal protection schemes in local area/same site	e.g. Upshore groynes, local sea wall

Table 2.3: Factors affecting beach morphology and beach drainage performance

Due to the large number of influencing factors, the potential scope of this investigation is large. Selected variables have been investigated, and these will be discussed in Chapter 4.

3. BRANKSOME CHINE FULL SCALE TRIAL

3. 1 Introduction

This chapter details a full scale beach drainage experiment which was carried out at Branksome Chine in Poole, Dorset. The project was financed jointly by the Borough of Poole (BoP) and the Ministry of Agriculture Fisheries and Food (MAFF). The aim of this chapter is to review the Branksome trial, highlight important practical considerations, present the results of the monitoring, and assess the trial outcomes.

Pumps were started in June 1998, and despite a number of unplanned out of operation periods, the trial continued for 12 months. The scheme was monitored closely for the first six months of the trial, during which time the system performance was variable. Monitoring techniques included surveys, weather observations, photographs and pump charts.

3.1.1 Background

Branksome Chine lies just west of the Poole/Bournemouth local authority boundary, and east of Poole Harbour and Sandbanks (Figure 3.1). This area of Dorset is renowned for its sandy beaches, natural habitats and seaside resorts, which attract many visitors each year. The local economy benefits from revenue generated from tourism, and the sandy beaches in Poole are a valuable asset.

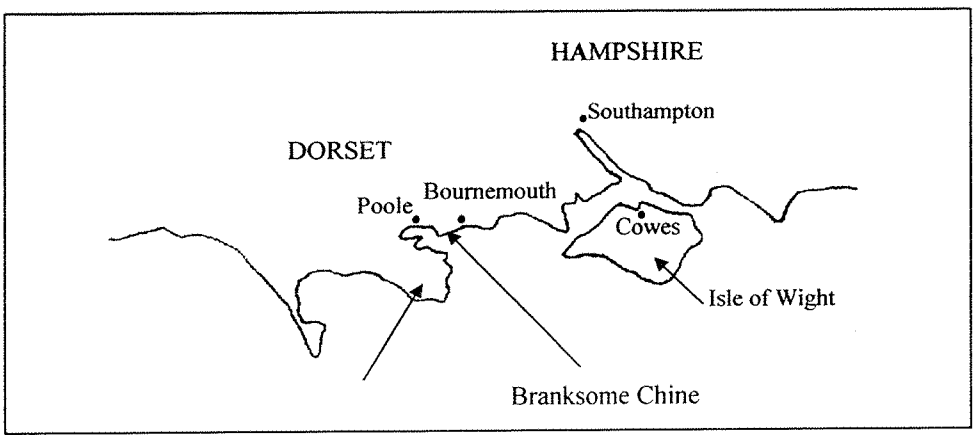

Figure 3.1: Area map

Branksome Chine is popular with both visitors and local residents, offering an extensive promenade along the top of the sea wall. There are a number of car parks and some small shops and public facilities situated behind the beach. Branksome is a desirable place to live with exclusive apartment blocks clustered around the cliffs behind the beach with views of Bournemouth, Old Harry Rocks and the Isle of Wight.

Figure 3.2 Branksome Chine beach

The beach at Branksome consists of between 1 and 3 metres of medium sand over a depth of silt and clay. The depth of sand was estimated from the sump excavation soil profile, a view of which is shown in Figure 3.3.

Figure 3.3 Soil profile revealed during sump excavation

The beaches along this stretch of coastline are flanked by cliffs, and as the name suggests, Branksome Chine represents the cross section of a truncated valley: the beach at Branksome Chine is backed by lower level land with cliffs rising up to either side. This feature is caused by cliff back cutting in the past revealing the cross section of a natural valley which approaches perpendicular to the shoreline, and is evidence that the area has experienced a history of erosion.

Since Branksome Chine is at the foot of a small valley, this area is a natural runoff collection point. However, much of the land run-off in this area is collected by the road drainage network, and discharged into the sea beyond the low water mark via a storm water overflow outfall.

The sandy beach forms the first line of defence against wave attack by dissipating surge energy and preventing run-up from reaching the base of the sea wall. When beach levels are reduced, waves may over-top the sea wall posing an immediate threat of flooding to low lying properties on the sea front. These are mainly beach huts, public conveniences and a few small businesses. In extreme cases low beach levels may allow wave attack to undermine the wall foundations, although this is not yet known to have occurred. If this situation did arise, wave attack may extend to the foot of the cliffs on either side of the chine posing a potentially serious threat to cliff stability and cliff-front properties. Low beach levels also pose a threat to the amenity value of the beaches. After stormy periods only a small beach area remains and some sections may be completely covered during high tide.

Despite the current shoreline protection measures the beach levels at Branksome continue to cause concern for local authorities. With traditional structures already in place, the local authority has been faced with a limited choice of new protection methods. Alternatives include riprap, a large breakwater, an offshore submerged rubble mound, and beach drainage.

An offshore breakwater was considered, but proved a controversial issue for decision makers. Submerged offshore rubble mounds are also known as artificial reefs, since they cause waves to break earlier, or prior to reaching the natural surf zone. The structures may be used to improve the recreational value of a beach, in particular for surfers and windsurfers (activities currently popular at Branksome Chine). Although offshore rubble mounds can provide an effective means of shoreline protection, the main disadvantages are that they are expensive, and are thought to pose a danger to some beach users (i.e. children). Given the high cost of the existing works at Branksome Chine, further expensive schemes could not be justified at the present time (although this is debatable).

A scale drawing of the area is shown in Figure 3.4. The beach is divided by wooden groynes that are 35m long and approximately 100m apart, and is backed by a concrete stepped sea wall which forms a promenade. Similar attempts have been made to reduce erosion at Bournemouth.

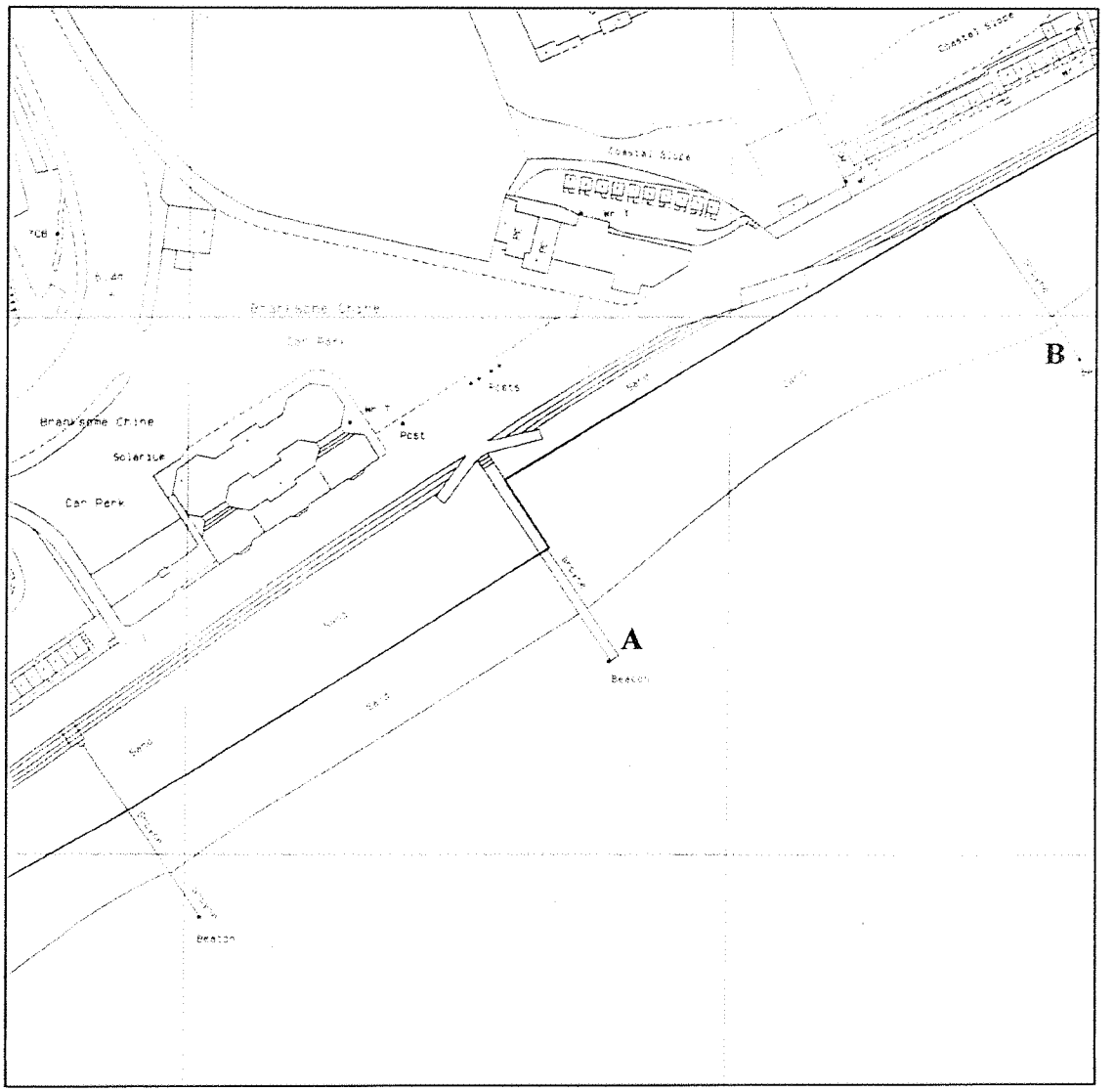

Figure 3.4: Plan drawing of Branksome Chine. Scale 1: 1250. (Reproduced with permission for examination)

The bold black line running across the beach denotes the mean high water mark. The groyne labelled A is a concrete groyne housing a storm water overflow outlet and is approximately 1.8m wide, while the remaining groynes are wooden. The concrete stepped sea wall can also be seen in Figure 3.4.

3.1.2 Aims and objectives

Previous studies have demonstrated the potential for improving beach stability through controlled drainage, as discussed in Chapter 2. However, the results of full scale trials are varied, and the application of the technique has been hindered by a shortage of practical information on the performance of beach drainage systems in the UK shoreline. The broad aim of the Branksome Chine trial was to investigate the application of beach drainage, and to establish whether this technique would be an effective shoreline stabilisation option for the Branksome Chine area.

The aims and objectives were different for the parties involved:

Borough of Poole

The principal objective was to investigate the suitability of beach drainage as a method of beach stabilisation for Branksome Chine.

The Ministry of Agriculture, Fisheries and Food (MAFF)

The primary objective for MAFF was to establish whether beach drainage could be considered as a viable coastal defence method for the UK. Given the high cost of coastal defence, MAFF was interested in determining the value of beach drainage as an economical protection measure.

The University of Southampton

This beach drainage trial was proposed and outlined prior to the involvement of the University of Southampton. The aim of the University was to maintain an objective approach to the experiment, and evaluate the scheme on the basis of scientific data and observations.

It was originally intended to investigate the performance of beach drainage systems using the full scale trial as a research tool. However, it quickly became apparent that this would be difficult due to:

a) the large number of variables in the field,
b) the lack of control over influencing variables,
c) the fact that variables rarely remained constant for any length of time, and
d) technical problems involving the sump and pump.

Therefore it was decided that the trial would be monitored and assessed as a pilot project, and practical aspects of the project are discussed in this chapter.

Despite the problems noted above, data were recorded regularly during the trial, and these have been used to:

a) demonstrate that the system performance varied during the trial,
b) understand why the system performance varied during the trial, and
c) investigate the system discharge.

The Branksome experiment provided an opportunity to demonstrate that beach drainage can influence the beach profile, and the trial highlighted several practical considerations and technical limitations.

3.1.3 Scope of study

The scope of the Branksome Chine trial was dictated by physical and financial constraints. However, it was important to be aware of the wide range of influencing factors identified in Chapter 2, section 2.6.

The investigation has focused on the following topics:

Effect of the drainage system on beach profile

The primary area of investigation was the effect of the system on the beach profile compared with the profiles of a number of control beaches.

The trial system was installed within one of the groyne bays, and was therefore restricted to a total length of approximately 100m. The drained section was between groynes A and B (shown in Figure 3.4), and the control beaches were 200m either side of the drained section (two groyne bays either side of bay AB). Hence a total of 500 metres of beach was surveyed.

System discharge

The system flow rate was investigated using a chart plotter connected to the pump control panel. Of particular interest was the relationship between discharge and tide level. This Chapter details the data collection techniques and results, and system discharge will be discussed in greater detail in Chapter 6.

Weather patterns

Another area of interest is the seasonal variation in weather during the trial period, since this may influence the interpretation of results. Weather data have been recorded for the trial period and will be discussed in section 3.4.2.

Local effects

Field notes were recorded to describe the distribution of sand on the drained and control beaches, since any accumulation or loss of sediment was likely to be influenced by the location of existing structures.

3.1.4 Considerations

It can be seen in Figure 3.4 that the mean high water (MHW) mark is not the same for the drained and controlled beaches. In particular there is a significant jump in the mean high water position from the drained beach to the control beach to the west of the drained section. The position of the MHW mark in Figure 3.4 indicates that the level of the beach between groynes A and B is lower than for the adjacent groyne bay to the west. This natural feature, which clearly existed before the installation of the drainage system, needed to be taken into consideration when assessing the success of the trial: a successful trial system may not necessarily result in an elevated berm in comparison to the control beaches, rather an equalising in the levels observed on either side of the concrete groyne A.

Experiment scale

A relatively short section (100m) of the shoreline was covered by the drain system. From Table 2.1 in Chapter 2 it can be seen that Branksome Chine was the shortest system to be installed to date. It is not known whether a minimum length of system is necessary for effective beach drainage. The small island of drained beach was likely to have been subjected to numerous influencing factors (e.g. cross shore currents, longshore drift, or aeolian sediment transport), and the extent of the edge effects is unknown.

The time scale for a beach drainage system to take effect was also uncertain. Data from previous test sites may not be applicable to sites such as Branksome, where characteristics (e.g. sediment supply) may be different. It is possible that due to external factors the rate of build up due to the drainage system may vary (see comments below).

Stabilisation and Accretion

Local knowledge suggests that sediment supply is limited (possibly due to dredging in Poole Harbour, reduced upshore cliff erosion, or historical reasons). Beach levels either side of the wooden groynes have been noted to be approximately equal on several occasions, which suggests that longshore sediment transport rates may be low.

Limited sediment supply is likely to affect the performance of a beach drainage system in this area, since a material supply is necessary for accretion to occur. The purpose of the drainage system might be to stabilise the material already present, and maintain the current beach levels while the control beaches continue to retreat. The effect of beach drainage on erosion and accretion are investigated using a physical model, which will be discussed in Chapters 5 – 8.

It is possible that the success of the trial may only become apparent when surrounding beach levels fall, and this would depend on the timescale for beach morphology in the Branksome area. Essentially, this means that the effect of the drainage system may be time dependent, and may not be immediately apparent: hence a long period of operation may be necessary to ensure a fair trial.

Comparison to Danish trials

In Chapter 3 it was noted that the beach drainage system at Hirtshals West in Denmark caused a significant widening of the beach (Vesterby, 1996). It was unrealistic to anticipate similar results for the Branksome Chine experiment since the site characteristics are not comparable (e.g. aspect, prevailing wind, sediment supply, beach width, local topography and structures). Due to limited knowledge at the time, it was difficult to accurately predict how the different site characteristics would affect the system performance.

3.2 Preliminary study

3.2.1 Introduction

A preliminary site investigation was carried out in February 1998 before the installation of the beach drainage system. The aim of the site investigation was to establish the characteristics of the beach and provide information to help design a suitable beach drainage system, including estimation of the required pump capacity.

Samples were collected from different depths and locations on the section of beach to be drained. These were then tested to determine the permeability and particle size distribution.

Sample Collection

Samples were collected from Branksome Chine trial beach on 2/2/98. Sediment properties were expected to vary with depth and location on the beach face, hence samples were collected.

Sample points were given an (x, y) co-ordinate where:

x = paces from concrete groyne,

y = paces from the foot of step 5 of the sea wall, where the top of the wall (promenade) is step 1. The sample locations and depths are given in Table 3.1

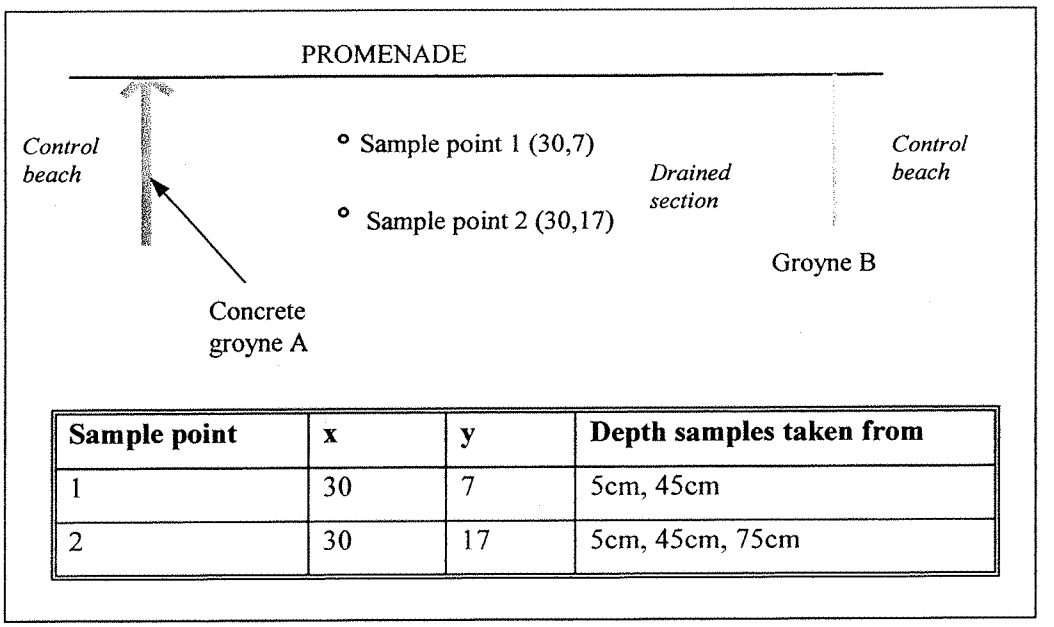

Sample point	x	y	Depth samples taken from
1	30	7	5cm, 45cm
2	30	17	5cm, 45cm, 75cm

Table 3.1: Location of sample points

3.2.2 Sediment Properties

Particle size distribution and soil classification

Dry sieving was carried out for each sample to establish the particle size distribution in accordance with BS 1377:1975, Test 7(a). A typical particle size distribution (PSD) curve is shown in Figure 3.5.

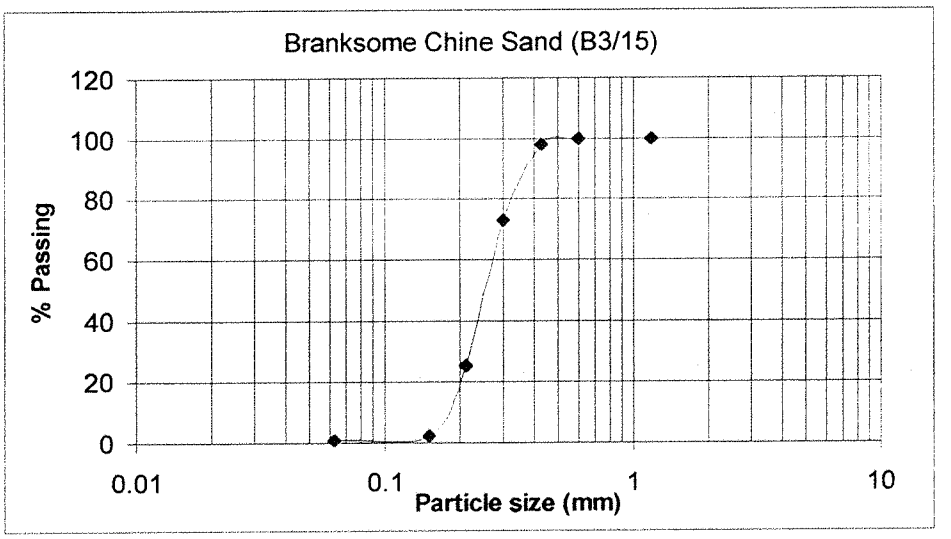

Figure 3.5: Particle size distribution curve for a typical sand sample from the drained section of beach (between groynes A and B)

There was some variation of sediment size with depth and location on the beach face, however, Figure 3.5 shows a typical sediment distribution curve. The particle size curves show that the beach material is a uniformly graded medium sand, with a 50% passing grain size (D_{50}) of 0.25mm.

Permeameter testing

Each sample was tested in a constant head permeameter according to guidelines set out by Head (1986). The permeameter test apparatus is shown in Figure 3.6.

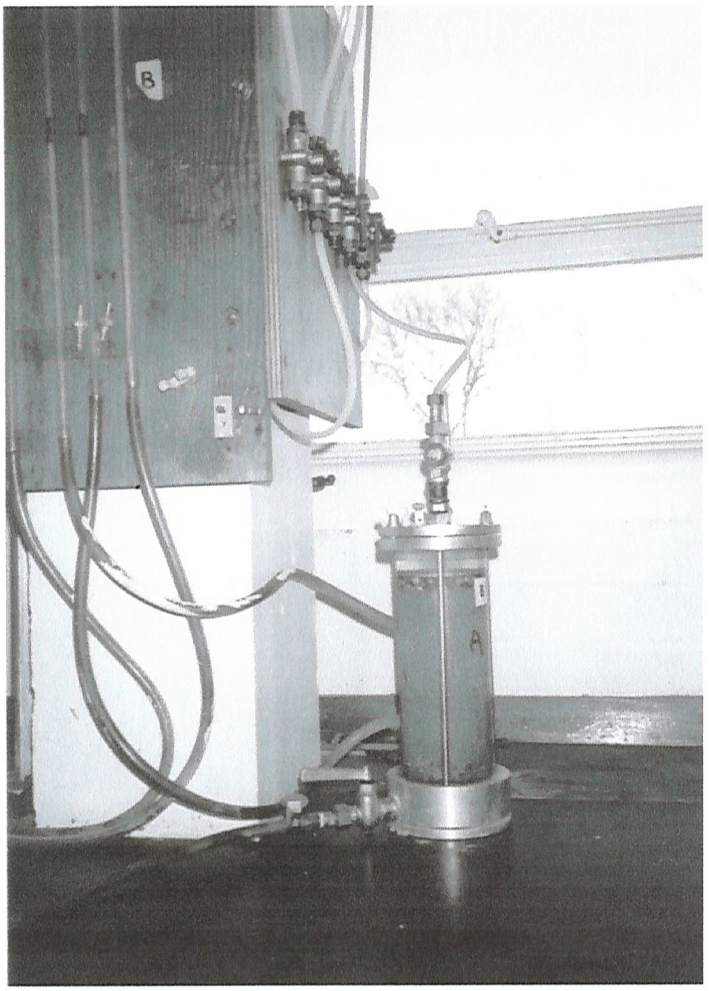

Figure 3.6: Permeameter test apparatus

Samples were tested in a loose and dense state. The loose sample was prepared by placing the sand in the permeameter, backwashing, then allowing the sand to settle. The dense sample was prepared by placing the sample into the permeameter cylinder in a series of layers. Each layer was gently compacted with a tamping rod, using approximately 10 strokes per layer. The prepared sample was dense, but not tightly compacted.

The discharge was recorded for a range of hydraulic gradients, and a typical set of results are shown in Figure 3.7.

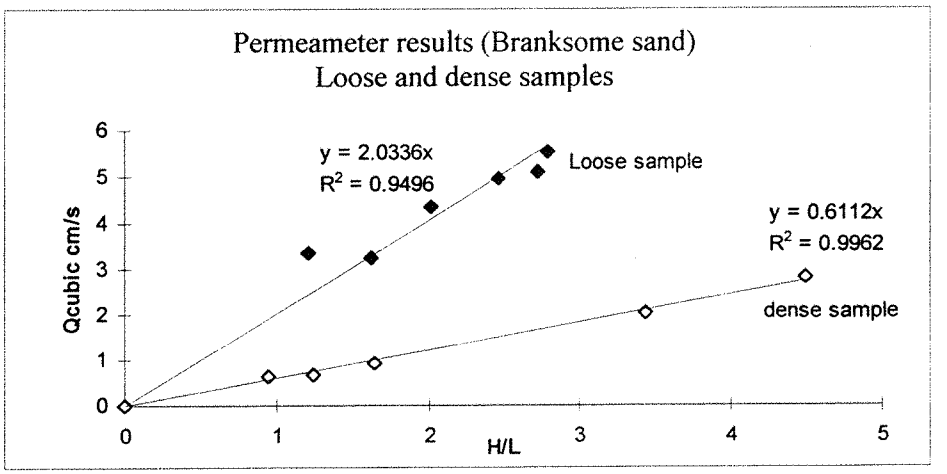

Figure 3.7: Permeameter data plot: Sample A (removed from 0.05m below the surface of the beach between groynes A and B)

The permeability was obtained using the Darcy equation (see Chapter 2):

$Q = Aki$

where Q = the discharge, i = the hydraulic gradient (= head drop/flow path length), k = beach material permeability, and A = the cross sectional area.

The gradient, m, for the graph in Figure 3.7 is equal to the product Ak in the Darcy equation:

$m = Ak$, hence

$k = m/A$, where A is the cross sectional area of the permeameter cell, and is equal to $45.36cm^3$.

The average permeability for the samples tested in a dense state was approximately 0.4×10^{-3} m/s.

Alternative method for permeability estimate

For uniform sands the permeability may be estimated from the D_{10} value (the largest particle size in the smallest 10% of the sample). This was carried out as a check:

$k = 0.01x\ D_{10}^2$

From the average PSD, $D_{10} = 0.18mm$, hence $k = 0.33 \times 10^{-3}$ m/s

Soil classification

The PSD data were used to calculate the following soil classification parameters, which were then compared to the Unified Soil Classification System, (Wagner, 1957 – see e.g. Craig, 1995).

- **Uniformity coefficient, C_U: $C_U = D_{60}/D_{10}$**

If $C_U<10$, then the sample may be regarded as uniformly graded. The higher the value of C, the greater the range of particle sizes.

- **Coefficient of curvature, C_Z: $C_U = (D_{30})^2/(D_{60} \times D_{10})$**

  If $1<C_Z<3$, then the sample may be described as well graded.

A summary of results is shown in Table 3.2.

Test Code	Sample Point	Depth Sample was taken from (cm)	Measured permeability (dense sample) (m/s x 10^{-3})	Theoretical permeability using D_{10} value (m/s x 10^{-3})	D_{10}	D_{30}	D_{60}	C_U	C_Z
A	1	5	0.14	0.31	0.175	0.235	0.31	1.77	1.02
B	1	45	0.38	0.31	0.175	0.22	0.29	1.35	0.95
C	2	5	0.34	0.31	0.175	0.205	0.26	1.48	0.92
D	2	45	0.61	0.44	0.21	0.265	0.35	1.67	0.96
E	2	75	0.43	0.32	0.18	0.245	0.31	1.72	1.07

Table 3.2: Summary of results

Results show that there is some variation in particle size and permeability with depth, which is approximately a factor of 1.5. In summary, the Branksome Chine sediment is a uniformly graded medium sand.

3.2.3 Beach slope

Figure 3.8 shows a typical cross section of the beach. The profile was recorded down the centre of the section of beach between groynes A and B during a period when the drainage system was not operating.

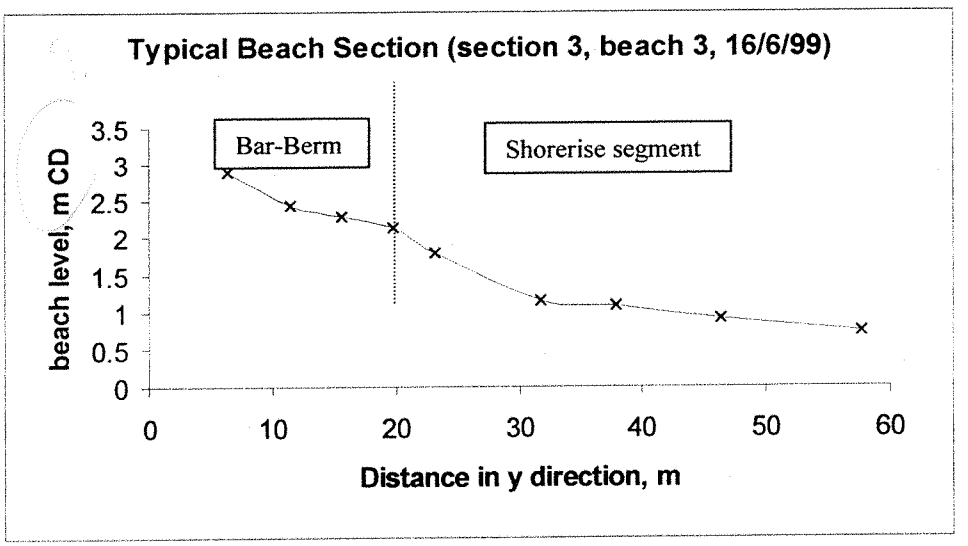

Figure 3.8: Typical Branksome Chine beach profile

The profile represents a compound profile, whereby two separate segments can be identified. The crest of the berm denotes the boundary between the two segments (Inman *et al.*, 1993).

For the section shown in Figure 3.8, the shorerise segment gradient is approximately 1/25, and the bar-berm segment has an average gradient of approximately 1/15. The beach drains were installed in the shorerise section of the beach (i.e. the part of the beach seaward of the berm). Equilibrium profiles are discussed further in Chapter 5.

3.2.4 Design pump rate

The following section describes how the seepage rate and system yield were estimated for the purpose of pump selection.

The seepage pattern around the beach drainage system is potentially complex, and it would be difficult to define the exact location of the phreatic surface, particularly during wave operation. To obtain an estimate of the typical system discharge three methods have been used:

- a simplified flownet sketch
- a more complex flownet produced by the Danish Geotechnical Institute (DGI)
- comparison of discharge rates from previous studies

The analysis below was carried out for practical purposes during the project design phase. After installation, the actual flow rates were recorded using a chart plotter. The actual and theoretical flow rates will be discussed in further detail in Chapter 6.

Flow net sketch

The flownet was sketched according to the conventional rules (e.g. see Powrie, 1997), with the following assumptions:

- The beach surface is horizontal
- The beach is completely flooded
- The still water level is maintained, and is level with the surface of the beach
- For simplicity, the theoretical beach drainage system consists of one pipe
- The flownet is assumed to be symmetrical about the beach drain
- The drain cover depth is 0.8m, and the depth to impermeable material is 1m

The following points should be taken into consideration:

- It is not known whether the water level is maintained when the beach drain is in operation
- The deepest samples were taken were from 45cm, however, it is possible that the sand at a depth of 1m (the likely drain installation depth) may be finer, coarser or more compacted.
- Samples tested in the laboratory to determine the permeability coefficient, k, were disturbed, and properties may vary to those of the *in* situ sample.
- The *in situ* sand may also have differing horizontal and vertical permeabilities that are not accounted for in the permeameter
- In the field the beach is subject to head fluctuations due to the tide. Hence the actual flow rate will oscillate according to the tide level.
- The beach slope is 1/18, and this will affect the flow path length (this has been approximated to horizontal, since 1/ 18 = 0.056)
- Head losses on entry to and exit from the pipe are unknown, and have therefore been estimated
- In the field the exact depth to impermeable material is unknown, however, the beach sand is known to overly layers of fine silt, and this material is likely to be effectively an impermeable boundary.

The flownet sketch used to estimate the seepage rate is shown in Figure 3.9.

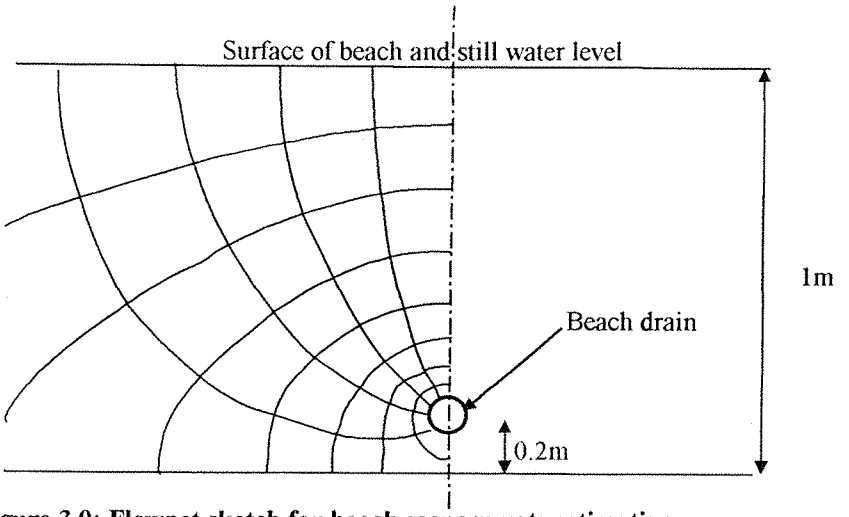

Figure 3.9: Flownet sketch for beach seepage rate estimation

The seepage rate is given by the following formula (see e.g. Powrie, 1997):

$q = H \cdot k \cdot N_F/N_H$

Where: q = flow per metre width of beach; k = permeability of beach material; H = total head drop; N_F = number of flow tubes; N_H = number of head drops

$N_F = 5 \times 2 = 10$

$N_H = 8$

e.g. $q = 0.8 \times 0.4 \times 10^{-3} \times (10/8) = 0.0004\ m^3/s$

= 40l/s per 100m run of pipe = 1.44 m^3 per hour per metre of system.

This simplified analysis was carried out to obtain an estimate of the flow rate for design purposes. In chapter 6, discharge calculation will be discussed in greater detail, and flow rates will be calculated for a range of tide levels.

Figure 3.10 shows a more complex flownet sketch prepared by the Danish Geotechnical Institute (DGI). The sketch does not conform to the conventional rules of flow net sketching, and it is highly unlikely that under wave action the beach drainage system will cause a significant draw down curve.

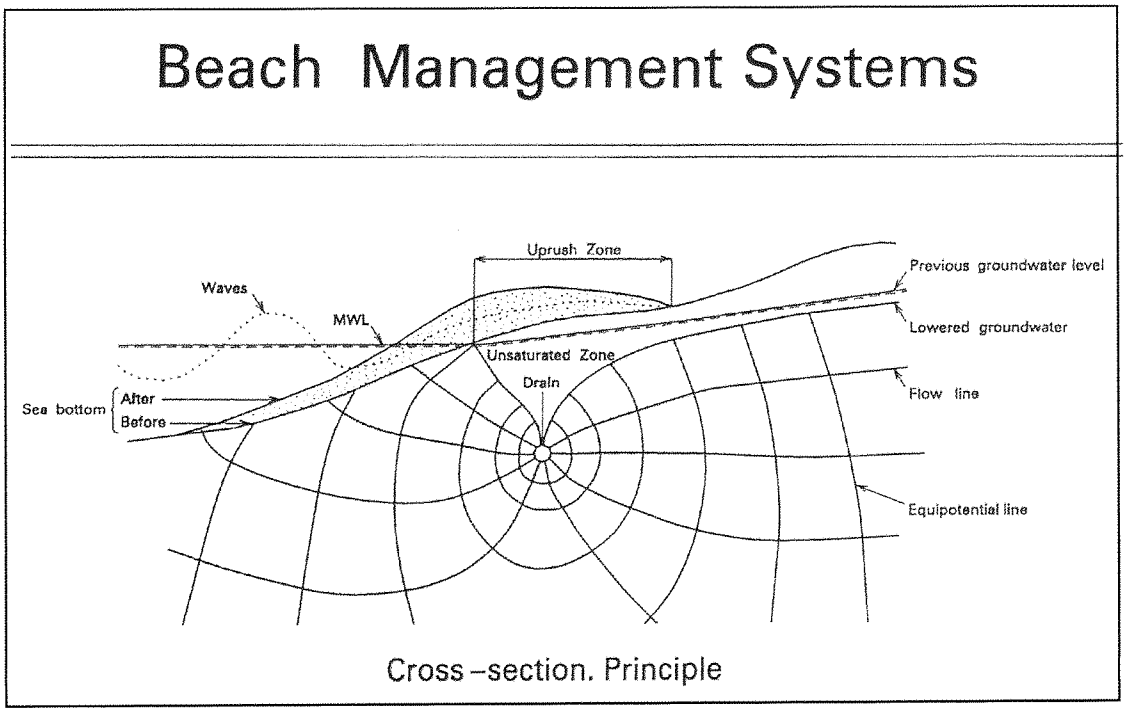

Figure 3.10: Beach drainage flownet sketch (Vesterby, 1996)

In this sketch it can be seen that the ratio of flow tubes to head drops is approximately 9:7, which is similar to the ratio obtained with the simplified diagram above. The seepage rate using the ratio 9/7 and the same head and permeability as above yields a seepage rate of 1.48 m^3 per m per hour.

Thus it can be seen that the seepage rate is likely to be in the order of 1.4 to 1.5 m^3 per hour per m. This is still likely to be an overestimate due to the assumptions noted above.

Assuming a 25 to 30% head loss (for example) on entry to the pipe, the anticipated seepage rate would be in the order of 1.1m^3/hr per metre run of system.

In Chapter 2, Table 2.1, it can be seen that typical initial flow rates for previous full scale systems range from 0.1 to 3.2 m^3/hr per m, while sediment sizes range from D_{50}

= 0.2 to 1.5mm. Figure 3.11 shows a graph of measured initial discharge against sediment size for the full scale data presented in Table 2.1 (Chapter 2).

Although the data are scattered, the trendline suggests that there is a reasonable correlation between D_{50} and discharge. The graph does not account for the fact that several of the full scale systems are likely to have slightly different cover depths and tidal regimes, and these may affect the measured flowrate. This may explain the scatter in the data shown in Figure 3.11.

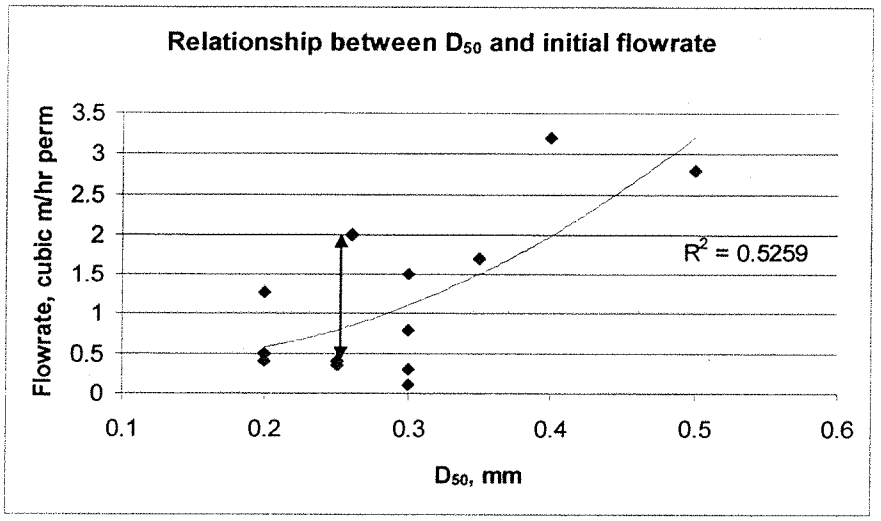

Figure 3.11: Graph to show the relationship between D_{50} and discharge.

The mean D_{50} sediment size for the beach at Branksome Chine is 0.25mm, and from Figure 3.11 this corresponds to a flowrate of approximately 0.8m^3 /hr per m (due to the data scatter a range of 0.4 to 2m^3/hr is not excessive).

In light of the above findings, it was anticipated that the drainage system would yield approximately 0.8 to 1.1 m^3/hr per m. This estimate has been based on theoretical considerations, an assumed 25 – 30 % headloss, and flow rates measured from previous trials.

In section 3.2.2 it was noted that the permeability varied by a factor of approximately 1.5, therefore this will also affect the discharge ($q \propto k$).

Pump capacity

Table 2.1 (from Chapter 2) shows that typical pump capacities for previous full scale systems range from 0.4 to 4.5 m^3 per hour per metre.

Due to the limitations of a single phase power supply and financial constraints, the maximum possible pump capacity was 0.65m^3 per hour per metre of system (two pumps with a maximum pump rate of 9 litres per min each). This is considerably less than the anticipated flow rate, and it was initially thought that this might pose a limitation on system performance.

Pump calibration

During the trial a chart plotter was connected to the pump control panel. The chart merely indicated when the pump was off or on, and did not provide a reading for the actual flow rate from the drainage system. The pump charts did not record head, so this had to be assumed. Prior to installation the pumps were tested to determine the head discharge relationship, so that the flow rate could be deduced from the pump charts and assumed head.

The flow rate from each pump was recorded for a range of pressure heads (H) using the apparatus shown in Figure 3.12. The valve was used to alter the pressure head in the pipe and Q was measured with an ultrasonic flowmeter. Figure 3.13 shows the measured relationship between discharge, Q, and head, H for each pump. In the field, the head depends on the water level in the sump, and this fluctuates according to the water table and tide level. This issue is discussed later in this chapter.

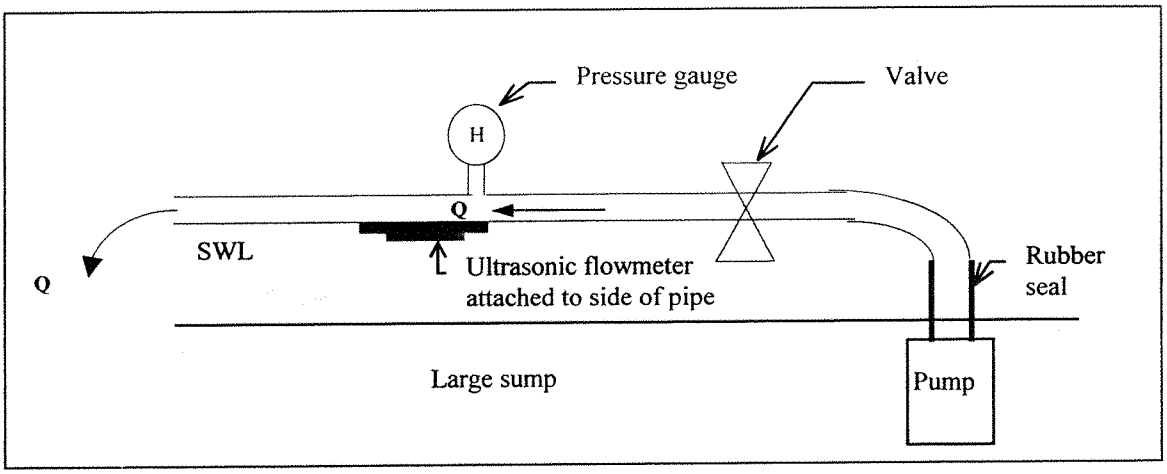

Figure 3.12: Pump testing apparatus

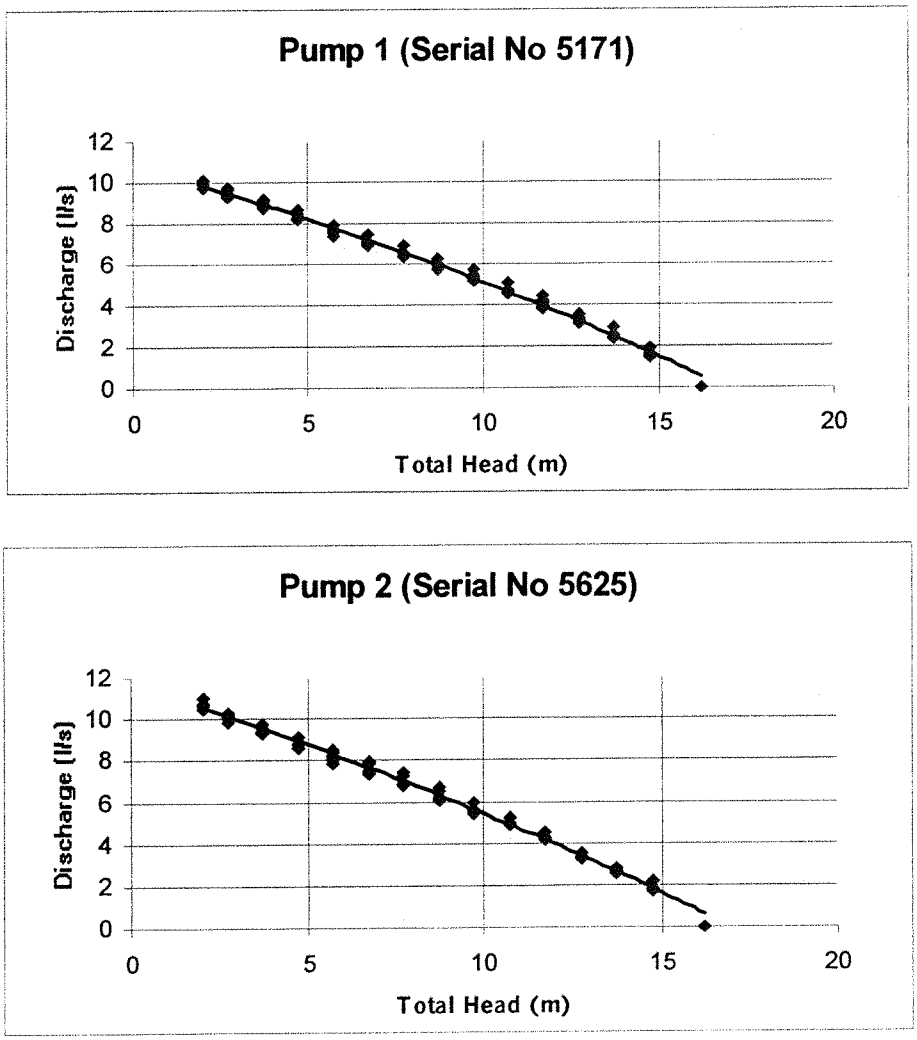

Figure 3.13: Head-discharge relationship for Branksome Chine pumps

Figure 3.13 shows that the actual pump rate is approximately 10 litres per second for a minimum head of two metres. Hence for two pumps, the maximum flow rate would be approximately 20l/s.

The pump on/off switch is activated by a depth gauge in the sump, (set at a depth of 2.5m). The depth gauges and four pipe inlets can be seen in Figure 3.14, which shows the inside of the Branksome Chine sump.

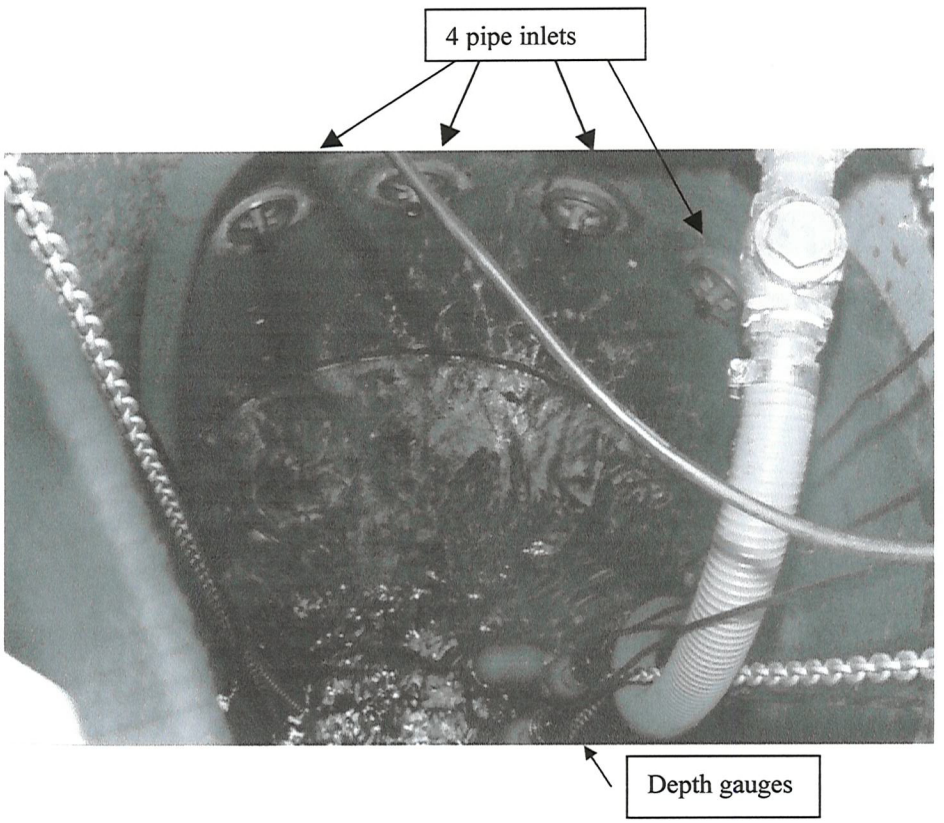

Figure 3.14: View down Branksome Chine sump

Flow rate will be discussed in further in section 3.4.3, and Chapter 6.

3.2.5 Additional considerations

Power supply

System design was limited by the single phase power supply. This restricted the pump capacity (discussed above), and hence the maximum system length. A three phase supply would have allowed the use of more powerful pumps, but this would have been expensive to provide since it is not available in the vicinity of the trial beach. It will be shown later in this chapter that the measured flow rate during operation was less than that previously calculated, so that pump capacity was not in the event a limiting factor.

Pipe length

The pipe length could not be longer than approximately 100m due to the groyne spacing, since it would be too expensive to span the system across more than one groyne bay. A larger system would also have required larger pumps and possibly a three phase power supply, thus substantially increasing the cost.

Previous trials have tended to use a minimum system length of 200m, and the Branksome Chine system was the shortest full scale installation to date. The minimum length requirement for an effective system is not yet known, and it is possible that length may be a limiting factor in terms of system performance.

Number of pipes

Four pipes were installed to investigate the effect of different drain locations on performance. During the trial several pipes were damaged, and parts were broken and removed from the beach. Hence it was not possible to investigate different combinations of the pipes, since it was necessary to use the pipes remaining.

3.3 System design and installation

The preliminary design was based on a typical Danish Geotechnical Institute (DGI) Beach Management System. The system consisted of 4 slotted PVC drainage pipes, and wrapped in a felt geotextile. Initially only two pipes were in operation, and it was intended to explore the effect of pipe location by shutting off different pipes for given time periods. However, it is later shown that parts of the system were damaged, and the investigation into pipe location was abandoned.

The drainage pipes were 100m long and installed approximately 1m below the surface of the beach. The pipes were laid parallel to the shoreline, approximately 1/3 of the distance from the low water mark to the high watermark (this location relative to the low and high water marks was recommended by the Danish Geotechnical Institute). The pipes drained by gravity to a sump and a submerged pump was used to discharge the collected water via an outfall back to the sea (in other trials the outlet has sometimes been used for a bathing pool, aquarium or salt water lagoon). Figure 3.15 shows a schematic diagram of the installed beach drainage system. For reference, the concrete groyne is the groyne labelled A in Figure 3.4.

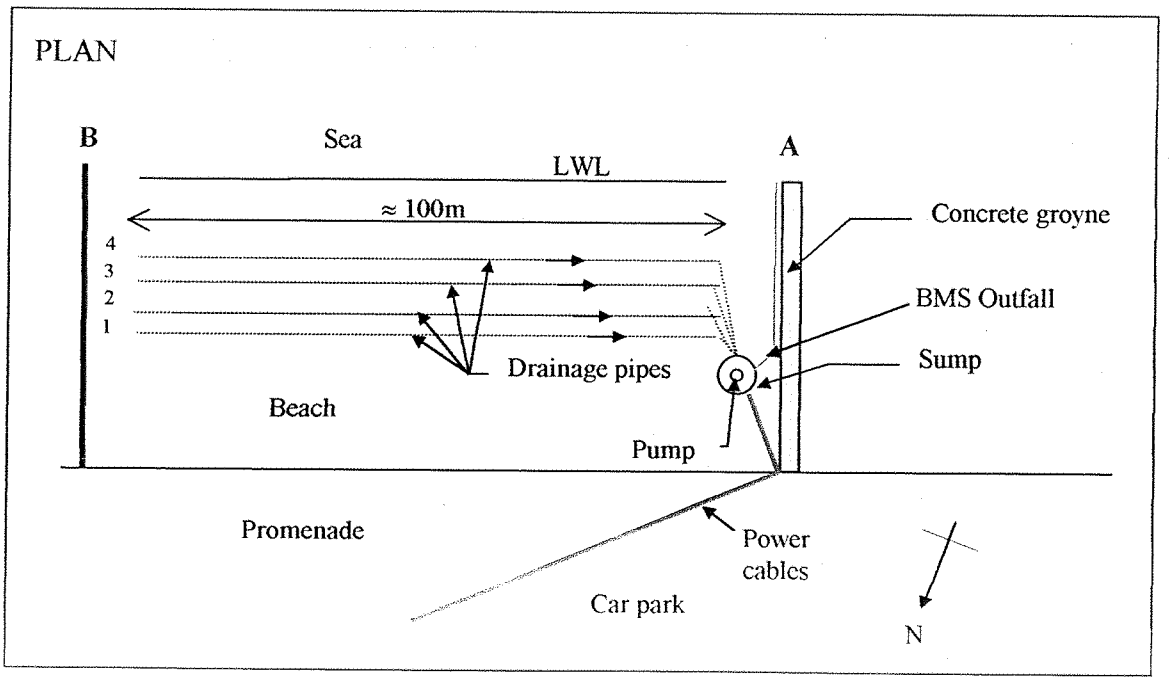

Figure 3.15: Schematic diagram of final system layout

The drain pipe used for the Branksome trial is shown in Figure 3.16. Installation was carried out during low water: a backhoe was used to dig a trench, in which the pipe was laid prior to back filling. This is illustrated in Figure 3.17.

The pipes are labelled 1 to 4 with pipe 1 being the nearest to the promenade as shown on Figure 3.15. The white lines marked on the edge of the concrete groyne in Figure 3.18 indicate the positions of the four pipes. The approximate pipe locations are 27m, 25m, 23m and 21m from the bottom of the flight of steps on the concrete groyne. These steps can be seen in Figure 3.20.

Figure 3.16: Drainage pipe ready for installation

Figure 3.17: Installation of beach drainage pipe

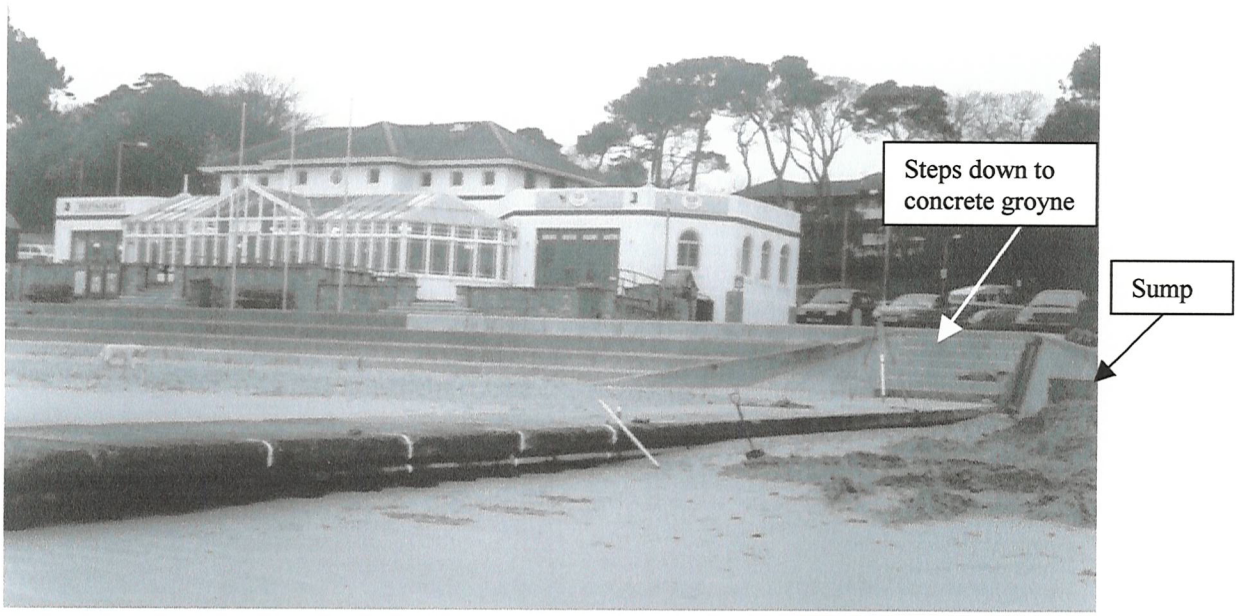

Figure 3.18: White marks on concrete groyne indicate the pipe locations

The pipes were installed so as to drain by gravity to a sump located in the west end of the groyne bay, near to the foot of the sea wall (Figure 3.18). Power cables were enclosed in a plastic pipe, which was laid under the car park to the control room (see Figure 3.15). The pump outlet was attached to the side of the concrete groyne (Figure 3.19) and allowed to discharge out to sea.

Figure 3.19: Sump outlet being fixed to the concrete groyne

3.4 Monitoring techniques and data collection

The scope of the project was outlined in section 3.1.3. The methods used for investigating each area of study are summarised in Table 3.3 below:

Area of Study	Monitoring Technique
Effect of drainage system on beach profile	Survey, field observations, photographs
System discharge	Pump cycle plotter and chart in control room
Influence of weather and wave regime	Local records
Influence on existing defence works	Field observations, photographs

Table 3.3: Monitoring techniques for selected study areas

3.4.1 Beach survey

Data collection

Beach levels were recorded between the foot of the sea wall and the low water mark along a 500m stretch of beach. Five groyne bays were selected for survey; the drained section, and two undrained groyne bays on either side. The bays were labelled 1 to 5, and each section is referred to as a 'beach'. These are shown in Figure 3.20. During the summer, surveys were carried out approximately monthly. For the remainder of the year the weather patterns and beach profiles were more dynamic and the surveys were carried out fortnightly.

A local grid was set up where the co-ordinate (0,0) was the centre of the landward end of the concrete groyne A. The x and y directions and (0,0) are indicated on the schematic diagram in Figure 3.20. Two survey stations were necessary, and these were set up on the promenade. Station A was located at (0,0), while station B was at (250.78, -20.16) metres: these are indicated in Figure 3.20.

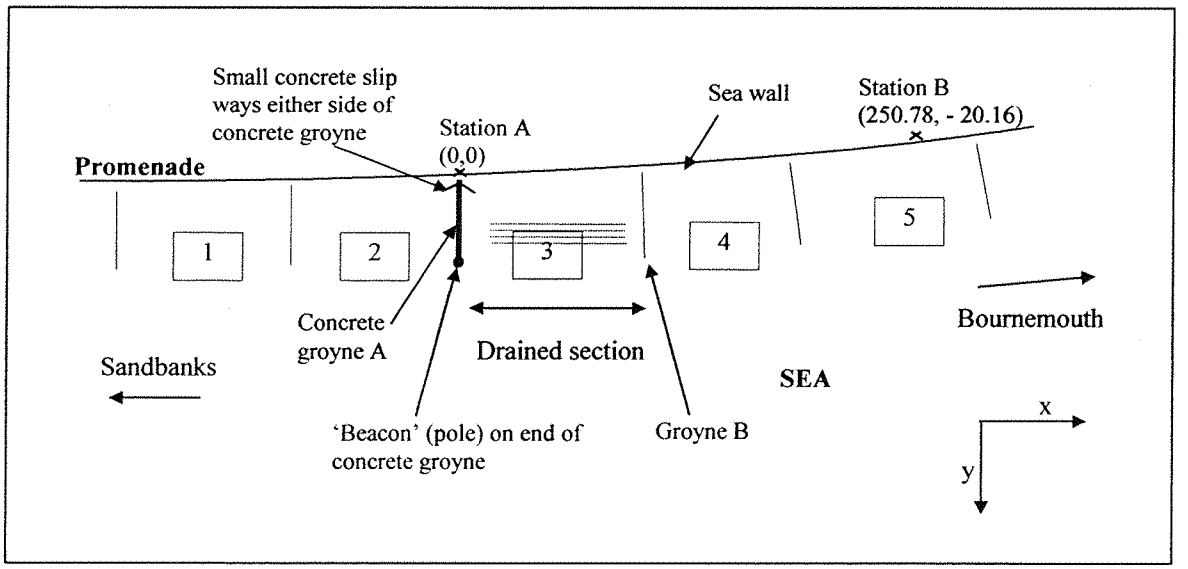

Figure 3.20: Schematic diagram of control beaches and drained section

A diagram detailing the location of (0,0) - survey station A - is shown in the field book extract in Appendix C. Data points were recorded at irregular intervals across the beaches depending on the amount of detail required. A typical data collection sheet is also shown in Appendix C.

Table 3.4 shows the survey dates, together with notes indicating when the system was in operation.

SURVEY NUMBER	DATE	NOTES	PHASE	
1**	6/5/98	Setting out	1	
2**	9/6/98	Survey before system is switched on. Survey #2	1	
3	7/7/98	First survey after pumps were switched on. Survey #3	1	← Pumps switched on
4	22/7/98	-	1	
5	4/8/98	Survey #5	1	
6	18/8/98	Survey #6	1	
7	3/9/98	Survey #7	1	
8**	17/9/98	Survey #8 System out of Operation due to siltation of the sump	1	← System damaged
9*	5/10/98	Survey #9	1	
10*	19/10/98	Survey #10	1	
11*	2/11/98	Survey #11	1	
12*	16/11/98	Survey #12	1	
13*	30/11/98	Survey #13	1	← New Installation
14	16/12/98	First survey after phase 2 pipes were installed. Survey #14	2	
15*	10/2/99	Survey #15: First survey after second installation. System known to be damaged for a second time	2	
16*	23/2/99	Survey #16 (station A readings invalid).	2	

Key:
*** System thought to be damaged. (Still working, but reduced efficiency)**
**** System thought to be out of operation**

Table 3.4: Survey Dates and system operation status

Survey data were entered into a spreadsheet and converted to (x,y,z) co-ordinates on a local grid. z = the level of the beach at (x,y) above chart datum (CD). Matlab was used to convert (x,y,z) co-ordinates into a 3D representation of the beach, and the 3D graph for each survey was then projected onto the horizontal plane to give a plan view and contour map of the survey area. A sample command sequence is shown in Appendix C.

A typical survey data plot is shown in Figure 3.21.

3D Graph

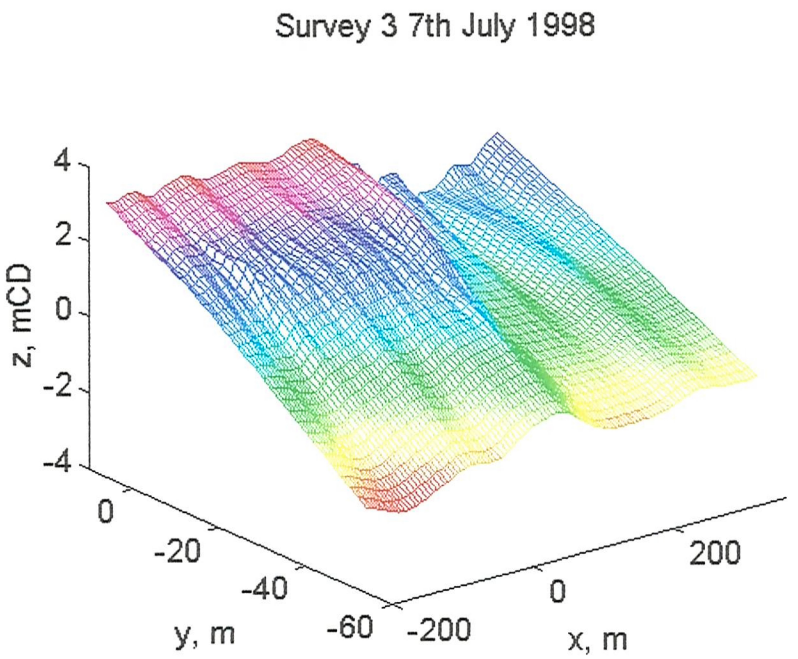

PLAN

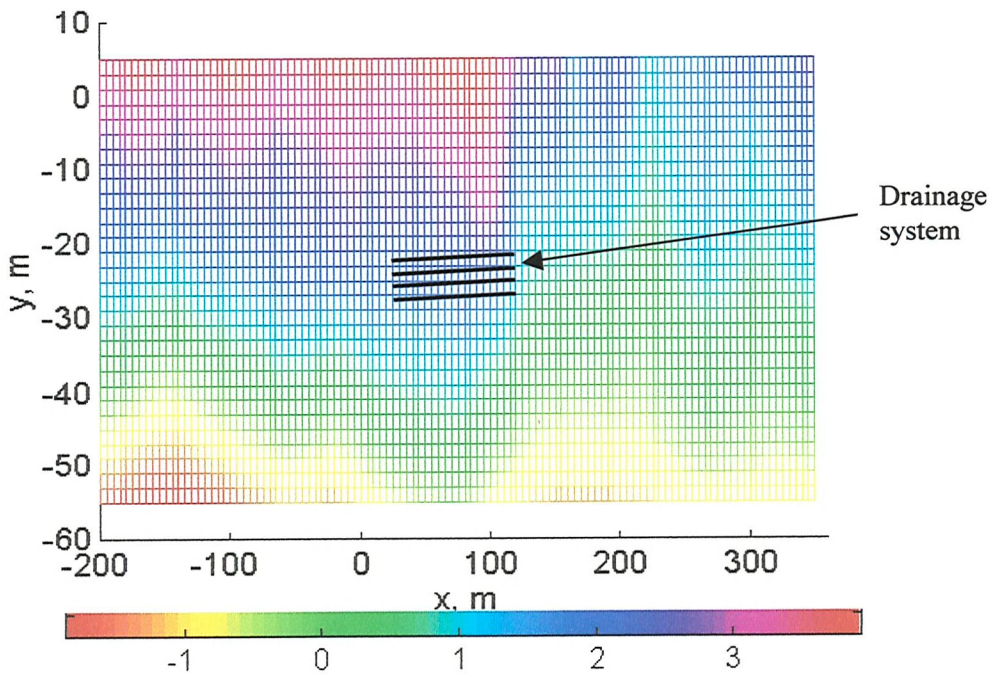

Figure 3.21: Typical processed survey data for Branksome Chine, 3/7/98 (colour bar indicates beach level in metres above chart datum). Drain was in operation when survey was carried out.

3.4.2 Weather data

A record was kept of the daily weather conditions in the local area. Information was recorded from the Sandbanks beach office (approximately 3 miles west of Branksome Chine) during autumn and winter and from Branksome during the tourist season. Data were recorded by the Borough of Poole Beach Inspectors (lifeguards) who are trained to estimate variables such as wave height and wind speed. A typical weather data collection sheet and a list of the raw data are given in Appendix E.

The data were estimated by observing nearshore conditions, and wave heights are likely to be affected by the proximity of the Isle of Wight and Isle of Purbeck (Figure 3.1).

3.4.3 System discharge

A chart plotter was installed in the pump control room to record the cycle of each of the two pumps. A typical section of the pump chart is shown below in Figure 3.22.

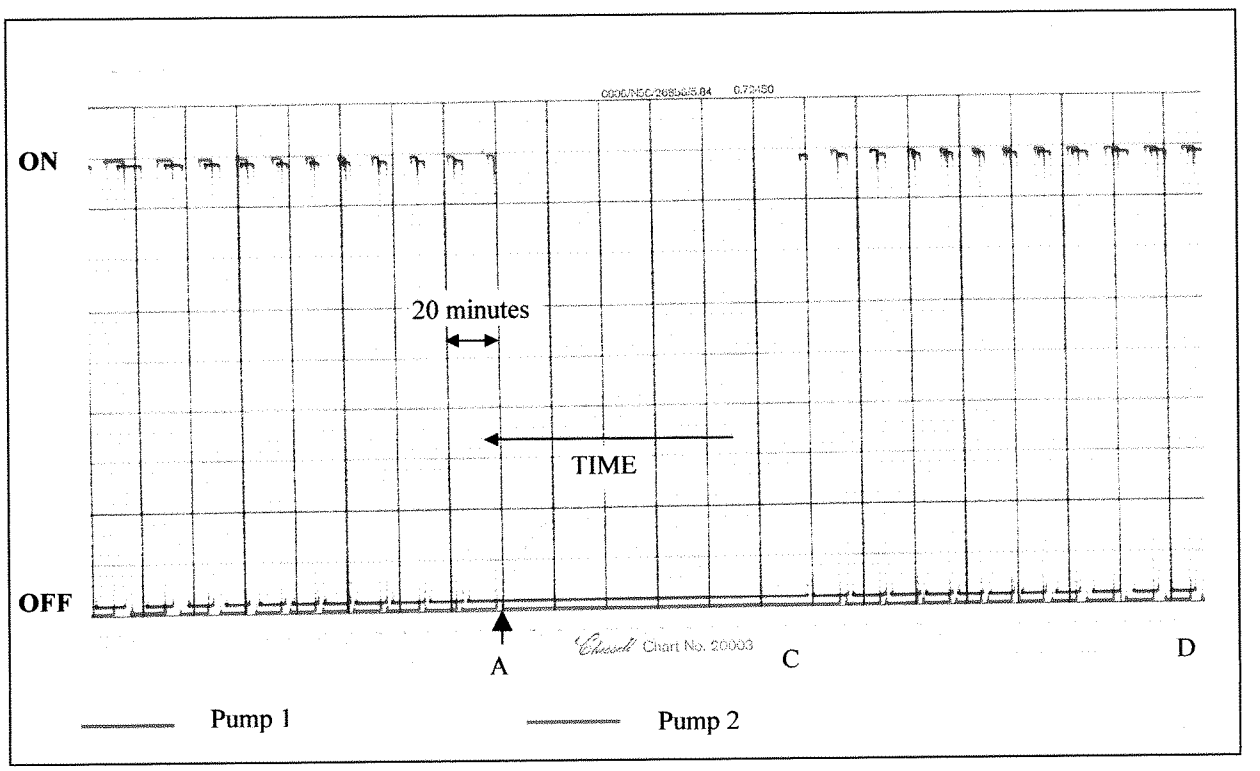

Figure 3.22 Section of pump chart (not to scale)

Each centimetre on the pump chart is the equivalent of 20 minutes. The date and time were marked on the beginning of the chart roll each time the roll was changed.

The corresponding tide chart for this period is shown in Figure 3.23.

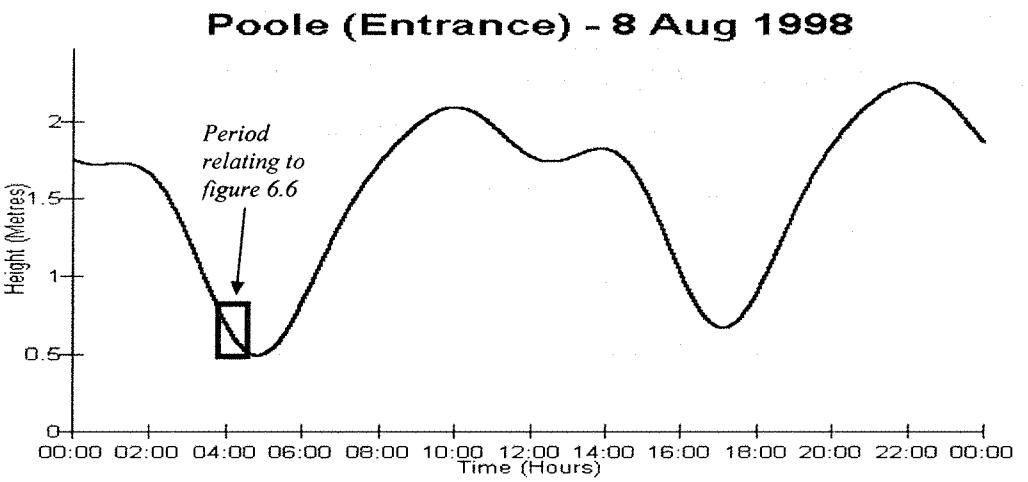

Figure 3.23: Tide chart for 8/8/99 (reproduced with permission for examination)

The pump chart indicates whether the pumps are on of off, with no indication of the actual flow rate. To determine the system yield, the pump discharge rate has been read from the head-discharge curves shown in Figure 3.13, and this value has been multiplied by the proportion of time the pump was on for a given time period. The proportion of time each pump was switched on was calculated simply by counting the intervals on the chart plot. Hence the flow rate would be averaged over a short time period, and instantaneous flow rates could not be obtained. The pump controls were designed to switch on when the level in the sump was approximately 2.5m.

Head-discharge relationship

The pumps were switched on when the level in the sump was approximately 2.5m. Including head losses in the outlet and exit pipes (using the Darcy equation for head loss due to friction in pipes - see e.g. Hamill, 1995), the total head is calculated to be

approximately 3m. Hence reading from Figure 3.13, the discharge for pumps 1 and 2 are 9.4 and 9.9 litres per second respectively.

This pump rate was multiplied by the % of time the pump was switched on (read from the pump chart) to give an average flow rate for a given time period. It was possible to average the flow rate over a relatively short time period of 20 minutes, and this was repeated for several consecutive 20 minute periods to give a range of different discharges for different times during the tide cycle. The tide level was read from tide charts, and example of which was given in Figure 3.23 (Belfield, 1999), and this was converted to still water level location relative to the drainage system in the horizontal plane using the beach slope (see section 3.2.3)

3.5 Results and discussion

3.5.1 Key project events

Despite the suspected system inefficiency in terms of discharge, the drainage system operated relatively effectively during the first two months of the trial. In September 1998 a period of prolonged strong winds and high waves affected the area, and a significant amount of material was lost from the beach. As a result, part of the system was damaged, and the effectiveness was considerably reduced. Further damage rendered the system out of operation, and in December 1998 the beach drains were re-installed and the sump was repaired. Further storms resulted in a second period of beach material loss and associated system damage. The pump rates for the second installation were significantly lower than those recorded initially. This is likely to be due to the new location (drains were installed further landward) and the loss of pipes due to system damage.

Table 3.5 summarises the important dates and events during the beach drainage trial.

DAY	MONTH	YEAR	ACTION
2	February	1998	***Preliminary site investigation:*** *Walkover survey.* *Collection of samples from different depths and locations to be tested for permeability.*
6	May	"	*Site visit - survey # 1*
12	June	"	*System switched on.* ***START DATE (phase 1)*** ***(a)*** *The drainage system flow rate is low in comparison to the theoretical value, and the discharges of previous trials.*
16	July	"	*Started collecting weather data* ***(b)*** *Survey data suggests that the system is having a positive effect on the beach profile. See survey data.*
29	July	"	*Installation of pump chart*
	August	"	*All beaches have relatively high levels of sand*

7	Sept	"	*(c) Some storm damage to drains identified on trial beach, and some of the pipes were exposed in places. This coincides with a period of poor weather (see section 3.5.3).*
10	Sept	"	*System known to be out of operation* *Removed manhole cover on sump to investigate.* *(d) Sump was filled with sand to beach level. This was due to a combination of high spring tides and storms. Sand may have been washed in through the manhole cover, which is not watertight, or through broken pipes.* *Pumps out of operation*
	Sept/Oct	"	*Sump cleared of sand. Pumps in operation again, but some pipes still damaged*
5	October	"	*The ends of three pipes were visible. A dry area over part of the landward drain indicated that some of the system was working. Some sections of the system are out of operation - assumed to be the lower (seaward) pipes. The damaged pipes have not been removed. General fall in all beach levels. Severe scour around groynes on beaches 4 and 5 (eastern control beaches). Damage perceived to be not as severe on drained beach*
2	December	"	*Recommendation to repair broken pipes before further storms occur.* *Pipes to be installed nearer to the high water mark (may be more effective if located on sloping section of beach, and less likely to be uncovered in storms.)*
3	December	"	*(e) Installation of new pipes. Installed* ***further landward*** *than previous pipes.* ***(Start of Phase 2)***
4	January	1999	*Storm damage to phase 2 system reported*
5	January	"	*(f) Site visit to investigate reported damage* *Beach levels fallen to lowest levels observed to date.* *Sump outlet was completely exposed with the beach level approximately 30cm below the outlet level. (See photographs later in this chapter for further evidence).* *Sump silted up to beach level once again. The concrete seal around the inlet for the pipes containing pump power cables was damaged*

			and a hole had appeared in the side of the sump. Most likely cause of siltation of sump. *Evidence that the system has been working, although it was found to be out of operation at the time of visit. A 'bump' or berm had formed on the drained beach, which was not visible on the control beaches (no survey available: photographs taken).*
Mid	January	"	*Pipes exposed - not known if old ones or new ones have been uncovered and washed up.* *A number of repairs were carried out, but the lost pipes were not replaced. Unknown which pipes have been removed or damaged. The sump was cleared and the pumps repaired. Shortly the sump filled with sand once again. This happened twice during this period. System not in operation.*
26	January	"	*Site visit to inspect reported damage and repair work.* *Beach levels recovered to an extent*

Table 3.5: Important project events

The project may be subdivided into three phases:

Phase 1: The first installation of a four pipe system was labelled phase 1 of the Branksome trial. This period is from February 1998 to December 1998, and is covered by survey plots 1 to 14.

Phase 2(new pipe location): A period of bad weather during early September caused extensive damage to the phase 1 drainage system (shown by large wave heights in Figure 5.23). The three lower pipes were damaged beyond repair and only the landward pipe remained intact. A new set of pipes was installed on the 3rd December 1998. The landward pipe from the phase 1 installation became the seaward pipe of the phase two installation. as shown in Figure 3.24.

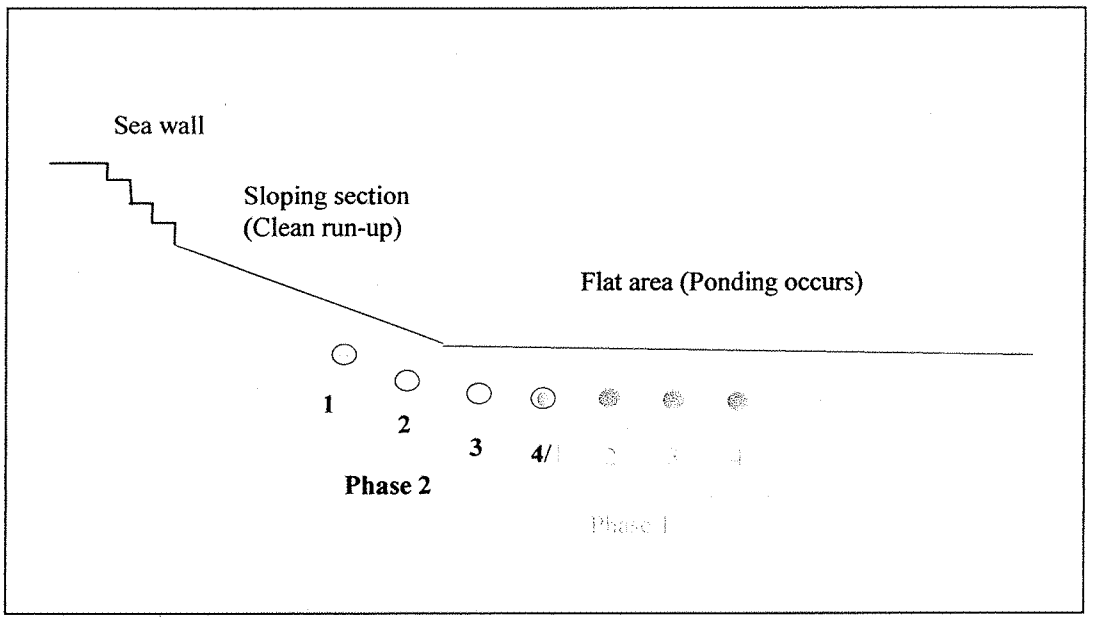

Figure 3.24: Schematic profile of the beach at Branksome (not to scale and with vertical exaggeration)

The pipes were installed further landward mainly to reduce the risk of damage during storms. The new pipes were also located on a more steeply sloping section of the beach, as opposed to the flat area as shown in Figure 3.28. On the flat section of the beach, ponding occurs during part of the tide cycle. During this time, the water is between ankle and knee deep, and the backwash moves over this depth of water instead of running down the surface of the beach.

In Chapter 2 it was noted that two of the possible mechanisms of beach stabilisation through drainage are backwash volume reduction and laminar flow phase extension. With ponding occurring, any further reduction in the backwash volume caused by the drain (in the phase 1 location) would be insignificant compared to this depth of water. Locating the pipes on a sloping section of the beach above this ponding area would allow for a 'clean' run up whereby the wave runs up over the sand, reaches a limit, then moves back down the sand surface with minimum interference from the next incoming swash. Further explanation of this theory will be presented in Chapters 4 and 8.

As discussed later in this chapter, the new pipe location resulted in a lower discharge rate, which led to reduced effectiveness. The phase 2 system was also damaged by prolonged storms, which affected the system performance. Therefore it would appear that any benefit gained by moving the pipes out of the ponding area was countered by the reduced discharge and storm damage.

Phase 3 (future installation): Consideration has been given to a full scale installation at Branksome Chine. The installation of such a scheme depends on several factors and will be considered in greater depth at a later date, outside the scope of this thesis.

3.5.2 Survey data

Graphs for surveys 2 to 11 are enclosed in Appendix D (there are no data for surveys 1 and 4 as noted in Table 3.4).

Survey Data

Data for surveys 2, 3 and 5 are shown in Figure 3.25a. The beaches are shown in plan, and the drained section is from x = 0 to x = 100 (beach 3). Beach 2 (control beach) is from x = -100 to x = 0, and beach 4 (control beach) is from x = 100 to x = 200. The colour bar indicates the level in metres above chart datum.

In the graph for survey 5 the groyne locations are indicated by a zigzag pattern of levels across the beaches. This occurred due to scour on the east side of the groyne and accretion on the west side and is particularly apparent at x = 0, x = 100 and x = 200 (this is where the groynes are located), and indicates long-shore drift (west to east).

Comparing survey 2 (June 9 1998) with survey 3 (July 7 1998), it can be seen that the beaches either side of the drained section experienced a loss of material on the lower part of the beach, while the beach levels in this area on the drained beach were maintained. The photograph shown in Figure 3.26a was taken on the same day as survey 3 (7/7/98) and also shows a raised area on the lower part of the drained section. A 3-dimensional graph of the survey 3 data was shown in Figure 3.21, which also shows the bump on the lower section of the drained beach.

After survey 3 all the beaches experienced an increase in level and there is little difference between the drained and control sections (see survey 5, Figure 3.25a).

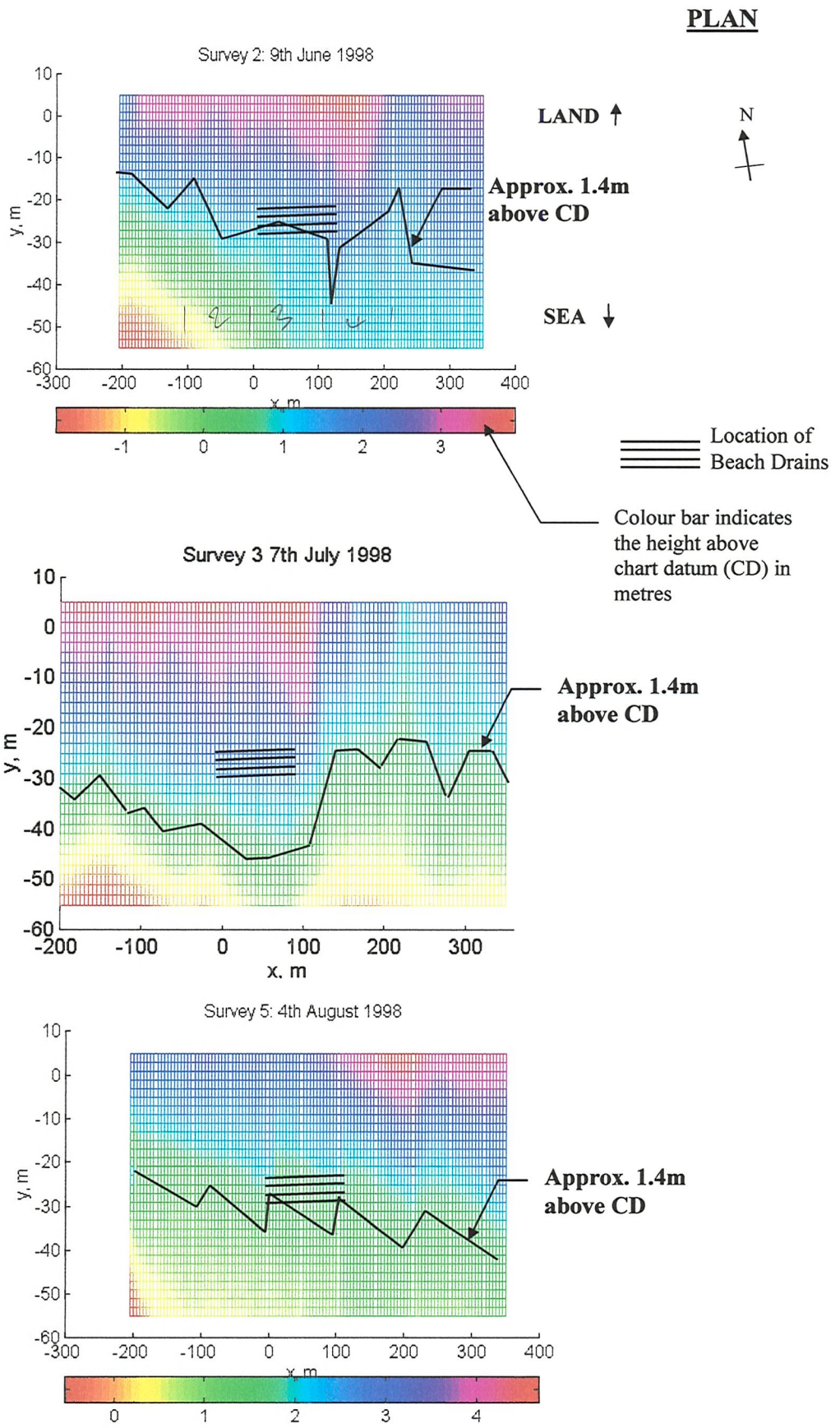

Figure 3.25a: Data for surveys 2, 3, and 5

On the 3rd September site visit observations and survey data revealed evidence of erosive conditions, although the system was still fully operational at the time of the visit. Coarse material had been deposited onto the upper beach, including whole shells and small pebbles, not normally present on the beaches at Branksome Chine.

The survey data also indicate the effects of erosive conditions as shown in Figure 3.25b. There is considerable material loss from the eastern control beaches, and the red areas at x = 100 and x = 200 indicate scour down the sides of the groynes which are located along these lines. This corresponds with a period of strong winds and large wave heights, which will be discussed in section 3.5.3.

The system was known to have been damaged shortly after survey 7, and as shown in the plot for survey 8 (Figure 3.25b), all beaches experienced a loss of material from September 3 to September 18. The effect of the drainage system can be seen to be reduced in the photograph shown in Figure 3.26b.

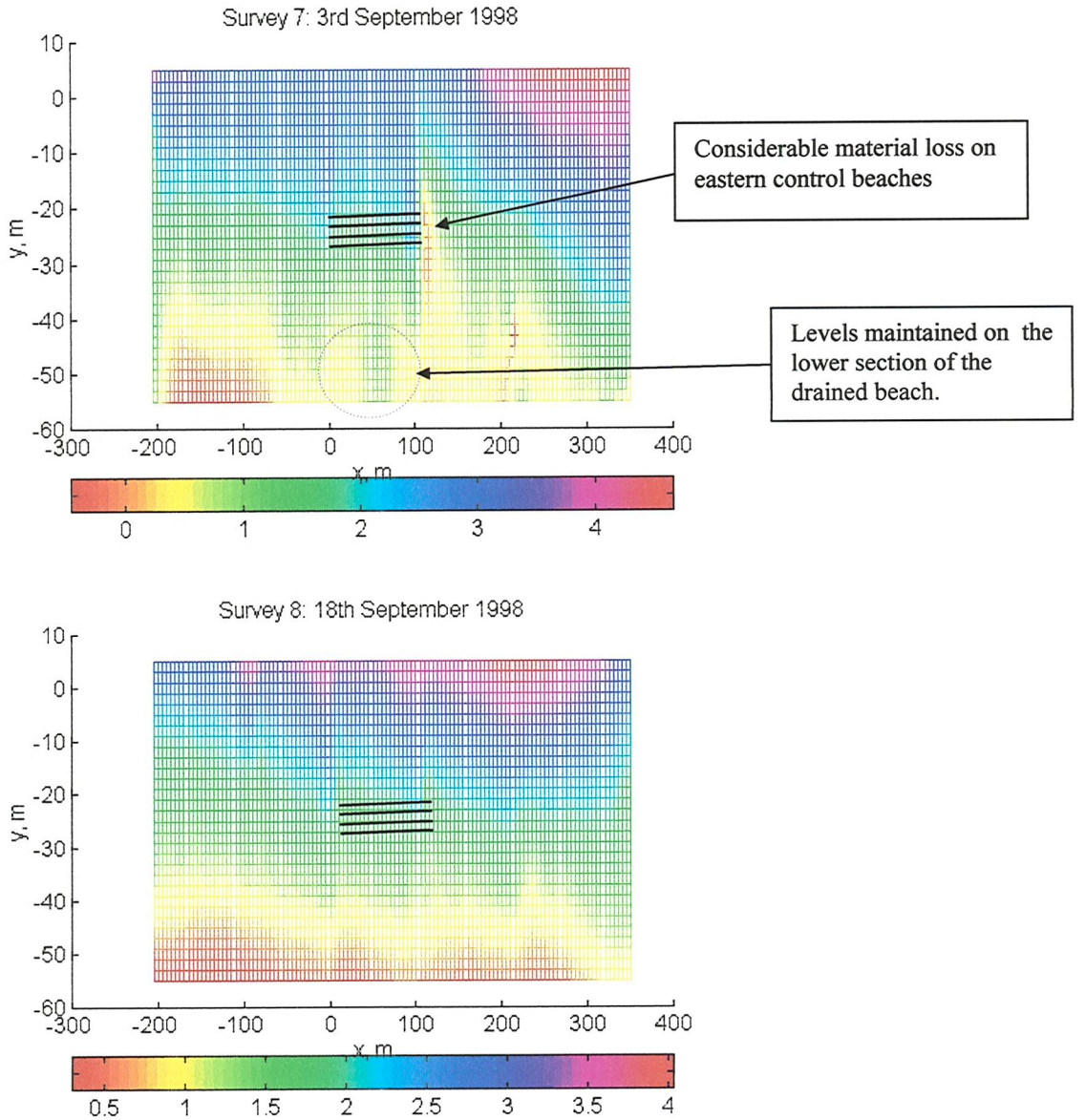

Figure 3.25b: Matlab plots for surveys 7 and 8. (Plan view – colourbar indicates the height above chart datum in metres).

Figure 3.26a: Photograph taken during survey 3, July 7 1998. System working efficiently

Figure 3.26b: Photograph taken on September 9 1998 shortly after storm damage to the system

3.5.3 Weather data

Wind direction

Figure 3.27 shows the frequency of occurrence of wind directions recorded at Branksome Chine and Sandbanks for a total of 236 days, from July 1998 to February 1999 (over the trial period).

The data show that the dominant wind direction is south-westerly, while southerly, south-easterly, and north-westerly winds are common. North-easterly and westerly winds are occasional, while northerly and easterly winds are relatively uncommon. With the most common wind directions containing an element of southerly, winds are frequently onshore or cross-onshore at Branksome. The area is sheltered from northerly winds by the local topography.

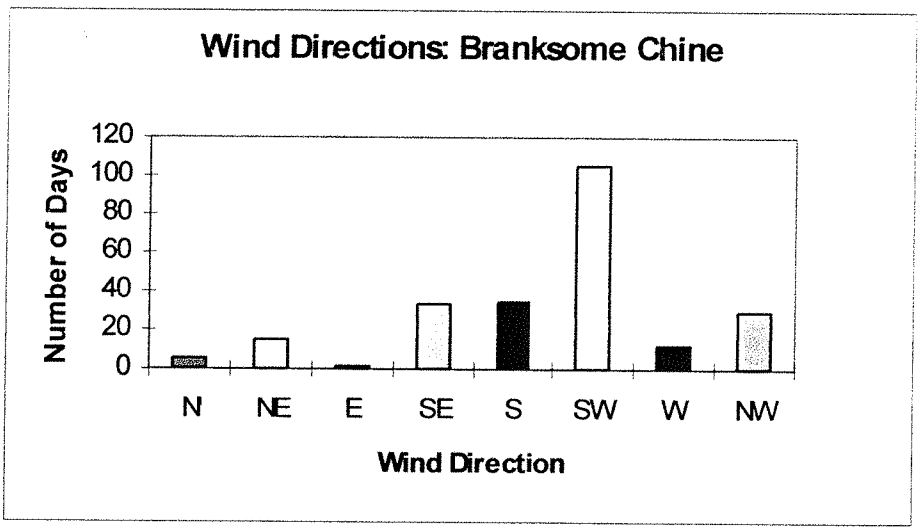

Figure 3.27: Bar chart to show the frequency of occurrence of wind directions

Wave height and wind strength

Figure 3.28 shows variation in estimated wind strength and wave height over time. The wind speed was estimated using the Beaufort scale (where each number relates to a physical observation related to strength), while the wave height was estimated in metres. The mean wave height is 0.45m, and the average wind speed is a Beaufort force 3. Raw data are shown in Appendix E.

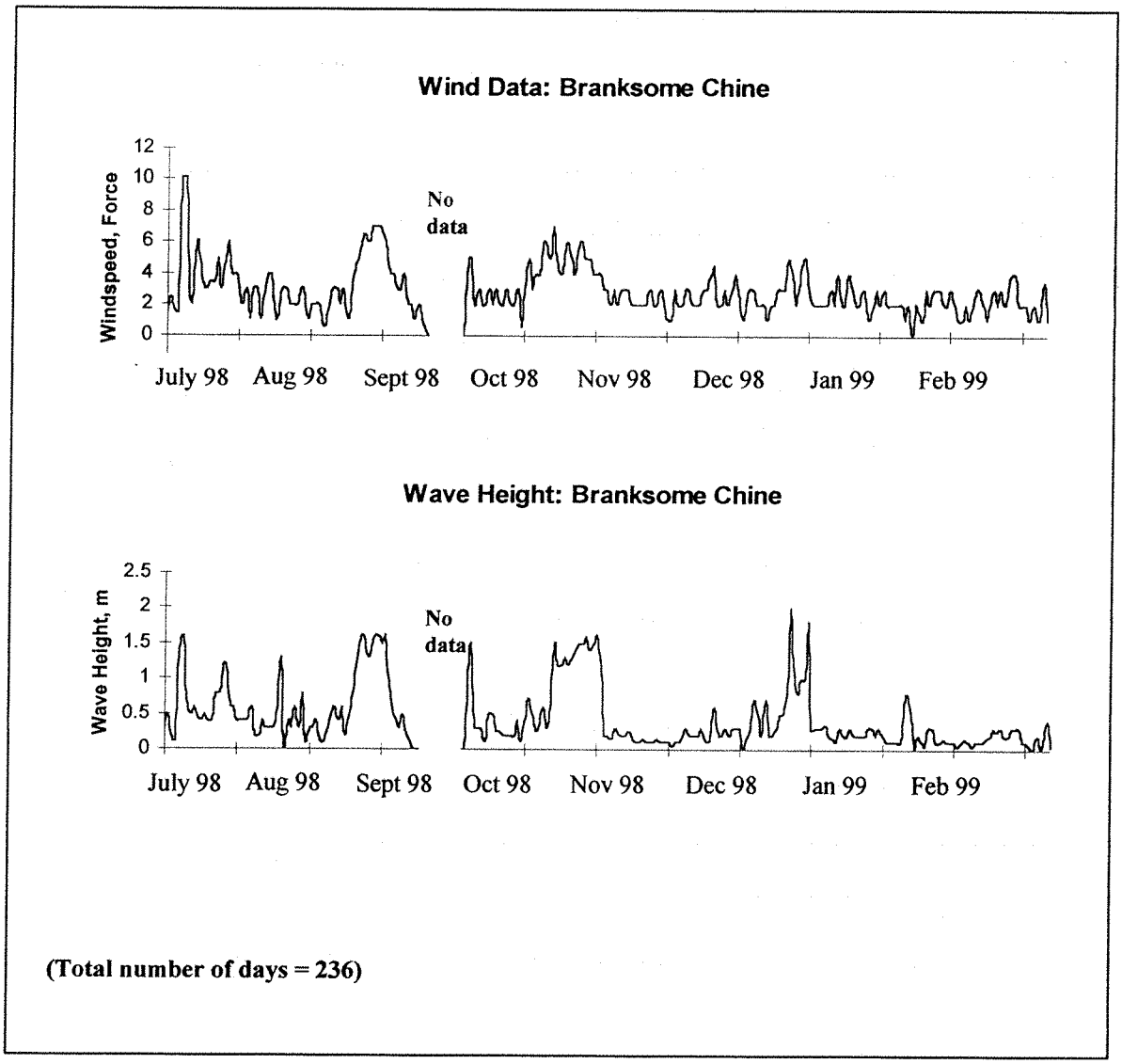

Figure 3.28: Branksome Chine weather data (No data from September 19 to October 7.

Estimation of wave period

Although wave period was not recorded, estimates of wind speed using the Beaufort scale were made by trained observers. It is therefore possible to estimate the typical range of wave periods for the Branksome Chine area using the weather data and deep water forecasting curves.

The forecasting curve used has been taken from King (1966), although the chart is based on work carried out by Bretschneider (1952). The forecasting curve provides a value for the deep water wave period and height as a function of wind speed and fetch.

The wave fetch was estimated using a scale map of the area (Harper Collins, 1993) for the different wind directions recorded in Figure 3.22. Table 3.6 summarises the estimated wave period derived from the forecasting curve (see e.g. King, 1966).

WIND DIRECTION	% OF TIME RECORDED	FETCH (MILES)	ESTIMATED PERIOD USING BRETSCHNEIDER CHART (S)	WEIGHTED PERIOD	TOTAL WEIGHTED PERIODS = 492.35. AVERAGE = 492.35/100 = 4.92S
NW, N, NE	21.2	(assume 2)	2	42.4	
E	0.4	10	2.7	1.08	
SE, S	28.8	100	4.6	132.5	
SW	44.5	700+	6.8	302.6	
W	5.1	10	2.7	13.77	
Average Beaufort Force = 2.78 = approximately 6.5 mph					

Table 3.6: Summary of estimated wind, fetch and wave period. (Fetch is estimated using maps)

The average estimated wave period is 4.9 seconds, while the wave period is likely to range between 2 and 7 seconds.

Prolonged periods of high wind speed and wave height

Three distinct periods of prolonged strong winds and large wave heights can be identified from Figure 3.28 (the exact dates of these events have been read from the raw data sets in Appendix E). These periods have been characterised by wind speeds in excess of Beaufort force 4 (strong breeze), or wave heights larger than 0.8m for more that 7 consecutive days. These events are summarised in Table 3.7.

EVENT DATES	AVERAGE WIND SPEED (BEAUFORT SCALE)	AVERAGE WAVE HEIGHT (M)	DOMINANT WIND DIRECTION
29th August to 9th September 1998	6	1.3	SE
19th October to 6th November 1998	5	1.1	SW followed by NE followed by SE (approx equal lengths of time)
28th December 1998 to 3rd January 1999	4	1.2	SW (3 days of southerly at end of period)

Table 3.7: Summary of prolonged periods of high wind speed and wave height

From Figure 3.28 it can be seen that some intermittent strong winds and high waves occurred during July 1998. On July 18, force 10 winds were noted, although conditions improved the following day.

3.5.4 System discharge

Head-discharge relationship

Figure 3.29 shows the relationship between SWL location (Y) and discharge recorded during August 1998 and during February 1999.

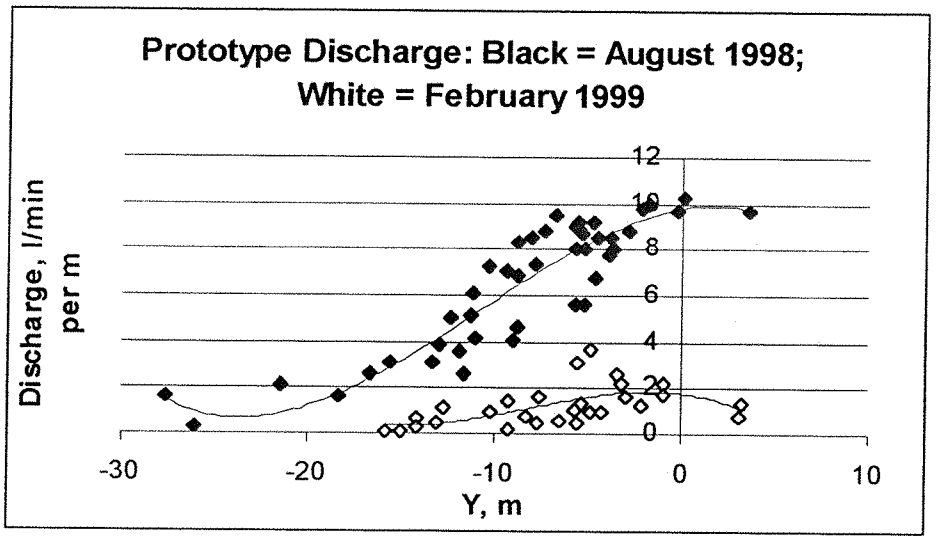

Figure 3.29: relationship between Y and discharge. Drain is located at Y = 0.

It can be seen from Figure 3.29 that there is a significant different in the system discharge for the two data sets. The mean discharge (taken at y = -10m) is approximately 6 l/min per m length of system (0.36 m^3/hour per m) for the August data set, and 1 litre/min per m for the February data set (0.06m^3/hour per m).

The drainage system discharge, even before the major system damage in September 1998 is low in comparison to previous trials, and is considerably lower than calculated in section 3.2.4. This is thought to be due to installation defects, such as poor choice of geotextile, lack of pipe rigidity, gaps in pipe joints and sump imperfections (allowing sand ingress). The Branksome Chine discharge rates will be compared to theoretical values and model data in Chapter 6.

The difference in the system discharge from August 1998 to February 1999 is due to storm damage that occurred during early September 1998, and at the end of December 1998 - beginning of January 1999. This will be discussed later in this Chapter.

Water table lag time

According to Emery and Foster (1948) the elevation of the water table follows the same pattern as the tide (although there is a lag time of approximately 1 to 3 hours). Figure 3.30 shows the fluctuation of discharge with time from 5.00am on 13/2/99 alongside the corresponding tide chart. It is difficult to define the lag time using the high water peaks due to the double tide. From the low water troughs in Figure 3.30 the lag time between the tide level and the pump rate minimums varies between 10 minutes and 1 hour – hence the average is 35 minutes. The tide chart in the figure is for Town quay, however, tide times for Branksome Chine are 30 minutes later than those for Town Quay. Hence the lag time varies between 40 minutes and 1 hour 30 minutes, and the average is approximately 1 hour.

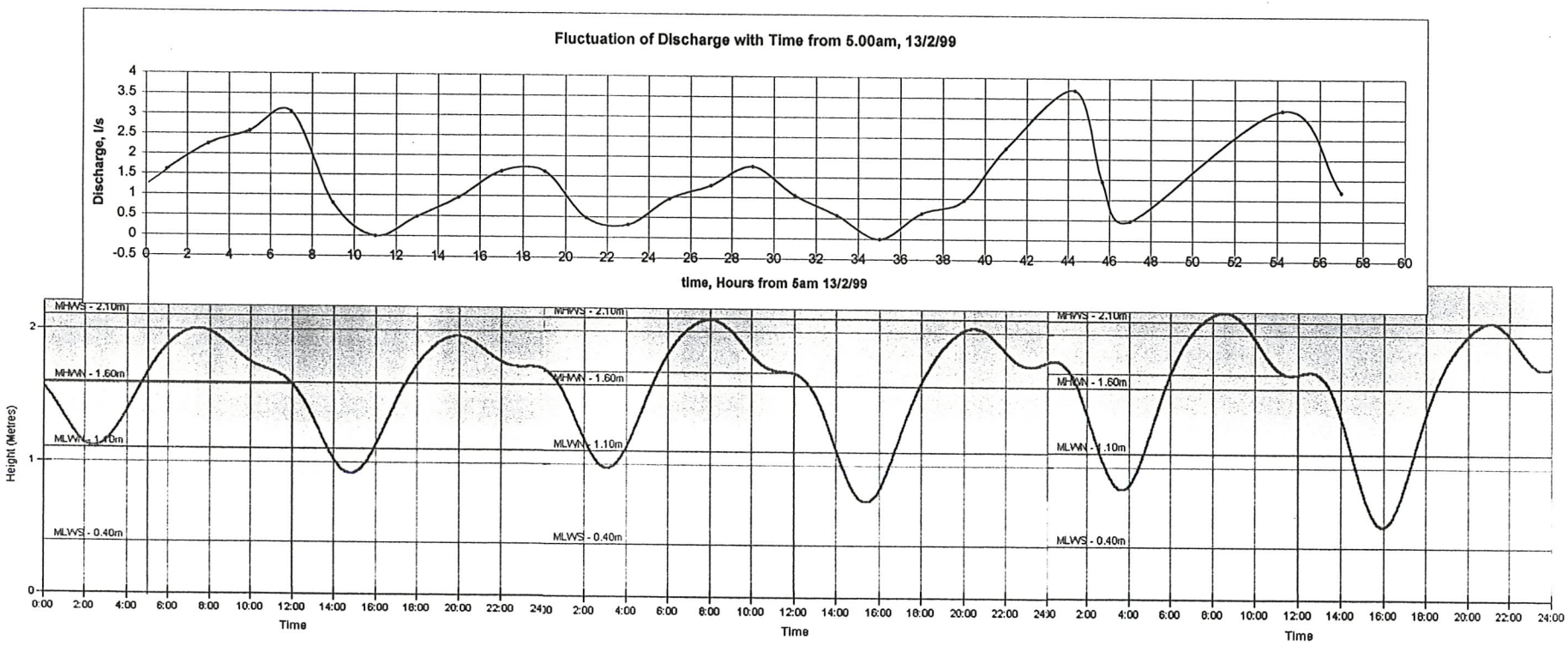

Figure 3.30 Graph to show the fluctuation of discharge with time from 5.00am on 13/2/99 alongside the corresponding tide chart (reproduced with permission for examination)

3.5.5 Photographs and additional field observations

The letters refer to Table 3.5.

(a) System damage shortly after installation

According to field observations, on June 12 1998 plastic was found to be blocking the drainage pipes, and this was thought to have been part of the pipe sleeving. Sand was found to be entering through two of the four pipes.

On July 29 1998 it was noted that the volume of water flowing from the landward pipe was higher than that of the seaward pipe, despite the fact that, with the tide in, the head difference for the seaward pipe was higher. This indicates that the seaward pipe was inefficient.

It is suspected that this was a result of installation defects, and it is likely that some of the sand may have entered via joins in the pipes.

(b) July and August 1998

Once the beach levels had recovered, the drainage system began to have a positive effect on the trial beach. The system performed effectively during July (see section 3.5.2).

(c) Pipe damage

After survey 5, a period of stormy weather caused damage to part of the system. The system is known to have been damaged on the September 6 due to a prolonged period of gale force SE winds and wave heights of over 1.5m, accompanied by spring tides. These high energy conditions continued for one week between August 31 1998 and September 7 1998. The beach aspect is SE, therefore the incoming waves would have been directly onshore. This combination of events resulted in a significant loss of beach material, and the loss of or damage to part of the system.

The lower beach drain (number 4) was found to be uncovered on September 6 1998 (Figure 3.31), and it is thought that part of the system was damaged during this exposure to the elements.

Figure 3.31: Uncovered beach drain 6/9/98

After this damage, the system remained in operation, but functioned less efficiently than during the summer. This was shown in Figure 3.26b. Although the dry area in Figure 3.26b indicates that the system is still working, there is water on the beach, which was not present in the photograph shown in Figure 3.26a (both photographs were taken at similar states of the tide).

The bulge shown in Figure 3.25a (survey 3) and the photograph in Figure 3.26a disappeared after the system was damaged. This result is significant since it

demonstrates that the bulge was not a local effect particular to this section of beach, but can be attributed to the presence of the drain system.

(d) Sump siltation

On several occasions sand was washed into the sump causing the pumps to switch off and rendering the system out of operation. On the first occasion sand is thought to have entered through damaged pipes (10/9/98), and the sand filled sump can be seen in Figure 3.32. The sump was unblocked and the damaged sections of pipe isolated.

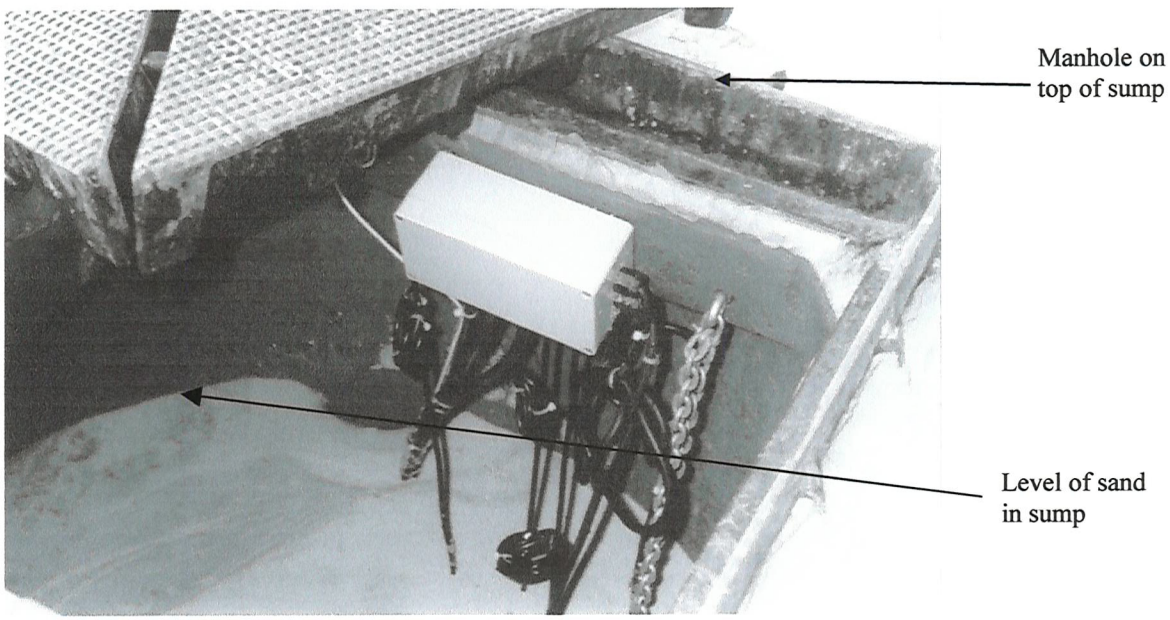

Figure 3.32: Sump silted up after storms (photograph taken on 10/9/98)

While the pumps were out of operation, the beach drainage system was unable to stabilise the beach. Poor weather conditions continued, further beach material was lost, and large portions of the beach drains were damaged or removed from the beach.

(e) Reinstallation

On December 3 1998 three new pipes were installed into the beach face. These were placed further landward than the previous installation (see section 3.4.4).

(f) Damage after reinstallation (phase 2 system)

Shortly after the second installation of pipes high tides and storms (see Dec/January prolonged storm in Figure 3.23) resulted in damage to the sump. The sump became filled with sand and the pumps were rendered inoperational. Figure 3.33 shows a photograph of Branksome Chine on the January 5 1999, and Figures 3.34 and 3.35 show the ensuing system damage.

Figure 3.33: Southerly storms at Branksome Chine, 5/1/99

Figure 3.34: Damage to concrete seal around power inlet

Figure 3.35:Damaged drainage system, 10/2/99

Since the pumps were out of operation during a period of erosive conditions (late December1998-early January 1999), the drainage system was unable to maintain the beach levels and defend itself against damage. During this out of operation period the reinstalled pipes were damaged, and when the sump was cleared of sand and the pumps restarted it was found that the system discharge was significantly reduced (this was shown in Figure 3.29).

Since the damage occurred so soon after reinstallation (phase 2), it is not clear whether the reduced discharge was due to pipe damage or due to the new pipe location, although it may be thought likely to be a combination of both.

With the reduced yield, the beach drainage system did not maintain the beach levels, and further pipe damage occurred. The second, clearly less efficient installation had little effect on the beach profile in comparison to the control beaches. Therefore the phase 2 installation was considerable less effective that the phase 1 system.

Marin *et al.* (1998) suggested that beach drainage is less effective during erosive conditions, and it is possible that the Branksome Chine system was less effective during the winter due to a seasonal variation in wave climate. However, Figure 3.28 shows that during February weather conditions were relatively mild, with recorded wave heights generally less than 1m. Conditions during the low yield period are comparable to those during July 1998 when the system had a positive impact on the beach. This observation is important, since it indicates that the reduced performance was likely to have been caused by the reduced yield, and not by seasonal weather patterns.

The effect of wave climate on drainage system performance has been explored using a physical model, which will be discussed in Chapters 5 and 8.

When the sump was filled with sand, the pumps automatically switched off. However, the pumps eventually ceased to operate permanently due to corrosion. This is shown in Figure 3.36. This is likely to be due to the effects of sea water.

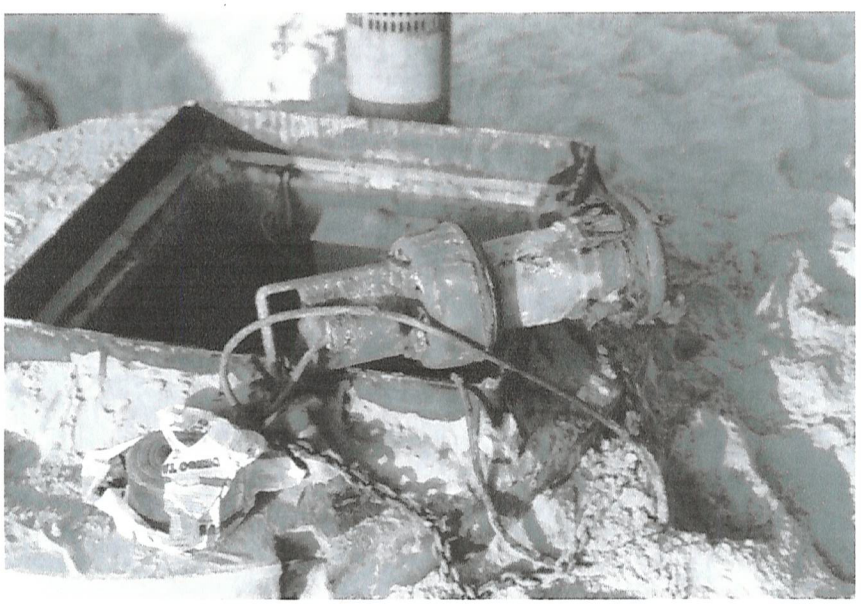

Figure 3.36: Corroded pump (June 1999)

3.6 Conclusions

The lag time between the minimum system discharge and low water at Branksome Chine is approximately 1 hour, and this gives an indication of the lag time between the tide and water table levels. This results compares with the findings of Emery and Foster (1948) which showed that the water table level lags behind the tide level by between 1 and 3 hours.

The measured system yield was considerably lower than the calculated value and those measured from previous trials. It is thought that installation defects, such as poor choice of geotextile, lack of pipe rigidity, gaps in pipe joints and sump imperfections (allowing sand ingress) are responsible for the initial lack of drainage system efficiency.

During the first two months of operation, there were no major storm events or inoperational periods (although the system was thought to be operating slightly inefficiently). The results show that during July 1998 the drained section maintained beach levels while sand was lost from the surrounding beaches. Therefore, when the pumps remained in working order the system was effective. Prolonged storms in early September 1998 damaged the phase 1 drainage system, and the sump was filled with sand. The system was reinstated in December 1998, but a second bout of prolonged storms in December/January 1998/9 caused significant system damage shortly after the phase 2 installation.

It is thought that the sump was insufficiently robust, the drain installation depth was too shallow, and the drains were inefficient. Future installations must address these issues and aim to

- design and construct a robust and watertight sump, and
- prevent system damage by maintaining pumps and preventing non-operational periods (install a warning system)
- prevent loss or damage to beach drains by installing the drains at an appropriate depth (i.e. it is necessary to take into consideration the beach levels at the time of installation in relation to the seasonal cycle)
- use improved installation techniques (e.g. ploughing technique, use of dewatering points around the excavation)

- take into account the beach levels at the time of installation and any likely seasonal fluctuations in beach level (historical records),
- reduce head losses
    - use a higher permeability, or no geotextile filter
    - use a gravel matrix around the beach drain (Vesterby 1996)
    - use drainage pipes with larger slots

Although the aim of the drainage system is to maintain the beach level, thus preventing itself from being damaged, it is still recommended that the system is installed as deep as possible within the beach, since inoperational periods (e.g. for reasons of maintenance) may be inevitable. It will be shown later in Chapter 8 that for a prolonged period of erosion, some loss of beach material will occur, even with the drainage system operating.

It would appear that as long as the system is maintained in working order, and the system is efficient (i.e. the system yield is adequate), then beach drainage would be an effective stabilisation option for this area. A full scale system with an appropriate installation depth, a minimum length of 200m and appropriate yield should mimic the results shown in the survey 3 plot and photograph shown in Figures 3.25a and 3.26a.

The results of this full scale trial indicate that a drainage system can stabilise the beach at Branksome Chine in the short term, however it is difficult to extrapolate results to predict long term performance. The findings do indicate that long term performance can be limited by the robustness and quality of the system and installation techniques, and the system must be able to withstand the range of conditions likely to be encountered for the duration of the design life. Results show that even with an effective system some material loss is inevitable during prolonged storms (see also Chapter 8), and perhaps a drainage system must be designed to withstand beach material loss likely to arise from a 1 in 20 (for example) year storm event. Thus historical records must be taken into account during the design stage.

A future project should aim to investigate the feasibility of a combined beach drainage/beach nourishment project, with groyne removal (since they are apparently ineffective) for Poole Bay.

4. INTRODUCTION TO PHYSICAL MODELLING: DISCUSSION OF KEY VARIABLES AND DEVELOPMENT OF BEACH DRAINAGE THEORY

4.1 Introduction

The broad aim of the work described in Chapters 4-8 was to investigate the effect of a range of variables on system performance using a physical model. This chapter introduces the variables to be investigated, and discusses the theoretical considerations that have guided the modelling.

The performance of a beach drainage system depends on many factors which occur in different combinations in the field environment. For example, a high water level may occur at the same time as large wave heights and cross shore currents. The Branksome Chine trial was a valuable pilot project in terms of gaining practical information about the operation, performance and maintenance of a full scale system. However, it was difficult to identify the effects of individual influencing variables because these could not be isolated. Full scale results indicate that drainage system performance is sensitive to drain location and discharge. The system was also subject to damage during storm events.

Physical modelling was therefore used to investigate some of the findings of the full scale trial in further detail, and to identify relationships between the principal controlling variables and system performance. The physical model has also been used to investigate the pore water pressure characteristics within the beach face around the drainage system, with the aim of gaining a further understanding of the mechanism of beach drainage.

To isolate the controlling variables, the model was simplified. For example, the model is two-dimensional and has no tide operating. Previous and concurrent studies have attempted to replicate field conditions, leading to the inclusion of many variables. The objective of using a model in this project is to isolate variables because the field is too complicated. However, it inevitably then becomes difficult to compare the results of the complex full scale trial with simplified model data.

Three important points have emerged from the literature review (Chapter 2):

- The scaling issue must be investigated if a physical model is to be used.
- Previous tests using a complex test matrix incorporating numerous variables have provided primarily qualitative data (i.e. data sets offering a comparison of different profiles). The relationships between individual parameters are yet to be investigated in isolation.
- Theories to explain beach stabilisation through drainage are yet to be discussed in detail and supported by evidence.

These issues have been addressed in this study, and are covered in Chapters 5-8.

Summary of modelling chapters

Chapter 5 discusses the design of an appropriate beach drainage model and test procedures, and investigates the scaling issues associated with beach drainage modelling. Dimensional analysis has been carried out to understand the relationship between the model and a theoretical prototype, and to help interpret the model results.

In Chapter 6, model and full scale (Branksome Chine) discharge data are compared and discussed. Scaling considerations indicate that the discharge and pore water pressure measurements in the model are likely to overestimate the values recorded in the field. In Chapter 7 the model pore water pressures are correlated to system discharge, and an empirical formula for pore water pressure is derived.

Chapter 8 describes several tests carried out to determine the relationship between drainage system performance and the principal influencing factors. Factors affecting beach drainage performance and beach morphology were listed in Chapter 2 (Table 2.8).

The physical model was used to carry out some preliminary experiments to investigate the use of an alternative drainage system design. This will be discussed in Chapter 9.

Variables to be investigated

The main variables, which have been drawn from discussion in earlier chapters and from previous work (e.g. Weisman *et al.,* 1995; Marin *et al.,* 1998), are:

- still water level location relative to drain, SWL (tide level, or head),
- pore water pressure, PWP (water table dynamics or drain drawdown),
- discharge, Q,
- wave climate, and
- beach profile response (volume change),

Each of the selected variables was investigated in turn, while other factors were held constant. Table 4.1 summarises the variables that have been investigated in test sets denoted A to F.

Test Set Code	**Controlling variable**	**Measured dependent variable**	**Variables held constant**
A	*Preliminary tests*		
B'	SWL location relative to drain	Q	wave climate
B	SWL location relative to drain	Profile	Wave climate
C	Q	Profile	SWL, wave climate
D	Q, wave climate, pressure probe location	PWP	SWL
E	Wave climate	Profile	Q, SWL
F	Wave climate, wave climate history	Profile	Q, SWL

Table 4.1: Summary of variables tested

No tide cycle was included during any of the tests, but test set B was used to investigate the effect of different tide levels by measuring the beach profile change in response to different still water levels. Thus the tide was simulated as a series of still water level increments in separate tests. In test set F, the beach was subjected to a range of successive wave climates, but the still water level was held constant.

The letters A to F in Table 4.1 are laboratory test codes that correlate to raw data sheets and spreadsheets. These are not necessarily discussed in alphabetical order in this dissertation.

In this chapter the main areas of discussion are:

1) system discharge and pore water pressure reduction,
2) swash zone energy dynamics,
3) relative energy removal,
4) laminar flow phase extension theory, and
5) wave climate

A summary of the laboratory experiment objectives will be given at the end of this chapter.

4.2 Discharge and pore water pressure reduction

There are two main processes that may be influenced by the presence of a beach drainage system:

1) the ability of the sediment to resist the shear force applied by the surge, and
2) the energy available to move the beach sediment (surge energy)

Both of these processes are affected by the drainage system drawdown, i.e. the depth of the new piezometric surface below the initial piezometric surface. The fact that water is being removed from the drainage system means that there is flow in the beach face, and pore water pressures are reduced. The exact location of the phreatic surface is difficult to define precisely in the case of a beach, because the beach face is subject to successive swash infiltrations.

4.2.1 Factors affecting discharge

Theory

According to Darcy (1856), the volumetric flow rate, q, through a porous medium is proportional to the head difference, H, sediment permeability, k, and the flow area, A, (defined by the geometry of the system):

$$q = Aki$$

The actual yield from the drainage system will be affected by any associated head losses. Therefore the factors controlling discharge are:

1) drainage system characterisation (e.g. hole/slot size and % open area),
2) sediment properties (permeability),
3) head difference between the source (still water level) and the drain, and
4) flow path length (geometry)

In the field the discharge may also be affected by blockage, pipe loss or pump faults. The effect of discharge on system performance has important design implications (i.e. pump selection).

Test set A: Drain hole size and % open area

One of the main aims of the preliminary tests, denoted set A, was to investigate model drainage system design, develop test procedures and characterise the model sediment. The effects of the following design variables on system discharge were investigated:

- pipe diameter
- drainage hole diameter
- geotextile type

Test set B': Head discharge relationship

The aim of test set B' was to investigate the relationship between head and discharge in the model, and compare this with the Darcy relationship and full scale data. Full scale discharge data were recorded at Branksome Chine and the head of water in the field has been deduced from local tide charts (see Chapter 3). The head-discharge data sets will be discussed in greater detail in Chapter 6.

4.2.2 Drain drawdown and pore water pressure reduction

Beach material has the ability to resist the applied shear force because the sediment grains are held in contact by an effective stress and there is friction between them. As noted in Chapter 2 the effective stress is the component of normal stress taken by the soil skeleton and for saturated soils the effective stress may be calculated using the Terzaghi equation:

$$\sigma_v' = \sigma_v - u$$

where σ_v' = the effective stress, σ_v = the vertical stress, and u = pore water pressure.

If the effective stress is zero, then the sediment has no shear resistance, and therefore behaves like a fluid.

The possible mechanisms of beach drainage were summarised in Chapter 2. It was noted that liquefaction may be responsible for beach face slumping and rapid material loss.

With beach drainage, a generally downward flow of water within the beach will result in sub-hydrostatic pore water pressures. This increases the shear resistance of the beach material, and also the amount of energy required for incipient motion.

The aim of test set D was to determine the spatial variation of pore water pressure caused by a beach drainage system, and investigate the effect of pore water pressure reduction on beach liquefaction. The effect of waves on pore water pressure has also been investigated.

4.2.3 Effect of discharge on system performance

The mechanism of pore water pressure reduction prevents the movement of particles that already exist on the beach. However, this cannot account for the fact that beach accretion occurs, and a second mechanism must exist to account for drainage-induced particle deposition.

One of the aims of test set C was to investigate whether *accretion* occurs in the swash zone when the drain is in operation, and if so to determine the nature of the relationship between beach accretion and system discharge. The change in beach volume over a period of time was determined for wave climate near to the boundary between erosion and accretion, for which in undrained conditions the beach volume change is very low (near to zero).

4.3 Swash zone energy dynamics and beach drainage

Surge energy

If the same quantity of water runs down the beach as runs up the beach, then the same quantity of material would be carried back and forth during each surge cycle (Bagnold, 1940). In an enclosed system, if no water has been removed from the swash zone and other losses are assumed to be negligible, then the wave energy during the backwash would mirror that of the incoming swash (see Figure 4.1).

Under natural conditions (with no drainage) water from the swash infiltrates into the beach, and this infiltrated water moves through the beach by gravity to rejoin the surge lower down the run-up zone. As the infiltrated water seeps out of the beach face, the water rejoins the surge causing the backwash volume to increase as it moves back down the run-up zone. The backwash gains momentum, and sediment particles deposited by the swash are re-entrained by the backwash.

Assuming no losses the total sum of potential and kinetic energy remains constant.

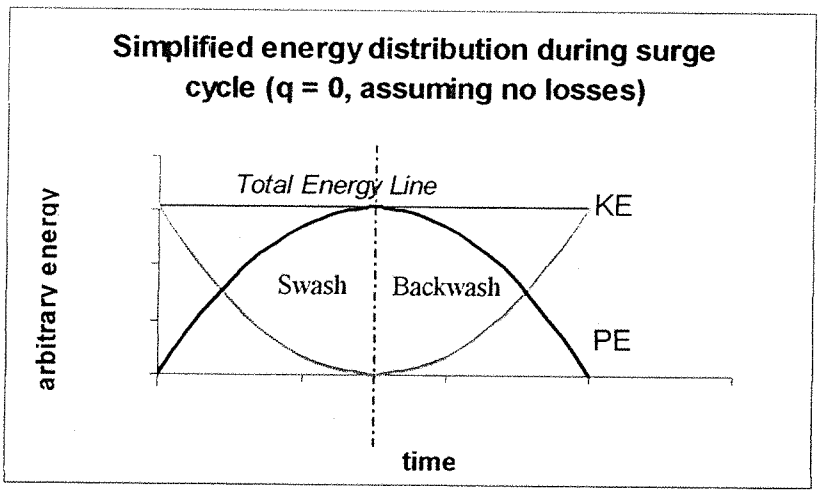

Figure 4.1: Simplified energy distribution during surge cycle (Wave period, T = time for one wave period). No losses.

In reality, energy is lost during the surge cycle due to percolation, turbulence, air entrainment and friction, as illustrated in Figure 4.2.

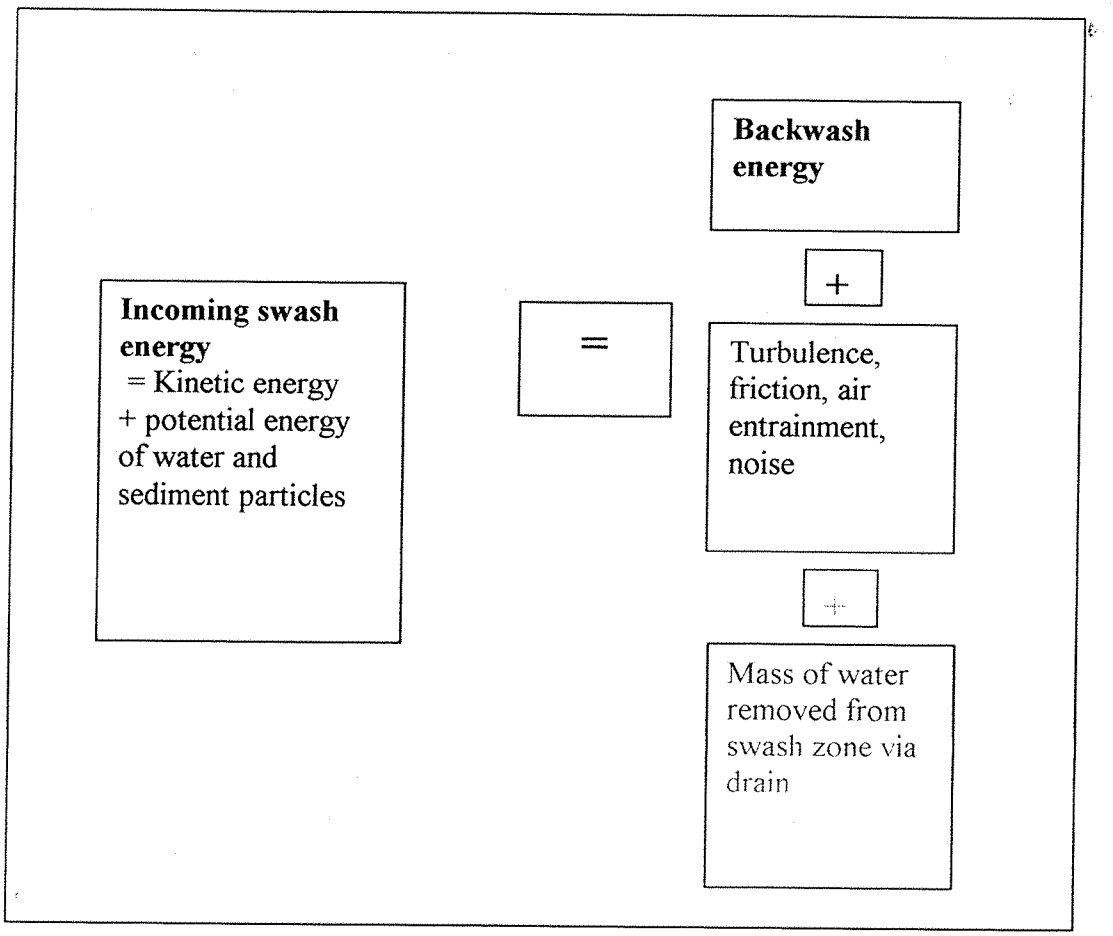

Figure 4.2: Summary of surge cycle energy transfers

Rapid deposition flow phase

As the surge moves up the beach, the velocity and wave volume decrease until the kinetic energy of the surge falls below that required for incipient motion. At this point, the sediment load is dropped by the surge. The threshold for particle entrainment may be determined using the Shields formula (Shields, 1936), as noted in Chapter 2 (see e.g. Chadwick and Morfett, 1993). Sediment deposition occurs most rapidly for a short phase at the upper extent of the swash when the kinetic energy is at a minimum, and there is a brief period of laminar flow (Grant 1948). This region is very small, and covers only the top (landward) few centimetres of the run-up zone. This area can easily be identified in the field by the existence of a small ridge of deposited sediment at the upper limit of the swash (Grant, 1948). Ridges of sediment deposition can bee seen in the photograph in Figure 4.3.

Figure 4.3: Sediment ridges left by the upper limit of the swash (Branksome Chine, Dorset)

In an erosive wave climate, the surge kinetic energy, or capacity to transport sediment, is sufficiently high at all stages of the surge cycle that entrained sediment is not deposited (with the laminar flow phase being negligibly brief). Furthermore, sediment from the beach face is taken up into suspension due to the high incoming wave energy (Grant, 1948).

During accretive wave climates, conditions are such that more material is carried forward in the swash than is transported back down the beach in the backwash.

Effect of beach drainage on swash zone energy dynamics

When the drainage system is operating, potential energy is lost since infiltrating water is removed from the beach face and cannot rejoin the swash during the backwash. This lost potential energy cannot be converted back into kinetic energy. By reducing the energy of the surge during the entire cycle, beach drainage alters the balance of swash energy to backwash energy in favour of accretion. Although this results in the backwash energy being less than the swash energy, it is important to look in further detail at the implications of this energy removal for sediment deposition.

In summary, the beach drainage system results in the following sequence of events:

- water in the beach face is taken away from the swash zone and into the collector pipe,
- this results in increased percolation rates into the beach,
- percolation has been identified by Bagnold (1940) as one of the causes of energy loss during the surge cycle,
- due to increased percolation, the surge volume experiences a net loss of energy during the complete cycle, since percolating water does not rejoin the surge at exit points lower down the beach,
- the reduction in surge volume (and hence energy) during the surge cycle results in a change in the balance of the swash/backwash energy , with the total energy of the backwash being less than the total energy of the swash.

4.4 Deposition phase extension theory

It can be seen that in theory the beach drainage system causes a change in the surge cycle energy dynamics in favour of accretion. However, the key issue is whether this energy loss actually causes the sediment load to be deposited. This section and the following section will examine two possible mechanisms by which surge energy reduction by beach drainage may result in increased sediment deposition.

Figure 4.4 shows schematically the potential and kinetic energy distributions during the surge cycle. The solid lines are for no losses, and the dashed lines allow for energy lost

from the surge due to water removal via the drainage system. When losses occur, the total energy line falls during the surge cycle.

Note that the diagram shows the curve for no losses at all, and a curve where all losses are assumed to be due to the drainage system. In reality there will be a combination of losses due to friction and percolation that would occur regardless of the beach drainage system.

Below a certain wave energy threshold, sediment cannot be carried. This is more commonly termed the threshold of motion, and according to Shields (1936) is a function of the Reynolds number and densimetric Froude number (discussed in Chapter 5), where the terms refer to the conditions at the grain. Although the threshold of motion is controlled by the grain dimension, it is also affected by the shear stress, τ, applied to the bed, which is a function of the wave energy.

According to Chézy formula[1]:

$\tau = \rho g R S_0$

Hence shear stress if a function of the hydraulic radius, R, where R = A/P (A = cross sectional area and P = wetted perimeter). As the wave depth, d, decreases, so the hydraulic radius, R, decreases

$\rightarrow \tau \propto d$

As the wave runs up the beach, the depth decreases, therefore the shear stress depends on the point in space and time during the surge cycle. If it is assumed that the wave depth and velocity decrease at the same rate (this is possible because the flow in non-uniform, since water runs into the bed as the surge flows up the beach) then the change in shear stress throughout the surge cycle may be approximated to the energy distribution shown in Figure 4.4.

Likewise, $\tau_{critical} = \rho\ g\ R_{critical}\ S_0$ (it is assumed that S_0 is constant).

$\rightarrow \tau_{crit} \propto d_{crit} \propto E_{crit}$

[1] There is no official published source for this famous equation. see Chow (1959) for further background)

where the subscript 'crit' denotes the value required for incipient motion. The critical energy line is illustrated in Figure 4.4.

Figure 4.4 illustrates how increased energy removal through drainage increases the length of time for while the surge energy is below the incipient motion threshold.

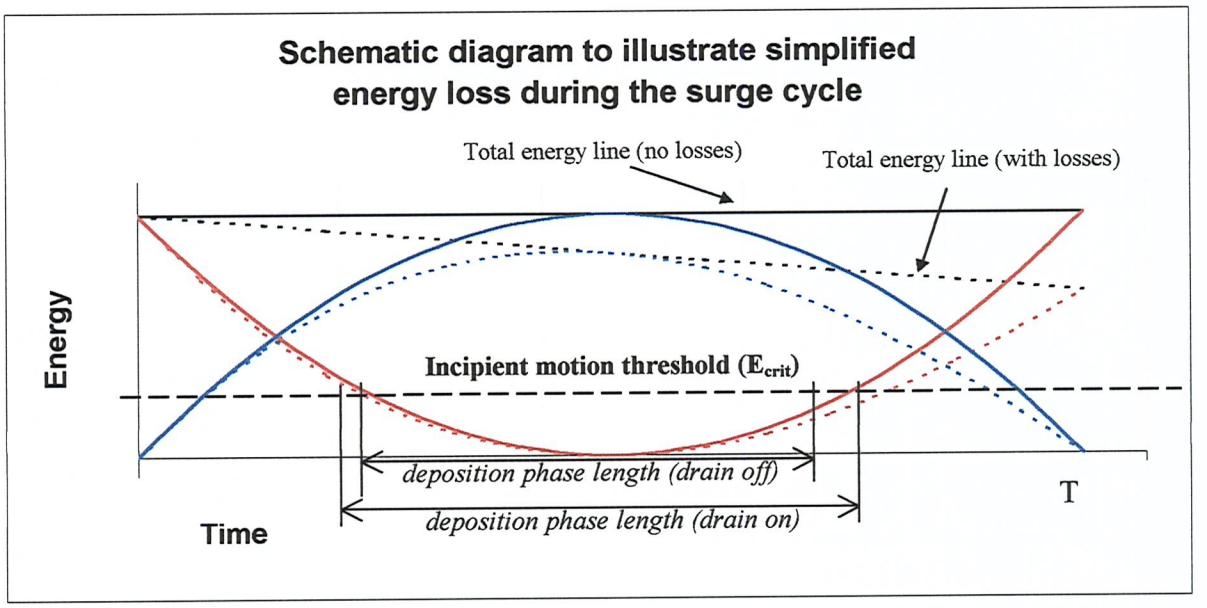

Solid line = No losses; Dashed line = Losses exaggerated
Red = kinetic energy; Blue = potential energy

Figure 4.4: Simplified energy distribution during surge cycle (T = 1 wave period).

If indeed beach drainage does increase the deposition phase, then one would expect to measure an increase in beach volume in the swash zone. This is not the same as recording less material loss than would otherwise occur, because this may be a result of the mechanism of effective stress reduction – which is slightly different to deposition phase extension.

If the effect of the beach drain were merely to increase the effective stress of the beach material, the one would expect the system only to be effective in retaining material that exists in an otherwise erosive wave climate.

For the mechanism of deposition phase extension to take effect, additional material must be added to the beach in an otherwise neutral wave climate.

Test Set C

An experiment was carried out to determine the volume of material gained in the swash zone during a monochromatic, neutral (neither accretive nor erosive) wave climate. Thus any material that accreted during wave operation could be attributed to the presence of the drainage system. The results of this experiment were compared with the above calculation, as will be discussed in Chapter 8, section 8.5.

4.5 Relative energy reduction

4.5.1 Theory

When a beach drain is in operation, there is a net movement of water from the water/sediment boundary to the drain, and hence there is greater percolation from the surge into the beach face. The volume of infiltrating water means that a mass of water has been taken from the surge, and therefore energy has been removed (see above section).

The surge energy reduction caused by the drainage system must be considered in terms of the ability of the wave to transport sediment since the energy removed may not be sufficient to induce particle deposition.

The effect of the drainage system (defined by beach volume change) might be expected to be greatest directly over the pipe since this is where the flow path from the water/sediment boundary to the drain is shortest. Hence this is the zone where infiltration rates will be highest, and volume, or energy removal will be the greatest.

The energy of the surge depends on the depth and velocity of the flow, which change as the swash propagates up the beach face (or retreats during the backwash). As the wave moves up the beach, kinetic energy is lost, potential energy gained, and the wave mass is reduced due to percolation. The area of the beach beneath the deeper part of the wave is subject to a greater shear force than the beach at the upper limit of the swash where the wave is shallow and slow moving (Fig. 4.5).

When wave energy is high the surge energy is significantly higher than that required for incipient particle motion on the beach face. A large amount of material is suspended in this region, as observed through the glass side of the wave tank (see Figure 4.6).

Figure 4.5: Photograph of retreating surge, Branksome Chine, Poole.

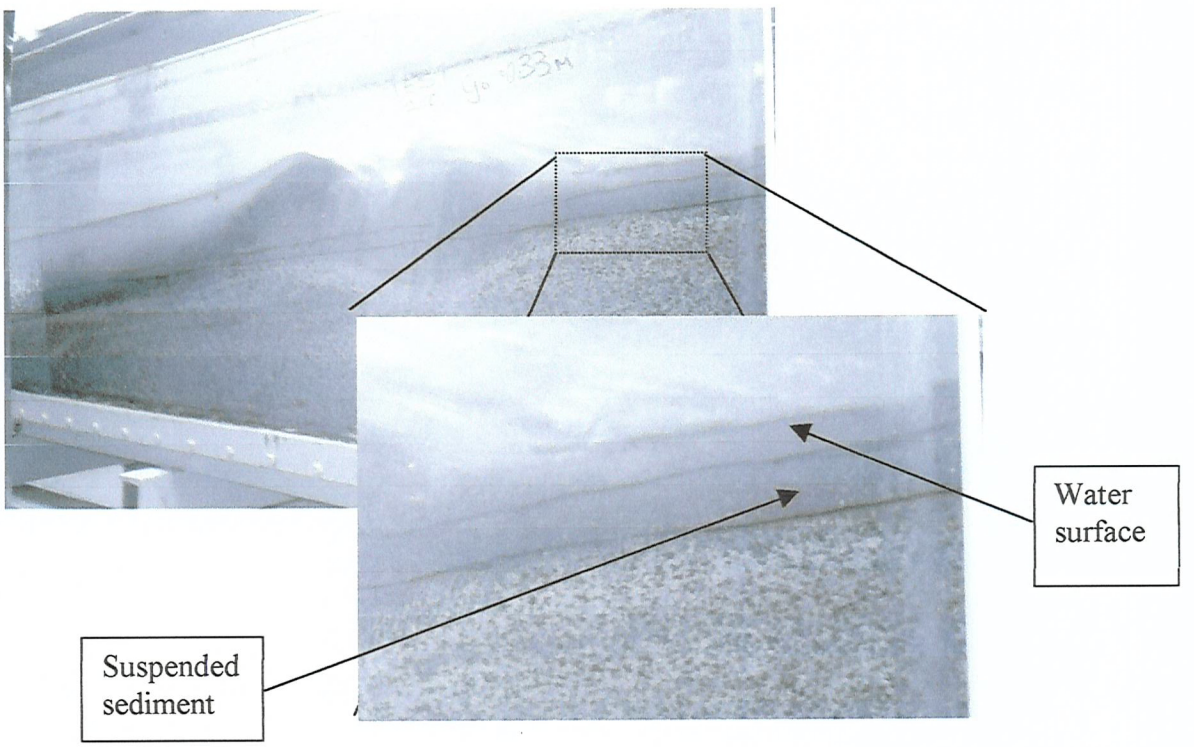

Figure 4.6: Suspended sediment in lower run-up zone.

In this part of the wave, the reduction in wave energy through water mass removal is not sufficient to reduce the total wave energy to below that required for particle motion. The ratio of energy being removed by infiltration to the total energy of the overlying wave is small. This ratio may be considered as $\Delta d/D$ where Δd is the (hypothetical) change in wave depth due to water being removed by the drainage system, and D is the total depth of the overlying wave at the point in question. As discussed in the previous section, the shear stress on the beach surface may be considered to be proportional to the wave depth, is the run-up is considered as open channel non-uniform flow.

If the shallow part of the wave is located over the zone of influence of the drain, then the amount of energy removed would be large in relation to the total energy of the wave, and it is more likely that this reduction will be sufficient to reduce the energy of the surge to below that which s required for incipient motion. In this case $\Delta d/D$ would be high.

As the SWL increases, the still water level mark on the beach face moves landward and the head above the drain also increases (Figure 4.7). Hence the discharge increases, percolation rates into the beach face are higher and more energy is removed in total. However, as the SWL moves landward, the depth of the wave above the drain also increases. Therefore the ratio $\Delta d/D$ may decrease, and with it the relative effect of the drain in terms of the energy removal in relation to the total energy of the overlying body of water.

If the shallow part of the wave, the part of the wave in the region of the upper limit of the swash, is over the zone of maximum influence of the drain then the relative energy reduction $\Delta d/D$ will be greater. This means that it is more likely that the rate of energy removal will be sufficient to cause the energy of the flow to fall to below that required for incipient motion.

It is not only the amount of water that is removed that is important, but also the part of the wave from which the water is removed: The effect of the drain on whether incipient motion will occur or not depends on the amount of energy removed in relation to the to the overall wave energy. For effective beach drainage enough water must be removed by the system such that the relative energy of the wave is reduced to below a threshold value. This will be discussed further in Chapter 8.

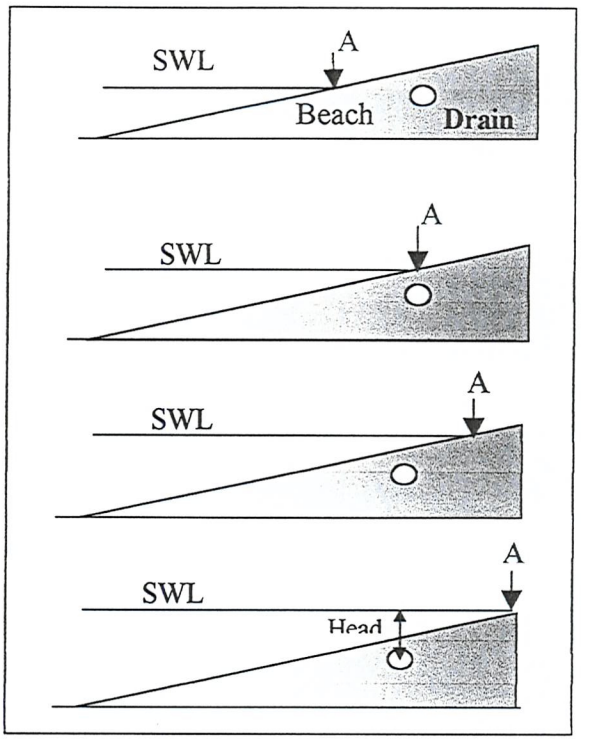

Figure 4.7: Schematic diagram of advancing SWL. A = SWL mark

This argument suggests that the performance will therefore depend on the position of the zone of maximum influence of the drain (or the drain drawdown pattern) in relation to the position of the wave (or the wave depth over the zone of maximum influence of the drain). According to the above theory, optimum performance will occur when the lowest energy part of the wave, the part of the wave in the region of the upper limit of the swash, is over the zone of maximum influence of the wave. In this instance Δd will be greatest, and D will be smallest, thus the relative energy removal denoted by the ratio $\Delta d/D$ will be at a maximum.

The ratio of $\Delta d/D$ has been used to illustrate the concept of relative energy removal, but it was not possible to measure accurately the wave depth in the experiments. On the basis of the above discussion we would expect to measure the optimum system performance when the upper limit of the swash is located over the zone of maximum influence of the drain. This has been investigated, and is discussed in Chapter 8.

4.5.2 Test set B

The main aim of test set B was to investigate the effectiveness of the drainage system for a range of different locations. The distance from the still water level mark to the drain was varied for each test to simulate different tide levels. This distance has been labelled y and is shown in Figure 4.8.

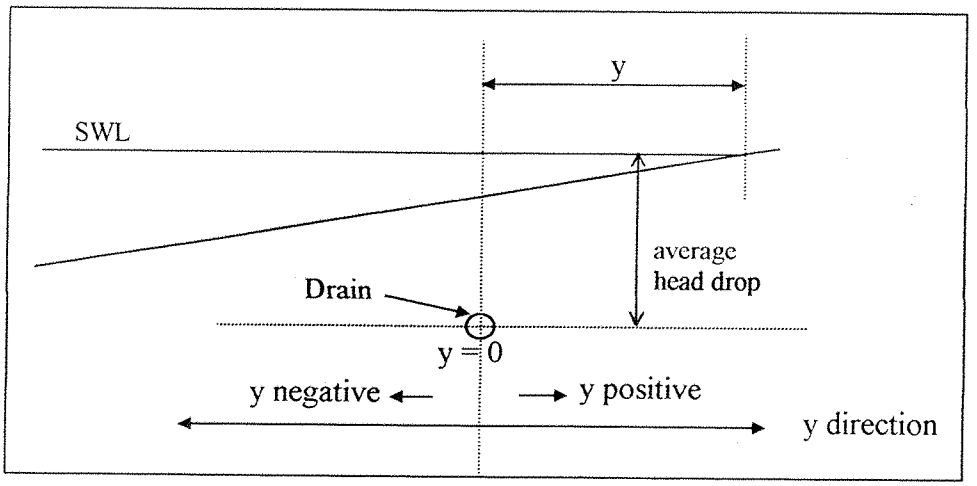

Figure 4.8: Distance from drain location to still water level mark.

While the relationship between average head drop (SWL) and discharge is likely to be positive (as suggested by the Darcy equation), a consideration of beach face dynamics suggests that the relationship between SWL and performance, denoted by beach volume change, will be more complex.

Theoretical shape of trendline

When the still water level is low, and still water level mark is considerably seaward of the drainage system, the beach volume change per unit time is unaffected by the presence of the drainage system because the swash zone is outside of the zone of influence of the drain. As the distance between the swash zone and the drain decreases the discharge will increase, and the drainage system will have a greater effect. Thus a positive relationship between performance and still water level (SWL) would be expected as the SWL is raised.

When the upper limit of the swash is over the zone of maximum influence of the drain optimum performance is likely to occur, since $\Delta d/D$ is at a maximum. After this point, the depth of the wave over the drain increases, and above any point on the beach face the wave energy is high in relation to the amount of energy being removed due to the drainage system. In the bottommost sketch in Figure 4.8, the upper limit of the swash (the part of the wave where the wave energy is low) is far from the zone of maximum draw down caused by the drain, thus the energy removal is minimal, and is therefore small even in relation to the energy of the wave at this point.

In test set B the above theory was investigated by quantifying the relationship between still water position and performance using the beach drainage model.

4.6 Wave climate

4.6.1 Change of beach volume with wave climate (test set E)

The main aim of this experiment was to observe the effect of wave climate on system performance. The results of this experiment have also been used to identify the wave regime that separates erosion and accretion.

Since beach drainage is thought to induce higher percolation rates (see section 4.3), it is possible that drainage may cause the beach to exhibit characteristics akin to undrained beaches consisting of coarser material. Model data have be recorded for drain on and drain off conditions, and these have been compared to published data for coarse and fine material.

Coarser beaches tend to differ from beaches consisting of finer material in three ways:

1) the foreshore profile is steeper (Bagnold, 1940)
2) a greater volume of material is gained during accretive wave conditions (Seelig, 1983)
3) a greater amount of energy is required to cause incipient motion, therefore there is a shift in the boundary conditions that separate erosion and accretion (Seelig, 1983).

These characteristics have been compared to the characteristics that arise from beach drainage, and are discussed in Chapter 8.

4.6.2 Wave climate history (test set F)

In Chapter 3, it was found that damage to the full scale system at Branksome Chine tended to occur during prolonged spells of erosive conditions. High water levels caused damage to the sump, while the loss of beach material resulted in the loss of parts of the drainage pipes. The aim of test set F was to simulate a series of consecutive mild and erosive wave conditions, and monitor the change in the beach profile at given intervals to observe beach profile recovery after a storm event both with and without the beach drainage system operating.

4.7 Summary

The mechanisms of beach drainage are ultimately governed by the system discharge. The discharge results in a reduction in pore water pressure affecting the shear strength of the beach material. Secondly, the percolation of surge water into the beach face increases, causing a reduction in the surge energy. These mechanisms are summarised in Figure 4.9.

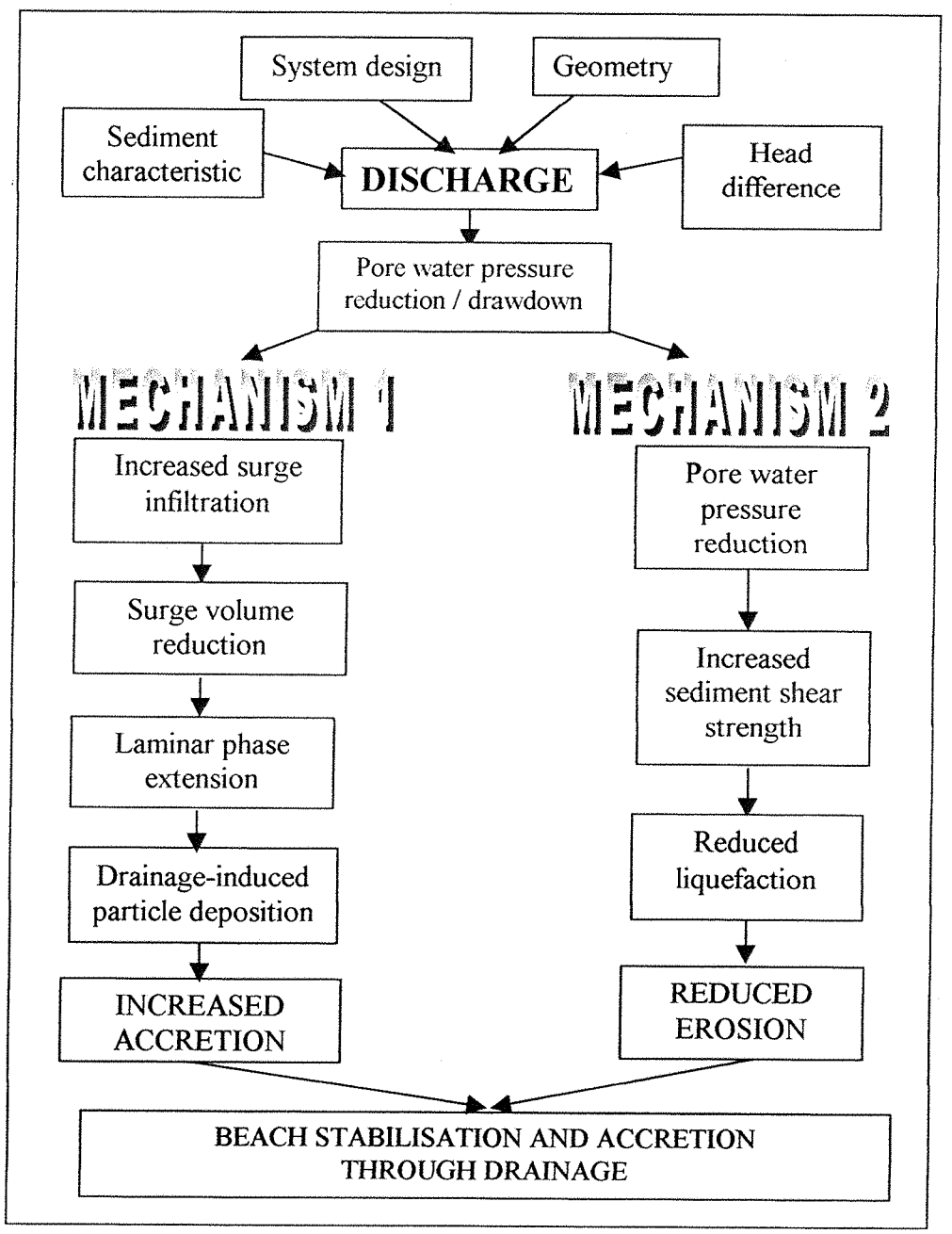

Figure 4.9: Diagram to summarise the mechanisms of beach stabilisation and accretion through drainage

The theories discussed in this chapter will be related to later in this thesis. Table 4.2 summarises each of the test sets to be discussed in Chapters 5-8,

TEST SET	TITLE	OBJECTIVES
A	Preliminary Tests	To establish suitable apparatus arrangement, explore some of the scaling issues and understand the behaviour of the ground Bakelite model sediment. To investigate the factors affecting discharge. To identify appropriate wave climates, beach slope and test time scale. Refine laboratory testing techniques (minimise scatter)
B'	Head-Discharge	To identify the head-discharge relationship in the model (and later compare these data to the full scale head-discharge data and the theoretical relationship).
B	SWL location	To evaluate the relationship between the drain location relative to the SWL and system performance. Identify the zone of influence of the drain in terms of beach profile change, and identify limits to performance. In this test, discharge is a dependent variable, since it is affected by the head of water over the drain system.
C	Discharge as a controlling variable	To investigate the relationship between discharge and performance when discharge is a controlling variable. The SWL is held constant, and q varied using a valve on the system outlet. The tests was also aimed at demonstrating that the beach drainage system can result in accretion in the swash zone.
D	PWP	To adapt pore water pressure transducers, commonly used in the field of soil mechanics, to measure the water table dynamics at different locations beneath the model beach. To determine the effect of beach drainage on beach liquefaction.
E	Wave climate	To identify a suitable criterion to differentiate between erosion and accretion for the model; to evaluate this for the Bakelite granules, and to quantify the effect of beach drainage on the erosion/accretion boundary condition. Compare the beach profile behaviour under beach drainage with that of a coarser beach.
F	Varied wave climate	To observe the system performance when the beach is subjected to a series of alternating erosive and accretive wave climate.

Table 4.2: Summary of test sets

5. DEVELOPMENT OF PHYSICAL MODEL

The aim of this chapter is to:

- describe the apparatus used for the experiments proposed in Chapter 4,
- discuss the development of appropriate test procedures and techniques, and
- investigate scaling issues.

The experiments described in Chapters 5-9 were carried out using facilities at the Chilworth hydraulics research laboratory and departmental Soil Mechanics laboratory. The hydraulics facilities have been used for previous coastal engineering model studies, and several of the data collection techniques used for this project have been developed in previous research projects (e.g. Marin *et al.* 1998). However, a significant amount of preliminary work was necessary to develop new methods for this project.

5.1 Apparatus

Two-dimensional model experiments were conducted in a glass sided wave tank (14m x 0.46 m x 0.5m), which is shown in Figures 5.1 and 5.2. The model used for this study has been simplified to include only wave action and seepage processes relating to beach drainage. The land flux is zero, and during each test run there is no tide operating. Instead, the effect of the tide is modelled as a series of head increments, by filling or emptying the tank between each of a series of tests.

Discharge

Water collected by the beach drain flowed under gravity to the sump which is located behind the beach and separated by a panel in the back of the tank (Figures 5.1 and 5.2). The sump was dewatered using a submersible pump, and discharge measurements were recorded using a sump depth gauge prior to pump submersion. Note that in Figure 5.1 the pump is located outside of the sump, however during the tests the submersible pump was placed inside the sump.

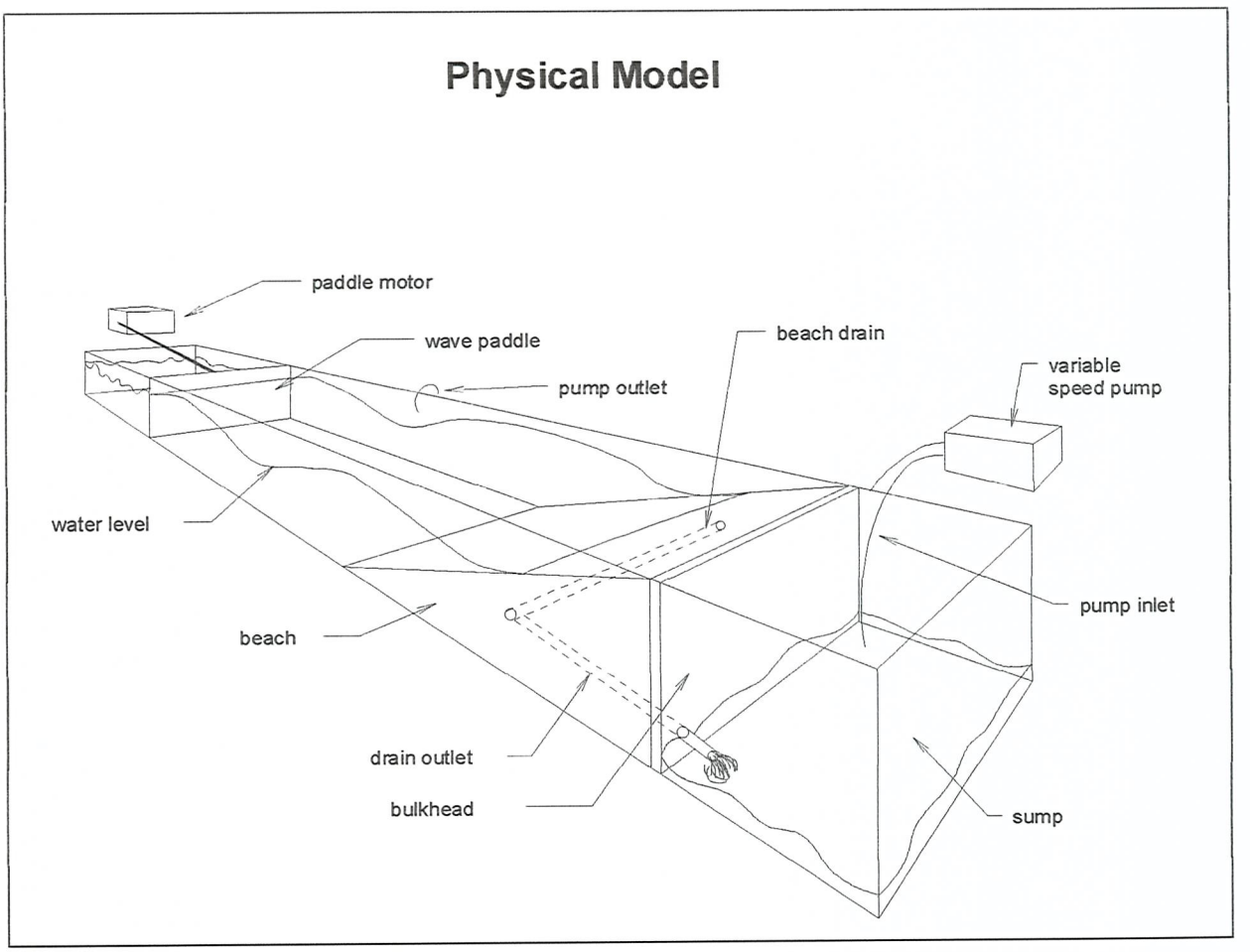

Figure 5.1: Schematic diagram of wave channel (drawn by R. Shaw)

Figure 5.2 Photograph of wave tank

Monochromatic waves

Waves were produced using a monochromatic wave generator (Figure 5.3). The frequency and wave length were altered manually, while the actual wave height and period were recorded electronically using surface penetrating wave probes. One of the wave gauges can be seen fixed to the trolley in between the two point gauges in the photograph below (Figure 5.4). Data were recorded as a voltage, and readings were calibrated and converted into water depth. Wave measurements were recorded in both the near shore and offshore regions to detect any wave reflection. Wave reflection resulted in some interference between the reflected and incident wave, and this lead to a relatively small fluctuation in the measured wave height (see section 5.4.5). It is assumed that all waves in the tank are shallow water waves.

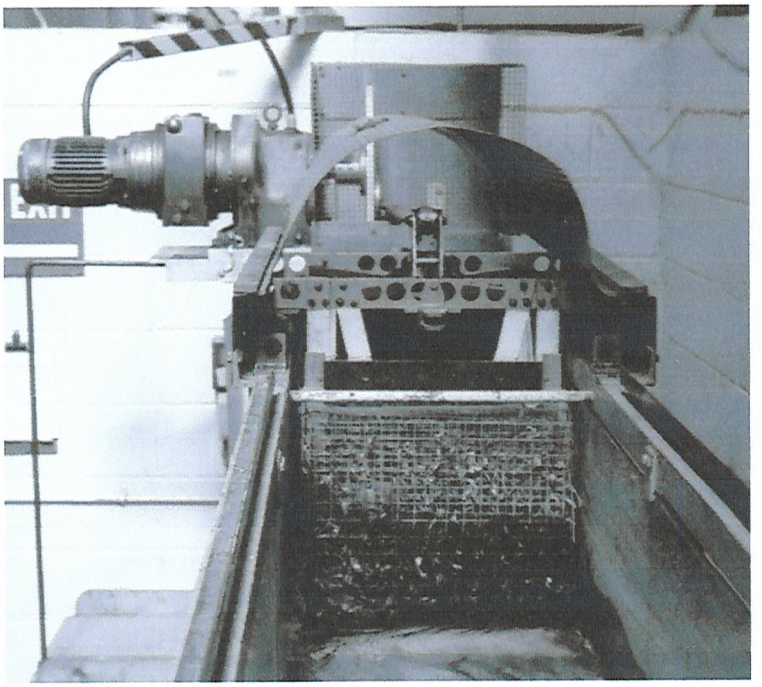

Figure 5.3 Wave generator

Figure 5.4 Two point gauges and surface penetrating wave probe fixed to moveable trolley.

Model beach

The model beach consists of a ground Bakelite model sediment. Bakelite is a dense plastic with a specific gravity ($G_s = \rho_{sediment}/\rho_{water}$) of 1.45 (the specific gravity of the prototype sand is 2.65). The 50% passing particle diameter is 0.51mm (see section 5.4.1), while that of the prototype sand is 0.25mm, and the initial gradient of the beach was approximately 6%. Sediment characteristics and beach slope are discussed in section 5.4.

Profile preparation and measurement

The profiles were prepared manually using a brick-layer's float and marker lines on the glass side of the tank as a guide. The beach levels were measured using a point gauge supported by a trolley which runs on the sides of the tank (Figure 5.4). The beach profile was measured along two sections, and was recorded at the beginning and end of each test. If the profile preparation was revealed to be insufficiently accurate during the initial profile measurement (as indicated by excessive discrepancy between the required 6% profile and the actual measurements), then the beach was reformed and the initial profile re-measured.

Still water level

The tank was filled or partly emptied to change the position of the still water level (SWL) intersect on the beach face. The distance between the SWL intersect and drain position in the horizontal direction has been labelled as y. The drain is located at y = 0; $y_{positive}$ = SWL landward of drain (drain flooded), $y_{negative}$ = SWL seaward of the drain. If y is negative, this does not necessarily mean that the drain elevation is higher than the SWL because the drain is buried several centimetres below the beach surface.

Pore water pressure transducers

The design and fabrication of the pressure transducers posed a technical challenge, and for this reason details of the pressure transducers are included in this section. Pore water pressure transducer (PPT) housing units were constructed in order to keep the electronics dry, while allowing the front portion of the transducer to be exposed to the water. Figure 5.5 shows a photograph alongside a schematic diagram of the PPT units.

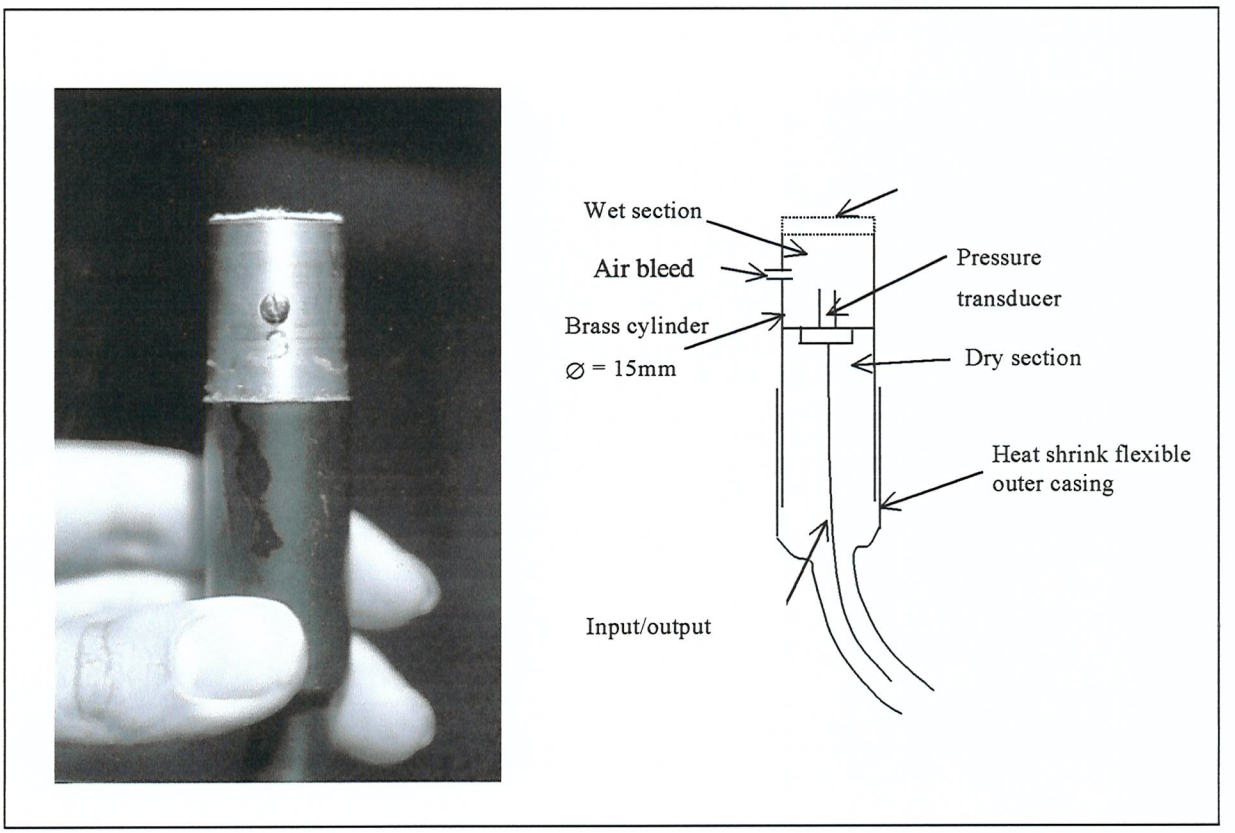

Figure 5.5 Pore water pressure transducers for use in model beach (not to scale)

The necessary watertight seals were made with silicone sealant, and the internal seals between the wet and dry compartments were made with o-rings. Four PPT units were made, and it was decided to mount them on a rigid rack in order to keep them in place when waves were operating. The PPTs were held on the rack with cable ties, and the PPT rack was fixed in place when mounted in the wave tank. Four PPT units and the aluminium rack are shown in Figures 5.6 and 5.7. The output pressure for the transducers was gauge pressure, therefore no adjustment for atmospheric pressure was necessary.

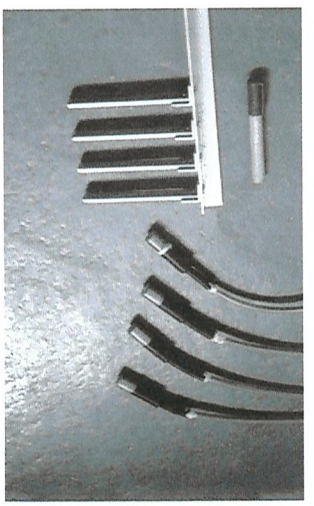

Figure 5.6: 4 pore water pressure transducer units and mounting rack

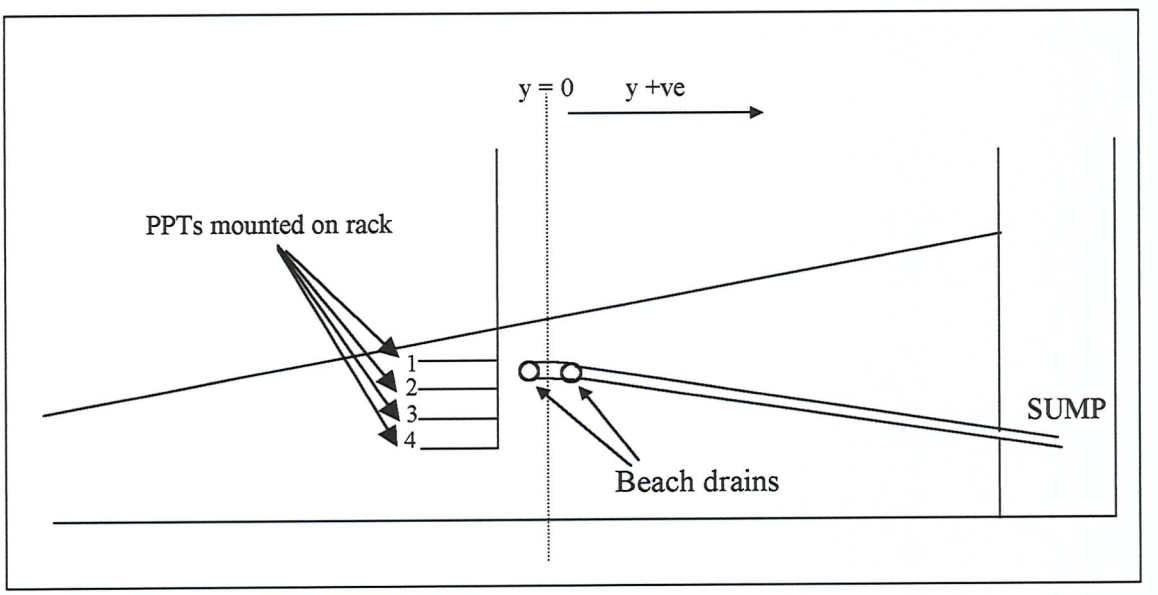

Figure 5.7: Schematic diagram of PPT rack in model beach. Drain is located at y = 0

Note that measuring the pore water pressure is different from measuring the water depth using manometer tubes. The pore water pressure (PWP) does not necessarily indicate the depth of water (PWP/ρg does not necessarily = depth), since conditions are not hydrostatic. It is preferable to have pore water pressure measurements rather than manometer levels because:

a) the pore water pressure affects the sediment shear strength, regardless of the water depth;
b) manual observations of manometer tube readings would be difficult to quantify (previous studies at the University of Southampton have used video recordings to evaluate the manometer level fluctuations with time); and
c) the exact water depth is affected by capillary action, and successive swash infiltrations, hence it is not clear exactly which manometer depth to use.

The transducer arrangement as shown in Figure 5.5 would remain watertight for several days, however, water ingress resulted in short circuiting of the PPT electronics on several occasions. In retrospect, epoxy resin would perhaps have been better for maintaining the watertight seal. Alternatively the electronic connections may be lacquered to provide a temporary watertight circuit a method previously used by the University of Bristol. Despite problems with water ingress, efficient planning lead to the recording of several data sets, and these will be discussed in Chapter 7.

The wet compartment within the PPT was de-aired using the air bleed valve (Figure 5.5), and trapped air in the wet compartment was as equally problematic as water in the dry compartment. Workshop fabricated PPT units were used instead of those commercially available since they were less expensive (more disposable), custom made for this specific problem, and more accurate.

Concurrent studies: University of Caen apparatus

In Chapter 2 it was noted that a concurrent study was carried out at the University of Caen. The apparatus used for this PhD project is akin to the University of Caen apparatus in terms of dimensions and general techniques. Both models use a 1:20 model to prototype linear scale factor for the important length dimensions, and wave probe instrumentation is the same. The principal differences are that the University of Caen model

- has an irregular wave paddle,
- uses sonar instrumentation for beach profile measurement,
- has a silica sand beach (D_{50} = 0.15mm),
- analyses data through comparing one profile to another,
- has no pore water pressure instrumentation, and
- is a model of a specific beach, and land flux and tides have been modelled.

There are several crucial differences in terms of the tests carried out and data analyses. The aim of the Southampton model experiment was to investigate each of the controlling variables in isolation. Tests were repeated several times for a range of values for the controlling variable, to determine the relationship between the dependent and controlling variables, and a graph was then constructed from which a trend could be identified.

In contrast, the Caen model is based on a specific full scale system (Les Sables d'Olonne, France), and all the principal variables present in the field have been modelled in the laboratory (namely the tide, land flux and wave climate).

5.2 Scaling

5.2.1 Principles of similarity

Linear Scale

The linear scale factor was determined by the wave tank dimensions, and a practicable value for the apparatus geometry was 1:20. All important linear dimensions have been scaled according this factor so that the model is geometrically similar to the full scale system. The principle geometric features were identified as the pipe depth, and pipe location (in the horizontal plane in relation to still water level). The pipe diameter and perforation hole size are less crucial since the amount of water that can enter the pipe is limited by other more dominant factors, and are thus not subject to the linear scale factor (these parameters have been investigated separately in section 5.4.2). The pipe was designed such that the system permeability was high in relation to the permeability of the surrounding material.

Parameters for a full scale system have been based on Branksome Chine full scale trial system, which was described in Chapter 3. All systems tested in the preliminary experiments have two pipes at 100mm centres and a cover depth of approximately 60mm, representing field pipes spaced at 2 metre centres at a depth of approximately 1.2m below the surface of the beach. Although four pipes were installed in the prototype beach, only two were operational at one time.

The impermeable boundaries of the sides and back of the wave tank, although not geometrically similar, do mimic the sea wall and groynes on the full scale beach. Branksome Chine is backed by a concrete sea wall, and under normal conditions the tide does not reach the foot of the wall. Therefore the effect of this wall is to provide an impermeable boundary at the rear of the beach which is effectively the same as the plastic false back in the model. The model is two dimensional with the sediment confined by the walls of the tank. In the field lateral movement is restricted by the existence of groynes which divide the beach at 100m intervals.

Kinematic Similarity

To achieve kinematic similarity, the model must reproduce to scale the flow velocities experienced in the prototype (e.g. Hamill, 1995). Kinematic variables for the beach drainage problem are: the velocity of the water percolating through the beach,

sediment fall velocity, system discharge (seepage velocity), and the rate of wave propagation up the beach (rate of beach face wetting). If the pipe permeability is sufficiently large in relation to the permeability of the surrounding material then the flow rate is limited by primarily beach permeability and still water level. Hence the principal kinematic factors are:

- beach permeability (rate of soak away)
- rate of beach face wetting (rate of wave propagation over the beach face)
- sediment fall velocity

Dynamic Similarity

This law requires the model to reproduce to scale all the forces experienced within the prototype (e.g. Hamill, 1995). The forces on the model system elements are: forces due to gravity, viscous shear, surface tension, forces due to elastic compressions and any pressure forces which arise due to motion. The resultant force is equal to the vector sum of these forces. For model-prototype similitude the ratio of the individual forces (model: prototype) must equal the ratio (model: prototype) of the sum of the forces.

It is not possible to satisfy this latter requirement, since no such model fluid is available, (Hudson and Keulegan, 1979). However, not all of the forces listed above are necessarily significant in the process under consideration, and hence surface tension and elastic compressions are assumed to be negligible in relation to gravity and viscosity.

Wave scaling is dominated by the force due to gravity, and all other forces may be assumed to be minor in relation to this dominant force. Gravity dominated processes are expressed by the ratio of gravitational to inertial forces, combined in the dimensionless group known as the Froude number (this will be discussed further later in this chapter).

Sediment transport modelling

The 2 main aims of using a physical model in this project were to

1. determine the effect of artificial drainage on beach formation for a range of conditions
2. explore the impact of beach drainage on pore water pressure in an attempt to understand the mechanism of beach stabilisation through drainage.

While physical modelling has the advantage of allowing for the visualisation of processes, and provides a good forum for the development of concepts and understanding, the interpretation of results must be approached with much caution.

This study is primarily a moveable-bed beach profile model. Scaling laws for moveable bed models are well documented (e.g Hughes), and suitable scaling criteria have been identified from previous work (e.g Bagnold, 1940; Kamphuis, 1975, 1985 and 1991; Dalrymple, 1989). However, since this is the first model investigation into drainage induced pore water pressure reduction in the swash zone, interpretation of the model results does not necessarily conform to previously used methods. Additional variables important to this model (i.e. not generally considered in more conventional coastal physical models) are the beach drain discharge and the beach pore water pressure.

Clearly, there are a large number of variables, not all of which conform to previous analyses. Therefore a dimensional analysis has been carried out to ensure that all possible dimensionless groups pertaining to the beach drainage model have been identified.

5.2.2 Dimensional analysis

Dimensional analysis of the beach drainage problem was carried out using the Buckingham 'Pi' theorem (Buckingham, 1914). The list of variables includes independent and dependent quantities for both the drainage system and surrounding environment, and these were divided into four categories. The set or variables, V comprise: V_1 (sediment properties) = {W_s, w, k, D_{50}, ρ_s}; V_2 (wave properties) = {T, H, L}; V_3 (fluid properties) = {ν, ρ_w, τ}; and V_4 (system properties) = {Y, D, V, q, P}. A summary of the symbols and definitions is given in Table 5.1.

Category	Variable	Symbol	Units	Dimensions
Sediment properties	Weight of sand particle	W_s	kgm^{-2}	MLT^{-2}
	Sediment fall velocity	w (or velocity, v)	ms^{-1}	LT^{-1}
	Permeability of beach	k	ms^{-1}	LT^{-1}
	Sediment dimension	D_{50}	m	L
	Density of sediment	ρ_s	kgm^{-3}	ML^{-3}
Wave properties	Period	T	s	T
	Height	H	m	L
	Wave length	L	m	L
Fluid properties	Viscosity	ν	m^2s^{-1}	L^2T^{-1}
	Density	ρ_w	kgm^{-3}	ML^{-3}
	bottom shear stress	τ	$Kgm^{-1}s^{-2}$	$ML^{-1}T^{-2}$
Swash zone and system properties	Still water level (tide level, or head)	Y	m	L
	Linear scale length dimension e.g. drain depth, diameter or position	D	m	L
	Volume of sand gained	V	m^3	L^3
	System discharge (where $q = f(Y, D, W_s, D_{50}, k, \nu, \rho_w, H, L, T)$	q	m^3s^{-1} per m → m^2s^{-1}	L^2T^{-1}
	Pore water pressure	P	$Kgm^{-1}s^{-2}$	$ML^{-1}T^{-2}$

Table 5.1: Summary of variables (Repeating variables have been shaded).

There are 16 variables, n, and three primary dimensions, m, = {M, L, T} = {mass, length , time} have been adopted. Hence there are $(n - m) = 13$ dimensionless groups. The repeating variables include a length dimension, velocity and fluid property.

Repeating variables:	**v**	**D**	ρ_w

The 13 dimensionless, or 'Π' groups may be obtained by combining each of the variables in Table 5.1 with the selected repeating variables. The dimensionless groups are listed in Table 5.2 below (not all groups are listed, since several contain the same dimensions, but with different meanings attributed – e.g. SWL, D_{50}, Y all have length dimensions and have been denoted by D).

$\Pi_1 = \frac{vT}{D}$	$\Pi_6 = \frac{v}{\sqrt{gD}}$
$\Pi_2 = \frac{D^3}{Vol}$	$\Pi_7 = \frac{Y}{D}$
$\Pi_3 = \frac{q}{vD}$	$\Pi_8 = \frac{v}{k}$
$\Pi_4 = \frac{\rho s}{\rho_w}$	$\Pi_9 = \frac{P}{\rho v^2}$
$\Pi_5 = \frac{\upsilon}{vD}$	$\Pi_{10} = \frac{\tau}{\rho v^2}$

Table 5.2: Dimensionless groups for beach drainage model

5.3 Discussion of dimensionless groups

5.3.1 Geometric similarity

Geometric similarity is determined by the ratio of lengths for the model and prototype: $\Pi_7 = Y/D$. The model has been designed so that this ratio (where Y and L are the principal length dimensions, e.g. cover depth, still water level location and pipe diameter) are the same for the model and the prototype.

5.3.2 Wave scaling

Froude number

The objective of the monochromatic model wave generator is to provide either erosive or accretive conditions for the model beach and to reproduce dynamically similar conditions to those likely to be encountered in the field. The main parameters relating to waves are the geometrical terms height, length and water depth, and temporal terms which are wave period and celerity (Chadwick and Morfett, 1993).

Scale models involving a wave tank would typically be based on similarity of the Froude number, $F = c/\sqrt{gD} = \Pi_6$, where c = wave celerity (see e.g. Chadwick and Morfett, 1993). The nearshore environment concerns shallow water waves since h/L <1/20, where h = water depth and L = wave length. In this case, the wave celerity, c, and wavelength, L may be approximated to:

$c = \sqrt{(gh)}$ and

$L = T\sqrt{(gh)}$

(where h = mean water depth)

→ c = L/T for shallow water conditions. Substituting into the Froude number:

$$F = \frac{L}{T\sqrt{gh}} \qquad [1]$$

For similitude:

$F_{model} = F_{prototype}$

$$\left[\frac{L}{\sqrt{gh}}\frac{1}{T}\right]_p = \left[\frac{L}{\sqrt{gh}}\frac{1}{T}\right]_m$$

$$\frac{L_p}{L_m}\frac{\sqrt{(gh)_m}}{\sqrt{(gh)_p}}\frac{T_m}{T_p}=1$$

The terms L and h are length dimensions, and are subject to the linear scale factor, which for this model is 1:20 (model: prototype). Hence:

$$\frac{20}{1}\frac{\sqrt{1}}{\sqrt{20}}\frac{T_m}{T_p}=1$$

$$\boxed{T_p = \sqrt{20}\ T_m} \quad \text{and} \qquad [2]$$

$$\boxed{H_p = 20\ H_m} \qquad [3]$$

Model wave conditions

The approach adopted in this study is based on that used by Bagnold (1940), whereby the range of possible dimensionless values likely to be found in nature is calculated for the full scale system, then the model values are calculated and compared. The model conditions are not selected to represent specific full scale conditions, rather a range of conditions similar to the range of conditions typically encountered in the field.

Table 5.3 shows the paddle stroke and motor speed settings used for the model tests.

Paddle stroke	Motor speed	Wave height (m)	Wave period (s)	Calculated wave length = T√gh (m)
10	2.5	0.0135	1.59	2.50
110	2.5	0.11	1.59	2.50
40	2.5	0.048	1.59	2.50
75	2.5	0.08	1.59	2.50
110	4.5	0.11	1	1.57
4	2.5	0.008	1.59	2.50
120	5	0.11	0.9	1.41
95	7.5	0.085	0.75	1.18
110	3.5	0.11	1.25	1.96
130	5	0.11	0.9	1.41

Table 5.3: Wave climates used in model tests

Table 5.4 summarises the range of wave periods and wave heights used in the model. These have been scaled up according to Froude's law to show the corresponding prototype conditions. The Branksome Chine data have also been included in this table to indicate the actual recorded range of full scale conditions.

Model range used for tests	Corresponding full scale conditions	Branksome Chine conditions (recorded)
0.75s < T < 1.59s	3.35s < T < 7.11	2s < T < 10s
0.008m < H < 0.11m	0.16m < H < 2.2m	0.2m < H < 1.5m

Table 5.4: Summary of range of full scale and model conditions (model conditions have been scaled according to Froude's Law)

As can be seen in Tables 5.3 and 5.4 the range of conditions tested in the wave tank are typical of the range of conditions likely to be encountered in the field. When tests were carried out for constant wave conditions, the wave climate with a paddle stoke of 110mm and motor speed of 2.5 tended to be used. Wave generator settings were abbreviated to 'paddle stroke/motor speed', hence the formerly mentioned climate becomes 110/2.5.

5.3.3 Sediment transport

i. General

Dimensional analyses for sediment scaling differ slightly from the analysis presented in section 5.2.2 above (i.e. these do not contain terms specific to the drain system). The aim of this section is to present the generic dimensionless set used for moveable bed models described in previous work, and then to discuss these in the context of the beach drainage model.

Kamphuis (1985 and 1991) derived a set of 5 dimensionless numbers for use in sediment transport models (see e.g. Hughes, 1993). These are:

$$\Pi_s = g\left[\frac{v_* D}{\nu}, \frac{\rho_w v_*^2}{\gamma_i D}, \frac{\rho_s}{\rho_w}, \frac{Y}{D}, \frac{w}{v_*}\right]$$

where:

v_* is the shear velocity ($= \sqrt{\tau/\rho_w}$); τ = bottom shear stress; γ_i = submerged sediment specific weight ($= \rho_s - \rho_w)g$; ρ_w = density of water; ρ_s =density of sediment particle

D = grain size; Y = length dimension

The above groups correspond to the dimensionless numbers Π_5, Π_6, Π_4, Π_7, and Π_8 (from section 5.2.2) respectively.

Specific gravity, G_s

The ratio of densities is simply the grain specific gravity.

Relative length

Y/D is simply a length ratio as discussed in section 5.3.1.

Grain size Reynolds number

The term

$$R_* = \frac{v_* D}{\nu}$$

is known as the grain size Reynolds number. In this instance, the Reynolds number relates to the *sediment* properties and the velocity term is the shear velocity, $v_* = \sqrt{\tau/\rho_w}$ (see e.g. Hughes, 1993; Chadwick and Morfett, 1993).

Densimetric Froude Number

The term

$$F_* = \frac{\rho_w v_*^2}{\gamma_i D}$$

is known as the densimetric Froude number. Both the densimetric Froude number and the grain size Reynolds number will be discussed later in this chapter.

Relative fall speed

The ratio of fall velocity to shear velocity is known as the relative fall speed. This will be discussed further in section 5.3.4.

ii. breaking zone

The above dimensionless set contains the term v_* for bed shear stress, which is the primary cause of sediment transport for bed-load dominated models. These apply therefore to the offshore environment, when suspended sediment is minimal and bed-load dominates.

As the wave approaches the beach and breaks, the mode of transport changes from bed-load dominance to suspended sediment dominance. The beach drainage model described in this thesis is concerned primarily with the beach profile in the surf zone – a region where the primary transport mode is sediment suspension.

Although bed-load may dominate for the final part of the wave run-up, sediment particles are in suspension for the majority of the swash-backwash cycle, and for the most part, sediment suspension dominates.

To make the scale criteria more appropriate for suspension dominated models Kamphuis (1991) replaced the term for shear velocity (v_*) with $\sqrt{gH_b}$. H_b is the breaker height, and may be substituted by the length dimension Y (since the wave height is scaled according to the linear scale factor). Thus the Kamphuis set of dimensionless numbers for sediment transport similitude in the breaking zone is:

$$\Pi_{bz} = g\left[\frac{\sqrt{gH_b}}{\nu}D, \frac{\rho g H_b}{\gamma_i D}, \frac{\rho_s}{\rho_w}, \frac{H_b}{D}, \frac{w}{\sqrt{gH_b}}\right]$$

Dean number

Dimensional analysis carried out by Dalrymple (1989) omitted the term Y and included terms for the wave height and period. The dimensionless groups comprise the grain size Reynolds number, the densimetric Froude number, the specific gravity and the Dean number, Dn, where:

$$Dn = \frac{H}{wT}$$

Sediment selection

Previous work investigating beach drainage systems (Weisman *et al.*, 1995) has used the Dean Number to scale the sediment. According to Weisman *et al.* (1995) a scale effect arises when using the sediment-fall-time parameter scale criteria. For given wave tank dimensions, waves are scaled down so that they fit into the available space, and therefore a reduction in wave period is in most cases unavoidable. To achieve model-prototype similarity using the sediment-fall-time criteria (H/*w*T), it is necessary to scale down the model sediment fall velocity. In the case of the Weisman *et al.* (1995) model this was achieved by reducing the particle size. The model beach is therefore subject to a higher frequency of beach face wetting, but due to the finer beach material, a slower rate of soak away. This combination results in a wetter beach face in the model than in the prototype (Weisman *et al.*, 1995).

In an attempt to minimise scale effects observed by Weisman *et al.* (1995) a model sediment with a lower specific gravity than that of the prototype, but a larger D_{50} was used so that a high permeability can be maintained while the weight of the particle is kept to a minimum.

While it is possible to select the specific gravity and particle size so that the densimetric Froude number and grain size Reynolds number criteria are satisfied, by doing this, it becomes impossible to fulfil the relative length and relative density conditions. F_* and Re_* are the axes on the Shields diagram for incipient motion (Shield, 1936) and ensuring that $[F_{*\,model} / F_{*\,prototype}] = [Re_{*\,model} / Re_{*\,prototype}] = 1$ ensures that the threshold of motion in the model and prototype are similar.

Kamphuis (1975 and 1991) warned of several problems arising from the use of lightweight sediments (from Hughes, 1993):

- transport rates are underestimated, and particles may go into suspension earlier than in the prototype
- lightweight sediment is relatively heavier when not submerged, which may lead to piling up of the material at the shoreline. These particles are then more difficult to move, and hence light weight sediment is not ideal for modelling bed-load phenomena such as accretion

- since the relative length is not scaled properly, the particles are disproportionately large in the model, which reduces the magnitude of sediment movement (this is thought to be the largest scale effect in lightweight models)
- lightweight sediment moveable beds are more porous because the particles are too large (thus relatively more wave energy is absorbed)
- liquefaction of will occur more easily
- the relative fall speed cannot be scaled properly, hence the sediment transport is not properly modelled

Clearly there are unavoidable scale effects concerning the use of a Bakelite sediment, however, this does not necessarily jeopardise the value of the results as a qualitative indication of beach profile response to beach drainage. Kamphuis (1985) concluded that lightweight sediment models are limited, and their use is now relatively rare. However, the beach drainage model described in this thesis aims to utilise the main disadvantage of a light weight sediment, (that the grain size is larger that it should be), to compensate for the beach face wetting problem that has arisen in the specific case of beach drainage modelling.

Weisman *et al.* (1995) found that the water in the model drained away more slowly than in the prototype, and that this problem was exacerbated by the reduced wave period, resulting in a 'wet' beach face, and underestimated results. It may also be inferred that underestimating beach volume change may lead to increased error margins, since the magnitude of change is small in relation to the accuracy afforded by the instrumentation and laboratory techniques.

Kamphuis (1985) states that lightweight sediment is not suitable for modelling beach accretion (where accretion is function of natural swash zone processes). However, in the context of beach drainage, accretion is in fact a phenomenon of drain discharge and thus infiltration rate or *particle size*. Therefore, if, as Kamphuis (1985) states particle sizes are *larger* than they should be in the lightweight model, then infiltration will also be disproportionately large, and therefore the effect of the drainage system exaggerated. Thus

a) the effect of the drainage system will be superimposed onto a background environment in which natural accretion is minimal
b) any accretion that does occur is likely to be attributed to the presence of a beach drain, and
c) accretion occurring on account of the drainage system will be augmented since it is a function of (among other things) grain size (since the accreted volume α Q as will be shown in chapter 8). This will make the trend more apparent, reduce the margin of error, and therefore allow for easy identification of the trend.

The primary disadvantage however, is that results are entirely qualitative, and undrained profile formation is unlikely to be representative of full scale behaviour. However, due to the above observations, the effect of the drainage system is exaggerated (hence unambiguous), and sensitivity to controlling variables can easily be identified.

5.3.4 Beach face wetness

The fact that Weisman *et al.* (1995) conclude that the beach face is wetter than that of the prototype, suggests that a means of quantifying the wetness of the model beach face in relation to the wetness of the model face would be useful, and that wave frequency and rate of soak away are important considerations in the model. Further more, research carried out for this PhD has demonstrated that beach drainage system performance is proportional to the system discharge (see Chapter 8), and according to Darcy's and Hazen's laws respectively (see e.g. Powrie, 1995), discharge is proportional to permeability and hence particle size. Since the principal aim of this experiment is to determine the effect of the beach drainage system (where the 'effect' is denoted by beach volume change in the swash zone), and 'effect' α Q α k α D, one could argue that infiltration rate and frequency of beach face wetting (since this is ultimately the supply of water to the beach face) are the most important considerations for this model.

In Chapter 7 it will be shown that pore water pressure is also proportional to system discharge, and that pore water pressure affects the shear resistance of the beach material.

Therefore the amount of water allowed into the beach face directly affects the magnitude of the discharge and thus the magnitude of the pore water pressure reduction and beach volume change (identified as a principal mechanism of beach stabilisation through drainage in chapter 4). One of the main aims of the model experiments described in this dissertation is to determine the effect of influencing variables on drainage system performance. Therefore similarity between the model and prototype in terms of seepage rate is an important scale criteria, and one which has important implications for the interpretation of results.

Development of a beach face wetness scale criteria

For hydrostatic conditions the amount of water entering the beach drain is controlled by the head of water (still water level), the beach material permeability, and the flow path length (geometry of the beach → beach slope). During wave operation the discharge also depends on the amount of water being supplied through swash infiltration.

The processes of beach face wetting and swash infiltration are complex because water is supplied to the beach face periodically, and therefore water seeps through the beach face in pulses. The area over which water is supplied to the beach face is denoted by the length of the run-up zone, and this is controlled by the wave height and beach slope. The frequency of beach face wetting is denoted by the wave period, T. Therefore the important parameters that affect beach face wetting and seepage rates are:

- beach material permeability (or particle size)
- beach slope
- still water level depth above drainage system
- run-up length (wave height)
- wave period

The problem with using the Dean number for scaling the model sediment is that the equation uses the sediment fall velocity, which is a function of both the grain size and density. Infiltration rate however, is affected only by the grain size (i.e. permeability), and in this instance the particle density is irrelevant.

To determine how wet the model beach face is in comparison to the prototype it would be more accurate to use a ratio of rate of wetting to rate of soak away. Thus the relative fall speed group (w/v), has been replaced by the ratio of two velocities, rate of beach face wetting, v : rate of soak-away, k (permeability):

$$\Pi_8 = v/k. \qquad [1]$$

The rate of beach face wetting may be equated to the rate of passage of the surge over the beach face. One cycle takes place over one wave period, T. During this time, the water travels twice the distance of the run-up length, R. Thus:

$$v = 2R/T \qquad [2]$$

The run up length is a function of the wave height, H where the maximum uprush is situated approximately 2H above the still water level, i.e. is a function of wave height (Muir-Wood, 1969). Assuming symmetry about the still water level, the total height from the lower to the upper limit of the swash is

$2H \times 2 = 4H.$

The beach slope, S_0, $= \tan \theta$. When θ is small, $\tan \theta \approx \sin \theta$. Hence:

$\tan \theta = 4H/R = S_0$

$\rightarrow R = 4H/S_0$. Hence equation [2] becomes:

$$v = 2 \times 4H/S_0T = 8H/S_0T \qquad [3]$$

Substituting [3] into [1]:

$$\Pi_8 = \frac{kTS_0}{8H}$$

Likewise with the Kamphuis dimensionless set for the surf zone, the wave height, H, may be replaced by the characteristic length, Y:

$$\Pi_8 = \frac{kTS_0}{8Y}$$

The above expression has been termed the beach face wetness number, W, and will be evaluated and discussed later in this chapter

5.3.5 Summary

Although several transport mechanisms occur in the swash zone, it will be assumed that the dominant mechanism is suspension, and hence the Kamphuis (1991) scale criteria will be used to determine model similitude:

$$\Pi_{bz} = g\left[\frac{\sqrt{gH_b}}{\nu}D, \frac{\rho g H_b}{\gamma_s D}, \frac{\rho_s}{\rho_w}, \frac{H_b}{D}, \frac{w}{\sqrt{gH_b}}\right]$$

The term $\frac{w}{\sqrt{gH_b}}$ will be replaced by the beach face wetness number $\frac{kTS_0}{8Y}$.

For complete similitude, all the scale criteria in the selected set of dimensionless products must be the same in the model as in the prototype. While it is not possible to satisfy all five groups simultaneously (due to practical limitations), a number of the criteria may be satisfied to achieve a degree of model : prototype similitude (see e.g. Hughes, 1993).

Since lightweight sediment models are relatively rare, and materials are not always readily available, it was decided to use a Bakelite sediment that had been previously used in the Chilworth Hydraulics laboratories for moveable bed studies. Hence it was not possible to select the grain size and specific gravity to satisfy the conditions for similitude exactly. Instead, the scale criteria have been calculated for the available sediment so that the deviation from complete similitude may be known (these will be calculated in section 5.5.1).

Before the dimensionless numbers discussed above were evaluated, preliminary tests were carried out to determine the model sediment properties. These are described in the following section.

5.4 Preliminary data collection (test set A)

5.4.1 Sediment characterisation

Particle size analysis

The sediment size distribution was obtained through dry sieving, which was carried out in accordance with BS 1377:1975, Test 7 (a). The particle size distribution (PSD) curve for Bakelite is shown in Figure 5.8a. A PSD curve for a typical Branksome Chine sand sample is shown in Figure 5.8b.

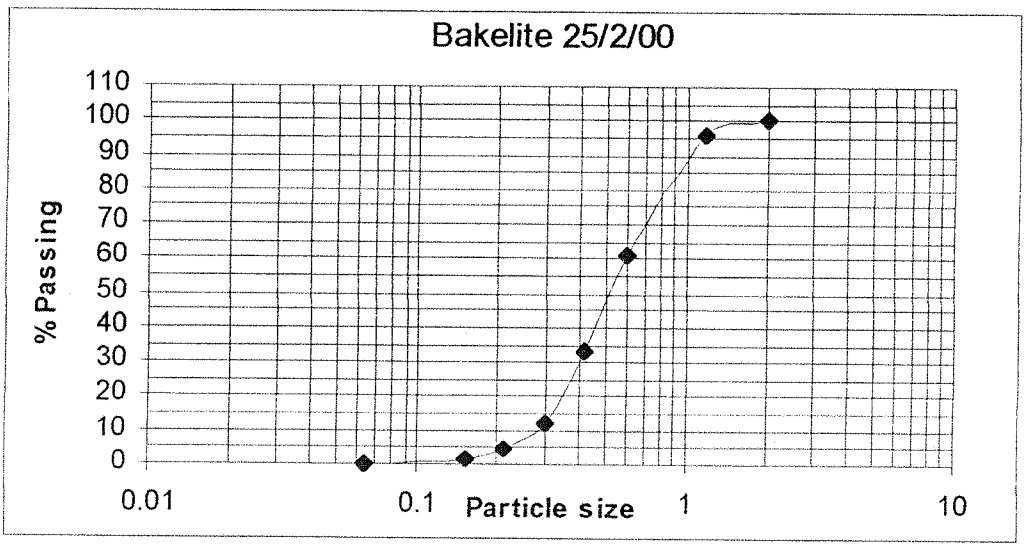

Figure 5.8a PSD curve for Bakelite used in model test.

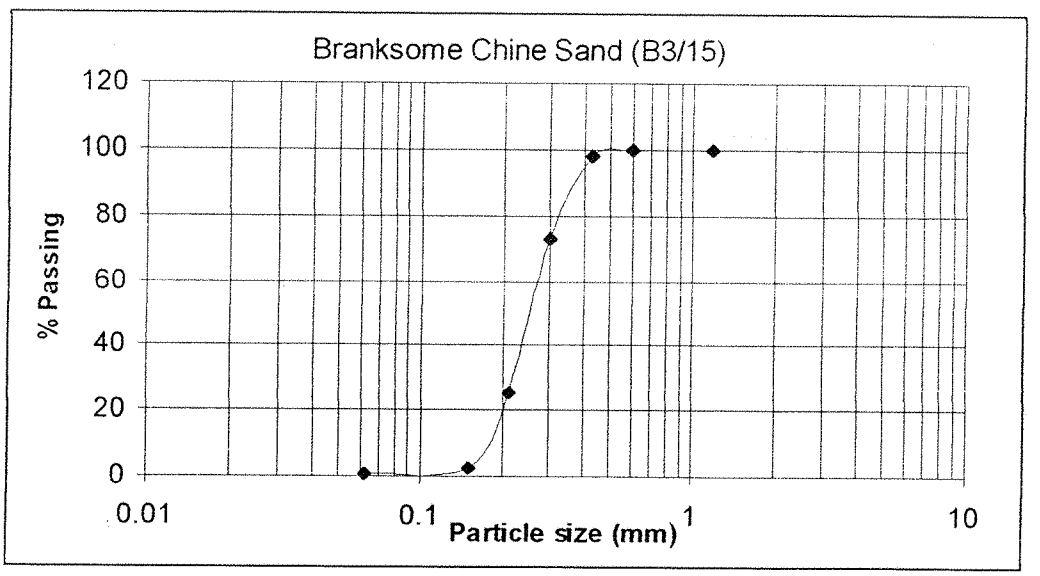

Figure 5.8b: PSD curve for Branksome Chine sand

The D_{50} particle size is 0.51mm, D_{10} = 0.28mm, D_{30} = 0.4mm, and D_{60} = 0.6mm. The coefficient of uniformity, $C_u = D_{60}/D_{10} = 0.6/0.28 = 2.14$; while the coefficient of curvature, $C_z = D_{30}^2/D_{60}D_{10} = 0.4^2/0.6x0.28 = 0.952$. The Branksome Chine and model particle size analysis data are summarised in Table 5.5.

PARAMETER	MODEL	BRANKSOME CHINE
D_{50}	0.51	0.28
D_{10}	0.28	0.18
D_{30}	0.4	0.23
D_{60}	0.6	0.34
C_u	2.1	1.6
C_z	0.95	0.98

Table 5.5: Summary of particle size analysis data for model and prototype

The higher the coefficient of uniformity, the larger the range of particle sizes present in the sample. A well graded soil has a coefficient of curvature value between 1 and 3 (see Chapter 3). The model sand C_U value was found to be larger than that of the field sediment, indicating that it consists of a larger range of particle sizes. However, both the model and full scale C_z values are approximately the same, and it can be seen that the C_u values both indicate a uniformly graded sediment.

Conclusion

Although the grain sizes are larger for the model Bakelite, in terms of the shape of the PSD curve the model sediment is similar to that of the full scale system. The range of particle sizes is slightly larger in the model, but the soils may be considered as equally uniformly graded.

Permeability

The permeability, k, was evaluated using a permeameter (shown and discussed in chapter 3). Samples were tested in both a loose and dense state. The permeameter head/discharge relationship is shown in Figure 5.9. The gradient of the curve equates to Ak, where A = cross sectional area of permeameter (= 45.36cm^2) , and k = permeability. A graph showing a summary of permeability values is shown in Figure 5.10.

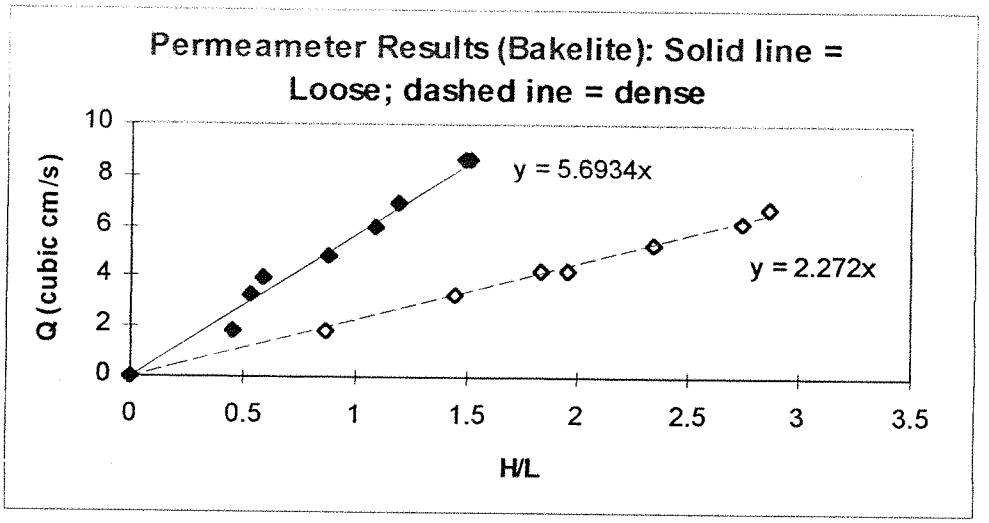

Figure 5.9: Permeameter test results for Bakelite in loose/dense state.

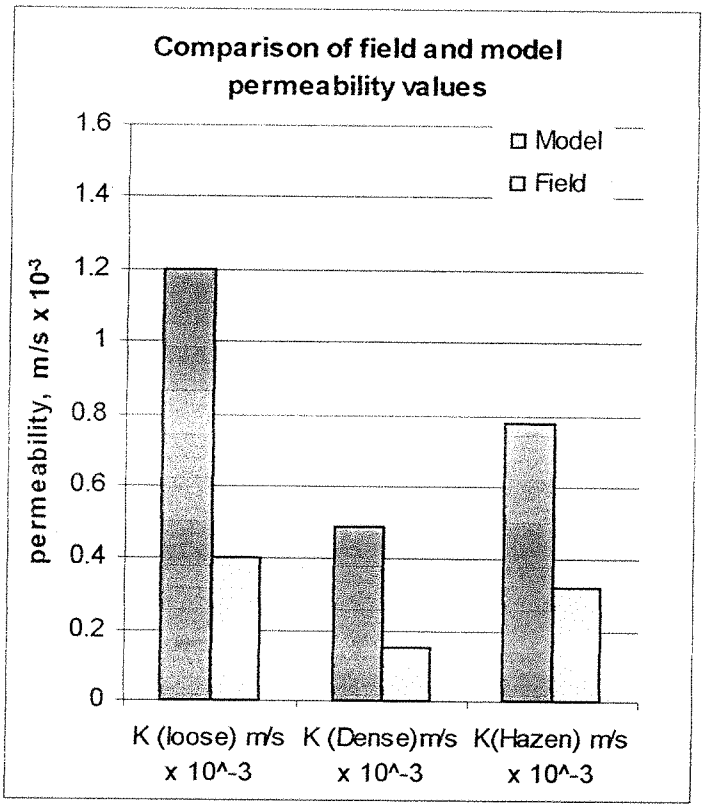

Figure 5.10: Presentation of model and field sediment permeability values

The model permeability ranges from 0.49×10^{-3}m/s when dense to 1.20×10^{-3}m/s when loose. k (dense) for the model is 0.00049m/s, which is 70% larger than k(dense) for the field sediment which is 0.00015. It was found that for both the Branksome Chine and model sediments the permeability was notably higher in the loose state. It is assumed that the main body of the beach is densely packed and the k_{dense} value was used to calculate the theoretical value of discharge (Chapter 6). The beach becomes densely packed due to overburden and wave action (the wave action 'shuffles' the particles into place so that they interlock). The profile is prepared with a float, and the sediment is smoothed into place, which will also contribute to a dense packing. Dense sediment packing was noted in the prototype beach.

Sediment weight

The specific gravity (G_s) of Bakelite was obtained using a narrow necked 'density bottle' (Marin *et al.* 1998), and the wet and dry bulk densities were measured by filling and weighing a 500ml beaker. When the wet density was measured the beaker was vibrated in order to de-air the pore spaces. The bulk density (for a densely packed sample), γ, was found to be:

$\gamma_{dry} = 7.51$ kPa

$\gamma_{wet} = 12.33$ kPa

$G_s = 1.45$

Sediment fall velocity

The sediment fall velocity was calculated using the specific gravity and particle diameter in the Stokes equations below (see e.g. Dyer 1990):

1) Stokes equation for laminar flow:

$$w = \frac{gD_{50}^{2}(G_s - 1)}{18\upsilon}$$

2) Stokes equation for turbulent flow:

$$w = [3.3g(D_{50}(G_s - 1)]^{\frac{1}{2}}$$

In summary, the calculated fall velocities are:

w_{model} (laminar) = 0.056m/s

$w_{prototype}$ (laminar) = 0.049m/s

w_{model} (turbulent) = 0. 086m/s

$w_{ptototype}$ (turbulent) = 0.116m/s

It can be seen that in the laminar flow equation $w \alpha D_{50}^2$, while for turbulent flow $w \alpha D_{50}$. When the laminar flow equation is used, the fall velocity for the model is just higher than that of the field, but for turbulent flow it is vice versa. To determine which value to use a Reynolds number is calculated for the sediment fall velocity, where $Re = wD/\upsilon$ (w = fall velocity, D = sediment diameter, υ = kinematic viscosity). If Re <1, then the sediment particles are said to fall slowly, and the laminar flow equation is used and *vice versa* (see e.g. Dyer 1990). Re was calculated to be greater than 1, thus the particles fall relatively fast and grain inertia dominates, therefore the turbulent flow equation is used. Therefore $w_{Bakelite}$ = 0.086m/s and w_{sand} = 0.116m/s.

Particle Shape

The Bakelite sediment was examined through a microscope to view the particle shapes. Photographs taken through a microscope are shown in Figure 5.11. The scale behind the sediment particles is in millimetres.

From Figure 5.11a it can be seen that a proportion of the larger diameter particles are in fact platy in shape. These particles are flaky in appearance, and can be degraded when rubbed hard between the fingers. Other particles are clearly granular and some almost spherical in shape (5.11b and c). These particle shape observations have implications for sediment permeability (but this is accounted for since it was measured using a permeameter), beach slope, fall velocity, geotextile blocking and hence discharge. These issues are discussed later in this chapter. All the prototype sand particles (Figure 5.11d) are granular, and the nominal particle size is smaller.

Figure 5.11a: Platy particles present in the Bakelite sediment sample (millimetre scale is shown behind the sample)

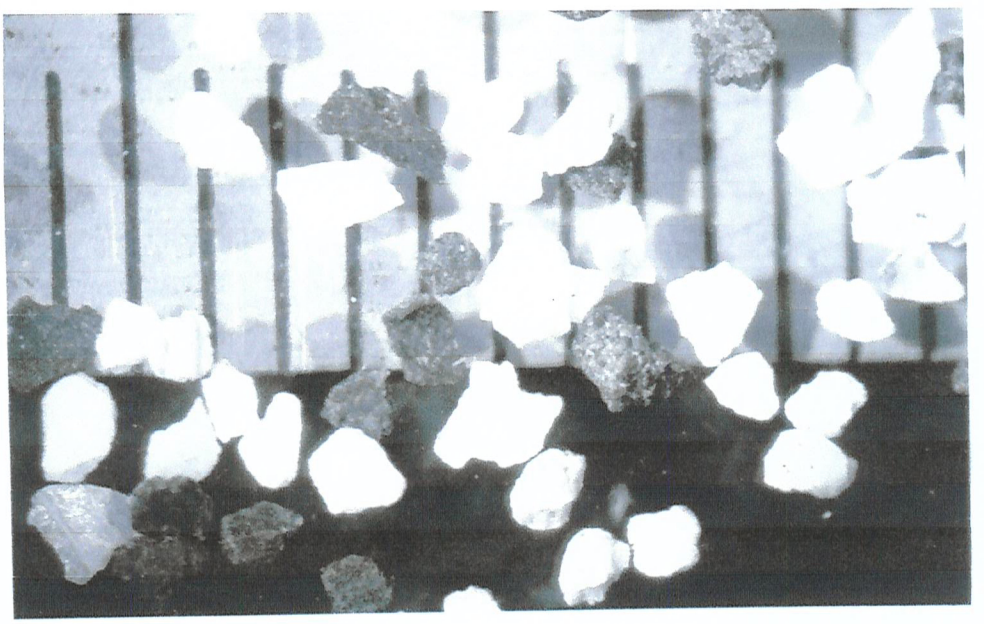

Figure 5.11b: Granular particles found in the Bakelite sediment sample (millimetre scale is shown behind the sample)

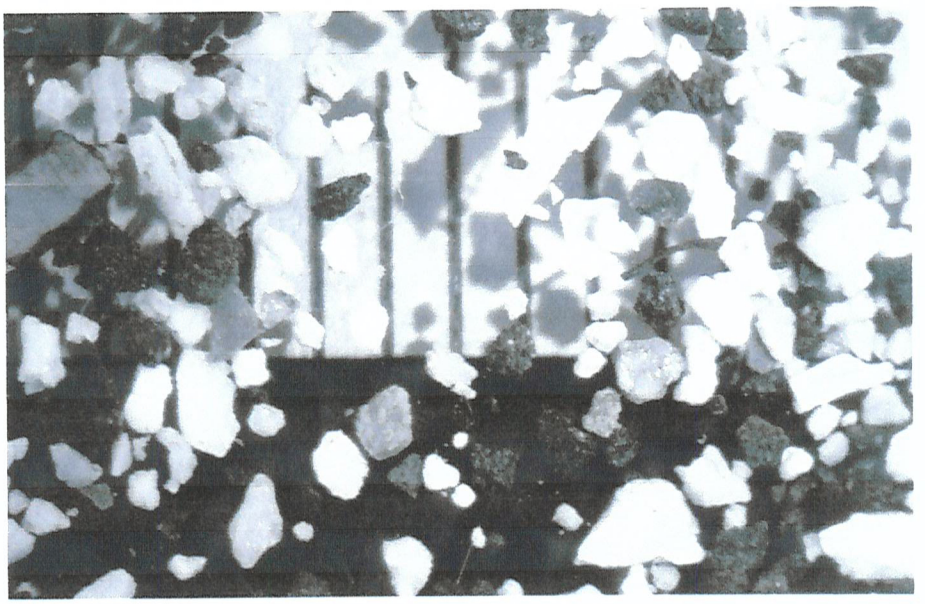

Figure 5.11c: Typical mixture of Bakelite particles (millimetre scale is shown behind the sample)

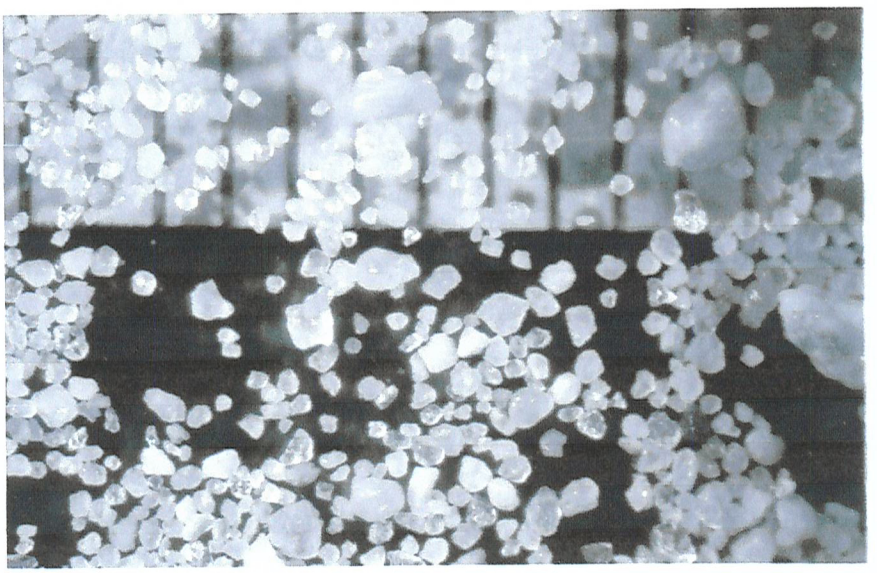

Figure 5.11d: Typical mixture of Branksome Chine sand particles (millimetre scale is shown behind the sample)

5.4.2 Investigation into factors affecting discharge

a) Drain characteristics

The drain system variables are: pipe diameter, geotextile properties, size and number of holes in pipe, cover depth and discharge. Preliminary experiments were carried out to determine the sensitivity of discharge to a number of these geometric features of the drainage system. Table 5.5 summarises the different systems tested, and the data in this table have been compared to identify the principle features that affect the system flow rate.

System 7 has half the hole area of system 1, and approximately 8 times less than system 2. There is some difference in the discharges, but all three values are in the same order of magnitude, and the data suggest that hole area has relatively little effect on system discharge. This is particularly clear in the case of systems 7 and 2 where the difference in hole area is a factor of 8, but the discharges are approximately the same (in fact, the discharge for system 7 is slightly higher than that of system 2). Comparing systems 2 and 3, it can be seen that pipe diameter also had relatively little effect on the system discharge.

The design parameter that has the greatest impact on system discharge is the type of geotextile used. Comparing systems 2 and 6 it can be seen that the use of a felt geotextile as opposed to a black plastic weave made a more significant difference to the system discharge. The gravel matrix filter layer (system 8) promoted a further increase in the discharge.

It will be assumed that provided they are sufficiently large, the pipe diameter and hole size are less crucial since the amount of water that can enter the pipe is limited by more influential governing factors. According to the Darcy equation the governing factors are head and permeability. The model drainage system is designed such that the pipe permeability is significantly higher than that of the surrounding material, rendering k and H the principal governing factors. The effect of still water level on discharge is investigated in further detail in Chapter 6.

System no.	Max. discharge l/min per m (SWL at y = -0.25)	Filter details	Pipe diameter (mm)		Hole diameter	No. of holes	Total area of holes (both pipes)
Set C			External	Internal	(mm)		$m^2 \times 10^{-3}$
1	4.41	black plastic close weave geotextile 0.2 mm thick	15	13	3	168	1.19
2	5.02	As above	15	13	6	179	5.061
3	5.34	As above	20	18	8	107	5.38
4		As above	15	13	As for	system 1.	Valve used to restrict outlet flow
5	0	n/a	No Drain	No Drain	0	0	0
6	7.56	synthetic fibre felt geotextile 2mm thick	15	13	6	179	5.061
7	5.26	black plastic close weave geotextile 0.2 mm thick	15	13	3 As for system 1.	98 Holes blocked using tape	0.692.
8	8.1	As for 6. Gravel matrix around drain	15	13	6	179	5.061

Table 5.6 Model System specifications (Shaded = system used for head discharge graph)

b) Sediment compaction / installation disturbance

During the course of a test, the flow rate was observed to reduce. After newly installing a system, the first discharge reading was always be the highest for that set of data. This may be attributed to the compaction of the disturbed sediment around the drainage system, and the process of particles being drawn against the geotextile by the inflowing water.

c) Change of flow path length with time

The flow rate was also observed to change during a test even when the system had remained in the beach for several days. The profile shape changes as it adapts to the wave climate, and because of this the flow path length to the drainage system also changes. During the test the still water level location migrates landwards or seawards as the beach profile changes shape. This is illustrated in Figure 5.12 which shows the relationship between system discharge and still water level location.

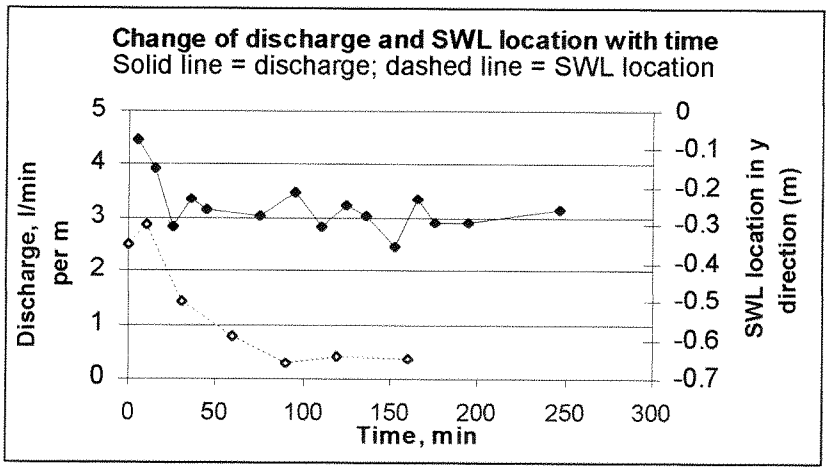

Figure 5.12: Change of discharge and still water level location (≈ flow path length) with time. Moderate wave climate

d) Drain efficiency and blockage

During the preliminary tests it was noted that the discharge may sometimes be inconsistent due to blockage, disturbance (due to installation) and back-washing (due to level differences in the sump and wave tank).

5.4.3 Beach profile

Geometric similarity between the model and prototype is preferable, since this allows for more accurate observation of physical processes (Hughes, 1993). One method of determining whether the model and prototype are geometrically similar is to compare the respective equilibrium beach profiles, since this dictates the ratio of horizontal and vertical length scales.

Theoretically, the final beach profile is independent of the initial profile, since the equilibrium profile will be a function of the sediment properties, wave climate and water level. If these variables are the same for each test, then the equilibrium profile would be the same at the end of each test (so long as the test time is greater than the time taken for the beach profile to reach equilibrium), regardless of the initial profile.

For the preliminary tests a 10% initial slope was used, and this has since been found to be steeper than the equilibrium profile. The problem with using this initial slope is that a relatively large amount of material must be removed from the beach face through back cutting before the new equilibrium profile is formed. Experience with the preliminary tests indicated that the model beach would take several hours to reach equilibrium, as the beach is back-cut and the new profile formed (Figure 5.13). Also, as the beach levels are lowered the drain cover depth changes considerably during the test. A schematic diagram of beach back cutting is shown in Figure 5.14.

Therefore, instead of starting with a steep profile, and waiting several hours for the beach to be back-cut, it was decided to form the initial beach profile near to the equilibrium profile. Thus a more gentle (near equilibrium) slope was used for the initial beach profile. By doing this, any influence of the drainage system becomes apparent in the early stages of the test.

An estimate of the equilibrium profile could be obtained by

- observing the new profile that was formed after back-cutting of the 10% slope,
- measuring the field profile (at Branksome Chine) and assuming that an equilibrium profile exists, or
- calculating the theoretical equilibrium profile.

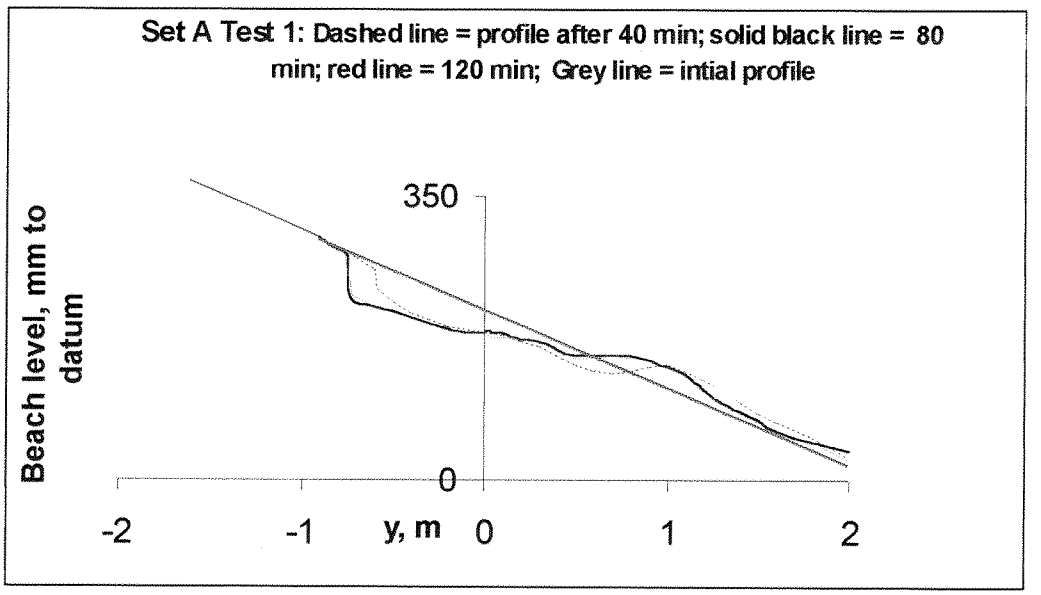

Figure 5.13 Erosion of 10% profile to less steep equilibrium profile (no drainage; moderate wave climate 110./2.5 - see section 5.4.6).

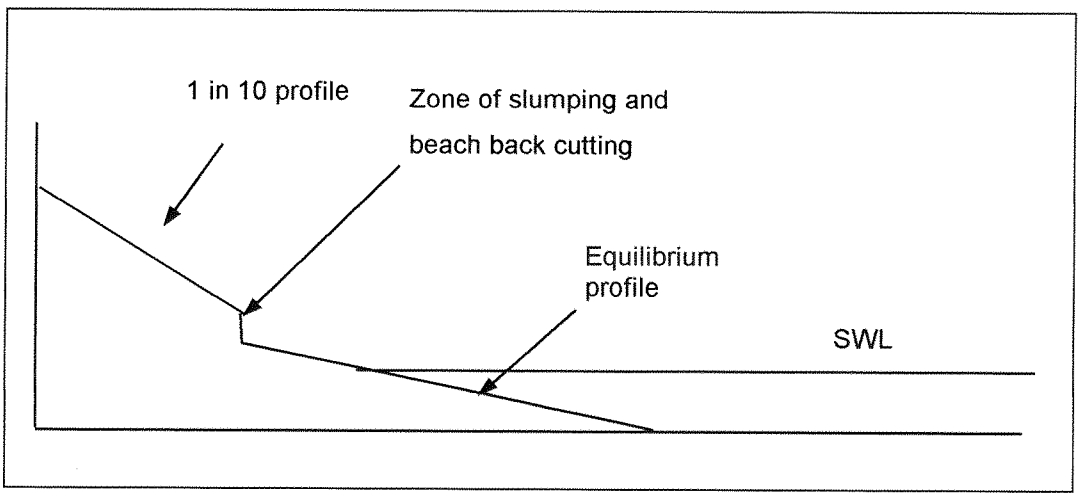

Figure 5.14 Schematic diagram of beach back-cutting

The theoretical equilibrium profile may be calculated using the profile expression derived by Bruun (1954) and Dean (1976, 1977):

$$h = A_s x^{\frac{2}{3}}$$

where h = still water depth at a horizontal distance x from the shoreline, and A_s is a dimensional shape parameter (length$^{1/3}$). The parameter A_s can be obtained from the empirical relationships suggested by Moore (1982) and Dean (1987 and 1991). The Dean (1987) and Moore (1982), graphs are available in 'Beach Processes and Sedimentation', by P. D. Komar (1998), page 279. Work and Dean (1991) developed more complex models to determine the parameter A_s. However, it was found that these did not significantly improve the accuracy compared with the Moore (1982) and Dean (1987) models.

In this section it will be shown that for a Bakelite model sediment the accuracy of the equilibrium profile equation is sensitive to whether when the A value depends on particle diameter (Moore, 1982) or sediment fall velocity (Dean, 1987).

1) Model equilibrium profile

According to the Moore (1982) relationship, if $D_{50} = 0.51$, then $A_s = 0.095$ (see e.g. Komar, 1998). The theoretical equilibrium profile based on this value of A_s is shown in Figure 5.15.

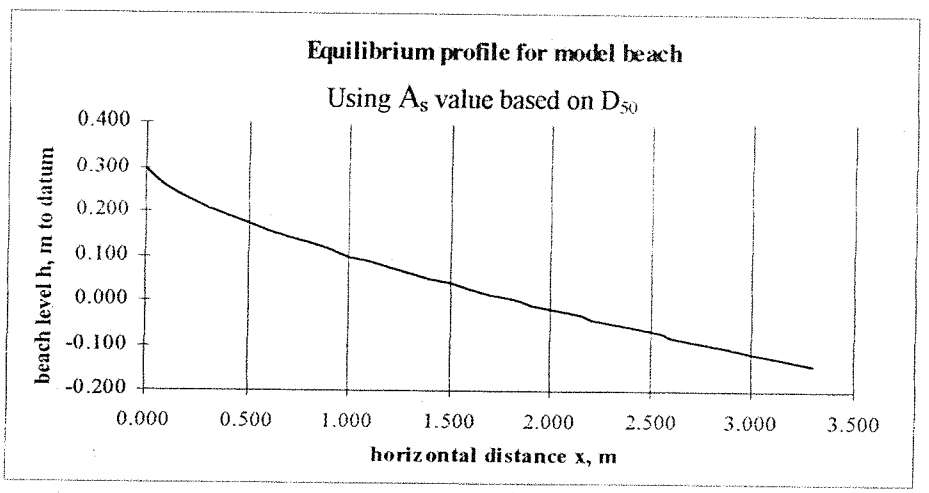

Figure 5.15: Theoretical equilibrium profile for model beach (For A_s value determined using D_{50})

The beach profile for the seaward section of the beach, when x >1.000 in Figure 5.15, is approximately 10% (the SWL intersects the beach at x = 0)

Experimental data

It was noted above that for model experiments with an initial profile of 10%, beach back cutting occurred resulting in a net loss of material. After an initial phase of back cutting, the model beach began to reach equilibrium: in Figure 5.13 it can be seen that there is little further beach profile change from t = 80 min to t = 120 minutes. The results indicate that the 1 in 10 profile is steeper than the equilibrium profile for the given conditions.

Fig. 5.16 shows a comparison of the actual and theoretical equilibrium profiles for the Bakelite model beach. (The theoretical profile is based on the Moore (1982) A_s value, which is dependent on the D_{50} sediment size).

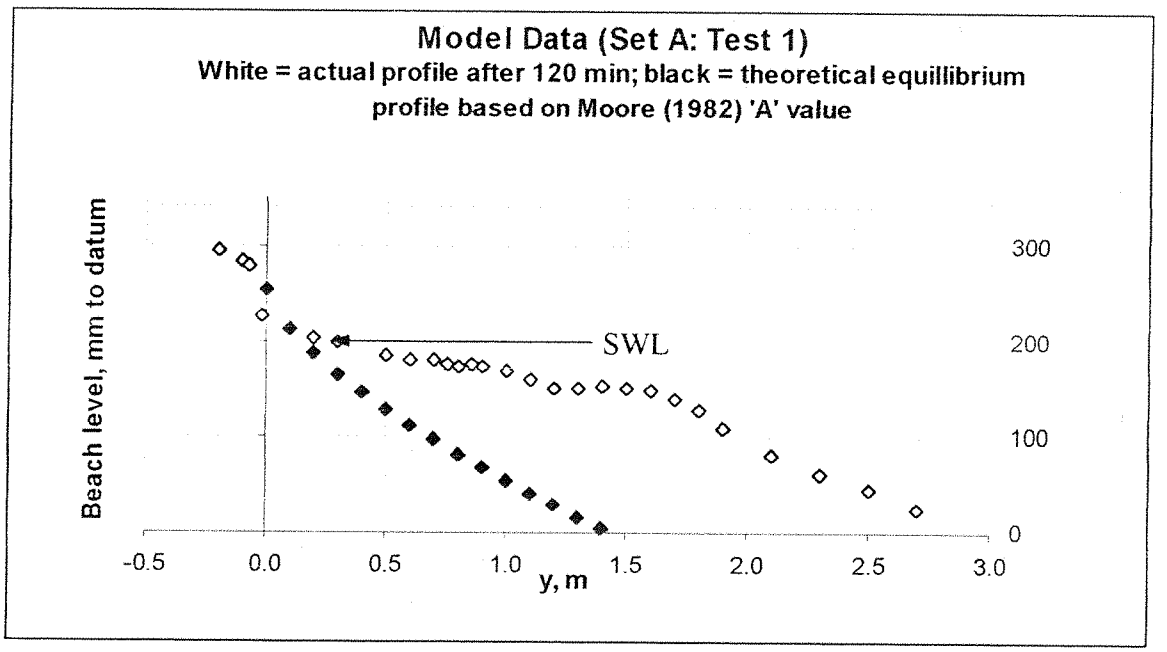

Figure 5.16: Comparison of actual and calculated model equilibrium profiles for the model

Clearly the predicted 10% beach profile is steeper than the actual equilibrium profile. It may be assumed that other factors are affecting the equilibrium beach slope, and that an 'A_s' value based solely on the D_{50} sediment size is inaccurate. Before

investigating this further the same procedure has been repeated for the field beach, to see whether the same problem occurs.

From Figure 5.16 it can be seen that the actual equilibrium profile is 5.4% (average).

2) Field profile

The Branksome Chine beach material has a lower D_{50} than that of the model, thus the Moore (1982) A_s value and associated equilibrium profile were different. In the case of the Branksome Chine sand, the A_s value (using the D_{50} value), is 0.09. This results in a gentler sloping equilibrium profile as shown in Figure 5.17 below (note that the datum for beach level is arbitrary in this figure).

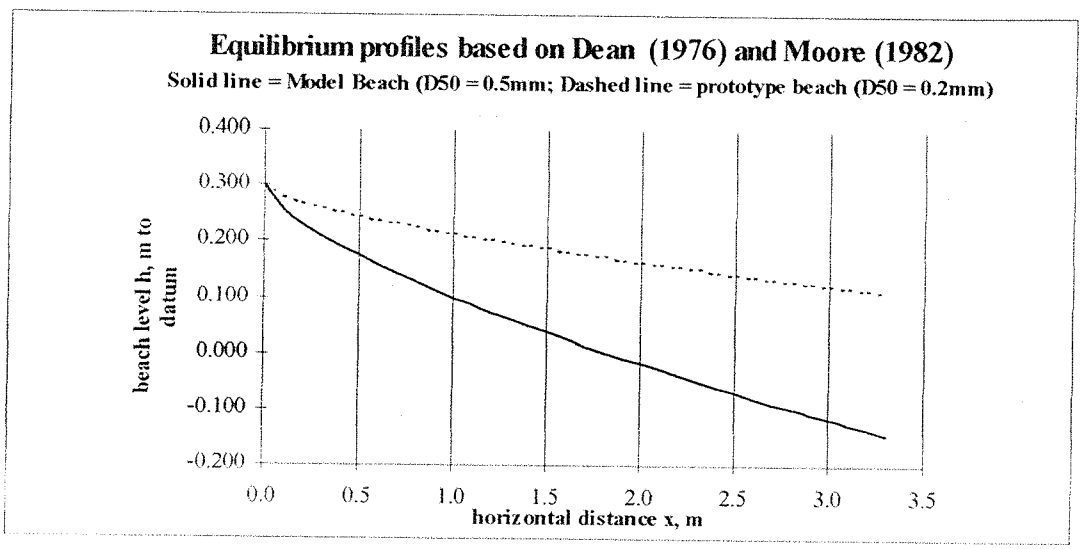

Figure 5.17: Comparison of calculated profiles using A_s value based on D_{50} value.

In the case of the full scale beach (Branksome Chine), the calculated equilibrium profile, below the SWL, is approximately 5%.

This can be compared to the actual beach profile as shown in Figure 5.18, which shows a typical beach section for Branksome Chine alongside the theoretical equilibrium profile. As discussed in Chapter 3, the beach profile at Branksome Chine is a compound profile, and cannot be described by a single Dean equilibrium profile (Inman *et al.*, 1993). For simplicity, the equilibrium profile has been compared to the

shorerise segment of the beach only (i.e. the part of the beach below the berm): in the full scale experiment described in Chapter 3 the beach drainage system was installed in the shorerise section of the beach.

The crest of the berm denotes the boundary between the two segments, and therefore the predicted profile applies seaward of this point. The mean sea level (or MSL) for this location is 1.4m CD (chart datum), and intersected the beach at y = 0.25m. This has been allowed for in the figure.

Clearly there is a much better correlation between the predicted and actual equilibrium profiles in the field data than in the model data.

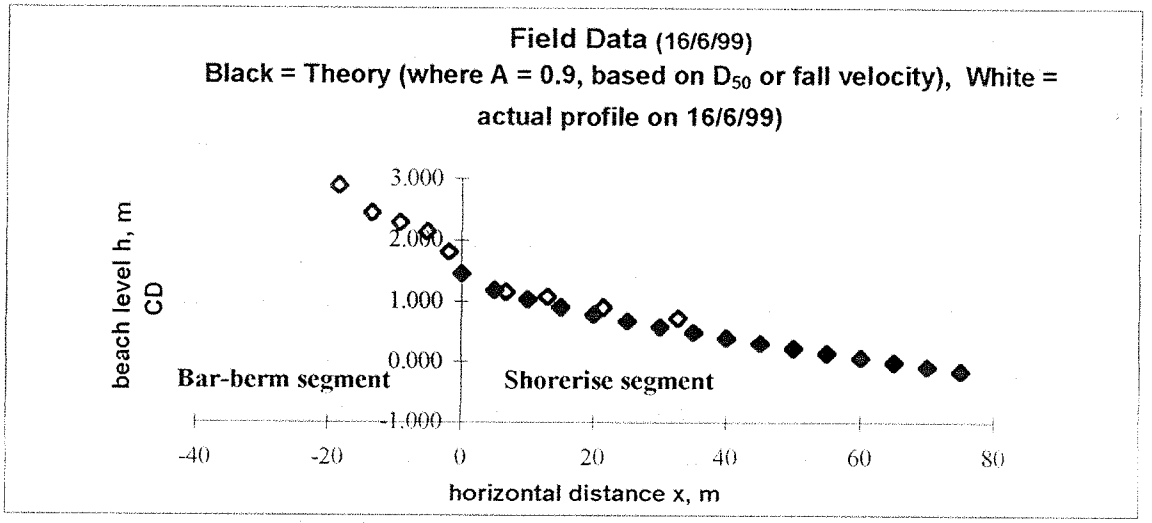

Figure 5.18: Comparison of calculated and actual prototype beach equilibrium profiles

It has been shown that when using the D_{50} curve to calculate the equilibrium profile, the actual equilibrium profile in the model is different from the calculated profile, while the actual and calculated profiles in the field demonstrates a good correlation. There are three main differences between the model and prototype sediment: The average grain size, the specific gravity and the particle shape. Therefore the value of A_s used in the theoretical profile equation must take these properties into consideration. The combination of these features is perhaps best accounted for by the sediment fall velocity rather than the nominal particle size.

If the model equilibrium profile is predicted using the A_s value found using the empirical relationship between *fall velocity* and A_s (Dean 1987), then a better correlation is obtained for the predicted and actual model equilibrium profiles. This is shown in Figure 5.19.

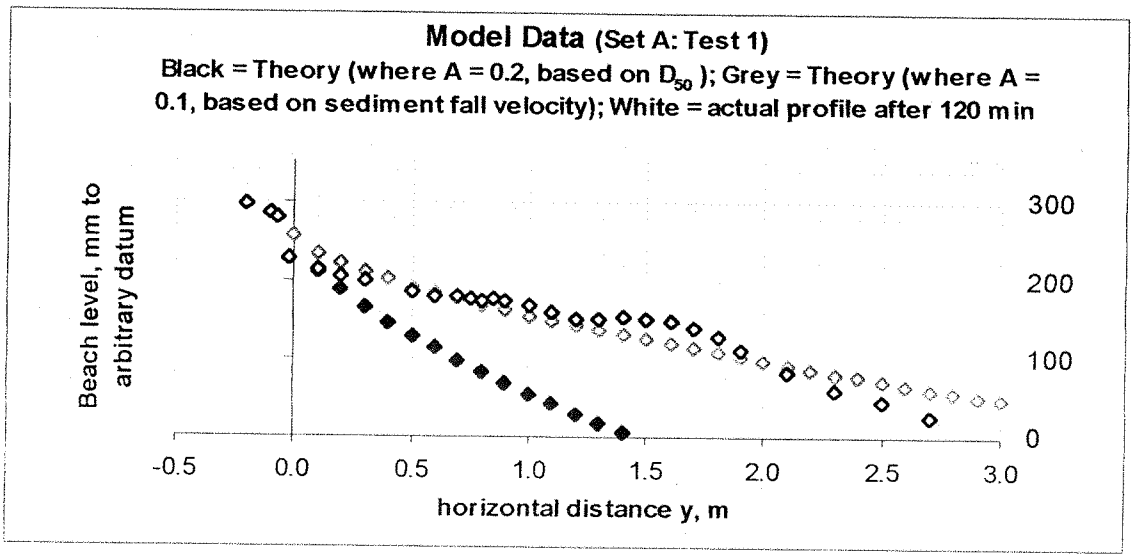

Figure 5.19: Correlation between calculated and actual model equilibrium profiles

For the Branksome Chine sediment the A_s value using the fall velocity is the same as the value obtained from the D_{50} curve, thus the same, good correlation remains.

As shown in Figure 5.19, the use of the scale parameter A_s, based on the sediment fall velocity, provides the best equilibrium profile prediction for the model. Clearly the sediment fall velocity is an important factor in determining the equilibrium beach profile.

The equilibrium profiles for the model and prototype are approximately the same (model = 5.4%; field = 5%). It is convenient that the model equilibrium profile is approximately the same as the field equilibrium profile since this allows geometric similarity in terms of the horizontal and vertical distances. This analysis has shown that the model and field sediment behaviour is similar in respect of equilibrium profile formation, despite the difference in characteristics (G_s, D_{50}, fall velocity and shape), and supports the argument for the use of Bakelite as a model sediment. The model beach profile is geometrically undistorted.

5.4.4 Test time scale

The initial model beach profile was prepared as a plane surface, and was therefore an approximation of the equilibrium profile. As the beach profile responds to wave action, various features, (e.g. a berm), are superimposed onto the calculated smooth equilibrium profile. When waves operate on the model beach, the profile responds and changes, and the rate of change decreases with time until an equilibrium profile is achieved (as discussed above). Hence it is necessary to determine an appropriate time scale during which the swash zone profile can respond. According to King (1966), the general character of the profile becomes apparent after the waves have been acting on it for a relatively short time (approximately half an hour), although the beach will take longer to reach static equilibrium. The Caen model tests (Briere 1999) had a test time of 12 minutes, while the undergraduate University of Southampton beach drainage tests (Marin *et al.*, 1998) used 10 minutes.

A number of model tests were carried out using a ten minute test time scale, but it was found that data were scattered (see Chapter 8). Model techniques were refined and practiced, but these did not reduce the data scatter, thus it was decided to investigate the test time scale in further detail. The profile change was recorded at regular intervals for a total of 5 hours in order to quantify the time taken to reach equilibrium. These data are shown in Figure 5.20.

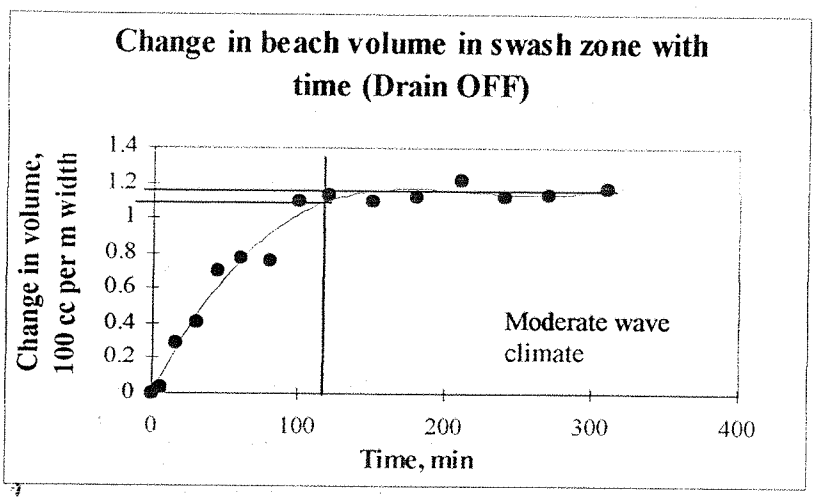

Figure 5.20: Change of beach volume in swash zone with time (no drainage)

Despite the fact that the initial plane beach profile was prepared near to the equilibrium profile, it is apparent that after just ten minutes the profile shape in the swash zone is in the relatively early stages of responding to the wave conditions. It was decided to increase the test time scale to 120 minutes for the remainder of the tests. After t = 120 minutes approximately 95% equilibrium is achieved.

5.4.5 Range over which profile is measured

The profile levels were recorded from the false back of the flume to approximately 1.5m seaward of the drain system (sometimes more or less as necessary). The lower extent of the measurements was some way below the still water level and lower surge limit, and seaward of the plunge zone. The initial plane profile was measured every 0.2m, while the profile after wave action was measured at irregular intervals according to the detail required. The beach volume was calculated using the trapezoidal rule, assuming straight lines between data points. Where profile change was rapid, data points were recorded at close intervals.

The total sediment volume in the tank remained constant, with any material accumulated at the top of the beach being taken from a source zone at the toe of the beach. During some tests the sediment was washed down towards the paddle end of the tank, and efforts were made to move any such migrated sediment back to the source zone. Therefore the profile measurement zone could experience net gains or losses. Gains and losses were found to be more distinct in the swash zone, and when an overall gain was measured, the majority of this was found to accounted for by berm build up in the upper swash zone. This is likely to be due to the use of a monochromatic wave generator. The beach volume change was measured in the zone from y = -0.4m to y = +0.4m.

This swash zone and upper section of the beach are important in the field since they form the 'amenity' area of the beach. This area is the useable zone, and the section of the profile that adds value to the beach as a recreational resource. Secondly, elevated levels in this zone may afford protection to any structures located directly behind the beach (such as a sea wall), and may contribute to flood protection.

5.4.6 Definition of erosion and accretion

Although the Froude number may be used to indicate similarity of the model and full scale waves, the number does not indicate whether erosion or accretion will occur since the sediment properties have not been taken into consideration.

Dean (1973) showed that the dimensionless group H/wT (sediment fall time parameter, or sometimes known as the Dean number) plays an important role in distinguishing between erosive and accretive conditions.

For each wave climate the beach volume change was recorded for a 120 minute test, and erosion or accretion was observed in the swash zone. This is summarised as E or A respectively in Table 5.7. The sediment fall time parameter (or Dean number, H/wT) which separates erosion from accretion was evaluated for the model by comparing beach volume change for a range of wave characteristics. The threshold Dean number when calculated using $w_{laminar}$ was found to lie between 1.4 and 1.6, and when using $w_{turbulent}$ it lies between 0.8 and 1.2. These values will be discussed later in Chapter 8.

The use of the Dean (1973) number for erosion/accretion prediction is a simplification (see Kraus *et al.*, 1991), and several more accurate techniques for profile prediction exist (Kraus *et al.*, 1991). However, for the purpose of the experiments described in this dissertation, the Dean number has been used to separate erosion and accretion for existing data (and not as a *predictor*). The Dean number has been applied to the model data merely as a simple method of defining the boundary that separates erosion and accretion for the purpose of comparing the difference between drained and undrained conditions. Note that the Dean number is not necessarily an accurate erosion/ accretion predictor, and the values that separate the two conditions apply only to the beach drainage model and profile range described in this dissertation.

Paddle stroke	Motor speed	Wave height (m)	Wave period (s)	Sediment fall time parameter, S (or Dean number , Dn)		Erosion (E) or accretion (A) in swash zone (drain off)
				$Dn_{laminar}$ Using $w_{laminar}$	$Dn_{turbulent}$ Using $w_{turbulent}$	
10	2.5	0.0135	1.59	0.16	0.099	A
110	2.5	0.11	1.59	1.15	0.79	A
40	2.5	0.048	1.59	0.55	0.35	A
75	2.5	0.08	1.59	0.92	0.59	A
110	4.5	0.11	1	1.79	1.28	E
4	2.5	0.008	1.59	0.092	0.059	A
120	5	0.11	0.9	2.18	1.42	E
95	7.5	0.085	0.75	2.02	1.32	E
110	3.5	0.11	1.25	1.42	1.02	A
130	5	0.11	0.9	2.18	1.42	E

Table 5.7: Wave climates used in model tests

5.4.7 Wave reflection

A thirty second plot for the nearshore wave probe for climate110/2.5 is shown in Figure 5.21. It can be seen that there is a small amount of fluctuation in the wave height, which is likely to be due to reflection. For the purpose of data analysis the mean wave height has been used.

Wave reflection is not of major significance since the beach reflection coefficient is low.

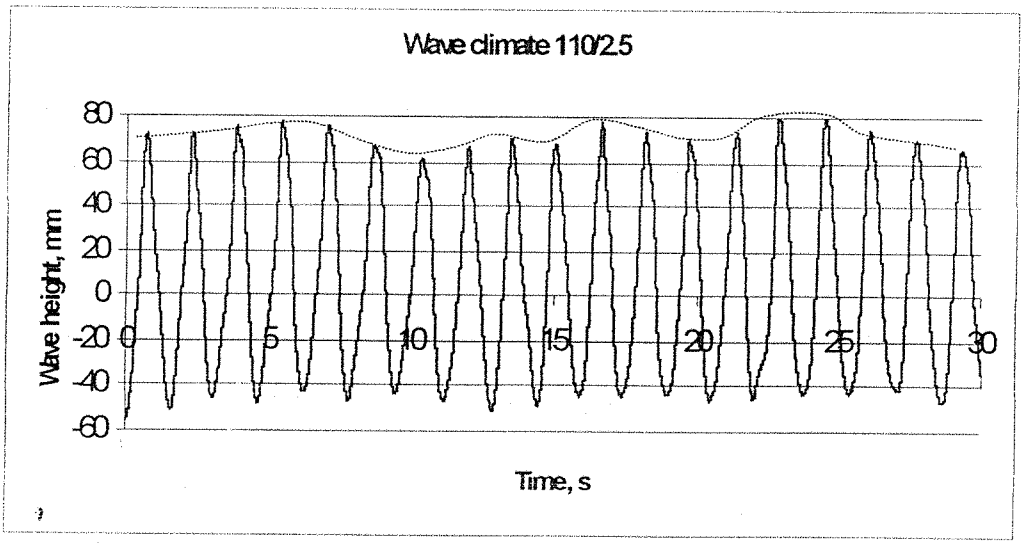

Figure 5.21: Nearshore probe output converted to mm and time (2.5/110). The dashed line indicates the fluctuation in wave height due to reflection.

5.4.8 Summary of parameters

Table 5.8 shows a summary of the model and full scale system properties. The university of Caen (Briere, 1999) and Weisman (1999) models were introduced in Chapter 2 (unfortunately some information is unavailable from the published literature), and details are included below.

System Properties	Units	Southampton Model	Branksome Chine	Caen Model	Caen Prototype	Weisman Model	Weisman Prototype
Linear length scale	m	1	20	1	20	1	6.97
Drain length	m	0.42	100	n/a	n/a	0.91	n/a
Drain diameter	mm	13	200	n/a	n/a	25.4	n/a
Number of drains	n/a	2	4 installed (2 in operation)	n/a	n/a	1	1
Drain spacing	m	0.1	2 (to centres)	n/a	n/a	n/a	n/a
Drain depth	m	0.06	1.2	n/a	n/a	n/a	n/a
Wave Properties							
Period	s	1.6	4.9	from 0.9 to 2	from 4 to 9	3	8
Height	m	0.11	0.45	0.04 to 0.07	0.8 to 1.4	0.12	0.835
Fluid density	Kg/m^3	1000	1050	1000	1050	1000	1050
Acceleration due to gravity (g)	m/s^2	9.81	9.81	9.81	9.81	9.81	9.81
Sediment Properties							
Stokes sediment fall velocity (laminar flow)	cm/s	5.6	4.9	0.018	n/a	0.018	0.046
Stokes fall velocity (turbulent flow)	cm/s	8.6	11.6				
D_{50}	mm	0.51	0.25	0.15	n/a	0.145	0.35
D_{10}	mm	0.28	0.18	n/a	n/a	n/a	n/a
C_u	n/a	2.1	1.60	n/a	n/a	n/a	n/a
C_z	n/a	0.95	0.98	n/a	n/a	n/a	n/a
Specific gravity (G_s) in fresh water	n/a	1.45	2.65	2.65	2.65	2.65	2.65
Beach slope (S_o)	n/a	5.6%	approx. 6%	7.5% upper 2% lower	7.5%upper 2% lower	0.025	0.074
Measured permeability (loose)	m/s $x10^{-3}$	1.2	0.4	0.109		0.109	0.64
Measured permeability (dense)	m/s $x10^{-3}$	0.49	0.15				
Calculated permeability (Hazen)	m/s $x10^{-3}$	0.78	0.32			n/a	n/a
Dry bulk density (dense packing)	kgm^{-3}	7.51	n/a	n/a	n/a	n/a	n/a
Wet bulk density[3]	kgm^{-3}	12.33	20	20	20	20	20

Table 5.8 Summary of model and full scale sediment properties

The linear scale is the same for the Southampton and Caen models, but the Weisman tests were carried out in a larger model wave tank, since the linear scale is only 1:6.97. Note that in the Caen model (Briere, 1999) it was attempted to use an initial profile the same as that measured in the field. However, the model uses a scaled down sediment particle size, and the thus the equilibrium profile for the model will be lower than that of the prototype. Hence the model beach is prepared to a profile steeper than the equilibrium profile. As the Caen and Weisman (1995) models used the same sediment, it may be assumed that the beach face wetness scale effect observed in the Weisman model (see section 5.3.3) will also apply to the Caen model, and therefore these results are also likely to be an underestimate.

Since the Caen model tank is smaller than the Weisman wave tank and the model sediment size is the same, the beach face wetness problem identified by Weisman *et al.* (1995) is likely to be exaggerated in the Caen model.

5.5 Discussion and conclusions

5.5.1 Evaluation and discussion of dimensionless groups

Geometric similarity

Taking two critical system dimensions from Table 5.6, i.e. drain spacing and cover depth, it can be seen that the model and full scale are geometrically similar (as designed):

$[G] = [d/D]_{model} = 0.1/0.06 = 1.67$

$[G] = [d/D]_{prototype} = 2/1.2 = 1.67$

$\rightarrow [G]_{model} / [G]_{prototype} = 1.$

Geometric similarity is also indicated by the fact that the model and field equilibrium profiles are the same, since the beach slope, S_0, is the ratio of horizontal to vertical length dimensions. Some linear variables are not geometrically similar, but it was argued that these have a relatively minor effect on system discharge (provided they are sufficiently large, e.g. pipe diameter and hole size). Also, the pipe lengths are different, but this is compensated for since discharge data will be analysed in terms of litres per minute per metre length of system.

Waves

As discussed in section 5.3.2 the range of wave conditions tested in the model is representative of typical full scale conditions.

Sediment transport

Since this is a moveable bed model, it was decided to opt for a light weight sediment model in an attempt to overcome the beach face wetting problem identified by Weisman *et al.* (1995). However, sediment selection was limited by availability, and the grain size and density were not ideal: the scale criteria set out by Kamphuis (1985 and 1991) for moveable bed coastal models have not been completely satisfied (for a lightweight model it is usually possible to satisfy the R_* and F_* simultaneously). Table 5.9 shows the scale criteria that have been evaluated for this model. Dimensionless groups were summarised in section 5.3 (note that as discussed earlier, the wave height, H has been replaced by the linear scale factor, Y, = 1:20 model : prototype).

Criteria	model	prototype	model/prototype
Grain size Reynolds number $R_* = \frac{\sqrt{gH_b}}{\nu} D$	1401	3071.74	**0.5**
Densimetric Froude number $F_* = \frac{\rho g H_b}{\gamma_i D}$	4358	16186.5	**0.09**
Relative sediment density $S = \frac{\rho_s}{\rho_w}$	1.45	2.65	**0.6**
Relative length $\frac{H_b}{D}$	1.96	80	**0.03**
Beach face wetting number, $W = \frac{kTS_0}{8Y}$	4.67×10^{-5}	3.20×10^{-6}	**14.6**

Table 5.9: Scale criteria (Kamphuis 1985 and 1991) evaluated for beach drainage model

For a lightweight sediment model, one would attempt to select the sediment weight and diameter such that the ratio of model: prototype values for R_* and $F_*$are unity. This has not been achieved with the available sediment. However, it has already been deduced (in section 5.3.3) that results are likely to be limited to a qualitative indication of beach profile response to artificial drainage, and results must be interpreted taking this into consideration.

The values in Table 5.9 agree with Kamphuis' conclusion that the greatest problem with using a lightweight sediment is the relative scale factor.

The disproportionately large grain size has overcompensated for the beach face wetting problem, and the wetting number W suggests that the model beach is 'drier' than that of the prototype. This indicates that results pertaining to the effectiveness of the drainage system may be an *overestimate* (in the case of the Weisman tests results were thought to be an underestimate). However, in terms of a qualitative study, this may be advantageous in highlighting the trend.

Summary of conclusions:

- The beach drainage model is geometrically undistorted
- the range of wave climates used in the model are typical of the range likely to be encountered in the field,
- the Bakelite properties have overcompensated for the beach face wetting problem, and the model beach is *drier* than the full scale beach.
- since the particle size is disproportionately high in the model, the discharge (which is a function of grain size) will also be disproportionately high (this will be discussed in Chapter 6). Since performance is proportional to discharge (see Chapter 8), results pertaining to the effectiveness of the drainage system will be an overestimate.
- interpretation of results is limited to a qualitative indication of beach profile response to artificial drainage
- qualitative data are valuable, since they indicate sensitivity to the range of variables tested

5.5.2 Considerations

Sediment properties

A limited number of samples (five) from the Branksome Chine beach has been used to characterise the full scale sediment. It is possible that the sediment may vary across the beach. However, the samples were collected from different depths within the beach, and the samples are therefore as representative as possible. It has been assumed that the main body of the beach sediment is densely packed, and the permeability from the dense sediment permeameter tests has been used for calculating the system discharge (see Chapter 6).

Rubbing the model sediment between the fingers (quite firmly) causes it to degrade. It is not known whether wave action is sufficient to cause this degradation throughout the course of the tests. If this were a major problem, then a reduction in the equilibrium profile would have been observed during the course of test sets. This was not the case, and it assumed that any effect of particle degradation on sediment grading is minimal.

Beach profile

Note that when the calculated and actual equilibrium profiles for Branksome Chine were compared, the actual measured beach profile was unlikely to be a true equilibrium profile, since conditions rarely remain constant long enough for the equilibrium profile to full develop.

Kamphuis (1995) carried out a comparison of two-dimensional (2D) and three-dimensional (3D) beach models. It was found that the use of a 2D wave flume instead of a 3D wave-basin did not have a significant impact on the time scale for beach profile evolution, but it did cause the shape of the resulting profile to be 'somewhat different'. While the 3D profiles were representative of the exponential profiles observed in the field, the 2D profiles tended to be more angular.

According to Kamphuis (1995) the turbulence that arises from the head on collision between the incoming breaking wave and the down-rush from the previous wave in the 2D model causes the profile to deepen just offshore of the SWL. From Figure 5.16 it can be seen that this was not the case for the Bakelite model.

Profile preparation

Sources of error include:

- human error due to manual profile measurement
- possible variation in the quality of initial profile preparation
- non-uniform compaction of initially prepared profile

The compaction of the initial profile was difficult to regulate, and a technique was developed using a float and guidelines marked on the side of the glass tank. The profile was prepared manually using a series of motions to smooth and compact the beach sediment. The quality of the initial profile was heavily dependent on this manual preparation of the beach material. This method took several preliminary trials to develop until profile preparation was consistent from one test to another. This relied upon having the same person available for slope preparation for all tests (which was the case for all of the wave tank experiments detailed in this thesis).

Model assumptions

The model beach was subject to monochromatic waves only, while the prototype is subject to a spectrum of wave heights and periods. Also, no tides were used during the model wave tests.

The model is only two-dimensional, while in the field longshore currents and cross shore sediment movement may occur which are not reproduced in the model. Field observations suggest that cross shore transport may alternate in direction at Branksome Chine. These conclusions were inferred by observing the location of the scour or accretion of sediment on either side of the groynes. Typical scour caused by long shore currents in shown in Figure 5.22. Often no long shore movement was evident (the levels either side of the groyne were even.)

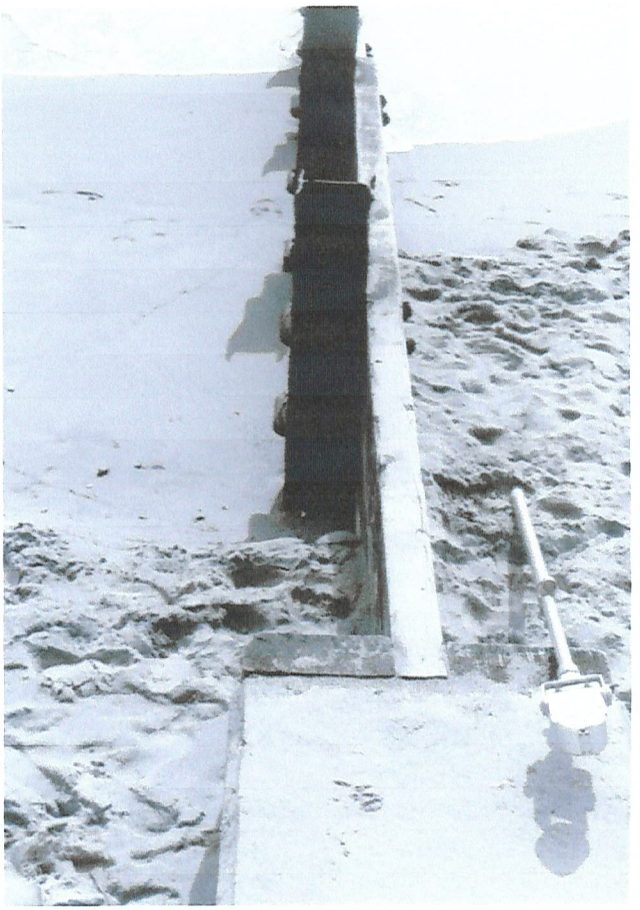

Figure 5.22: Scour down side of groyne caused by long shore currents.

Another important point to note is that the model drainage system does not replicate the land run-off contribution to the water table dynamics (land flux). The accuracy of this model representation of the full scale system will therefore depend on the prototype site in question. The beach at Branksome Chine is surrounded by a large urban area where a vast proportion of the land is covered by impermeable material (roofing, concrete, roads) land run-off is collected by the local storm water run-off drainage network. Any through flow is fed onto the beach via weep holes in the sea wall. While occasionally some evidence of weep hole flow and land run-off was noted (Figures 5.23 and 5.24), this was rare. For much of the time no weep hole discharge was noted. In view of this discussion, it can be seen that despite the limitations due to the dimensions of the model tank, the boundary geometry is not unlike that of Branksome Chine.

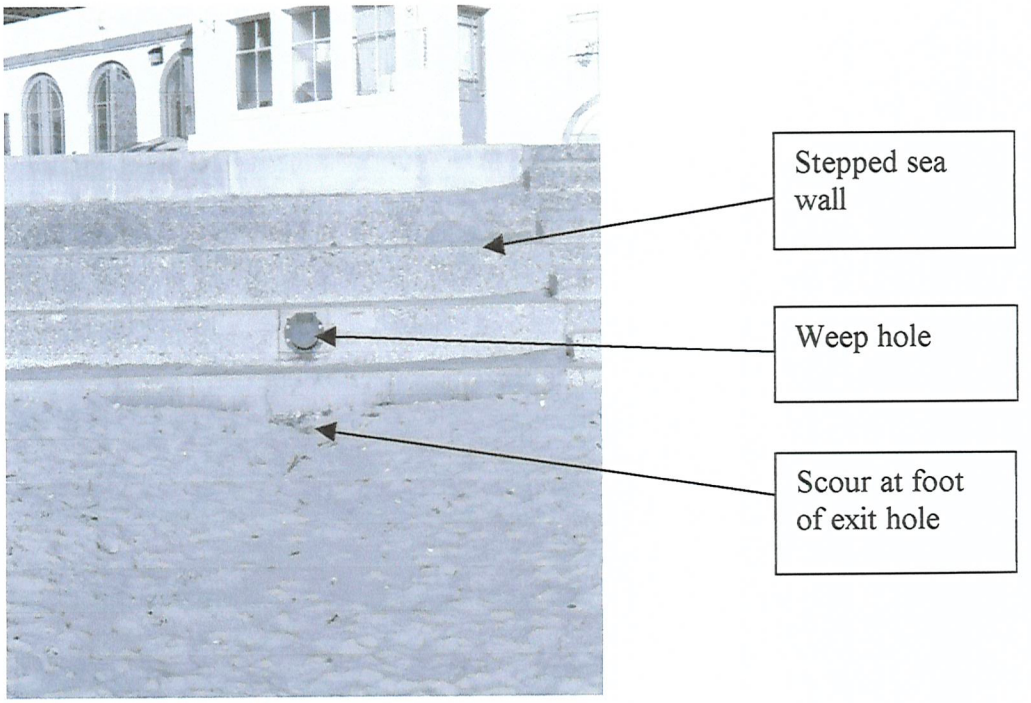

Figure 5.23 Scour in area of weep hole exit points (occasionally noted). Beach levels are unusually low in this photograph;

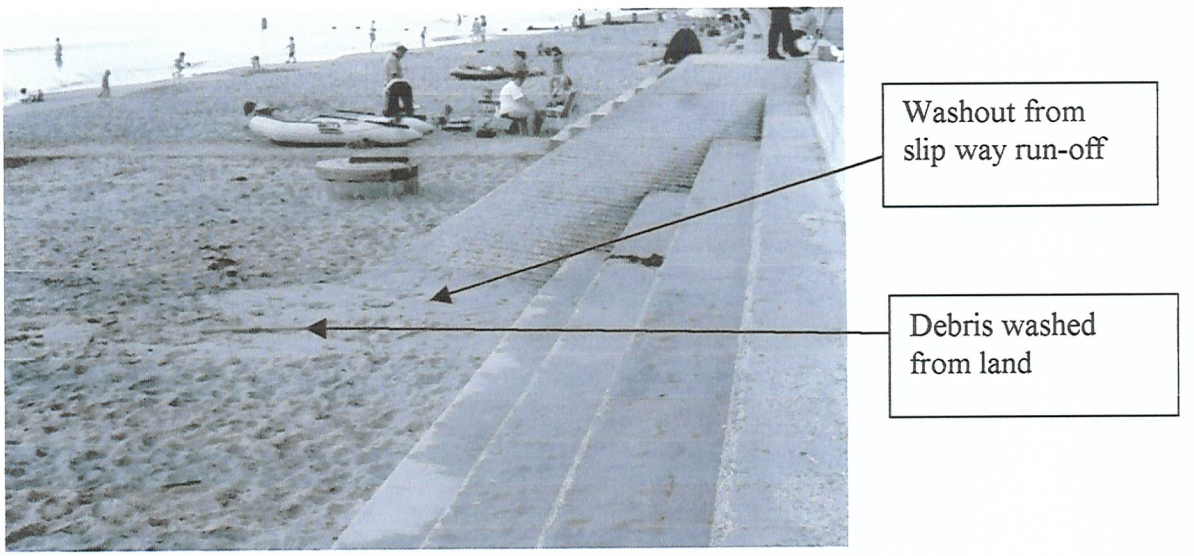

Figure 5.24 Evidence of land run off after heavy rainfall (Branksome Chine, Dorset)

6. INVESTIGATION INTO SYSTEM DISCHARGE

The aim of this chapter is to investigate the head discharge relationship for the

- full scale system,
- physical model, and
- theoretical model.

The measured and calculated head-discharge data for the full scale system were discussed in Chapter 3. This chapter presents the discharge measured for the model, and discusses the differences between the model, field and theoretical discharges.

6.1 Beach drainage model

Data collection

Discharge data were collected from the model drainage system, which was discussed in Chapter 5. The discharge data for the full scale system were recorded several weeks after installation. During this time the sediment that was disturbed during installation would have become generally settled down around the drainage system. Similarly, model test data were collected from a drainage system that had been operating for several days (i.e. after a prolonged set of tests).

Results from the investigation described in section 5.4.2 suggested that pipe diameter and hole area have relatively little influence on the system discharge (so long as they are above a minimum value). Therefore hole size was not scaled down for the model, as this is not a critical scaling dimension. The model and full scale systems are geometrically similar, thus the cover depth, pipe diameter and position in the horizontal plane were all scaled using the 1:20 linear scale factor.

The model discharge was measured while the 110/2.5 wave climate was operating (see section 5.4.5). The still water level was changed by partly emptying or filling the tank, and the still water level was allowed to reach equilibrium within the beach before the discharge was recorded. Discharge from the drain outlet was recorded using a depth gauge in the sump and stop watch.

Sign convention

The parameter y is the distance in the horizontal plane between the drain location and the point where the still water level intercepts the beach face and (illustrated in Figure 6.1). The head is linearly related to the horizontal distance by the constant beach slope S_0 (which is the same for the model and full scale beaches).

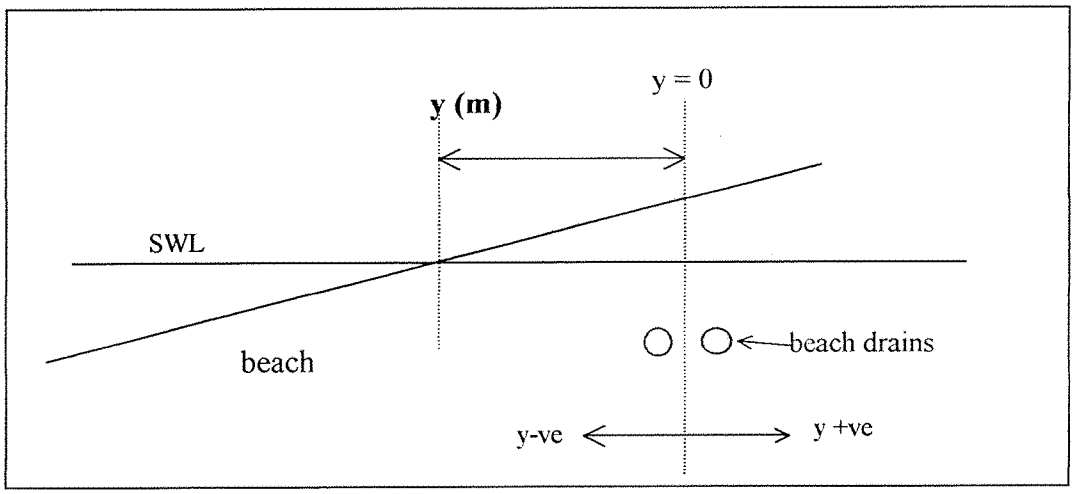

Figure 6.1: Schematic diagram to show y

Results

Figure 6.2 shows the relationship between discharge and the still water level location in the horizontal plane.

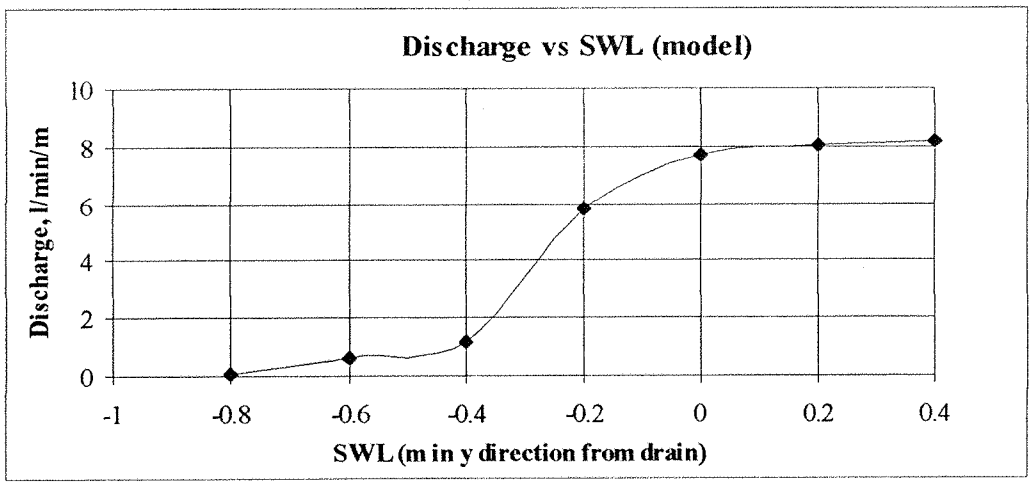

Figure 6.2: Relationship between discharge and still water level location

Scaling considerations

The permeability of the beach material was measured using a permeameter (section 5.4.1), and it was found that the permeability of the model beach was larger than that of the Branksome Chine sediment. The effect of this can be understood through the evaluation of the beach face wetness number, W, which was developed and discussed in Chapter 5. The ratio of permeability to rate of beach face wetting, W, was used to give an indication of the wetness of the beach face.

$$W = \frac{kTS_0}{8H}$$

It was found that W was 4.5 times larger in the model than in the field, indicating that the model beach was drier than the full scale beach.

Given that the beach drain permeability is high in relation to the surrounding material, then if the head difference is constant, the discharge is controlled primarily by the permeability of the beach material. Water cannot enter into the drain at a faster rate than it is allowed to pass through the surrounding beach material. Likewise, the amount of water entering is limited by the rate at which it is being supplied to the beach face. Hence it may be assumed that the system discharge will be affected by the beach face wetness factor, W. If the pore spaces are occupied by water, then no more can enter. The 'drier' beach face is likely to provide more opportunity for water infiltration in the run-up zone, and hence result in a higher discharge.

6.2 Discharge calculation

The drainage system discharge was calculated using Darcy's Law (1856):

$q = Aki$

where q = volumetric flowrate through a porous medium, A = cross sectional area, k = soil permeability, and i = hydraulic gradient (= head difference/flow path length).

In Chapter 3 a simplified flownet sketch was used to solve the Darcy equation: the system geometry was drawn to scale, and the region of flow was divided into head drops and flow tubes, where the elements in the mesh formed curvilinear squares, or an approximation thereof (see e.g. Powrie, 1997 pp 96-113). When using a flownet to solve the Darcy (1856) equation, the flow rate, q, is given by the following formula:

$$q = kH\frac{N_f}{N_h}$$

where q = flow rate per metre, k = permeability, H = head, N_f = number of flow tubes, and N_h = number of head drops (see e.g. Powrie, 1997).

In Chapter 3 only one flownet was used to obtain an estimate of the mean flowrate for the full scale system. However, the aim of this chapter is to compare a range of calculated and actual flow rates, so a series of flow nets has been sketched to simulate a range of tide levels. The information gained from numerous flownet sketches is summarised in Figure 6.3, which shows the ratio N_f/N_h obtained for a range of SWL locations. The flownet sketches were drawn similarly to the flownet described in Chapter 3, but for different still water levels. Similar assumptions apply, but in this case a sloping beach was included. Flownets were sketched with the profile of the beach and still water level intersecting at the point y, where y is the distance in metres from the drain in the horizontal plane (see Figure 6.1). The ratio N_f/N_h shown in Figure 6.3 applies to both the model and full scale systems since they are geometrically similar.

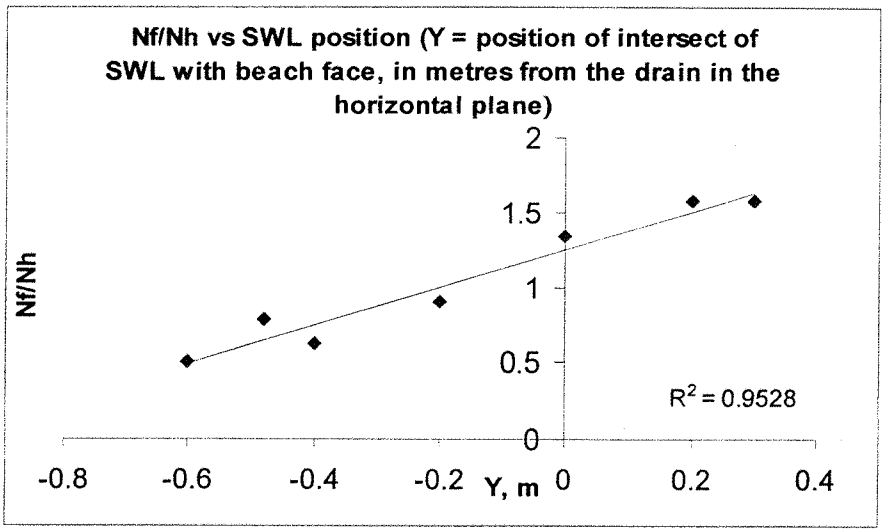

Figure 6.3: Relationship between N_f/N_h and still water level position

In Chapters 3 and 5 the permeability coefficients (k) for the full scale and model beach materials were estimated using a permeameter. It was noted that the permeability varied according to the packing of the sediment, and that since the permeameter sample was disturbed, the packing was likely to be different from the *in situ* sediment. A summary of the permeability values is given in Table 6.1.

PERMEABILITY COEFFICIENT, k	MODEL SEDIMENT	FULL SALE SEDIMENT (FROM BRANKSOME CHINE)
dense	0.5×10^{-3} m/s	0.15×10^{-3}m/s
loose	1.2×10^{-3} m/s	0.4×10^{-3} m/s
calculated using the Hazen formula (see Chapters 3 and 5) $k_{Hazen} = 0.01D_{10}^2$	0.8×10^{-3} m/s	0.3×10^{-3} m/s

Table 6.1: Permeability coefficients (see Chapters 3 and 5 for details)

The permeameter test results show that the permeabilities of both the model and Branksome Chine sediments vary considerably according to the packing of the sample (by a factor of approximately 2.5). In addition to this, the laboratory sample densities may not necessarily be representative of the *in situ* density since the sample

was disturbed. Also, the *in situ* density may vary with depth due to historical changes in the wave climate under which the sediment was deposited. Samples from different depths were tested in Chapter 3 and the results suggest that there is some variation in the particle size distribution with depth, and permeabilities varied by a factor of approximately 1.7.

If, as is likely, the *in situ* material is anisotropic this will also affect the accuracy of the discharge calculation. Difficulties in measuring the *in situ* density are well known.

The head difference was taken to be the depth of water above the level of the drain. The discharges for a range of y values were calculated using a spreadsheet and the results are presented in the following section.

6.3 Comparison of measured and calculated discharge

Figures 6.4 and 6.5 show the calculated discharges for the full scale and model drainage systems respectively. Three discharge values were calculated using each of the different permeability coefficients.

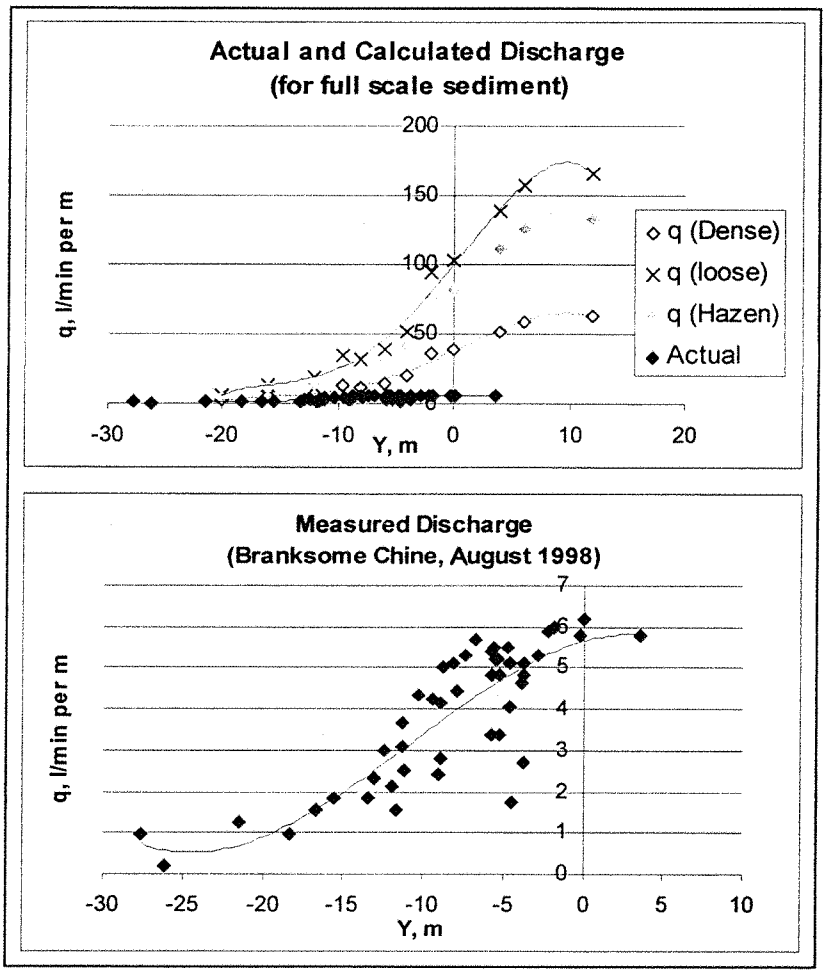

Figure 6.4: Calculated flow rate using different values for k (full scale sediment)

Figure 6.4 shows that for the full scale system there is a large difference between the calculated and measured discharge values regardless of the permeability coefficient used. For Branksome Chine the actual and theoretical values require a correction factor of approximately 6 for the k_{dense} curve, and 15 for the k_{loose} curve.

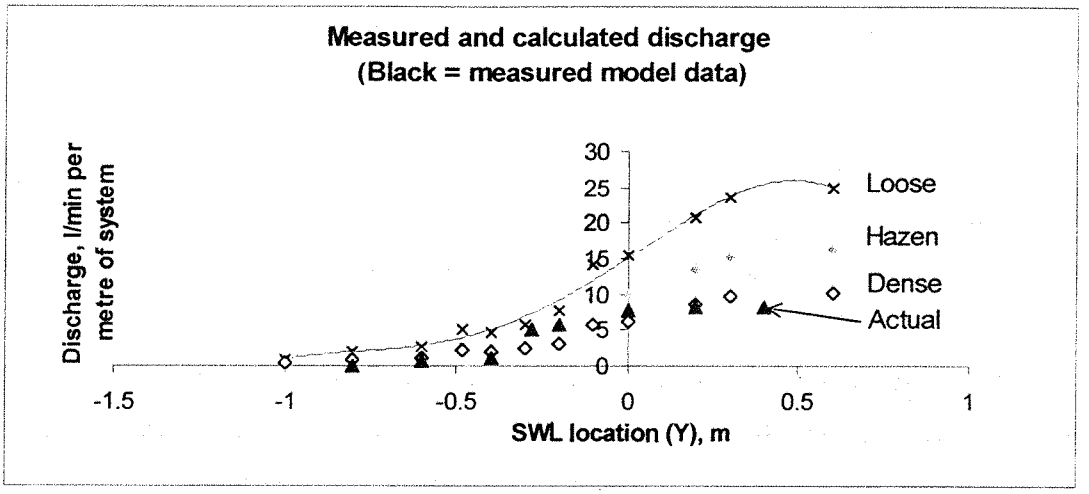

Figure 6.5: Calculated flow rate using different values for k (model sediment)

For the model system there is a good correlation between the measured data and the calculated discharge when k_{dense} is used. The sediment in the model beach was though to be densely packed due to wave action, overburden and preparation method. As noted during preparation of the model beach profile the sediment is difficult to dig into and the model sediment was observed to be densely packed after each test. The model sediment was purposely compacted with the float during profile preparation (see Chapter 5).

It is possible that in the field, the sediment is even more densely packed than the tested sample due to overburden and wave action. However, this is unlikely to account for the discrepancy observed in Figure 6.4. The k_{dense} calculated discharge values are in the order of six times higher than the actual discharge, and it is unlikely that the field void ratio is six times smaller than the densely prepared laboratory tested sample. This discrepancy is likely to be accounted for by a combination of factors that were not taken into consideration by the calculation. These include:

1) losses on entry to the pipe,
2) loss or damage to beach drains (see comments in Chapter 3),

3) variation in sediment packing density throughout the beach cross section (resulting in anisotropic permeability),
4) errors in evaluating the permeability coefficient, k in the laboratory (e.g. disturbance of sample),
5) the flownet assumes that there are no waves operating, and equilibrium exists. In reality, a steady state is not reached, and the water level in the beach is not the same as the tide level (this is because of the lag time noted by Emery and Foster (1948), which was discussed in Chapters 2 and 3).

Points 1), 2) and 3) are much less significant in the model: full scale geotextile was used in the model, and it is likely that losses are less significant for the 1:20 scale system. The model drainage system was in good condition and free from damage or incontinuities and the permeability is more uniform since the sediment was placed by hand into the tank and not deposited as a series of layers over a long period of time.

It is known (see Chapter 3) that the drainage system was operating inefficiently, even during the early stages of the trial. As discussed in Chapter 3, installation defects, sand ingress, pipe damage and head losses on entry to the pipes are all though to have contributed to this initial system inefficiency.

In September 1998 major damage resulted in pipe loss, and the system was reinstalled in December. Shortly after the reinstallation, further storm damaged caused a significant reduction in system discharge. The discharge rates before and after the major storm damage were discussed in Chapter 3.

The data in Figure 6.4 were recorded *before* the major storm damage had occurred, and it is thought that even at this stage the system was generally inefficient.

6.4 Comparison of model and full scale discharge

In order to compare the model and full scale discharges the data have been non-dimensionalised. The discharge was non-dimensionalised using Pi group three from section 5.2.2, and the length was simply divided by the linear scale factor (Pi group seven):

$\Pi_3 = q/vL$ (where q = discharge per metre, v = velocity and L = length dimension) and $\Pi_7 = Y/D = y/L$.

For the purpose of this analysis it is convenient to use v = permeability (k) and L = D = linear length scale (= 1:20 see Chapter 5). This is because the permeability and head are the two main variables that differ from the model to prototype. The head is linearly related to the scale factor L.

Figure 6.6 shows the non-dimensionalised plots for the model and full scale data. The vertical axis is the non-dimensionalised discharge, q/kL, while the horizontal axis is the non-dimensionalised y value, y/L.

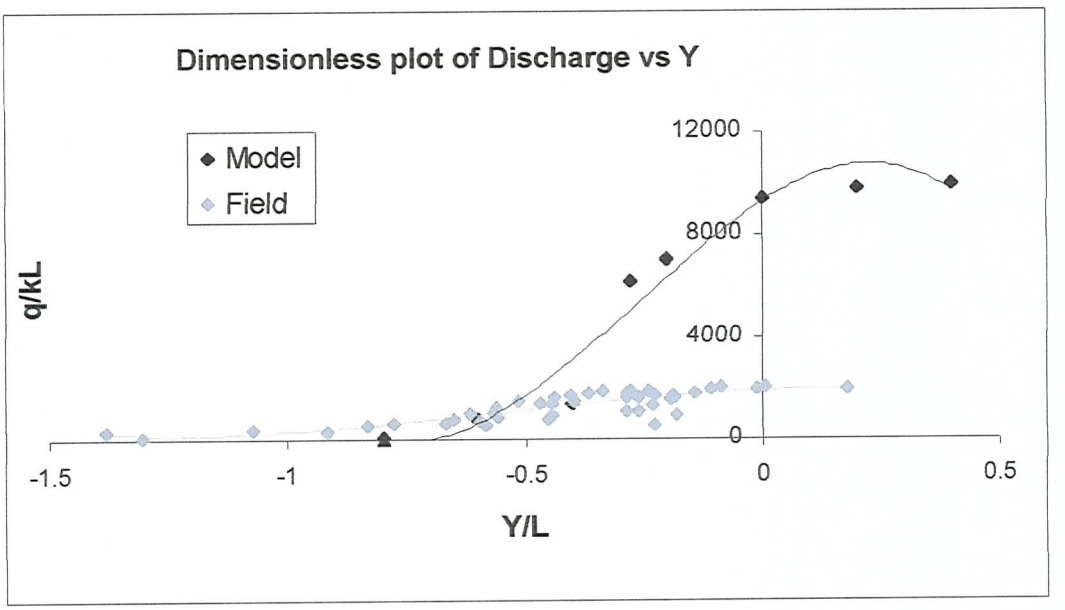

Figure 6.6 Non-dimensionalised model and prototype data

Figure 6.6 demonstrates that the non-dimensionalised model discharge is higher than that of the full scale system. The non-dimensionalised model data is a factor of approximately 5 greater than the full scale data (estimated by eye). As discussed in section 6.1 the beach face wetness factor, W, is likely to distort the model percolation processes, and result in a disproportionately high discharge in the model drainage system.

Other factors which may contribute to the discrepancy are:

- the full scale system may have more entry losses than the model (and possibly some exit losses),
- installation defects may have caused system inefficiency
- an unknown portion of the full scale system it thought to have been damaged shortly after installation
- greater set-up may occur in the model beach due to the relatively narrow beach width (this will increase the head, and therefore increase the discharge), and
- the model set up may also be higher than that of the full scale system because the wave heights for the 110/2.5 wave climate represent relatively large full scale waves (see Chapter 5), and set-up is dependent on wave height.

6.5 Comparison of full scale discharge with previous trials

In Chapter 3 the full scale discharge was compared with that of other full scale installations. A graph was drawn to show that relationship between particle size and discharge for previous trials, and this is shown again in Figure 6.7. The data suggest that there is a correlation between sediment size and discharge, and although the data are scattered, this may be explained by the fact that the data do not account for different cover depths and tidal curves for the various sites.

From Figure 6.7 the discharge for Branksome Chine, where D_{50} = 0.25mm is approximately 0.8m^3/hr per metre length of system. The mean measured discharge during August 1998 was 0.36m^3/hr per metre, and during February 1999 was 0.06m^3/hr per metre (see Chapter 3).

The discharge from the previous trial trendline is 2.5 times larger than the Branksome Chine discharge. Even before the severe September storms the discharge for the Branksome Chine system was considerably lower than the value suggested according to the trend shown by previous trials (for further discussion see Chapter 3)

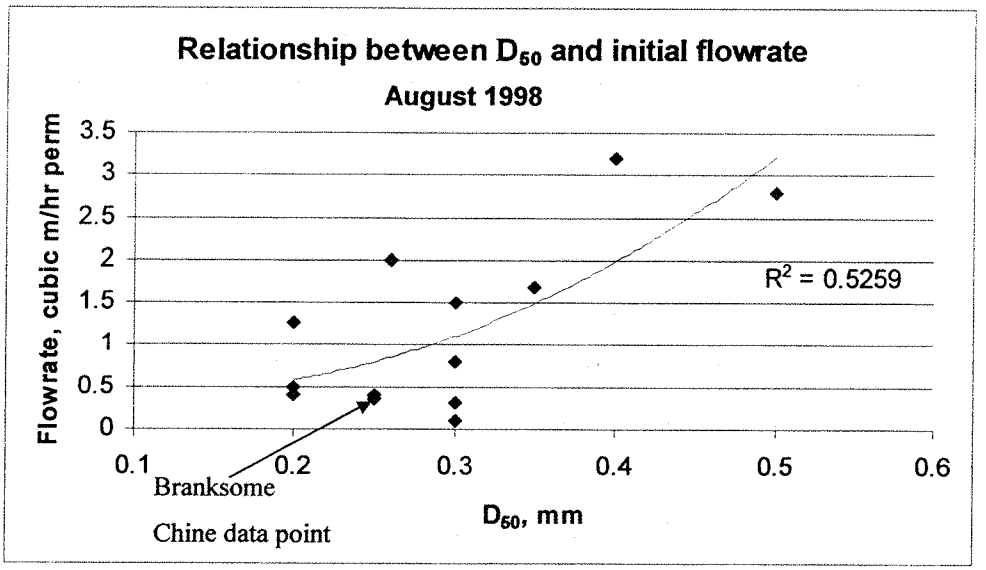

Figure 6.7: Graph to show relationship between D_{50} and flowrate (Data source: see Appendix B)

6.6 Discussion and conclusions

In Chapter 3 the trial system pump selection was discussed, and it was noted that it is necessary to estimate the system flowrate during the design stage. This could be done in three ways:

1) calculating the seepage rate using the flownet and applying a factor to allow for head losses
2) using model data and an appropriate scale factor (data suggest that the beach face wetness factor might provide a suitable scale factor, although further work is needed)
3) estimating the flow rate using discharge data from previous trials
4) using an improved method of seepage rate calculation (e.g. finite element package, or using a more detailed flow net if boundary conditions are known)

Methods 1) and 3) were used in Chapter 3. In the case of discharge calculation, estimation of the correction factor is difficult since important factors such as sediment void ratio, pipe entry losses, and the effect of wave action (e.g. set-up) are unknown.

Even assuming a dense packing the calculated flow rate was an overestimate of the actual discharge measured from the Branksome Chine system. In general soils with less than 20% fines (as is the case with the model and full scale sediments) tend to overestimate or underestimate the actual measured flow rates by a factor of three or less (Preene and Powrie, 1993). However, the measured flow rate for the full scale system was approximately a factor of 6 smaller than the calculated flow rate.

The flow rate may be calculated using an alternative method of solving Darcy's Law (1856), e.g. the use of a finite element package. However, even with the use of complex numerical models assumptions and simplifications are unavoidable (especially regarding boundary conditions), and the estimation will only be as good as the data entered into the package. A more important means of improving the accuracy of the discharge is the estimation of the system head losses, data that must inevitably be entered into any numerical model.

According to Preene and Powrie (1993) a careful flow rate calculation will not usually result in an estimate of more than × or ÷ three. However, for the Branksome Chine

trial full scale trial the flow rate is a factor of approximately 6 lower than the calculated value (using k_{dense}). Therefore taking this into consideration, the difference between the measured and actual data (for the full scale data) is at least a factor of three.

Hence in summary:

- the calculated flow rate is **x6** greater than the measured full scale value (less a maximum flownet inaccuracy allowance of x3) → **x3**
- the model flow rate is a factor of approximate **x5** greater than the full scale value
- the flow rate estimated form the trendline obtained from previous trial is approximately **x2.5** larger than the Branksome Chine value.

One of the key issues in predicting system discharge is the estimation of the likely head losses due to system inefficiency.

It could be argued that the physical model is a preferred means of full scale flowrate estimation, because some losses at least are accounted for. The problem is that it is not known whether the losses in the model system are representative of those in the field. The physical model is also able to simulate the effect of waves more realistically (with fewer assumptions) than a numerical model. Likewise there are likely to be scale effects which affect the interpretation of the results. The beach drainage model is certainly affected by scale effects, and it is possible that these are in part responsible for the discrepancy between the model and full scale discharge values.

The comparison to previous trials method has the advantage that other systems are likely to incur similar head losses/inefficiencies due to installation defect. However, the comparison indicates that the Branksome Chine system is a factor of 2.5 less efficient than the trend would suggest. Clearly head losses and system defects will vary for different trials, and the trend from previous trials should only be used as a guide.

Comparison of physical and theoretical models

There are six variables, which must be evaluated to calculate the discharge: head difference, flow path, beach material compaction (permeability), losses, location of local impermeable boundaries (boundary conditions in general) and wave set-up. Table 6.2 summarises the main comparisons and contrasts for the physical and theoretical models.

CONSIDERATION	✔ = ACCOUNTED FOR; ✘ = NOT ACCOUNTED FOR	
	Theoretical	Physical
Head	✔	✔
Flow path length	? The flownet provides an estimate only. The flow net sketch does not include the features superimposed onto the beach profile by wave action.	✔ Model beach features are similar to those formed on the full scale beach.
Beach compaction (permeability)	✘ Must be assumed. Complications due to waves operating in prototype	? Effect of wave action on beach material compaction is simulated in physical model. Overburden is less, and the surface of the beach is prepared manually.
Losses on entry to pipe	✘ must be assumed (or ignored)	? Losses may be disproportional to the prototype. Will depend on design of system. Can mitigate the problem by using similar materials.
Effect of waves (set up)	✘ The simplified flownets assume hydro- and geostatic conditions. A more complex model could account for this, but assumptions need to be made.	✔ The physical model may be run with waves operating, thus all geo- and hydrodynamics are accounted for (but must be aware of scale effects to interpret the results)
Location of boundaries confining flow	✔ Can be located as required	✘ Limited by the geometry of the wave tank
Installation defects and system damage	✘ Installation defects/inefficiencies unknown.	? Some accounted for, but may not necessarily be representative of the full scale system.

Table 6.2: Comparison of physical model and theoretical methods of discharge prediction.

7. PORE WATER PRESSURE

7.1 Introduction

As already stated there are three main mechanisms that may explain beach stabilisation through drainage:

1) Surge volume reduction resulting in energy loss and laminar flow phase extension,
2) Seepage cut-off, and
3) Pore water pressure reduction resulting in increased beach shear strength.

These mechanisms involve two fundamental components: the ability of the moving water to transport the sediment, and the ability of the sediment to resist the force that is attempting to move it. They all rely on the fact that the drainage system causes a drawdown, and therefore depend on pore water pressure reduction.

The aims of this chapter are to:

- investigate the effect of beach drainage on pore water pressure,
- explore the effect of waves on drainage induced pore water pressure reduction,
- derive an empirical expression for the relationship between pore water pressure, system discharge and distance from the beach drain, and
- determine the effect of drainage on beach liquefaction (investigate mechanism 3).

One of the principal innovations presented in this thesis is the measurement of pore water pressure in the model beach under the influence of both waves and a beach drainage system, as discussed in this chapter.

When the drained beach is subject to wave action it is geotechnically and hydraulically dynamic because:

- the beach face is subject to a cyclic shearing force and the sediment particles are being moved by the surge,
- water from the surge percolates into the beach, and moves through the beach face under gravity to rejoin the surge during the backwash (or moves towards the drainage system), and
- pressure waves move through the beach (Chappell *et al.*, 1979).

7.2 Data collection

The apparatus and model drainage system used for this experiment were discussed in Chapter 5. The still water level, beach sediment and wave climate were constant for all tests, and a monochromatic wave generator was used.

Pore water pressure data were recorded at different locations in the horizontal and vertical plane to obtain a grid of data points. Tests were carried out with and without waves operating, and with the drain off and on alternately. Time was allowed between tests for pore water pressure equilibration. A summary of tests carried out is given in Table 7.1.

A wave climate was selected such that neither erosion nor accretion occurred during undrained conditions. Wave climate 110/2.5 was selected, since it was shown that after several minutes of operation, relatively little beach volume change occurred (with drain either off or on. See Chapter 5, Figure 5.12 for details). This wave climate was used so that pore water pressure data could be recorded while the flow path length (beach geometry) remained relatively constant.

The tests codes in Table 7.1 correspond to raw data sheets and spreadsheets, and are not necessarily discussed in order in this chapter.

LABORATORY TEST CODE	SUMMARY	WAVES
D1	Drain on then off alternately (preliminary test)	-
D2	Drain on then off alternately (preliminary test)	110/2.5
D4, 5, 6	Investigation into the variation of PWP with discharge	-
D7	Investigation into PWP response time	-
D8	Repeat of test D1	-
D9	Repeat of test D2	110/2.5
D11	As for D8, but the top probe was placed just below the beach surface	-
D12	As for D9, but the top probe was placed just below the beach surface	110/2.5

Table 7.1: Summary of laboratory tests (pore water pressure measurement)

Instrumentation

Pressure transducers were discussed in Chapter 5. An array of four pore water pressure transducers was mounted onto a rigid metal rack and the pressure transducer units were held in place with cable ties. The pressure transducers were spaced 45mm apart on the rack, and the top probe was labelled probe 1, and the bottom probe 4. Figure 7.1a shows a typical pressure probe arrangement in the model beach. The pore water pressure transducer (PPT) output was calibrated and converted to kilo Pascals.

Unfortunately water ingress occasionally rendered one or more of the pressure transducers out of operation (the probe array with probe 1 out of operation is shown in Figure 7.1a). The pressure transducer units housing the electronic components tended to stay dry for between 6 and 24 hours.

Sign convention

The horizontal plane has been labelled the y plane, and the drainage system is located at y = 0. y-positive is landward of the drain, while y-negative is seaward of the drain. (this convention is shown in Figure 7.1a). In this diagram, the rack is located 0.3m landward of the drain, hence the rack position is labelled y = +0.3m

Still water level

A fixed still water level location, where the water level mark on the beach surface is 0.25 metres seaward of the centreline of the drainage system (y = -0.25m) was used in these tests. The upper limit of the swash was located at y = +0.1m (just landward of the drain). These are indicated in Figure 7.1b.

The effect of the still water level (SWL) location on system performance is discussed in Chapter 8, where it will be shown that the optimum location is at y = -0.25m.

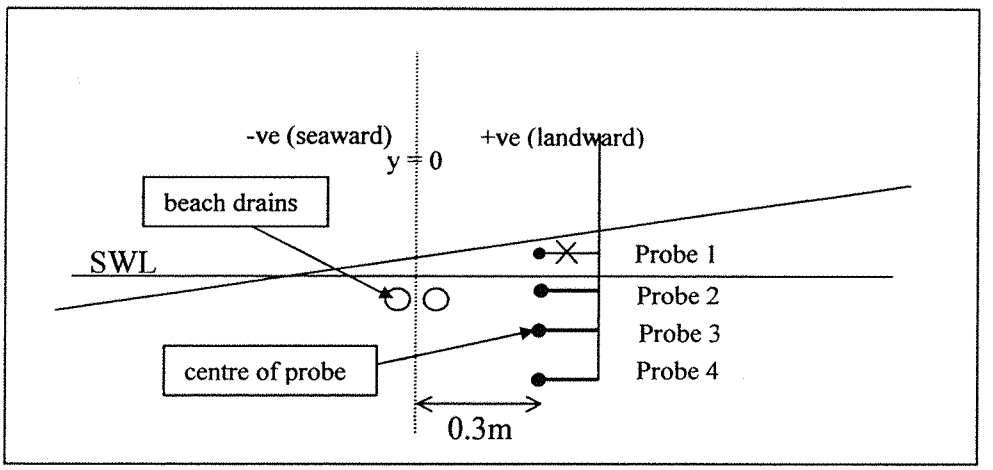

Figure 7.1a: Schematic diagram indicating the probe locations for Figures 7.2 and 7.3 (in this figure probe 1 is out of operation).

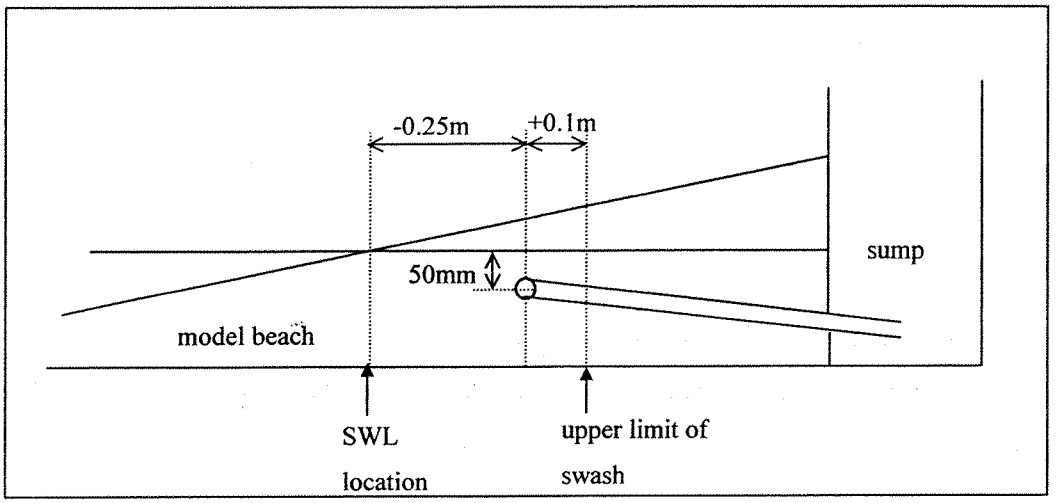

Figure 7.1b Schematic diagram showing SWL and upper limit of swash

7.3 Pore water pressure response time

Many of the tests described in this chapter involved recording the pore water pressure with the drain alternately off and on. The aim of the test described in this section was to determine the time taken for the pore water pressure (PWP) to respond and equilibrate after switching the drain on. To determine the PWP response time a stopper was removed or replaced from the drainage system outlet while the data logger was recording.

Figure 7.2 shows the change in pore water pressure with time (no waves were operating). During this test the topmost probe on the rack was out of operation. Probe 2 was located 22mm below the SWL, and the three vertically aligned probes were 45mm apart.

To obtain the data shown in Figure 7.2 the stopper was removed from the drainage system outlet at t = 16 seconds. In this figure approximately 60% of the total change occurs in the first 20 seconds after the bung is removed, although equilibrium is reached after several minutes (in some instances this was found to be less).

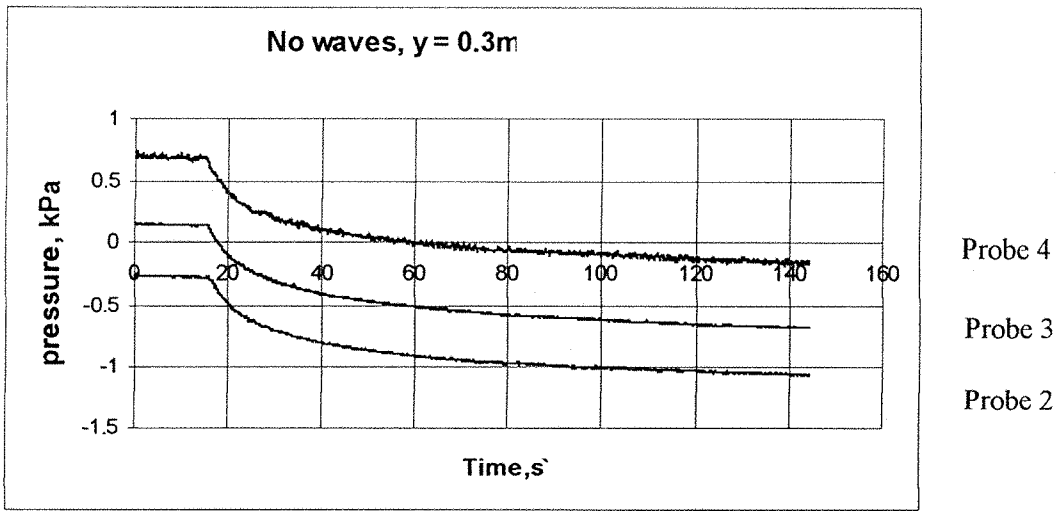

Figure 7.2 (Probe 1 is out of operation) Change of pore water pressure with time when bung is removed from the drainage system outlet during data recording. No waves operating.

The opposite pattern to that shown in Figure 7.2 occurs when data recording starts with the outlet open and the bung is then replaced (Figure 7.3). In Figure 7.3 the bung was replaced after 9 seconds.

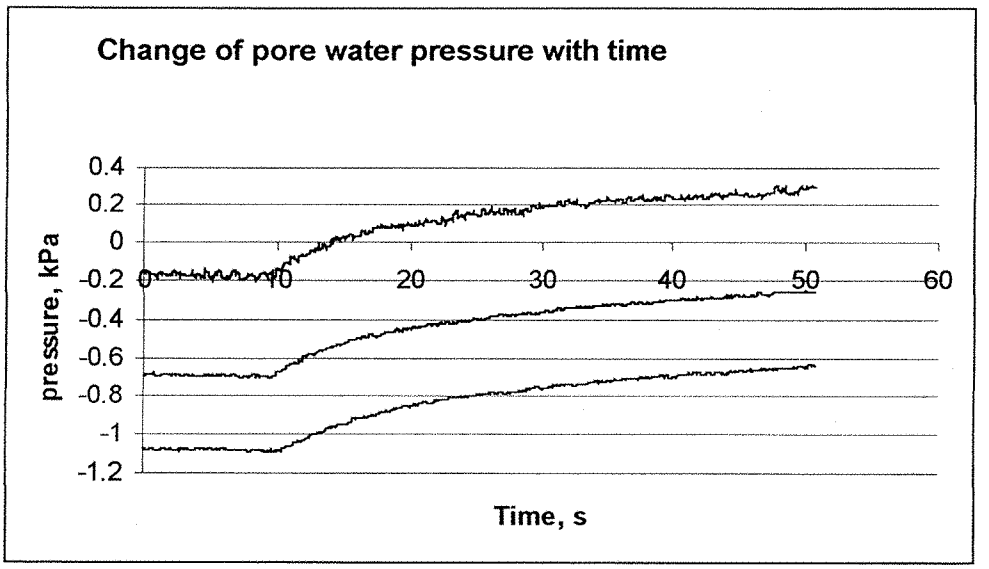

Figure 7.3 Change in pore water pressure with time when the bung is replaced during data recording. No waves operating.

7.4 Effect of waves on pore water pressure

7.4.1 Pore water pressure fluctuation

The pore water pressure transducers were sufficiently sensitive to record cyclic pressure fluctuations during wave operation. Figure 7.4 shows an example of pressure probe data for wave climate 110/2.5 (wave climates were discussed in Chapter 5). Probe 1 was not working, and probe 2 was located on the surface of the beach (the probes were as usual 45mm apart).

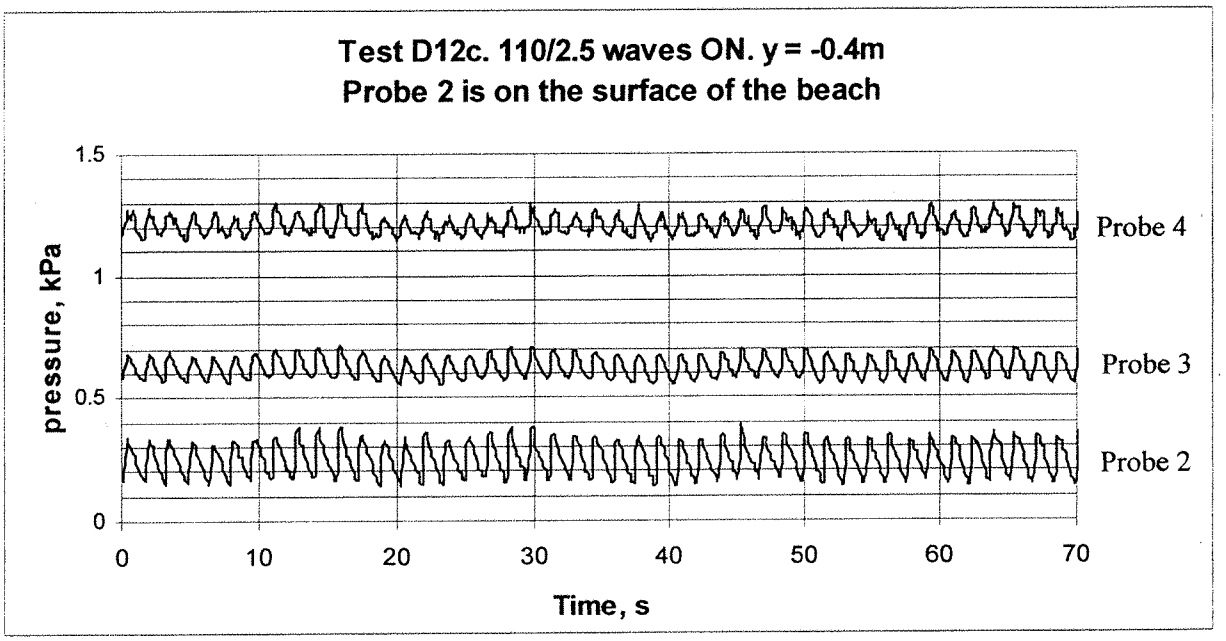

Figure 7.4: Fluctuation of pore water pressure with time (Test D12c). Probe 2 was on the surface of the beach. The probe rack was located 0.4m seaward of the drain (y = -0.4m).

For the data shown in Figure 7.4 the bung in the system outlet was removed at time, t = 16 seconds. The drainage system had relatively little effect on the pore water pressure in the beach in this case, since the probe was located 0.4m seaward of the drain, outside of the zone of influence.

The presence of waves results in a fluctuation in the pore water pressure at all depths. From Figure 7.4 it can be seen that the amplitude of the fluctuation decreases with depth.

Offshore water level data were also recorded using a wave probe located just seaward of the toe of the beach. The water depth (wave) and pore water pressure data loggers were started simultaneously. Figure 7.5 shows a plot of water level and pore water pressure against time for approximately 6 wave cycles. The pore water pressure probe was located on the surface of the beach.

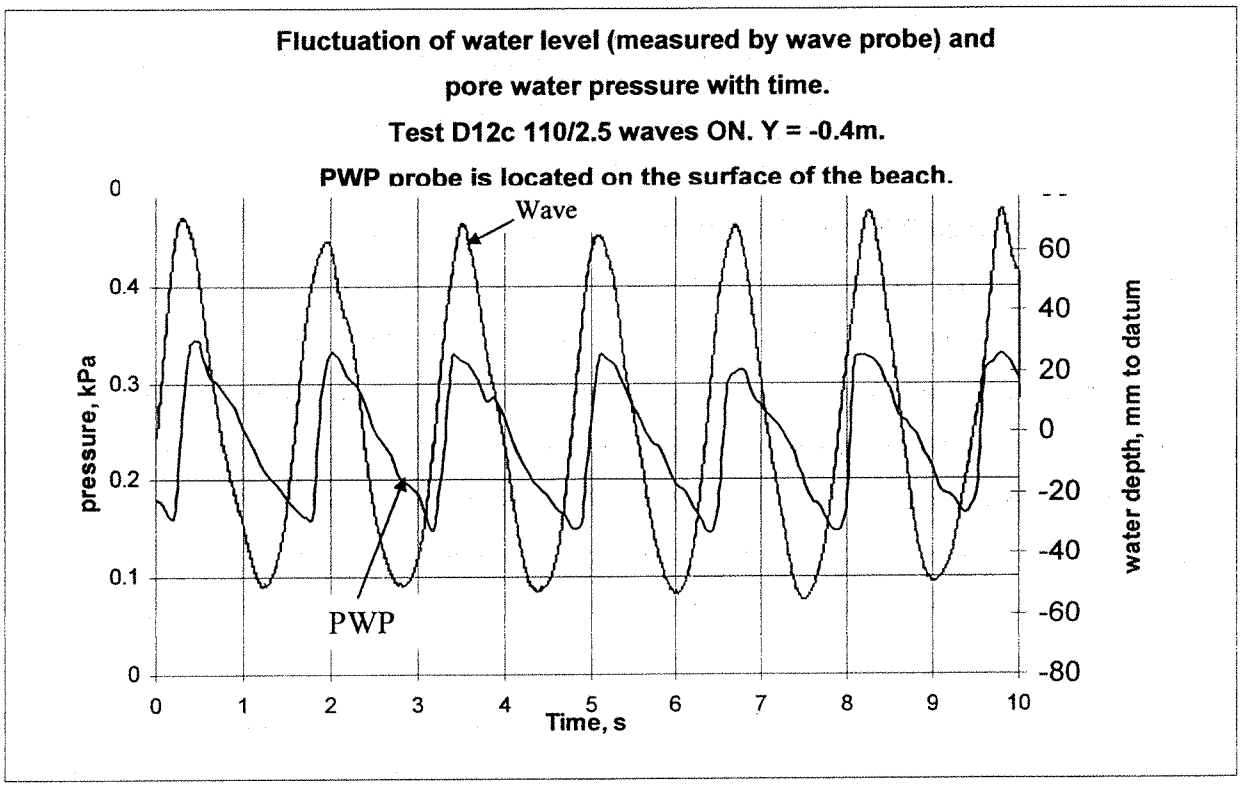

Figure 7.5: Corresponding wave probe and pore water pressure (PWP) transducer outputs for test D12c (y = -0.4m, 110/2.5 waves on). The PWP probe is located on the surface of the beach.

The pore water pressure waveform mimics that of the incoming wave, and the wave period is the same for the water level and transducer outputs (= 1.55 seconds).

The waveforms for the wave probe output are approximately symmetrical, and there is little disturbance in the majority of the waves. The waveform for the pore water pressure data is more skewed, and the rising leg is considerably steeper than the falling leg.

The wave and pore water pressure (PWP) probes were located 6m apart in the horizontal plane. Therefore an incoming wave will pass the wave probe some time

before the pore water pressure probes. This lag time has been evaluated by comparing the output from a pressure transducer placed on the surface of the beach and the wave probe output. In Figure 7.5, PWP probe 2 is located on the surface of the beach. The phase difference is between the water wave and PWP peaks is approximately zero, indicating that a wave crest passes pressure transducer 2 at the same time as a crest passes the wave probe. Obviously this will not be the same wave crest, because the wave and pressure probes are located 6m apart, however, the crest phase difference is zero. The difference between the troughs is different to that of the wave crests and is approximately 0.4 seconds.

The above effects are likely to be because the pore water pressure probe is located in the wave run-up zone, while the wave probe is seaward of the toe of the beach: In the run-up zone the incoming swash propagates up the swash zone with greater impact than the receding backwash. The incoming wave plunges and rushes up the beach relatively quickly, with most of the surge water above the surface of the beach. By the time the backwash begins some of the surge water has soaked into the beach, and this water moves back down the run-up zone as through flow, rejoining the surge lower down the run-up zone. The infiltrated water moves more slowly through the beach, and the kinetic energy of the backwash is reduced. There is no plunging at the beginning of the backwash, and the water retreats down the beach relatively gently, hence the skewed pore water pressure pattern observed in Figure 7.5.

7.4.2 Effect of waves on mean pore water pressure in the vertical plane

It has been found that the presence of the waves results in an increase in the average pore water pressure for a given transducer location. Figure 7.6 shows pore water pressure data recorded with the probe rack in the same y location as for Figure 7.4, however, in this case no waves are operating.

For both plots (Figures 7.4 and 7.6) , transducer 1 was out of operation, and probe 2 was located on the surface of the beach. In Figure 7.6 the bung was removed from he drain outlet at time, t = 7 seconds. A slight dip in the pressure readings can be seen after 7 seconds, but this is relatively small. This is because the pressure transducer rack is located 0.4m seaward of the drain (y = -0.4m), and is likely to be beyond the zone of influence of the drainage system. The special variation in pore water pressure will be investigated later in this Chapter, and also in Chapter 8.

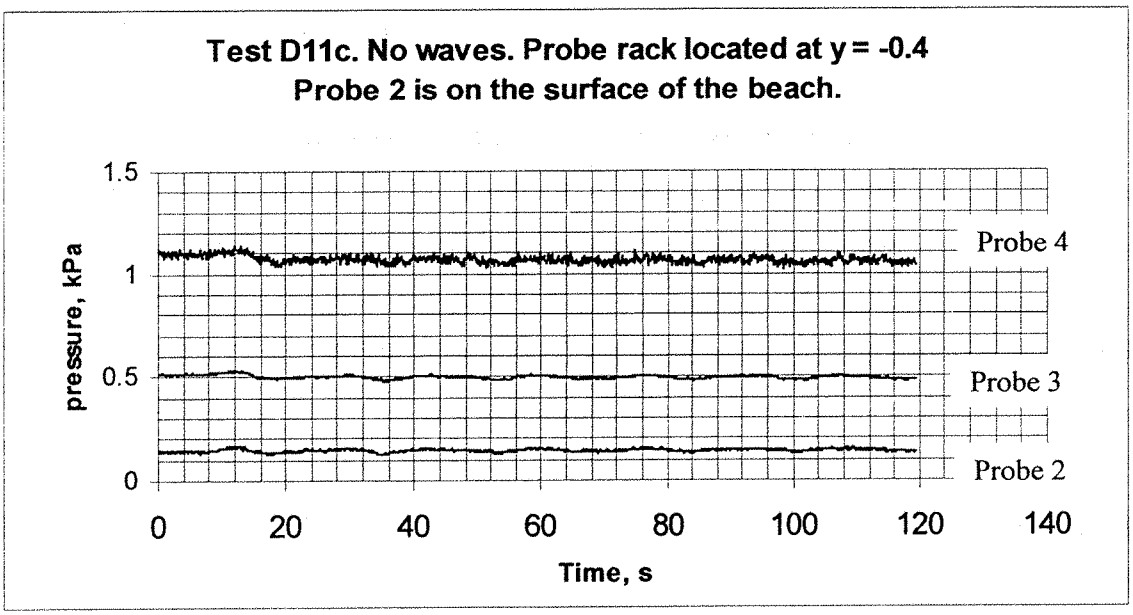

Figure 7.6: Pressure plots for Test D11c, where y = -0.4. No waves operating.

From Figure 7.6 it can be seen that the average pressures for transducers 2, 3, and 4 from t = 20 to t = 30 (drain on) are 0.14kPa, 0.5kPa and 1.06kPa respectively. From Figure 7.4 the corresponding pressure readings are 0.26kPa, 0.63kPa and 1.21kPa. These values are summarised in Table 7.2.

PROBE	LOCATION IN HORIZONTAL PLANE, M FROM DRAIN	LOCATION IN VERTICAL PLANE, M BELOW BEACH SURFACE (MM)	PRESSURE (KPA) (DRAIN ON)		DIFFERENCE IN PRESSURE (WAVES ON – WAVES OFF) KPA
			Waves off (hydrostatic)	Waves on (dynamic)	
1	-	-	-	-	-
2	-0.4	0	0.14	0.26	0.12
3	-0.4	45	0.5	0.63	0.13
4	-0.4	90	1.06	1.21	0.15

Table 7.2: Summary of pore water pressure data from tests D11c and D12c.

It can be seen that the waves result in a pore water pressure that is greater than the hydrostatic pressure by approximately 0.14 kPa.

The data suggest that the pore water pressure difference occurs at all depths, however, only 3 depths are presented in Table 7.2.

Effect of waves on beach pore water pressure for a range of depths

Table 7.3 shows the pore water pressure readings when the pressure transducer rack is located at y = 0 (between the two beach drains). Two sets of data were collected for this rack location: the first one was with the top transducer (probe 1) located 22mm below the SWL (or 34mm below the beach surface) to produce probe readings labelled 1, 2, 3, and 4, and the second test was carried out with the top probe (probe 2') located on the beach surface to produce probe readings labelled 2', 3' and 4'.

The wave generator was switched on for all the readings shown in Table 7.3, and the discharge was constant for all tests (= 9.3 l/min per m). Average pore water pressures were read from PWP plots by eye. Figure 7.7 shows the relationship between pore water pressure and depth for the test data tabulated in Table 7.3.

Rack position y = 0						
					Head at depth	
	Probe depth	Probe depth	PWP reading		of probe due to	
	below beach	below	KPa	KPa	PWP (H, mm)	
Probe code	surface (z, mm)	SWL (d, mm)	Drain OFF	Drain ON	OFF	ON
2'	0	-12	0.05	0.05	5.0968	5.0968
1	34	22	0.59	0.37	60.143	37.717
3'	45	33	0.39	0.16	39.755	16.31
2	79	67	0.89	0.6	90.724	61.162
4'	90	78	0.99	0.66	100.92	67.278
3	124	112	1.21	0.96	123.34	97.859
4	169	157	1.79	1.55	182.47	158

Table 7.3: Average pore water pressure readings when the probe rack is located at y = 0. 110/2.5 waves ON

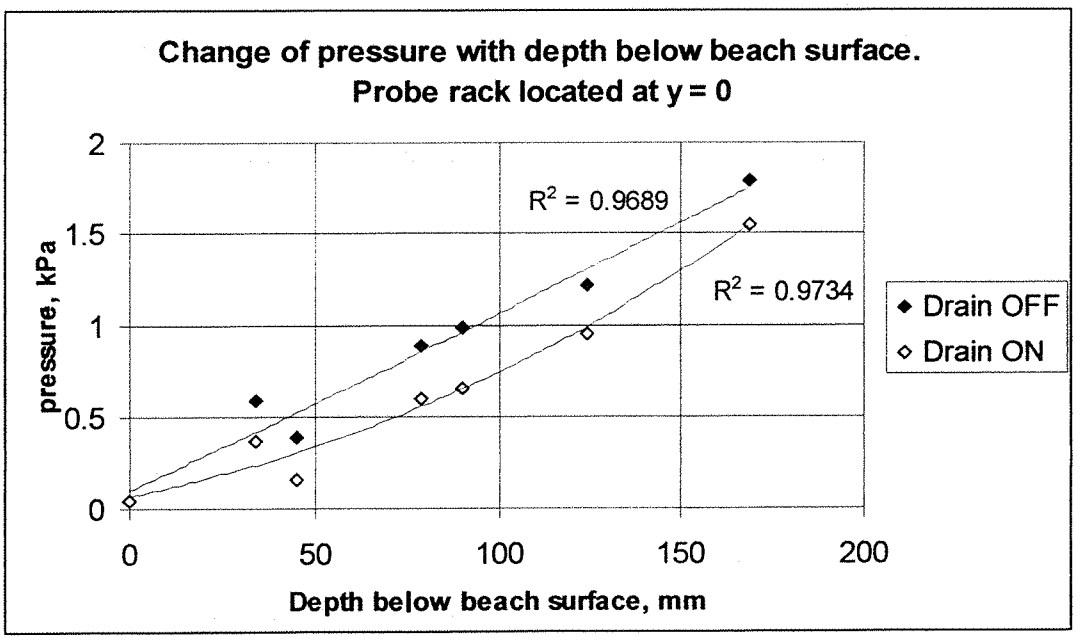

Figure 7.7: Change of pore water pressure with depth when probe rack is located at y = 0. 110/2.5 Waves ON.

The pore water pressure measured on the beach surface (z = 0) is the same with the drain off and on, but the two trendlines diverge with increasing depth below the beach surface. Even at a depth of just a few centimetres there is a significant difference between the drain off and drain on pressure reading.

Results indicate that although the beach drain cannot reduce the pressure immediately on the surface of the beach, the effect of the drainage system increases rapidly with depth, and may therefore be valuable in increasing the stability of the layers of sediment directly below the beach surface.

When the waves were switched off, it was found that the beach drainage system had a greater effect on the beach pore water pressure. Figure 7.8 shows the relationship between pore water pressure and depth for the same pressure transducer locations as for Figure 7.7, but with the wave machine switched off.

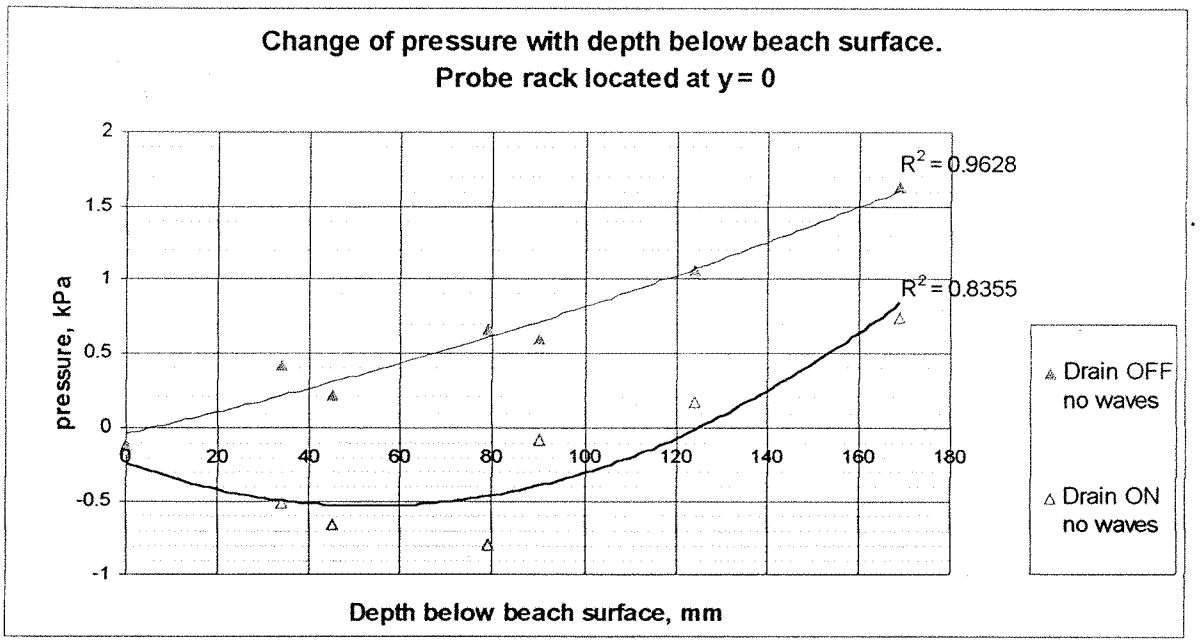

Figure 7.8: Change of pore water pressure with depth. Pressure transducer rack is located at y = 0, no waves.

Figure 7.9 shows the pore water pressures recorded with and without waves operating when the drainage system was switched off (these data sets are taken from Figure 7.7 and 7.8). When the two data sets are compared on the same graph, it can be seen that wave operation results in an elevation of the beach pore water pressure at all depths. The pressure elevation may be assumed to be constant for all depths, since the two lines are parallel.

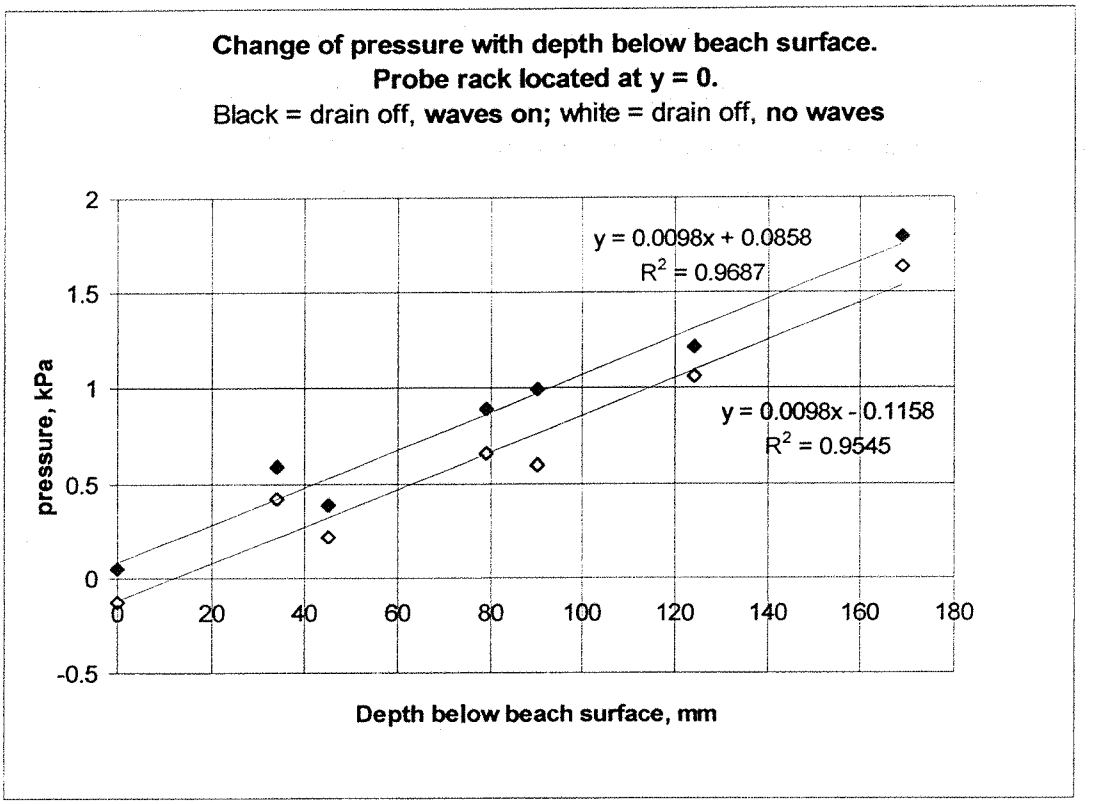

Figure 7.9: Change of pore water with depth with beach drain off. Black = with waves operating; white = without waves operating.

7.4.3 Effect of waves on mean pore water pressure in horizontal plane

Effect of wave action on pore water pressure when the beach drain is off

It has been shown that pore water pressure elevation in the vertical plane due to wave action is constant with depth. In this section, the effect of wave action on pore water pressures in the horizontal plane is investigated.

Figure 7.10 shows the change in pore water pressure with distance from the beach drain in the horizontal plane. These data were recorded using a probe located 0.067m below the still water level, and with the drainage system off. The grey line shows the change of pressure with distance from the drainage system with waves operating, while the black line is the hydrostatic pressure recorded with the wave generator switched off.

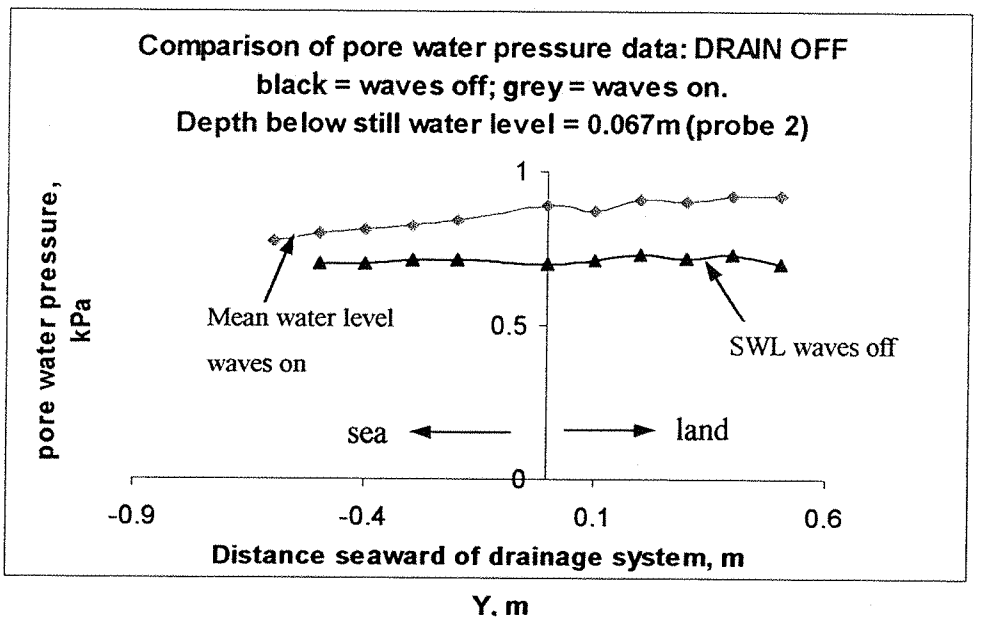

Figure 7.10: Pore water pressure measured 0.067m below the still water level, with and without waves operating (drain off).

Figure 7.10 shows that a variation in pore water pressure occurs in the horizontal plane. However, the increase in pore water pressure due to the waves is not constant for all positions in the horizontal plane. When the wave generator is on, the pore

water pressure gradually increases as y increases (for the range tested), while the black line (waves off) is approximately horizontal.

Figure 7.11 shows the trendlines for the data sets shown in Figure 7.10. From this figure it may be extrapolated that the set-up is zero at y = -1.3 (i.e. 1.3m seaward of the drain). At this point the pore water pressure is the same as that measured in hydrostatic conditions. This observation will be used later in this chapter.

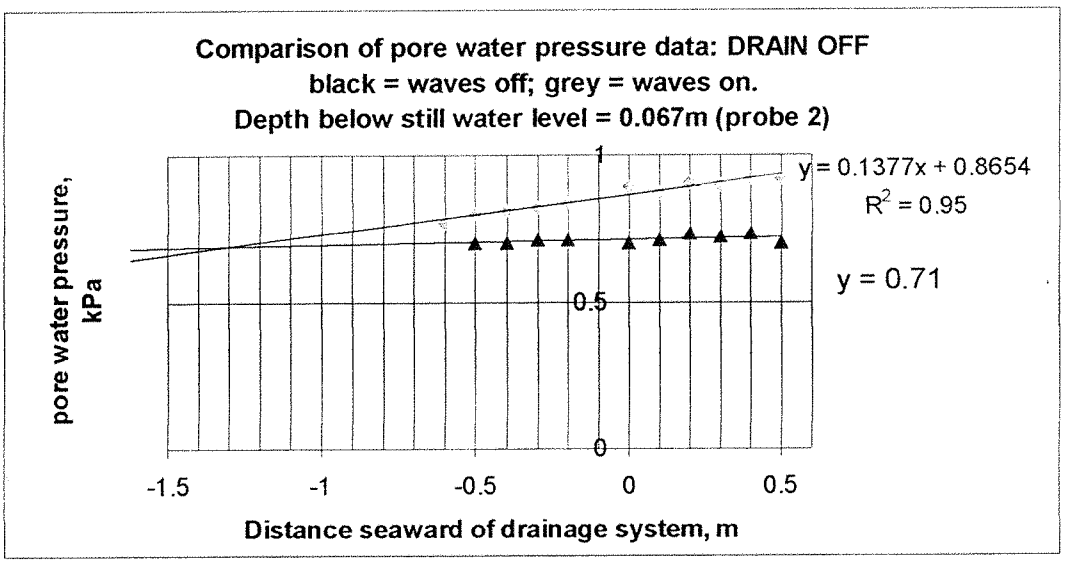

Figure 7.11: Same data set as shown in Figure 7.10 : trendline though data points.

Wave set-up

The elevation in pore water pressure shown in Figure 7.10 may be explained by the phenomenon of wave set-up. Set-up is an increase in the water level beneath the beach caused by the breaking waves and surf in the swash zone (Bowen, Inman and Simmons, 1968). It is '...a seaward slope in the water surface that provides a pressure gradient or force that balances the onshore component of the... momentum flux of the waves' (Komar 1998).

It is possible that the wave set-up in the model is exaggerated due the relative narrow width of the wave tank (= approximately 0.45m). In the model, wave motion is confined to two dimensions by the sides of the wave tank, and waves are monochromatic. Hence successive swashes regularly coincide with the returning

backwash, and the two collide directly. In the field, waves are irregular, and are not restricted from lateral movement.

For the model data, the location of the maximum set-up is unknown since the pressure is still increasing at y = +0.5m. The set-up is the difference in pore water pressure (between the waves on and waves off test) divided by ρg (ρ = density of water, g = acceleration due to gravity):

$P = \rho g d$ (d = depth of water)

$\rightarrow d = P/\rho g$

For probe 2 located at y = +0.5m, the pressure when waves were operating was recorded to be 0.95kPa, while the hydrostatic pressure was 0.7kPa.

Δd (metres) $= \Delta P/\rho g \rightarrow \Delta d = (0.95-0.7)x1000/9810$

$\Delta d_{model} = 25mm$

According to Chadwick and Morfett (1993) the maximum wave set-up is approximately 20 to 30% of the breaking wave height. Hence for the given wave climate, H = 0.11m (this is actually a shallow water wave height), the maximum set-up ranges between 22 and 33mm (mean = 28mm). This calculation suggests that the set-up in the wave tank is not exaggerated, since it corresponds to the theoretical prediction.

Affect of wave action on pore water pressure when the beach drain is in operation

The presence of waves also affects the pore water pressure when the drain is in operation, as shown in Figure 7.12. In this instance, the difference between the drain off and drain on lines is significantly greater, indicating that wave action has a marked effect on the influence of the drainage system.

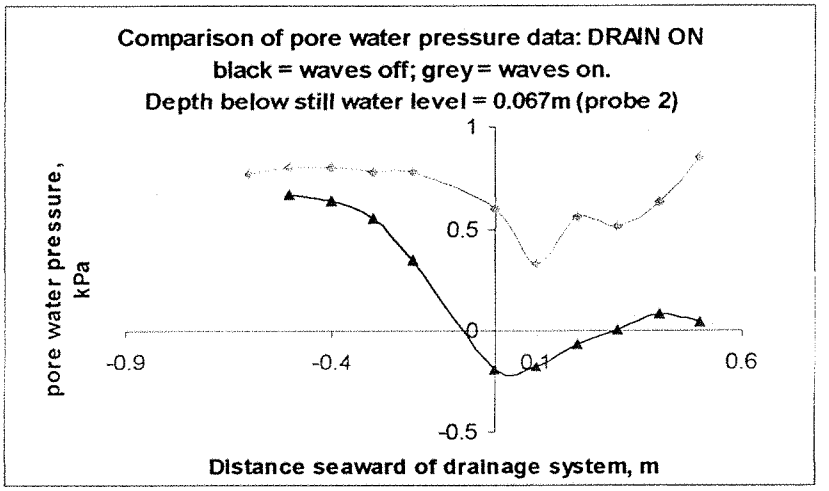

Figure 7.12: Pore water pressure readings for probe located 0.067m below the SWL when the drain is on. Grey = waves ON; black = waves OFF. The beach drain is located at y = 0.

When the waves were off, the maximum pore water pressure reduction occurred at approximately y = 0 (in line with the drain), however, when the waves were in operation, the maximum reduction occurred at approximately y = +0.1m, just landward of the drain. As in the case of the vertical plane, the presence of waves reduces the effect of the beach drainage system.

Set-up reduction

It has been shown that the beach drainage system effectively reduces the set-up within the beach. The wave set-up is an important factor influencing the mean shoreline position above which the individual waves occur (Komar, 1998). Hence reducing the set-up will affect the total run-up height. Unfortunately this was not investigated for this project, however, further investigation into the effect of beach drainage on the run-up length for individual waves is recommended. This research would have important implications for shoreline protection.

7.5 Spatial variation of pore water pressure (waves operating)

In section 7.4 the effect of waves on pore water pressure in the vertical and horizontal planes was investigated. Pore water pressure data have been recorded for a range of vertical and horizontal locations to produce a grid of data points within the beach cross section.

As discussed in section 7.2, four probes were mounted on a rack, which was placed in the beach at a given horizontal distance from the beach drain. Pressures were recorded for a range of depths below the still water level.

Figure 7.13 shows the relationship between pore water pressure and depth below the still water level for a range of different locations. All values are average pore water pressures. The distance from the probe rack to the drain in the horizontal plane (in metres) is indicated at the top of each chart. The top left chart in Figure 7.13 shows the pore water pressure data when the probe is furthest seaward of the drain, while the rack location for the bottom right chart is the furthest landward of the drain. The black data points were recorded when the drain was off, while the white data points were recorded with the drain on.

At y = -0.4 there is no difference between the drain on and drain off pore water pressure readings throughout the depth of the beach. For y = -0.3m and –0.2m the difference is relatively small. The drainage system is most effective between y = 0 and y = +0.3m. There is a small effect at y = +0.5m, but by y = +0.6 the drainage system is ineffective again.

Beach drainage system effective zone

From Figure 7.13, it can be seen that the drainage system is effective between approximately y = -0.3 and y = +0.5m, and the optimum effect is at y = +0.1m. Note that this is for the given SWL location. The effective zone and optimum are likely to be affected by the SWL location (see Chapter 8).

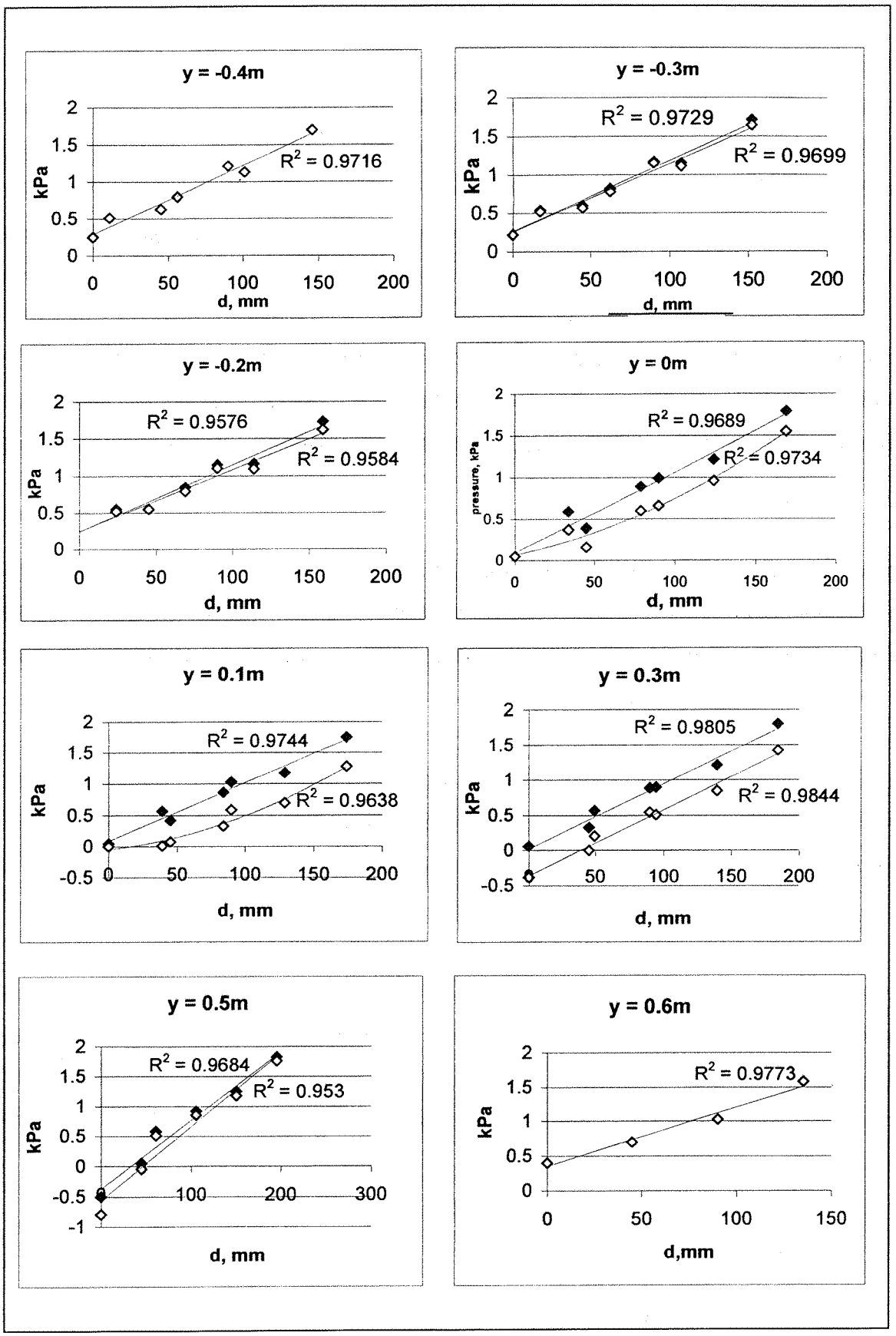

Figure 7.13: Graphs to show change of pore water pressure with depth for different probe rack locations (waves operating). Black = DRAIN OFF; white = DRAIN ON; Drain is located at y = 0.

Pore water pressure distribution

Figures 7.14 a and b show a cross section of the model beach and lines of equal pore water pressure. The top graph (Figure 7.14a) shows the pore water pressure distribution when there was no drainage, and the bottom graph (Figure 7.14b) for when the drain was on. The lines of equal pore water pressure have been interpolated from the data shown in Figure 7.13 using a spreadsheet. The horizontal axis is the distance in the horizontal plane from the drainage system, while the vertical axis is the depth, d, below the still water level. The horizontal axis, d = 0 is the still water level, and the position of the beach drainage system is indicated in Figure 7.14b. A moderate wave climate was in operation for both tests (wave climate 110/2.5: see Chapter 5).

The lines of equal pore water pressure with no drain operating are approximately horizontal, straight and parallel. It can be seen that drainage system was effective between y = -0.2m and 0.5m, and the optimum pore water pressure reduction is at y = 0.1m.

When the drain is operating, the lines of equal pressure remain parallel, which indicates that the drain is equally effective at all depths. This may be as a result of the impermeable boundary at the back of the wave tank, since it would be expected that the influence of the drain would decrease with depth.

The zone of influence of a full scale drainage system can be seen in Figure 7.15. This photograph shows the beach drain at Town Beach in Newquay (discussed in Chapter 2). The location of the drain can be identified by the dry area on the beach. (Note that the people picnicking on the beach are seated on the driest part of the beach over the drain).

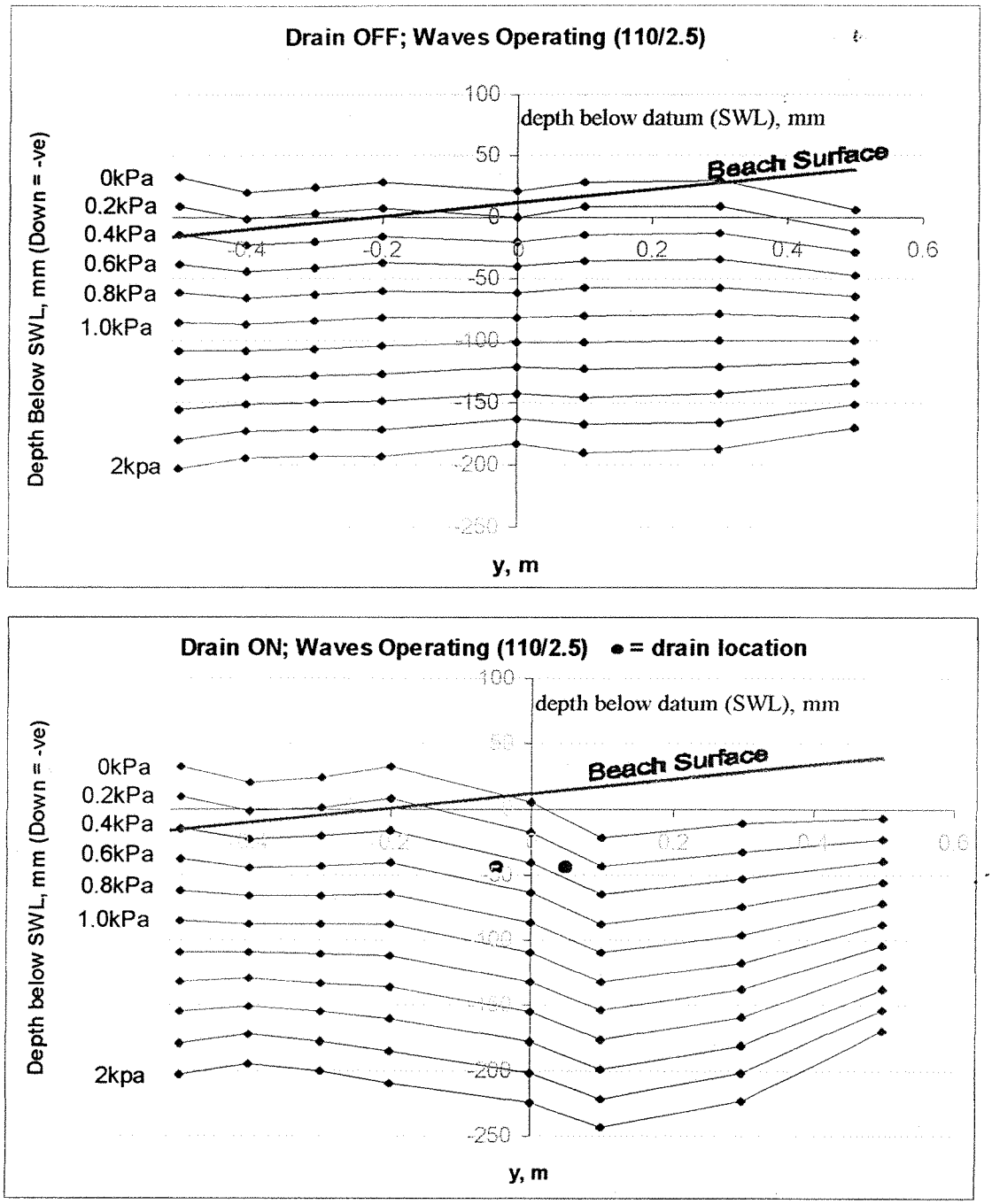

Figure 7.14a and b: Pore water pressure distribution. (a) Top graph = drain OFF; (b) bottom = drain ON. Waves operating in both instances. (All values are average pore water pressures)

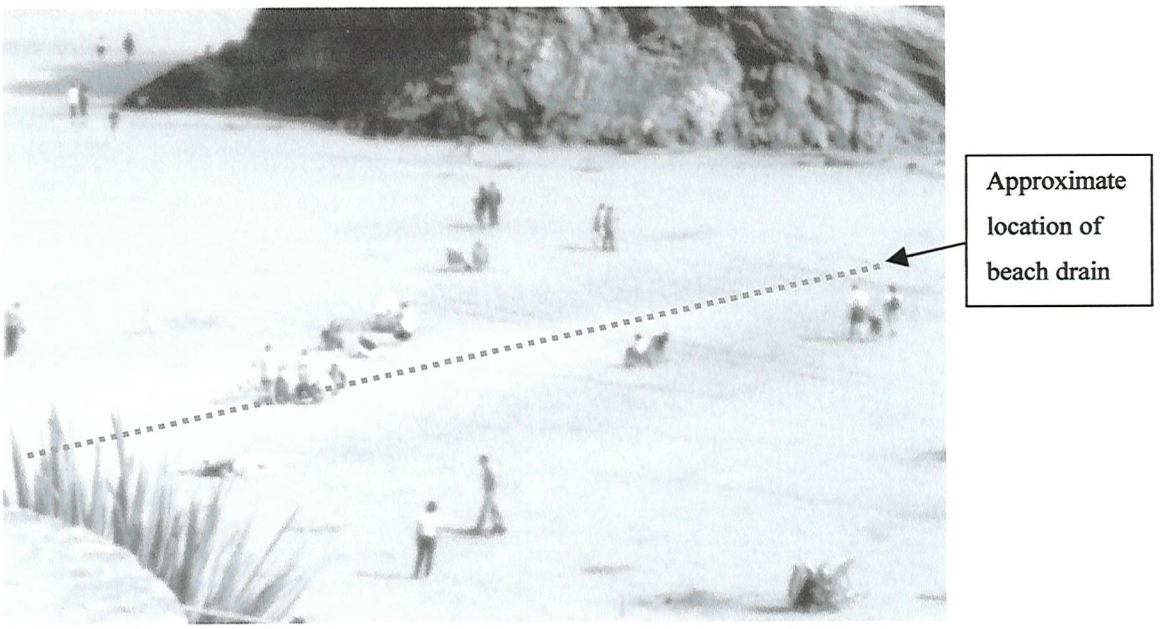

Figure 2.15: Towan Beach during low water

7.6 Relationship between discharge and pore water pressure (no waves)

For a given probe rack location, the pore water pressure was measured for a range of discharges. Pore water pressure data were recorded with the probe rack located in different positions relative to the drainage system. No waves were operating for these tests.

Probe rack located within the zone of influence of the drainage system

Figure 7.16 shows the change of pore water pressure with discharge with the probe rack located within the zone of influence of the drain at y = -0.2m.

There is a difference of approximately 0.3kPa between q = 0 and q = 5l/min per m. The gradients for the four probes are approximately the same, although the gradient becomes slightly lower the nearer to the surface of the beach the probe is located. This observation is likely to be a coincidence, since for other data sets, the gradients of each of the curves for probes 1 to 4 are approximately the same, and do not necessarily ascend from probe 1 to probe 4.

A good correlation is observed with the linear trendline, and the data demonstrate that the relationship between pore water pressure and discharge is approximately linear.

Probe rack located outside the zone of influence

Figure 7.17 shows that when the probe rack is located outside the zone of influence of the drainage system the gradient is zero.

Probe rack located on the boundary of the zone of influence of the drainage system

Figure 7.18 shows the PWP vs discharge plot for the four pressure probes with the rack located at y = -0.4m. The low gradients of the lines in Figure 7.18 show that this probe location is near the limit of the effect of the drainage system. The difference in the PWP between q = 0 and q = 5/min per m is only 0.05kPa.

Probe Rack located at y = 0

The maximum gradient is achieved when the probe rack is located between the two beach drains at y = 0. The data recorded for y = 0 are shown in Figure 7.19. There is a good correlation with the linear trendlines, which have a mean gradient of 0.185.

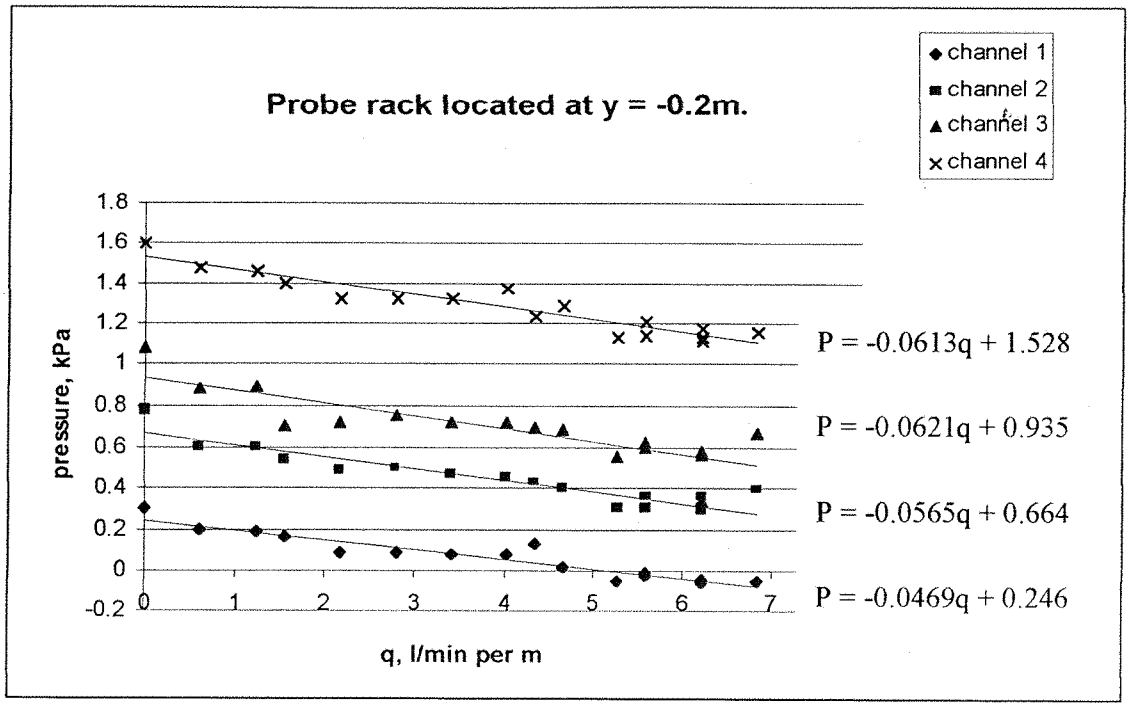

Figure 7.16 Relationship between pore water pressure and discharge. Probe rack located at y = -0.2m. Probe 1 is 24mm below the beach surface, and 22mm below the SWL.

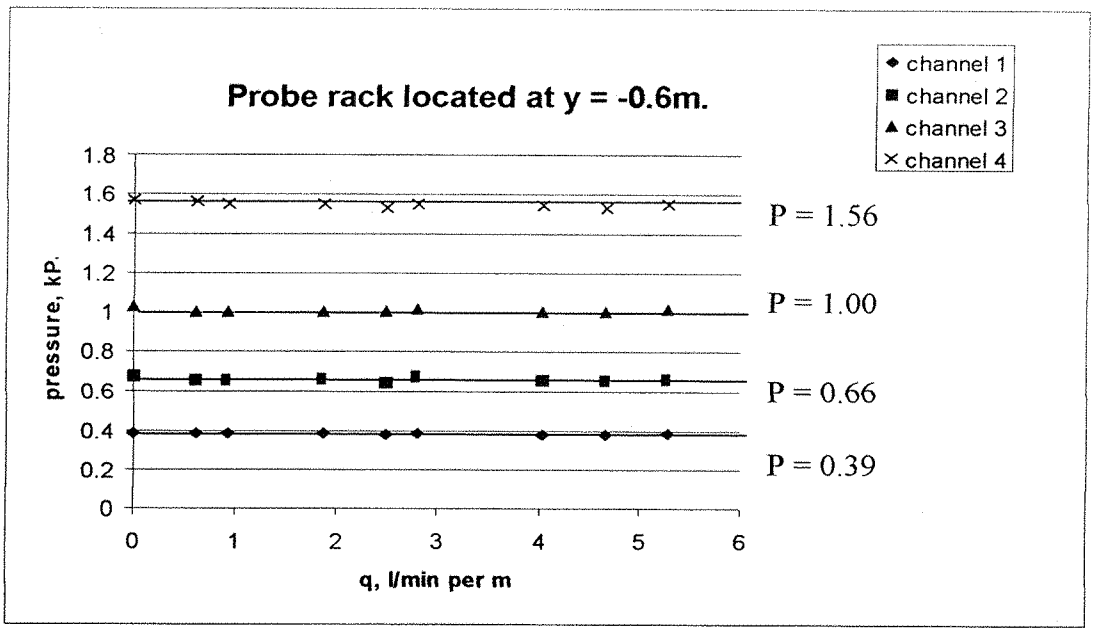

Figure 7.17: Relationship between pore water pressure and discharge when the probe rack is located at y = -0.6m. Probe 1 is 0mm below the surface of the beach, and 22mm below the SWL.

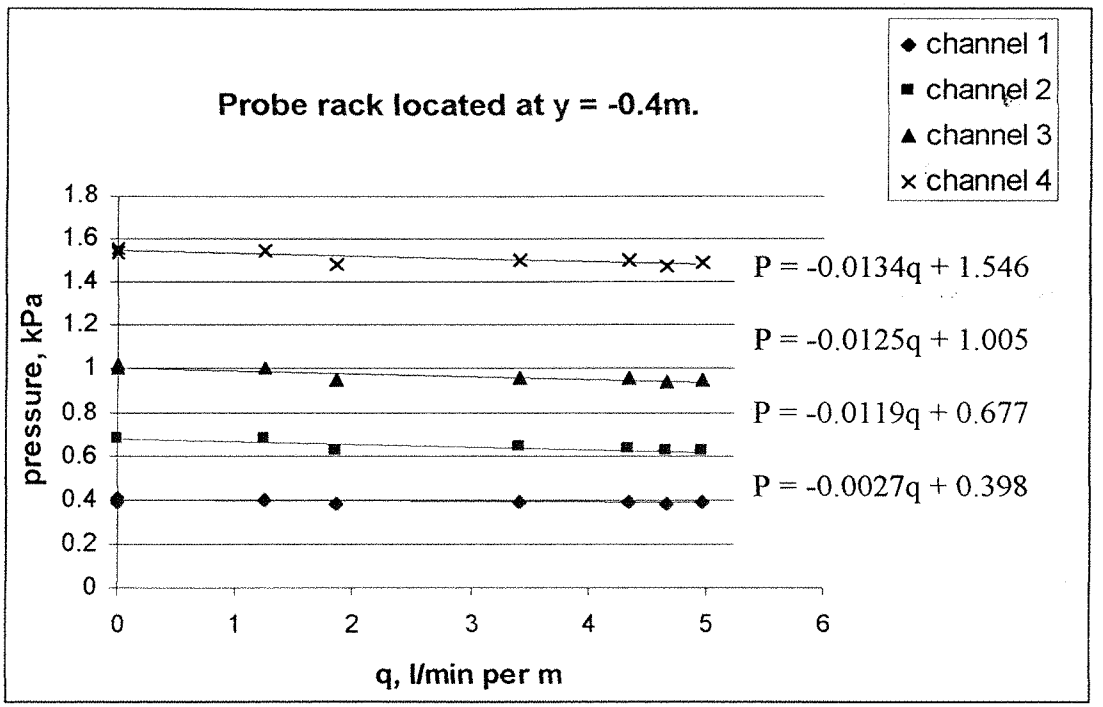

Figure 7.18: Relationship between pore water pressure and discharge when the probe rack is located at y = -0.4m. Probe 1 is located 11mm below the surface of the beach, and 22mm below the SWL.

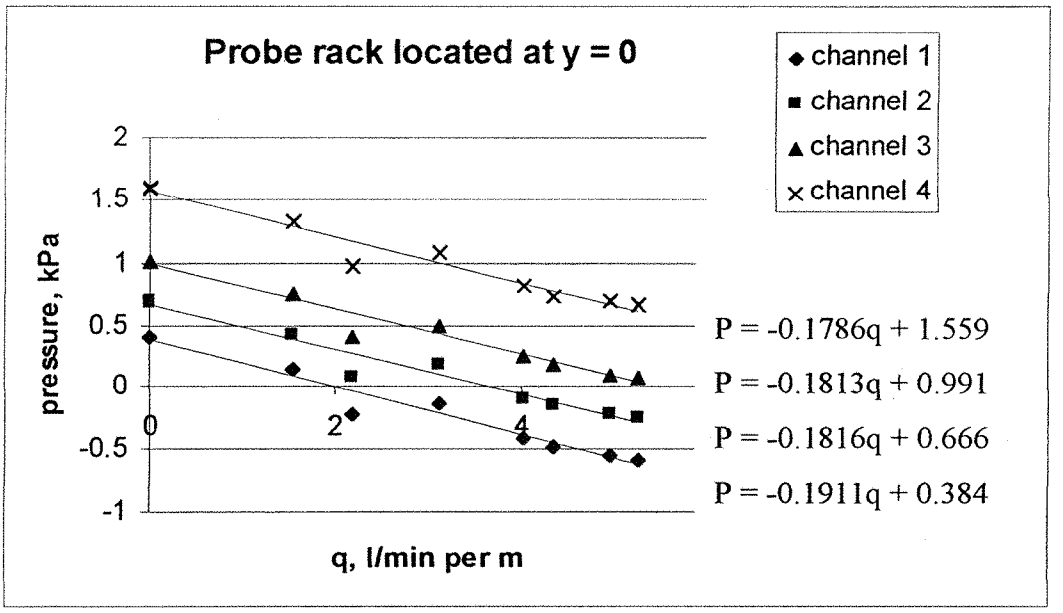

Figure 7.19: Relationship between pore water pressure and discharge when the probe rack is located at y = 0. Probe 1 is 34mm below the surface of the beach, and 22mm below the SWL.

Discussion of data

It should be noted that there is a discrepancy between the probe output for channel 1 and the given water depth in Figures 7.17, 7.18 and 7.19. As shown in Figure 7.16, the probe reading when the pressure transducer is buried 22mm below the still water level should read approximately 0.22kPa when q = 0 ($P = \rho gh$). Figures 7.17, 7.18 and 7.19 show the pressure for probe 1 to be approximately 0.4kPa, suggesting a water depth of 40mm. However, it can be seen that for the remaining probes (2, 3, and 4) the static head is more accurate: the probe depths below SWL are 67mm; 112mm; and 157mm while the pressure readings (when q = 0) are 0.67kPa; 0.10kPa and 1.56kPa respectively. Clearly the probe readings for channels 2, 3, and 4 correspond to the measured water depth much better than for probe 1, suggesting that the probe 1 reading is an anomaly. It is interesting that one probe in the set of four should provide an anomalous reading, since all four probe measurements were recorded simultaneously, and the probe positions on the rack were fixed with a rigid fitting. The discrepancy may have been caused by air ingress (since probe 1 is the top probe and is the unit most likely to have been accidentally lifted above the SWL during moving).

In terms of data analysis, the gradient of the probe 1 data set (Figures 7.17, 7.18 and 7.19) is not anomalous, and corresponds with the gradients of the probe 2, 3, and 4 data. This suggests a systematic error, which also indicates possible air ingress, or even (but less likely) an electrical fault.

Relationship between pore water pressure and discharge for different rack locations in the horizontal plane

The above graphs show that the relationship between pore water pressure and system discharge is approximately linear, and varies with the probe location. The distance in metres from the drainage system in the y direction controls the gradient of the linear trendline, while the vertical location, in metres below the still water level, controls the intercept. (Note that the intercept simply represents hydrostatic conditions.)

Further data sets were recorded, and a summary of the gradients is shown in Table 7.4. The data presented in Table 7.4 are shown graphically in Figure 7.20. The vertical axis is the rate of change of pore water pressure with discharge, or the gradient read from the graphs of pore water pressure vs discharge. The steeper the gradient ($\Delta P/\Delta q$), the more effective the drainage system. The horizontal axis is the distance in metres from the beach drain to the probe rack.

Probe location (metres from drainage system)	Average gradient = ΔP/Δ q
-0.6	-0.0035
-0.4	-0.0161
-0.2	-0.0567
0	-0.185
+0.2	-0.152
+0.4	-0.1702
+0.5	-0.1233

Table 7.4: rate of change of pore water pressure with discharge for different probe rack locations. ΔP = change in pore water pressure, Δq = change in discharge

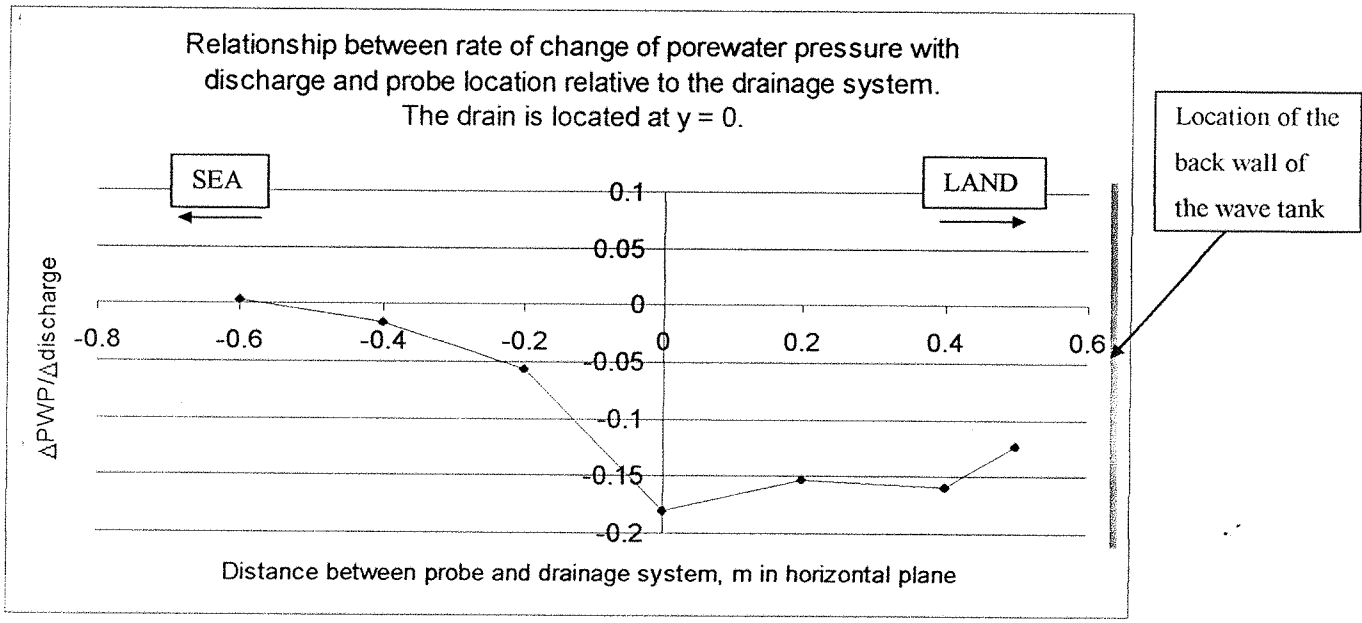

Figure 7.20: Relationship between ΔP/Δq and probe rack location in horizontal plane

The maximum gradient occurs at y = 0, when the probes are located between the two beach drains. The drainage system has an effect on beach pore water pressure when the probe rack is located less that 0.6m seaward of the drain.

The graph is not symmetrical about y = 0, and this is likely to be due to:

- the proximity to the rear of the wave tank,
- increased wave set-up due to the restricted width of the wave tank (this will be discussed later in this chapter), and,
- because the seaward side of the drainage system is continuously inundated with water.

7.7 Relationship between pore water pressure and controlling variables

In this section the analysis introduced in section 7.6 is extended to derive an empirical formula quantifying the relationship between pore water pressure and the controlling variables.

7.7.1 No waves operating

In Figure 7.20 it was shown that the pore water pressure reduction produced by the drain is not symmetrical about y = 0. For simplification, the data points seaward of the drain, the area most vulnerable to instability and slumping, will be analysed.

Figure 7.21 below shows the part of the graph seaward of the drain only, and a trendline has been fitted to the data set. Although there are only four points on this plot, each of these points has been obtained from a graph containing numerous data points (see e.g. Figures 7.16, 7.17, 7.18, 7.19).

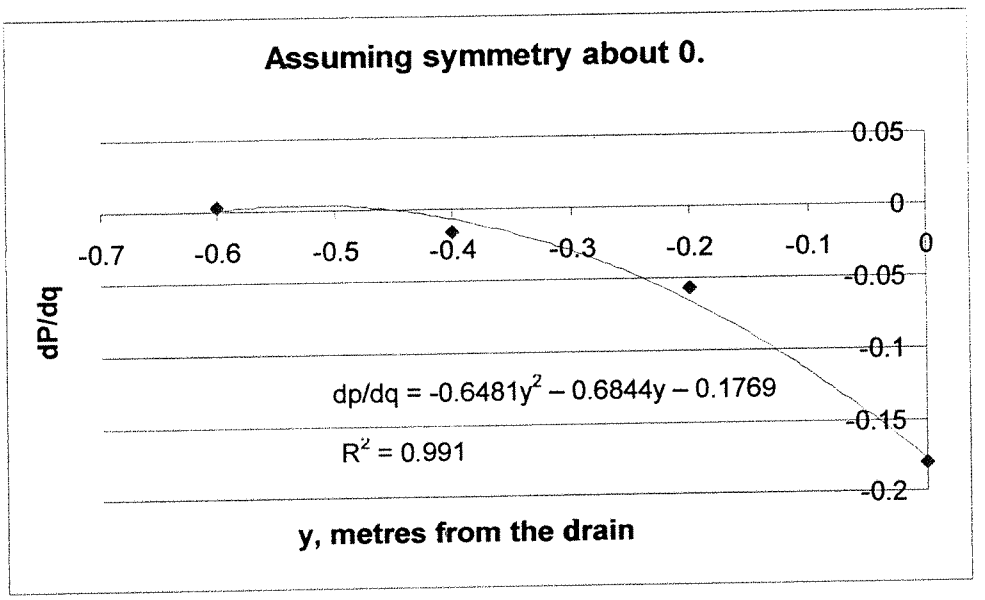

Figure 7.21: Relationship between ΔP/Δq, for probe rack locations seaward on the drain only

The equation for the trendline in Figure 7.21 is

$$\Delta P/\Delta q = -0.648y^2 - 0.684y - 0.177$$

where $\Delta P/\Delta q$ is the rate of change of pore water pressure with discharge.

Hence

$$dP = (-0.648y^2 - 0.684y - 0.177)\ dq$$

$$P = \int(-0.648y^2 - 0.684y - 0.177)\,dq$$

Therefore:

$$P = -q(0.648y^2 + 0.684y + 0.177) + C$$

C is a constant, and has been evaluated by measuring the pore water pressure at a given depth below the still water level when q = 0, i.e. C may be equated to the hydrostatic pressure. Figure 7.22 shows the relationship between depth and pressure when the drainage system is switched off. Four data points were recorded for each depth value.

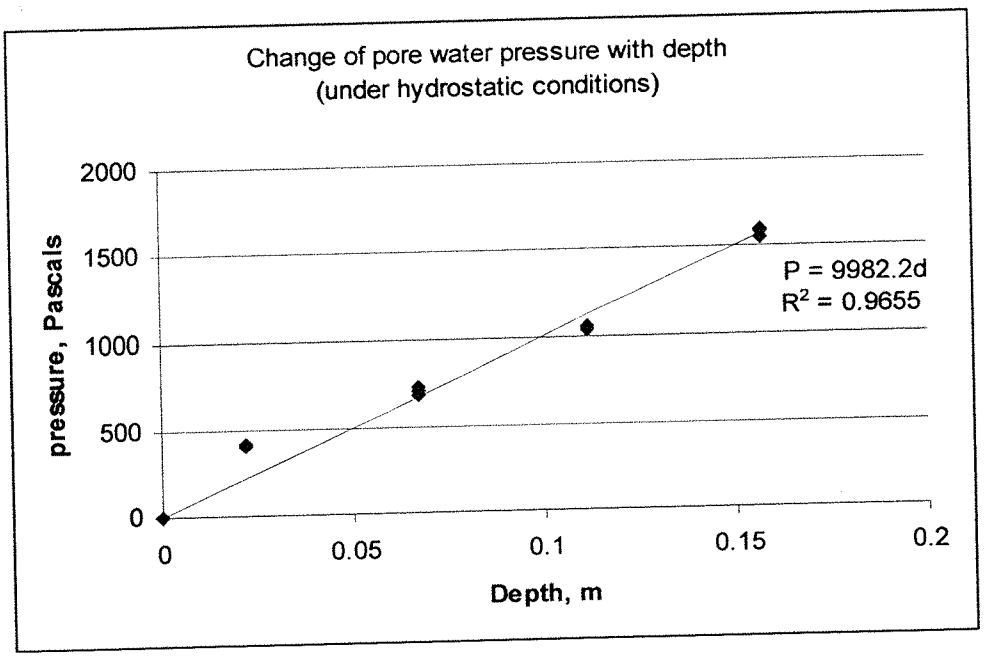

Figure 7.22: Relationship between depth and pore water pressure for hydrostatic conditions (model data measured using pressure transducers)

P (kPa) = 9.81 (kN/m^3) x d (m)

According to the measured data (Fig. 7.22) $P(Pa) = 9982.2d$

→ P (kPa) = 9.98d

Hence the constant, C = ρgd, and the relationship between pore water pressure, discharge and probe location becomes:

$$P = -q(0.648y^2 + 0.684y + 0.177) + \rho gd \qquad [1]$$

More generally:

$$P = \rho gd - f(q)$$

Note that there will be a maximum possible value of q based on a full drain and the permeability of the beach material.

P = pore water pressure, kPa; q = discharge (l/min per m), y = distance in horizontal plane from probe to drainage system, ρgd = static pressure in kPa, ρ = the density of water, g = acceleration due to gravity and d = depth below still water level (m). This relationship applies for a monochromatic moderately mild wave climate (110/2.5), with no tide operating, a fixed SWL location of 0.25m seaward of the drain, and a model drain depth of 50mm.

Figure 7.23 shows the relationship applied to a range of system discharge values. The empirical formula (equation 1) applies to hydro- and geostatic conditions, however, later in this chapter this relationship is compared to data collected during wave action.

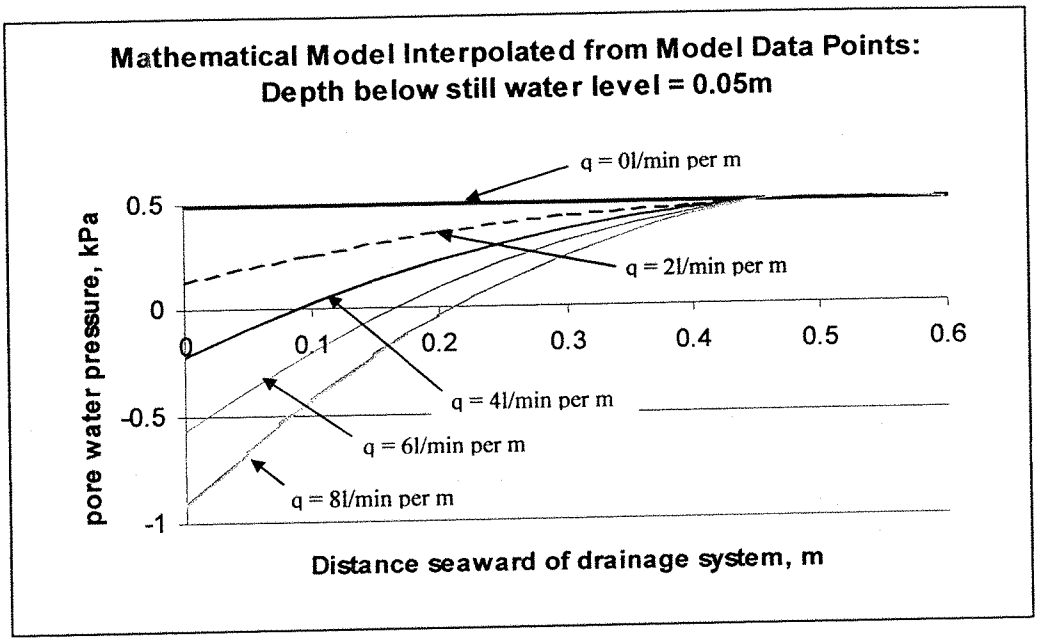

Figure 7.23: Empirical model (derived from physical model data) applied to a range of discharge values.

7.7.2 Waves operating

The empirical equation discussed in the previous section was derived from model data that were recorded when no waves were operating. However, in section 7.4 it was demonstrated that when the wave generator is on, the mean pore water pressure is increased. Therefore the formula above will not apply during wave operation due to wave set-up, and a new expression must be derived to account for this.

The equation for the relationship between pore water pressure, discharge and location in the horizontal plane, y, was evaluated in the same way as for the case where no waves were operating (see section 7.7.1). However, in this case, data were not recorded over the full range of discharges, and instead the $\Delta P/\Delta q$ gradient was evaluated using data from the extreme cases drain off and drain on (where q = 15l/min per m) only. Table 7.5 shows the $\Delta P/\Delta q$ values obtained for different probe rack locations, and Figure 7.24 shows a graph of the data tabulated in Table 7.5.

DISTANCE FROM DRAIN IN HORIZONTAL PLANE (M)	GRADIENT = $\Delta P/\Delta$ Q
-0.6	0
-0.5	0
-0.4	-0.00067
-0.3	-0.00267
-0.2	-0.004
0	-0.01933

Table 7.5: Table to show $\Delta P/\Delta q$ for different probe rack locations

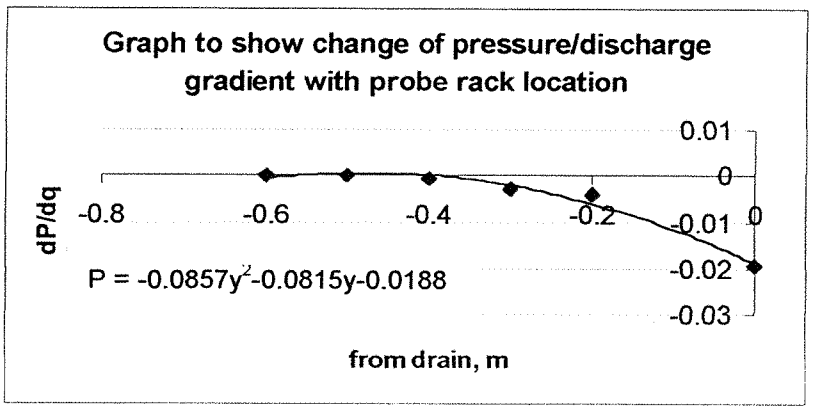

Figure 7.24: graph of data tabulated in Figure 7.16

In this case:

$$P = q(-0.0857y^2 - 0.0815y - 0.019) + C \qquad [2]$$

With no waves operating, the intercept C was equated to the hydrostatic pressure, ρgd. However, it has been shown that when waves are operating the pore water pressure with no drainage is greater than hydrostatic due to wave set-up. Therefore the intercept, C in this case needed to be evaluated by deriving a formula for the pore water pressure when q = 0 during wave action.

In section 7.4.3 it was shown that set-up reduces seaward, and that for a given location in the horizontal plane, the pore water pressure measured with waves operating will be equal to hydrostatic. This was observed to occur at approximately y= -1.3m (see Figure 7.11). The parameter y_h has been introduced, where y_h is the value of y at which the pressures are hydrostatic. In this case, y_h = -1.3m.

Figure 7.25 shows the pore water pressures measured when q = 0 for four different probes in different locations in the horizontal plane. The horizontal plane sign convention y has been used in this figure, where the beach drain is located at y = 0, and y +ve is landward of the drain, while y –ve is seaward of the drain.

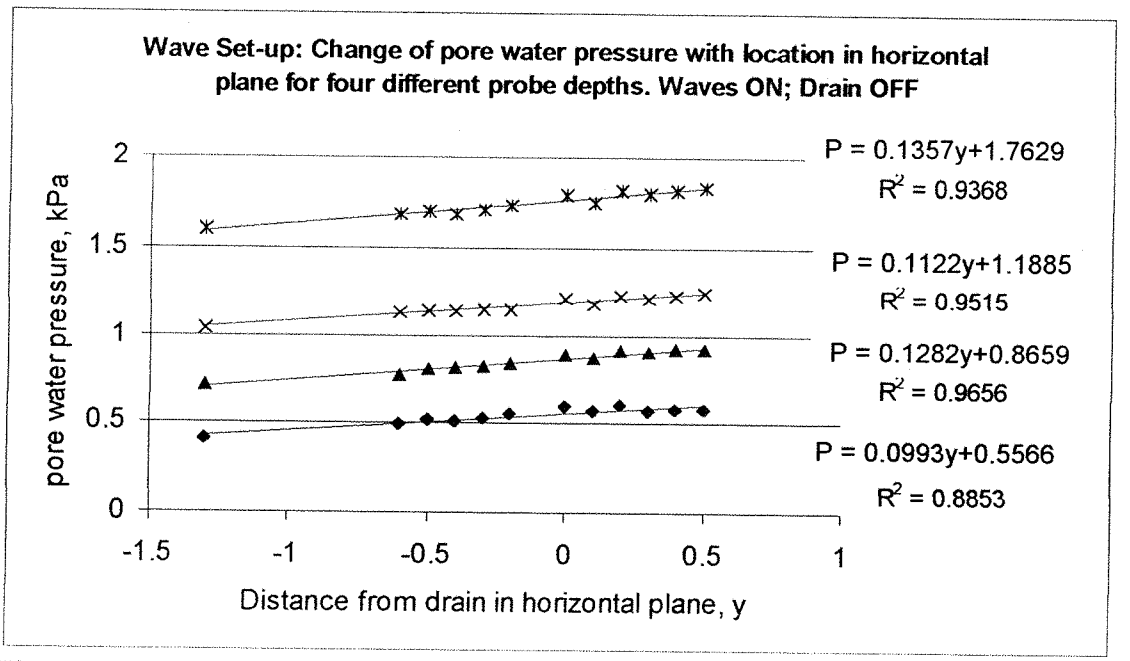

Figure 7.25: Change of pore water pressure with distance from the beach drain. Drain is off, and wave generator is on. Probe 1 is 22mm below the SWL and the four probes are 45mm apart and vertically aligned.

The generic equation for the trendlines shown in Figure 7.25 is: P = my+c, where P = pore water pressure when q = 0, m is = the gradient (dP/dy), y is the distance from the drain in metres, and c is the intercept with the vertical axis. The hydrostatic pressures for probes 1, 2, 3, and 4 are 0.41kPa, 0.71kPa, 1.04kPa and 1.60kPa respectively, and extrapolating from Figure 7.25 these can be seen to occur at y = -1.3m.

When the term y_h is used in place of y, the intercept, c, is shifted, and becomes equal to the hydrostatic pressure, ρgd. Therefore:

$$P_{(\text{when } q=0)} = my_h + \rho gd.$$

For simplicity, it has also been assumed that all the gradients in Figure 7.25 are the same, and the average gradient of the four lines is 0.11.

Therefore in this case the equation for the intercept C becomes:

$$C = 0.11(y+1.3) + \rho gd \qquad [3]$$

Substituting [3] into equation [2], the expression for pore water pressure when waves are operating becomes:

$$P = q(-0.086 - 0.815 - 0.019) + [(0.11(y+1.3)) + \rho gd]$$

More generally:

$$P = \rho gd + m(y - y_h) - f(q)$$

Where m is the set up gradient, and y_h is the distance from the drain to the point at which P = hydrostatic. Note that this equation applies for the physical model described in Chapter 5, and for a constant wave climate (H = 0.11m; T = 1.59s).

7.8 Effect of drainage on effective stress

Since the beach drainage system causes a reduction in pore water pressure, this affects the effective stress of the beach material (the ability of the sand to resist shear).

As previously stated the effective stress is the difference between the overburden (soil + water) and the pore water pressure. Should the effective stress of a soil become zero, then it has no resistance to shear, and behaves as a fluid (known as fluidisation or liquefaction). This can only occur if excess pore water pressure occurs (the pore pressure at a point below the beach surface is greater than the static head at that point).

Observations through the side of the tank indicate that the top layers of sediment move due to wave action in the swash zone. The sediment particles move freely without shear force resistance since the particles are no longer in contact. Below these layers, the bed begins to resist shear, since the particles are held in place due to the weight of the overlying material (overburden).

The purpose of the investigation described in this section is to determine the impact of beach drainage on the beach material shear resistance.

7.8.1 Data analysis

The data used in section 7.5 (Figure 7.13) have been used to evaluate the effective stress for all the probe locations for which pore water pressure data were recorded.

According to the Terzaghi (1936) equation quoted in Chapter 2:

$\sigma' = \sigma - u$ (where σ' = effective stress; σ = vertical stress; u = pore water pressure)

Several assumptions have been made:

- the overburden comprises the direct vertical stress only
- the material below the still water level is fully saturated
- the beach material is uniformly compacted

- the overburden of the saturated overlying material is calculated using the wet bulk density of Bakelite (= 12.3kN/m^3)
- additional overburden arises due to the weight of the water overlying the surface of the beach, the magnitude of which is denoted by the pressure probe reading on the surface of the beach (as noted on page 196 additional readings were recorded to determine the pressure on the surface of the beach)

Hence:

$$\sigma' = \left(\gamma_{wb} z + \gamma_w \left[\frac{P_s}{\rho g} \right] \right) - P_z$$

Simplifying:

$$\sigma' = \left(\gamma_{wb} z + P_s \right) - P_z$$

where:

γ_{wb} = wet bulk density of Bakelite

z = depth below beach surface

γ_w = bulk density of water (= ρg)

P_s = pressure measured on surface of beach (at a depth h below the still water level: P_s=ρgh)

ρ = density of water; g = acceleration due to gravity

P_z = pressure recorded at depth z below the beach surface (= probe output for given location)

These parameters are summarised in Figure 7.26.

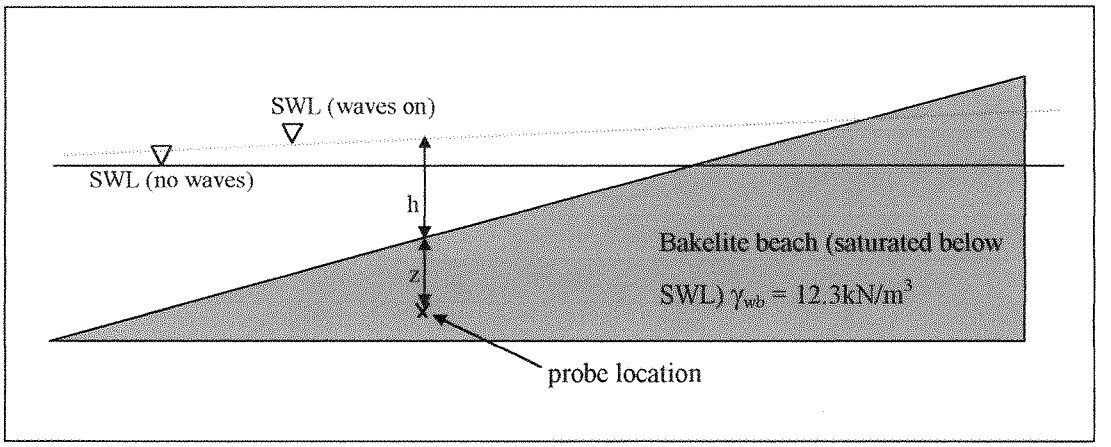

Figure 7.26: Diagram to show parameters used for effective stress calculation

Table 7.6 shows an example spreadsheet, with data for the probe rack located at y = -0.4m (0.4m seaward of the drain in the horizontal plane). Data have been recorded at 6 different depths below the beach surface (z).

Y = -0.4			Unit weight of Bakelite	12.3kN/m^3			
Probe code	Water depth from surface of beach to MWL	z (m) depth of beach above probe	PWP Data OFF K Pa	PWP Data ON K Pa	Dist from SWL probe (m)	Effective stress K Pa OFF	Effective stress K Pa ON
2'	0.025	0	0.25	0.25	0.011	0	0
3'	0.025	0.045	0.63	0.63	0.056	0.1735	0.1735
2	0.025	0.056	0.8	0.8	0.067	0.1388	0.1388
4'	0.025	0.09	1.21	1.21	0.101	0.147	0.147
3	0.025	0.101	1.13	1.13	0.112	0.3623	0.3623
4	0.025	0.146	1.7	1.7	0.157	0.3458	0.3458

Table 7.6: Example spreadsheet for effective stress calculation

Example: Probe 3'

from probe 2`

$$\sigma' = \gamma_{wb} z + P_s - P_z = (12.3\text{kN/m}^3 \times 0.045\text{m}) + 0.25\text{kPa} - 0.63\text{kPa}$$

σ' = 0.55 +0.25-0.63 = 0.17kPa (for drain on and drain off since probe is located beyond the zone of influence of the beach drain)

The change of effective stress with depth was plotted for each probe location (drain off and drain on). Data for a range of rack locations are shown in Figure 7.27.

Outside of the zone of influence of the beach drain, at y = -0.6m, it can be seen in Figure 7.27 that the effective stress increases with depth, and is the same for both the drained and undrained conditions. At y = -0.3m the beach drainage begins to influence the effective stress below the beach surface and, due to the reduction in pore water pressure, the drain results in a higher effective stress for a given beach depth (see graph for y = -0.3m in Figure 7.27). The drain has the greatest effect on beach strength between y = 0 and y = +0.3m.

At y = +0.3m and y = +0.5m the beach drain causes a difference in effective stress at z = 0. This is thought to occur because at these probe rack locations the mean water level is below the surface of the beach. For the remainder of the rack locations (y = 0m, and seaward of this point) the mean water level is above the surface of the beach, and hence the effective stress = 0 when z = 0 for both the drained and undrained conditions (i.e. the drainage system has no effect on the surface of the beach when it is flooded).

Note that the data were recorded for a fixed SWL location of y = -0.25m, a monochromatic wave climate (110/2.5), no tide and a Bakelite sediment where D_{50} = 0.51mm, and G_s = 1.45.

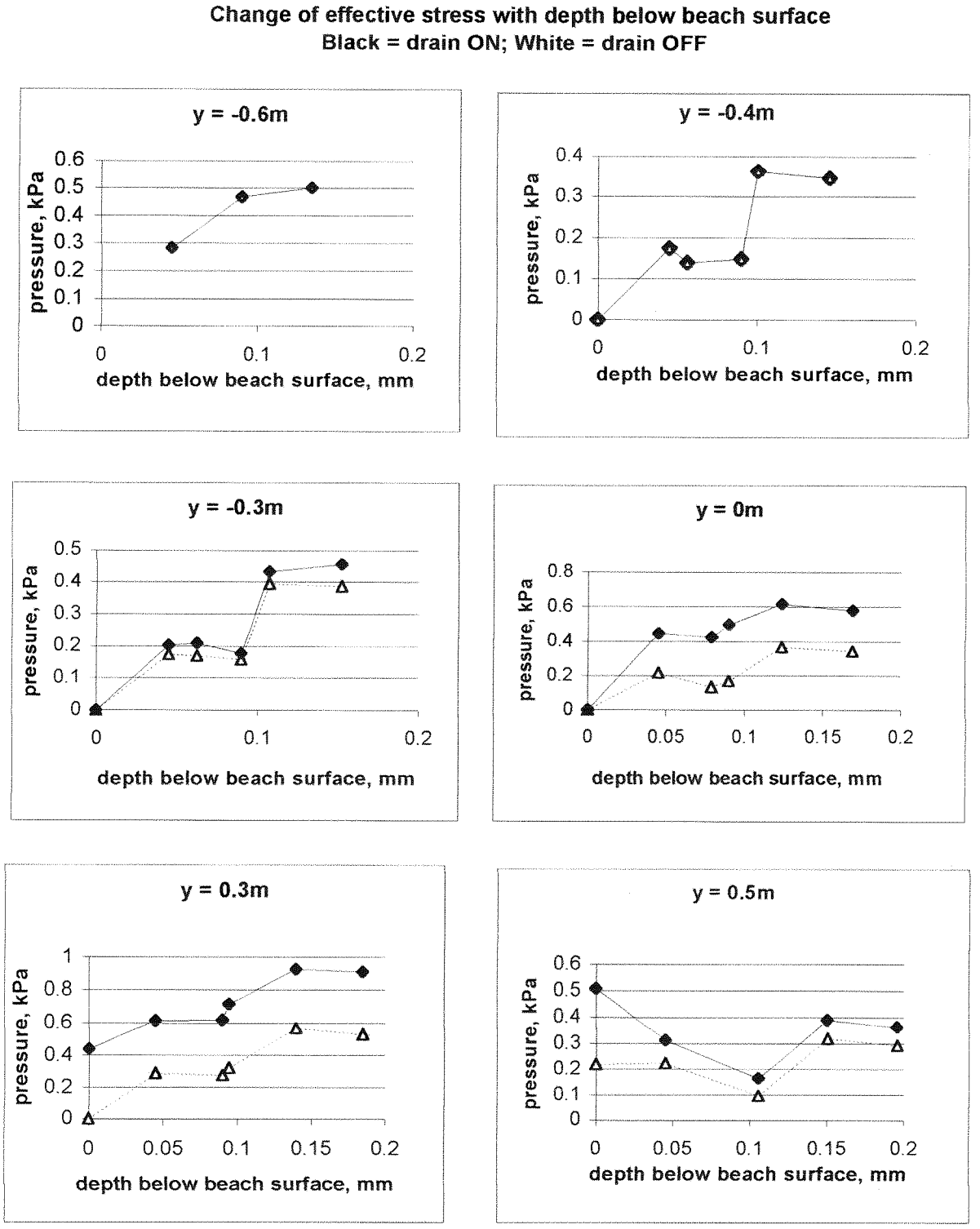

Figure 7.27: Graphs to show change of effective stress with depth for different probe locations

7.8.2 Discussion

Scale effects

As noted by Kamphuis (1975) liquefaction occurs more easily with a lightweight sediment model (where the relative length ratio is not unity) than for a sand model where linear length scales are properly reproduced (source: Hughes, 1993). Therefore the effective stress values in Figure 7.27 are likely to be an overestimate due to inherent scale effects associated with a Bakelite sediment model.

Effective stress

The model shows that, due to pore water pressure reduction, beach drainage results in effective stress increase. However, it is difficult to determine the actual value of the effective stress, particularly during wave action, because it is difficult to determine the exact overburden for a given point in time and space (particularly that due to the 'static' head for a snapshot in time).

Water table and drawdown

The beach is subject to relatively high frequency successive swash infiltrations, and due to the limitation of the beach permeability the water does not have time to soak away before the next swash inundation. For example, to reduce the water table level to 0.02m below the mean water level, water fed to the surface of the beach by the run-up would need to travel 0.02m before the next swash inundation. However, the permeability of the beach is only in the order of 0.5×10^{-3} m/s, hence even with a hydraulic gradient of 1 it would take 40 seconds for the water to travel this distance. The wave period is considerably shorter than this (1.6s), and the water to needs to travel much faster (40/1.6 = 25 times faster) to physically drain away from the surface of the beach before the next lens of water is added to the beach face. This simply isn't possible in the case of a fine grained beach material.

Hence it is apparent that due to the low beach material permeability in relation to the wave period, the actual water level in the beach is not affected by the drainage system since it cannot respond quickly enough to the relatively rapid wave inundations. This conclusion is, however, conjecture and this topic is recommended for further investigation in future work.

Additional considerations

Additional assumptions listed earlier may also affect the accuracy of the results. These are namely that the beach material is unlikely to be isotropic, since compaction and therefore bulk density will vary spatially. It must be highlighted that the bulk density is considerably less for Bakelite than for a natural sand, while the water density is the same.

7.8.3 Future work

Further study must seek to develop a method to accurately determine the mean water depth during drainage and wave operation. In the above analysis this has been calculated from the reading on the top probe. However, due to the dynamic nature of the surf zone, it is not known whether the output from the probe on the surface of the beach encompasses lateral forces due to water movement, and it cannot be certain that dividing by ρg automatically converts this reading to the head of water at that given temporal and spatial location. Further work must aim to:

1) develop a method for determining the mean water depth/drawdown (one possible method may be to filter out horizontal pressures using a physical attachment).
2) develop a numerical model based on the rate of wetting and rate of soak-away to quantify the actual draw down in mean water level that occurs This model may be used to validate the physical model.
3) explore the temporal variation in drawdown dynamics, pore water pressure reduction and effective stress
4) verify the drainage induced effective stress increase for the Bakelite sediment model using a full scale sand (and preferable a full scale wave tank).

7.9 Conclusions

The above sections have demonstrated that the beach pore water pressure depends on:

- whether the drain is in operation
- the length of time the drain has been on or off (lag time)
- whether waves are operating or not
- distance from the beach drain in the horizontal plane
- depth below the still water level
- the drainage system discharge

Response time

When the bung was removed from the drain outlet, the pore water pressure responded quickly, dropping rapidly at first, then more gradually with time. Equilibrium was reached after approximately 100 seconds.

Effect of waves

The pore water pressures recorded in the beach face were found to fluctuate during wave operation. The pore pressure cycles mimicked those of the water waves, although the shape of the waveform was more skewed. This result is likely to be because the pressure probe was located within the beach, while the wave probe was offshore. The pore water pressure wave amplitude was noted to reduce with depth below the beach surface.

The presence of waves resulted in an increase in the mean pore water pressure. This elevation was constant with depth, but was found to increase linearly with the distance in the horizontal plane (in the sea → land direction). This phenomenon has been identified as wave set-up, and it was argued that the set-up in the model is likely to be slightly exaggerated.

When waves were operating, the reduction in pore water pressure due to the drainage system was less than for hydrostatic conditions.

Probe location

The drainage system was effective within the range y = -0.4m to y = +0.55m, and the optimum pore water pressure reduction occurred when y = +0.1m.

It was found that when the surface of the beach was inundated with water (i.e. within the run-up zone) the pore water pressure on the surface of the beach was not affected by the beach drain. However, pore water pressure reduction due to the drainage system increased rapidly with depth, and immediately below the beach surface there was a significant reduction in pore water pressure due to the beach drain.

Above the run-up zone a significant difference in pore water pressure was measured on the surface of the beach when the drain was both off and on.

Relationship between pore water pressure and controlling variables

The pore water pressure reduction caused by the drainage system was affected by the distance from the drain in the horizontal plane, the system discharge, and whether waves were operating.

For hydrostatic conditions the relationship between pore water pressure, P, discharge, q and distance from the drain in the horizontal plane, y is given by the following empirical equation (for the seaward side of the drain only):

$$P = q\left(-0.648y^2 - 0.684y - 0.177\right) + \rho gd$$

and more generally:

$$P_{No\ waves} = \rho gd - f(q)$$

When waves were in operation it was noted that the pore water pressure was elevated due to wave set-up.

A similar analysis was carried out to determine the empirical relationship between pore water pressure, discharge and probe location during wave operation, and this is given by the following equation:

$$P = q(-0.086 - 0.815 - 0.019) + [(0.11(1.3 + y)) + \rho gd]$$

hence the general equation is:

$$P_{waves\ operating} = \rho g d + m(y - y_h) - f(q)$$

Where m is the set up gradient, and y_h is the distance from the drain to the point at which P = hydrostatic.

This formula applies to the beach drainage model, where the beach consists of a Bakelite sediment with a D_{50} particle size of 0.51mm, and fall velocity, w of 0.056m/s. There is no tide operating, the land flux is zero, and the SWL location is fixed at y = -0.25m. It has been assumed that the relationship between pore water pressure and discharge (for a given probe location) is linear. The wave climate is also constant (H = 0.11m; T = 1.59s).

Effective stress

Model data show that beach drainage increases beach shear strength within the range y = -0.3m to y = +0.5m. Results may be an overestimate due to the use of a lightweight sediment, and it is recommended that findings are verified using a full scale sand.

Sources of error include:

- the bulk density of Bakelite is less than that of natural sand
- isotropy was assumed for the beach material
- errors may have occurred in the calculation of the actual mean water depth during wave operation, since the drawdown caused by the drainage system is unknown.

8. FACTORS AFFECTING SYSTEM PERFORMANCE

8.1 Introduction

The objectives of the experiments discussed in this chapter were to explore the factors influencing system performance, and where possible identify the trend between each of the controlling variables and the resulting change in beach volume. The factors investigated are:

- system discharge,
- drain location (relative to SWL location), and
- wave climate.

It was necessary to ensure that the relationship observed as a result of each test set could be attributed wholly to the variable under investigation and was not a compound function of several variables. Hence each of the above variables was investigated in turn and where possible in isolation from each other.

A summary of tests was given in Chapter 4, and the apparatus, test procedures and model scaling issues were discussed in Chapter 5.

System performance was quantified by measuring the beach profile at the beginning and end of each test, and calculating the change in beach volume in the swash zone during the test. The swash zone is considered the useable area of the beach, and any stabilised or accreted sediment in the swash zone will contribute to the protection of the shoreline. In the model the swash zone is defined as the area of beach 0.4m landward and 0.4m seaward of the still water level mark (measured horizontally).

8.2 Discharge as a controlling variable (test set C)

8.2.1 Introduction

In Chapter 4 it was noted that the system discharge depends on the head of water, beach material permeability, and system geometry. Discharge may also be affected by head loss at entry to the drain and limited by pump efficiency.

Some head losses will occur with any beach drainage system. In a fully operational system these will consist of

- some losses on entry to the pipe due to water passing through the geotextile and pipe holes,
- friction losses over the length of the pipe, and
- exit losses if the outlet is submerged.

Additional losses may occur when the system is damaged, blocked or broken in places. For example, the discharge may be reduced due to

- blinding of the geotextile filter by compacted surrounding beach material or fines,
- loss of sections of pipe through storm damage,
- sediment entering the pipe through broken sections causing blockage and/or pump damage, or
- one of several pumps being out of operation (e.g. power cut, sump damage, salt water corrosion causing parts to seize, accidental inactivation – this occurred during the Branksome Chine trial because the off switch was located in a general purpose store room).

The aim of the experiment described in this section was to determine the relationship between system performance and discharge, and to investigate whether this relationship is affected by wave climate.

The test duration was 2 hours (this was discussed in Chapter 5), and between each test the beach face was prepared, measured, and the system outlet valve adjusted to a new position. During the test the discharge was recorded, and at the end of the test the

profile was re-measured. The change in volume in the swash zone was calculated on a spreadsheet using the trapezoidal rule. Data points were recorded at close intervals to allow for the fact that the trapezoidal rule assumes straight lines between data points. The wave machine was initially set to a moderate climate (2.5/110), then a second data set was recorded for a more erosive wave climate (4.5/110). Wave climates were discussed in Chapter 5.

8.2.2 Results

General observations

Figure 8.1 shows a side elevation of the model beach profile after 12 minutes under a moderate wave climate. Figure 8.1a shows the profile with the drain system off, and 8.1b shows the profile with the drain in operation. The black circles on the side of the tank indicate the positions of the two drains. Comparing the level of the beach at point A (which is the centreline between the two drains), the drain off profile (8.1a) shows the surface of the beach crossing the centimetre scale on the side of the tank at approximately 3.5cm. In the drain on photograph (8.1b) the surface of the beach at point A crosses the scale at approximately 6.5cm. Therefore the crest of the berm caused by the drainage system (this berm can be seen in Figure 8.1b) is approximately 3cm higher with the drain on than with the drain off. All conditions were the same for each of the tests shown in Figure 8.1: the initial profile, SWL and wave climate were the same.

Figure 8.2 shows the measured profile after a 2 hour test during which an erosive wave climate was in operation. The solid line shows the beach profile at the end of the test when the drain outlet valve was half closed (q = 5.1l/min per m), while the dashed line shows the profile after the test during which the drain outlet was fully open (q = 8.1l/min per m). The grey line shows the original beach profile. For the given wave climate it can be seen that the drainage system prevents erosion that would otherwise occur, and a berm is created in the upper swash zone that is not present in the undrained test.

The system is significantly less effective with the reduced discharge. This test was repeated for several different discharges for both mild and erosive wave climates.

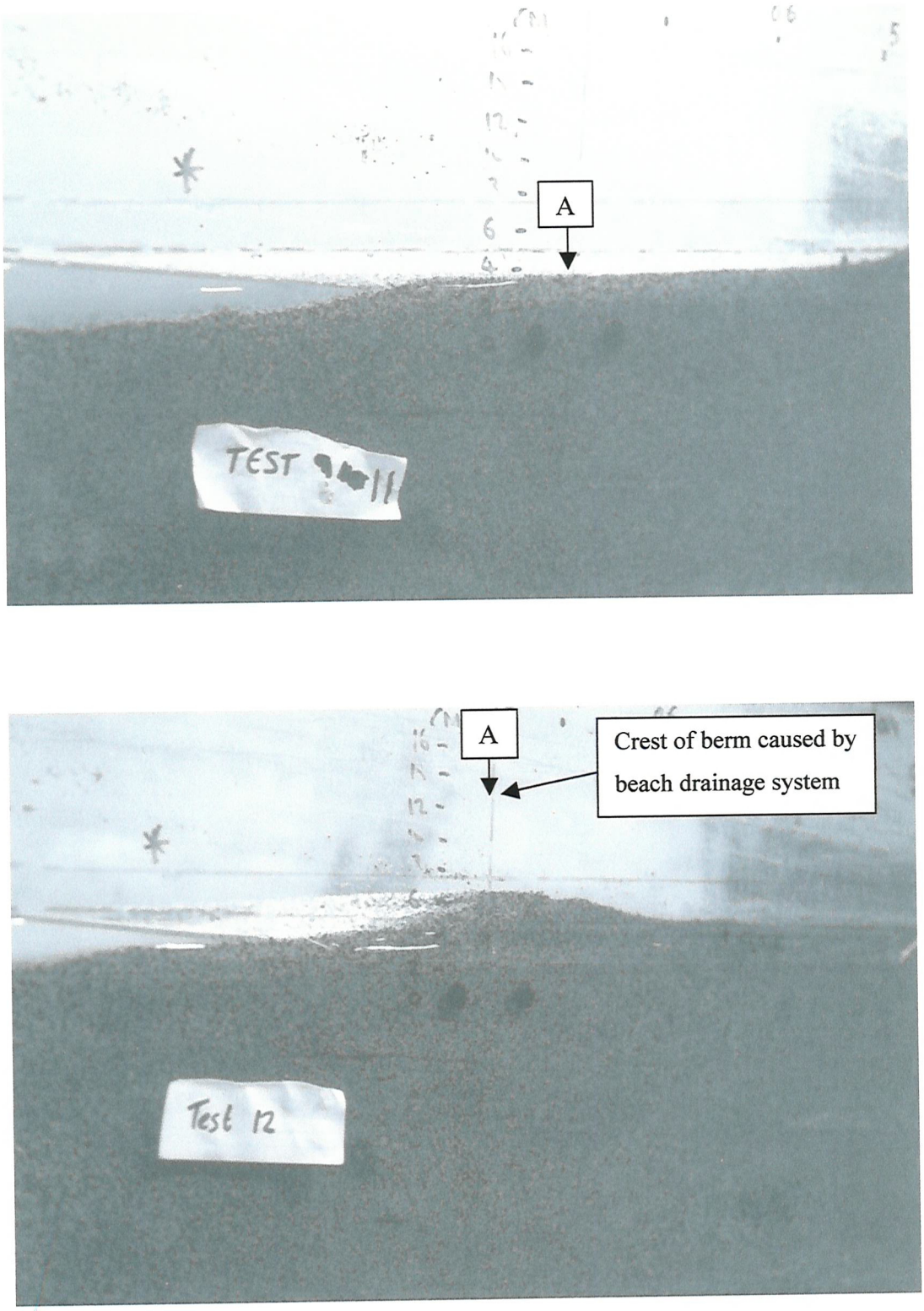

Figure 8.1 a (top) beach profile after 12 minutes – drain off; b (bottom) beach profile after 12 minutes – drain on.

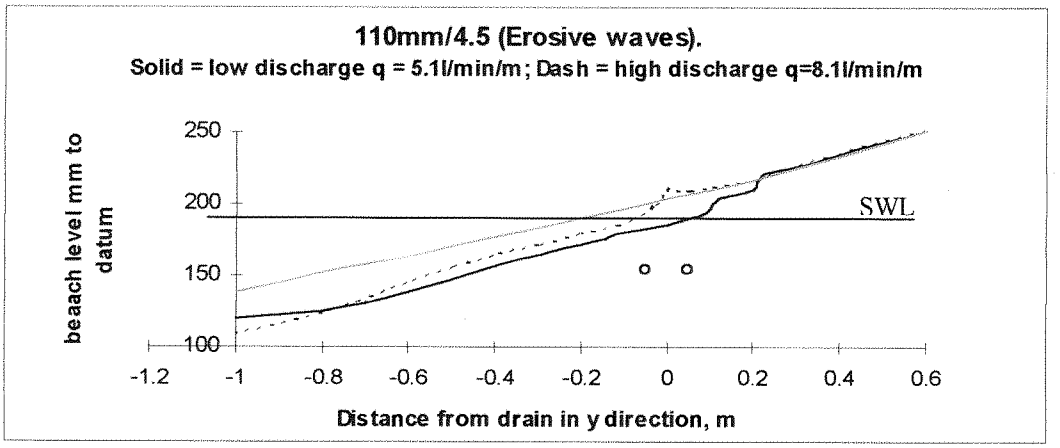

Figure 8.2: Beach profile after 2 hour test (erosive wave climate). Dashed line = high discharge; solid line = low discharge.

Test C1

Figure 8.3a shows the relationship between system discharge and beach volume change during a series of 2 hour tests. A relatively neutral wave climate (110/2.5) was used, where the beach volume change for undrained conditions was approximately zero (this climate is referred to as the milder of the two climates tested in set C).

For the purpose of identifying the trend of the data points, two trendlines have been fitted as shown in Figures 8.3b and c. Clearly there is a positive relationship between beach volume change in the swash zone and system discharge. The linear trendline suggests that the beach volume change is proportional to the discharge. Only a slightly better fit is achieved with the polynomial, and the relationship is still approximately proportional from q = 0 to q = 5l/min per m.

Test C2

The test was repeated using a more erosive wave climate (climate 110/4.5), and Figure 8.4 shows the results of test C2. The data were more scattered for test C2 than test C1, although the same procedures had been followed. The increased scatter may simply be a result of the beach volume change being more variable under a more extreme wave climates.

The C2 data set indicates that there is also a positive relationship between beach volume change and discharge for the more erosive wave climate, and this relationship is also approximately linear.

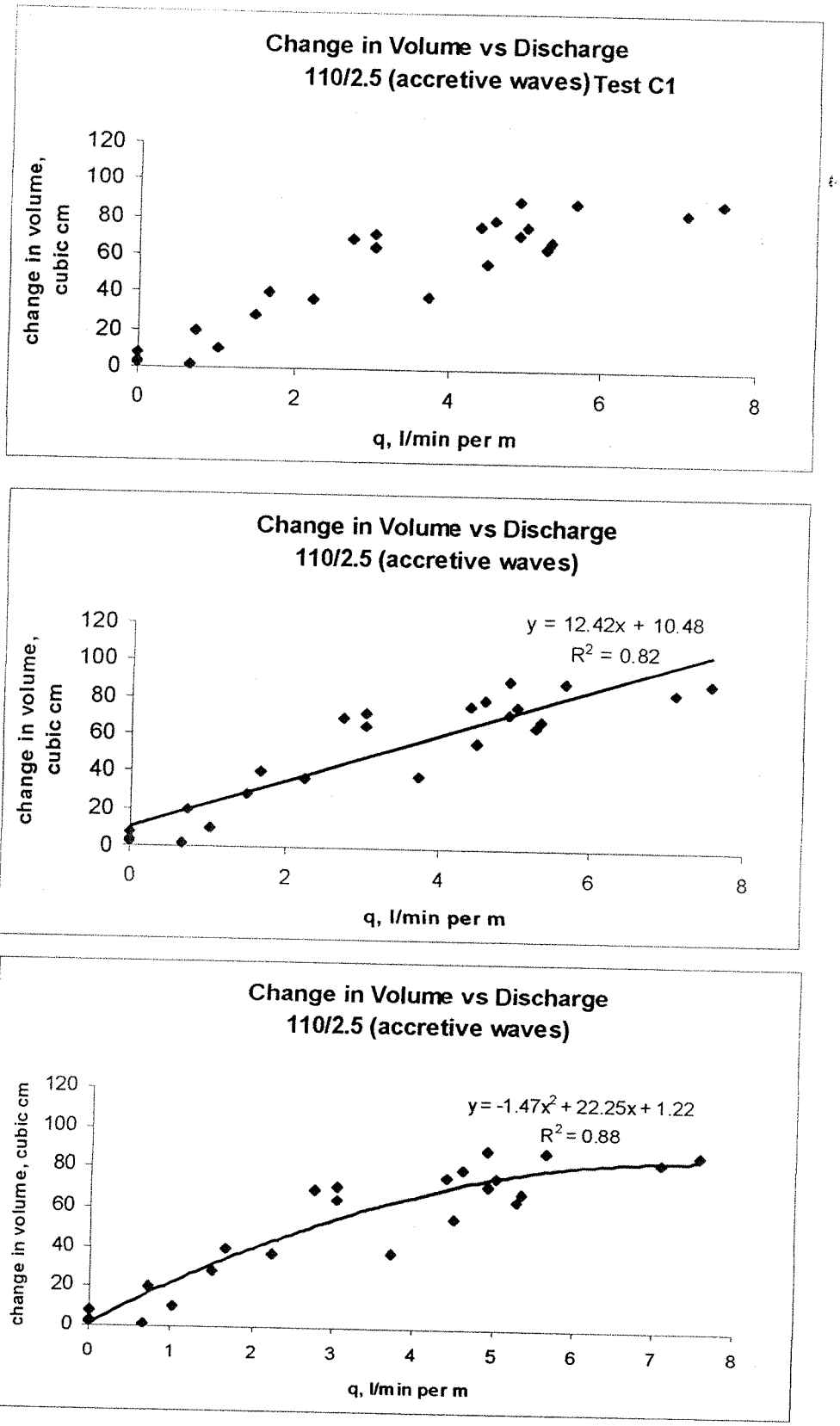

Figure 8.3 Model relationship between discharge and performance (moderate wave climate - test C1): a (top) data points; b (middle) linear trendline; c (bottom) polynomial trendline

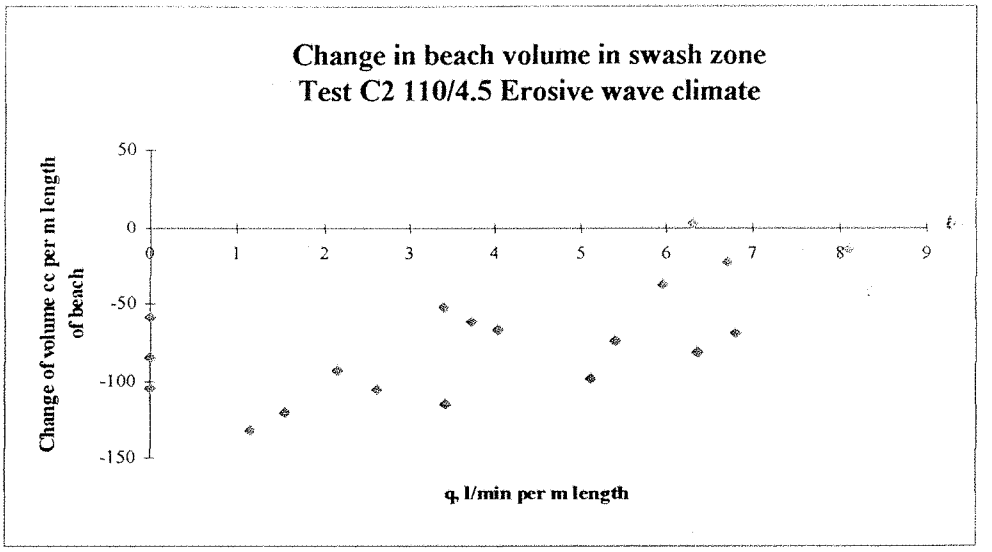

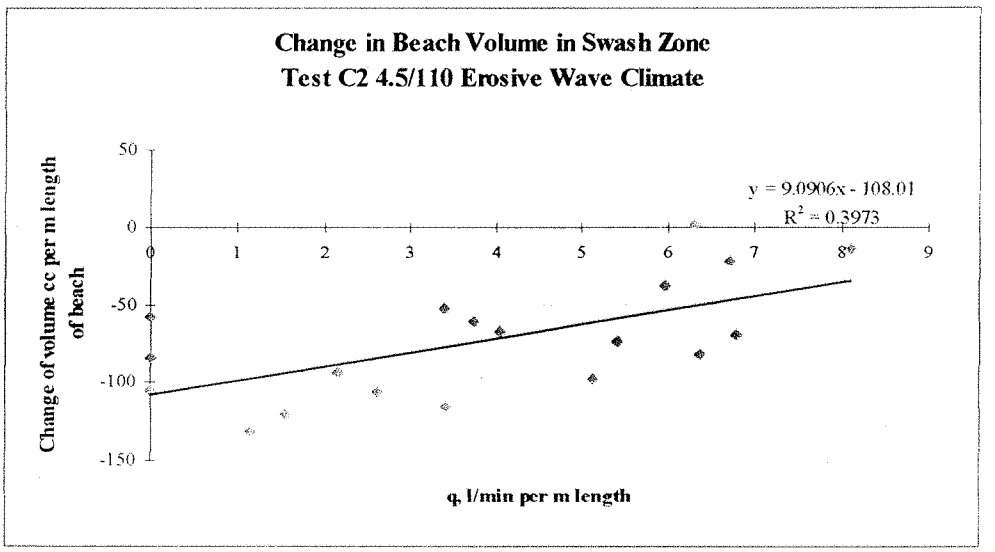

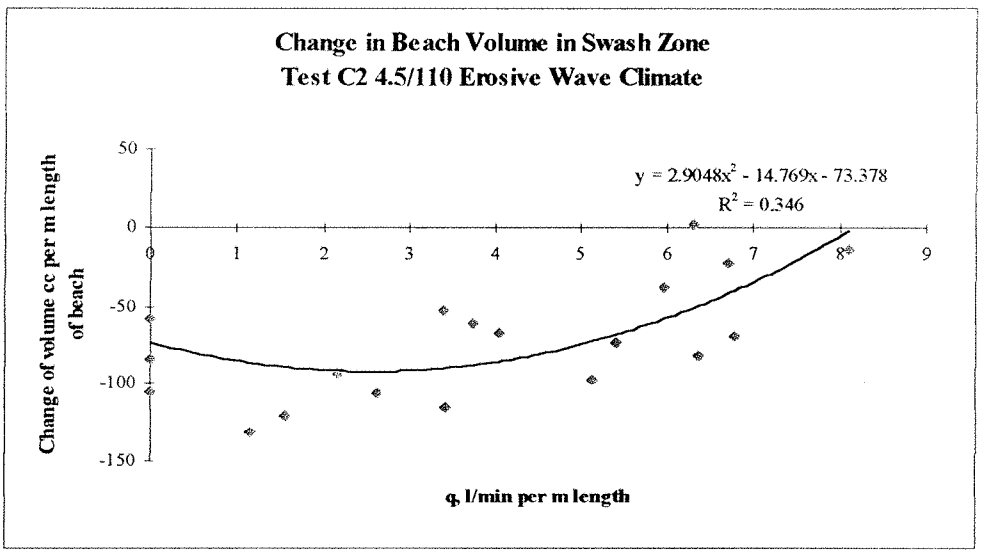

Figure 8.4: Relationship between beach volume change and discharge for more erosive wave climate (4.5/110, test C2) a (top) data points; b (middle) linear trendline; c (bottom) polynomial trendline

8.2.3 Discussion

Comparing the polynomial trendlines for both wave climates, the data suggest that there is a slightly different relationship for the mild and erosive wave climates: The trendline for the erosive wave climate suggests that there is a plateau from q = 0 to q = approximately 4 l/min per metre (see Figure 8.4c) and that the rate increases as q increases. This is different to the trend suggested for the test C1 plot (Fig. 8.3c), which indicates that the rate of change of volume with discharge decreases as q increases.

The shape of the polynomial trendline for the erosive wave climate indicates that it is possible that a threshold value of q exists below which the system is ineffective. It may be that there is a threshold discharge value below which the system is ineffective, after which point the relationship between volume change and discharge is linear (Figure 8.5). Note that for the erosive wave climate data from point C to D in Figure 8.5 the gradient of the graph is the same as that of data set C1.

The data suggest that the minimum discharge requirement for effective beach drainage increases as the wave climate becomes more erosive (for the neutral wave climate = approximately q = 0; while for the erosive climate = approximately q = 3.8l/min per m).

This interpretation of the data in Fig. 8.5 is supported by the results observed in the full scale trial: During the first summer of operation the discharge was high, and an increase in beach levels on the drained section of beach was observed (see Chapter 3). However, the system was damaged during the fourth month of operation, after which it was repaired. The reinstated system had a significantly reduced yield (see Chapter 3), and survey data indicate that this system was ineffective. No significant difference in beach levels between the drained and undrained beaches was observed, despite that fact that *some* discharge was obtained from the system. However, this yield was lower than that of the original installation, and the results indicate that below a certain threshold yield the system had no significant effect.

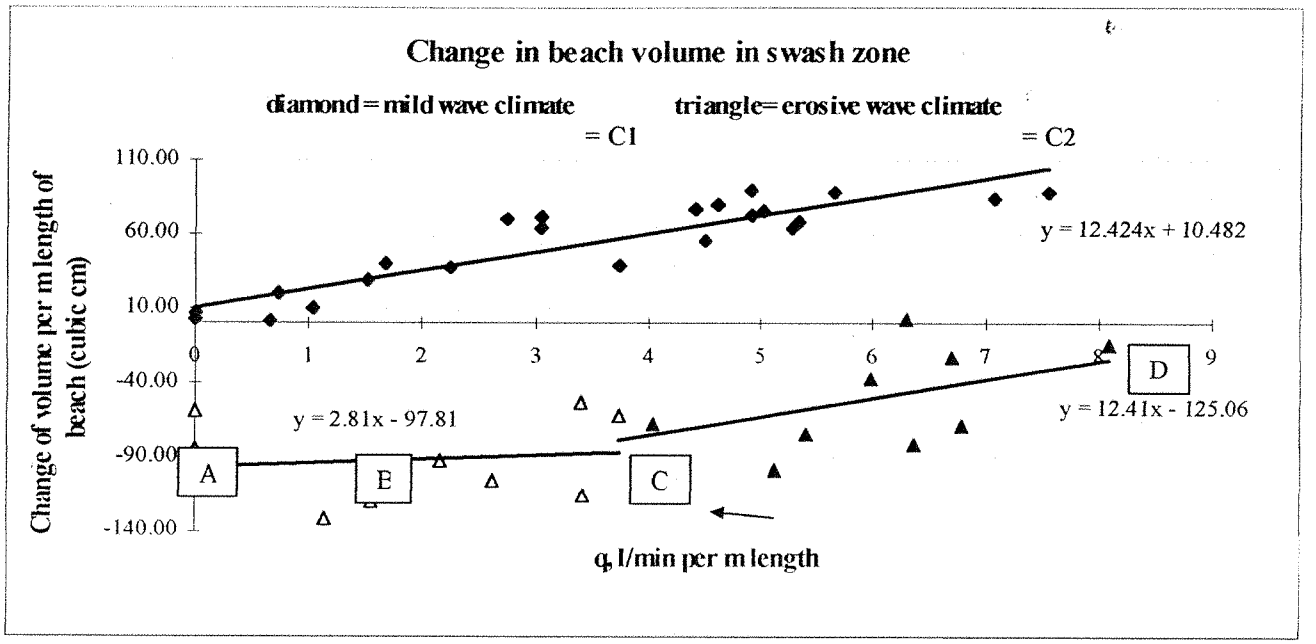

Figure 8.5: Alternative trendlines for data set C2. (White triangle = test C2, from q = 0 to q = 4l/min per m; black triangle = test C2 from q = 4l/min per m to q = 8l/min per m).

The discussion in Chapter 4 concerning the effect of beach drainage on incipient motion also supports the interpretation of the data shown in Figure 8.5. For a highly turbulent, high energy body of water moving over the surface of a drained beach, it is possible that energy can be removed from the wave without any impact on whether incipient motion will occur or not.

When the total wave energy is high, the energy removed is not sufficient to reduce the total wave energy to below that required for deposition. In the discussion of test set B (in Chapter 4), this concept was examined in terms of relative energy removal. The highest wave energy occurs where the wave was deepest and fastest moving (in the lower run-up zone), while the least kinetic energy occurs when the wave is slowest, and shallowest (at the upper limit of the swash).

The argument can be applied to wave climate. For the same point in the wave (e.g. the mid-runup zone), the higher the wave height and lower the wave period, the greater the wave depth and velocity at that given point. The energy removed from the wave must be considered in relation to the total energy of the wave at that point. If the total energy of the wave is high, then a given amount of energy removed from the surge will not be sufficient to lower the energy to below that required for incipient motion: for example at point B in Figure 8.5, although a discharge exists, the change in beach volume in the swash zone is approximately the same as the volume change when $q = 0$ (point A). Eventually a threshold will be reached (point C) when the amount of energy removed is sufficiently high in relation to the overall kinetic energy of the wave that the wave energy is reduced to below that required for incipient motion and sediment particles are deposited (as discussed in the laminar flow theory section in Chapter 4). After this point the higher the energy removal, the greater the volume deposited (CD on figure 8.5).

The data suggest that the threshold discharge theory is possible, but the scatter in data set C2 leaves room for debate.

It must be noted that only two wave climates were investigated in test set C. It will later be shown that the drainage system performance (or performance vs discharge gradient as discussed above) is approximately the same for moderate wave climates, but for extreme climates (very mild or very erosive) the drainage system is less effective (see section 8.4: test set E).

Maximum discharge

Q = 8.1l/min per was the maximum possible discharge for test set C. This value was obtained using a gravel matrix around the pipe. No further increase in Q could be achieved under the natural head, and it is thought that at this point Q is limited by the permeability of the beach material. This is illustrated by the still water level-discharge relationship shown in Figure 8.6 (data are from Chapter 6). The graph in Figure 8.6 plateaus at q = approx. 8l/min per m, and no further increase in q can be obtained despite the increase in head.

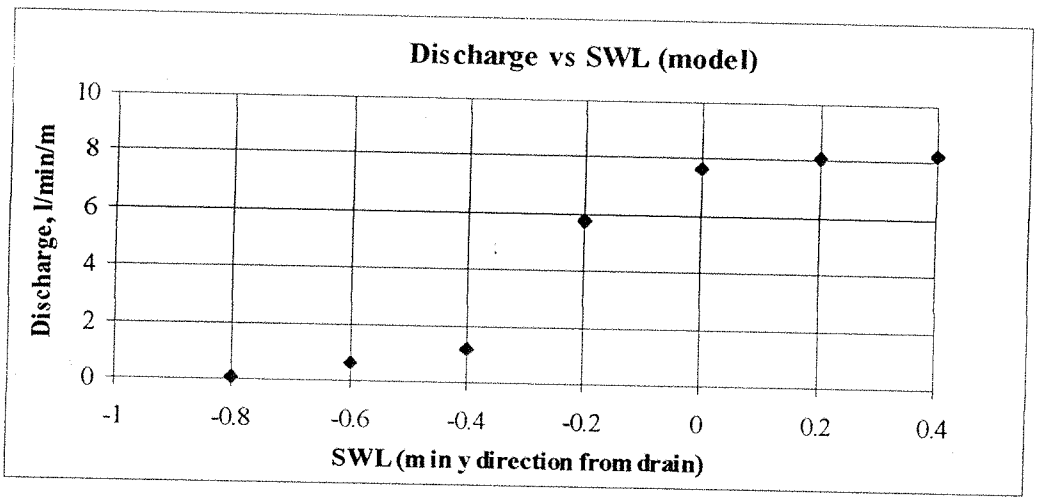

Figure 8.6: Discharge-head relationship (measured model data)

Sediment deposition

The test time for set C is two hours, therefore the theoretical estimate of volume change in the swash zone is 28cubic cm for q = 9l/min per m. This estimate of volume change is based on the assumption that the beach volume change with no drainage is zero, i.e. it is an estimate of the extra volume of sediment deposited due to the existence of the drainage system. According to the model data, for the milder wave climate, when the drain is off, the beach volume change in the swash zone is relatively near to zero.

The beach volume change may be expressed as a volume change per 1l/min per m increase in discharge, or let us call it an 'accretion gradient'. For the test C1 data set (and the C2 set for q greater than 4l/min per m), the accretion gradient is approximately 6cc per l/min per m per hour.

In test C2, the drainage system does not necessarily cause 'accretion' to occur, since the overall change in beach volume is still negative. Thus the beach drainage system causes less erosion than would otherwise occur.

It is difficult to translate the model beach volume change data to a field situation where the waves are irregular and therefore surge energy is far more complex due to irregular swash/backwash interference. The magnitude of beach volume change does not necessarily represent the magnitude of material likely to be accreted in the field because, in addition to the scaling limitations discussed in Chapter 5, irregular waves, cross shore currents and local bathymetry have not been accounted for in the model.

In Chapter 5 it was deduced that due to the excessively large grain size in the mode, beach permeability and hence discharge are disproportionately large, and beach volume change due to drainage is likely to be an overestimate.

8.2.4 Set C Experiment: Conclusions

Practical aspects

Beach drainage causes an accretion of material in the swash zone that would otherwise not occur. The accreted material in the model takes the form of a berm of material, and lies in the region of the upper limit of the swash (note that the model waves were monochromatic). This berm has two main benefits in terms of human use of the shoreline environment:

1) It increases the useable area of beach, since it increases the volume of beach material above the water line. This improves the area of beach accessible to users, thus increasing the amenity value of the beach. This benefit is particularly important for the Branksome Chine trial site, since the area is a popular holiday destination, and beach material loss threatens the attraction of the beaches by reducing the space available for amenity use.

2) The elevation of the beach is increased, which provides visible, physical protection of the shoreline. Not only does this provide a tangible defence for the shoreline through increased beach levels and a larger volume of material, but also promotes confidence among beach users and the local population. Because the beach drainage system is sub-surface, it is difficult to see a visible return for investment, and the appearance of a notable berm on the drained beach, as was the case at Sailfish point in Florida (Vesterby, 1996), is beneficial to local authorities who ultimately derive funds for coastal defence from tax payers' contributions.

Design implications

The fact that performance is approximately proportional to the system discharge has important implications for system design and maintenance. Full scale results demonstrate that if the system yield is reduced and erosive conditions occur, then the system cannot protect itself, and beach levels are liable to fall. In the case of the Branksome Chine trial, this resulted in the uncovering and damage of the drainage pipes. Robust design and prompt maintenance are essential in order to maintain the system yield and prevent beach material loss.

Threshold discharge theory

The data suggest that the beach volume change in the swash zone is proportional to the system discharge (or yield), although it is possible that a plateau exists for the erosive climate data set (test C2). Both field observations and theoretical considerations support the concept of a threshold discharge. The threshold discharge is the minimum discharge required for a given wave climate for the beach drainage system to begin to have an effect.

Yield capacity

The highest discharge that could be obtained was approximately 8 l/s per m, and the level in the sump was maintained below the outlet pipe level. It is thought that the discharge is limited by the permeability of the beach material and geometrical constraints. Therefore any pump with a maximum pump rate greater than the maximum rate at which it is possible to have water flowing out of the drain outlet will have redundant capacity. It is important to know the upper limit of the system yield to avoid pump over-design, since pumps are the main source of capital and running cost for a beach drainage system.

Considerations

The data for test C2 were scattered, and the correlation coefficient for the fitted trendline was approximately 0.4. It is recommended that further experiments are conducted in order to confirm the interpretation of the data.

8.3 Still water level relative to drain location (test set B)

8.3.1 Introduction

The results of the full scale trial suggest that the system performance depends on the distance between the drain and the intersect of the still water level with the beach face (the distance y in Figure 4.8 – see Chapter 4). When the Branksome Chine full scale beach drain was moved further landwards, a lower discharge was measured, and the system was visibly less effective (see Chapter 3).

In laboratory test set C (discussed in the previous section) it was shown that the relationship between discharge and performance is approximately linear, when the SWL is constant and discharge is the controlling variable. However, as discussed in Chapter 4, theoretical considerations suggest that the relationship between still water level is non-linear, and an optimum and limits exist.

In test set B, the distance between the drain and SWL was changed by filling or emptying the tank, thus simulating a tide in a series of head increments. In chapter 6 it was shown that the discharge measured at the system outlet increases with head as the still water level mark moves landward (see also Figure 8.6 above). If the increase in beach volume were simply proportional to the volume of water (energy) removed from the surge, then one would expect to observe a positive relationship between SWL and performance. However, a consideration of the processes operating indicates that in reality the relationship is not so straightforward. This is because the drain system causes a non-linear pore water pressure reduction pattern as shown in Chapter 7 (section 7.5).

In Chapter 7 it was found that the zone of maximum influence of the drain lies slightly landward of the drain centreline, at approximately y = 0.1m (i.e. 0.1m landward of the drain centreline), and the limits to the zone of influence were approximately y = ±0.4m. In addition to this, the depth and velocity of the surge, and therefore the energy of the flow (and hence the shear force exerted into the bed by the surge) varies from the bottom to the top of the run-up zone. Therefore even on the beach surface, the total energy of the wave and the amount of energy removed varies.

Whether the kinetic energy of the surge will be reduced to that required for incipient motion depends on both the total energy of the wave, and the amount of energy removed, and this was referred to in Chapter 4 as relative energy removal.

According to the argument presented in Chapter 4 the greatest relative energy removal may be achieved when the wave its at its thinnest, and when energy removal is greatest. Hence the optimum performance is likely to occur when the upper limit of the swash is over the zone of maximum influence of the drain.

The system performance will reduce as the drain becomes flooded, because the relative energy decreases (the surge depth over the zone of maximum influence of the drain increases, and therefore relative energy decreases).

Tests were carried out using the model beach drainage system described in Chapter 5. Each test was run for ten minutes, and the profiles before and after wave operation were recorded. Experimental procedures were discussed in Chapter 5. A long test time scale was undesirable for this experiment since during a period of two hours the position of the still water level mark on the beach face migrates according to the evolving profile shape (Figure 5.12, Chapter 5). Some SWL migration is unavoidable by virtue of the fact that the beach drainage system causes an increase in beach volume, and thus a change in the profile. The test time scale of ten minutes was selected in order to provide a measurable, but not excessive increase in beach volume during the test. Since the test timescale was relatively short, the *initial* rate of accretion was measured, as opposed to the equilibrium condition.

For each test the position of the still water level and the position of the upper limit of the swash were recorded. In the graphs discussed below, the change in beach volume is plotted against the position of the upper limit of the swash. The distance between the upper limit of the swash and the drain may be referred to as the overlap (y_o).

8.3.2 Results

Figure 8.7 shows the change in volume recorded for different still water level positions for both the drain off and drain on tests. The vertical axis is the change in beach volume in cubic centimetres per m width of beach. The horizontal axis is the overlap.

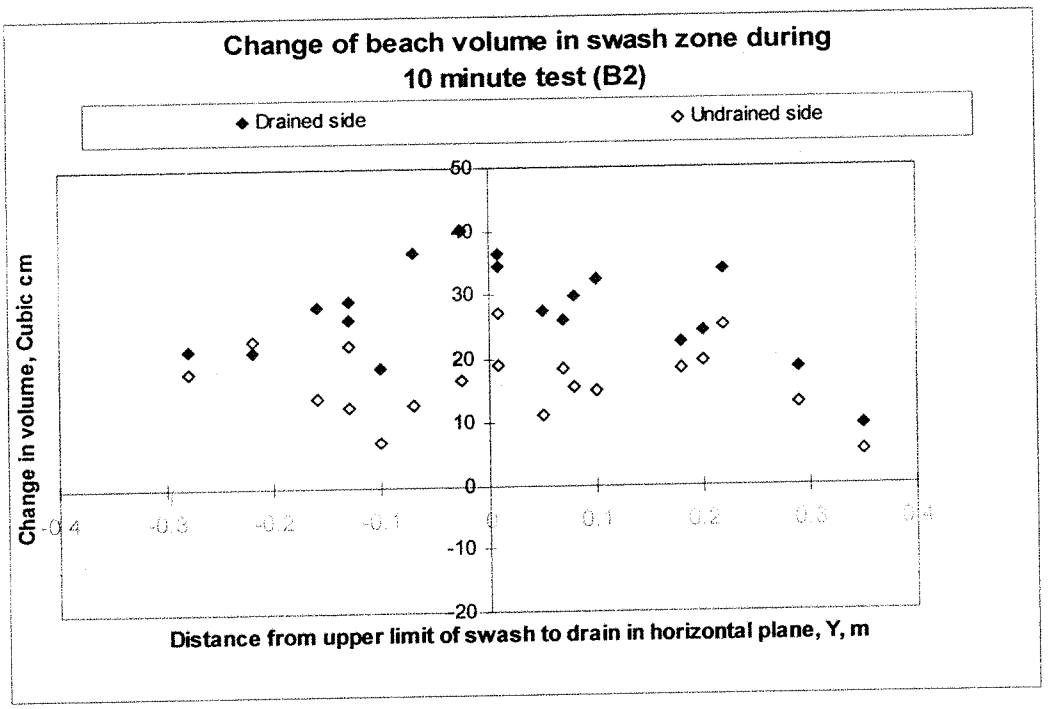

Figure 8.7: Relationship between change in beach volume and overlap.

Due to the limited timescale, the change in beach volume during the tests is relatively small. This results in a greater margin of error than in other tests, since the precision and accuracy of the profile measuring techniques are the same, and as can be seen in Figure 8.7 the data are scattered. However, it is possible to identify some trends in the data, which support the relative energy removal theory:

- All except one of the data points for the drain on data set lie above the drain off data points.
- The difference between the drain off and drain on data points is greater in the region $y_o = -0.2$ to $y_o = +0.2$.
- When the SWL is located some distance from the drainage system, the difference between the change in beach volume for the drain off and drain on scenarios is considerably reduced. Thus the two data sets converge at the extremities of the horizontal axis.

To highlight these observations, trendlines have been fitted to the two data sets (Figure 8.8). It can be seen that the optimum performance occurs when the upper limit of the swash is located at approximately $y_o = +0.05$.

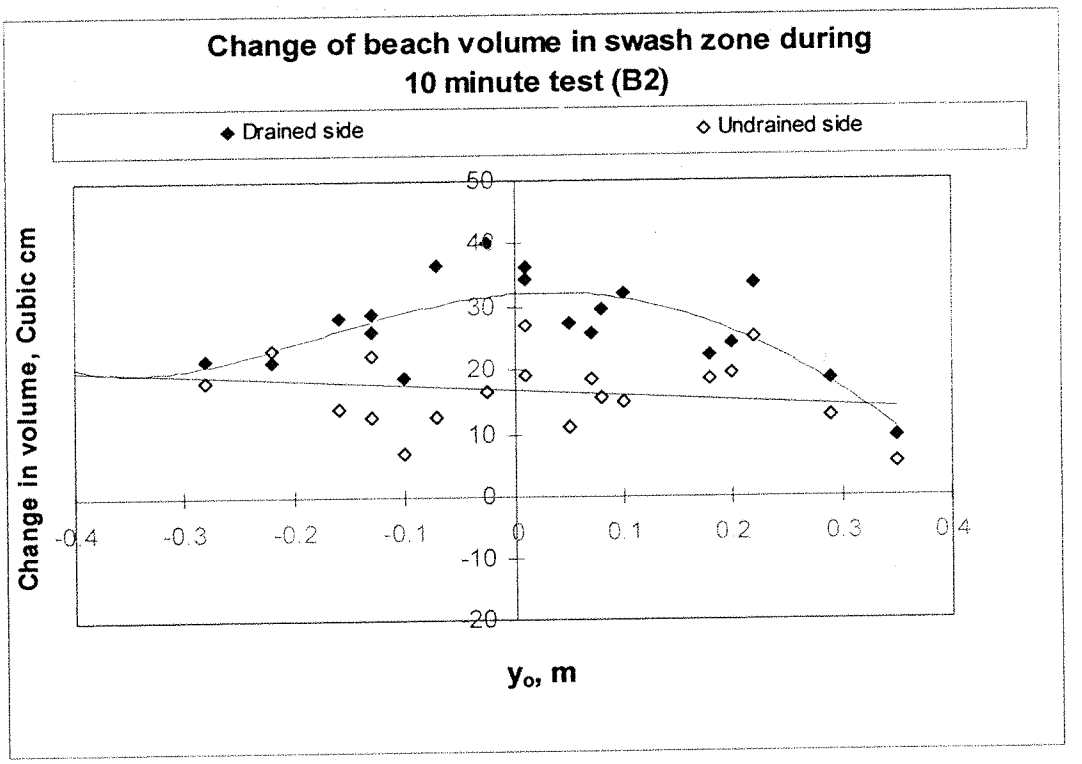

Figure 8.8 Relationship between change in beach volume and position of upper limit of swash relative to the drain (drain off and drain on data sets). Trendlines superimposed to highlight correlation.

8.3.3 Discussion

Figure 8.9 shows the data from Figure 8.8 alongside the drawdown diagram presented in Chapter 7. It can be seen that the greatest pore water pressure reduction occurs at approximately $y_o = +0.1$m.

The data suggest that the optimum performance occurs when the upper limit of the swash is located approximately over the zone of maximum influence of the drain.

The optimum performance occurs when the upper part of the wave, the upper run-up zone where the wave is shallowest, is located over the part of the beach where the maximum pore water pressure reduction occurs. The relative energy removal is high, and beach drainage can prevent the entrainment of sediment particles, resulting in accretion as indicated by Figure 8.8.

When the upper limit of the swash is located further landward, the part of the wave over the zone of maximum influence of the drain is relatively deep and fast moving, and flow is likely to be turbulent and more able to transport sediment particles. Hence for an overlap of 0.3m, the difference in beach volume change between the drain on and drain off tests is considerably reduced.

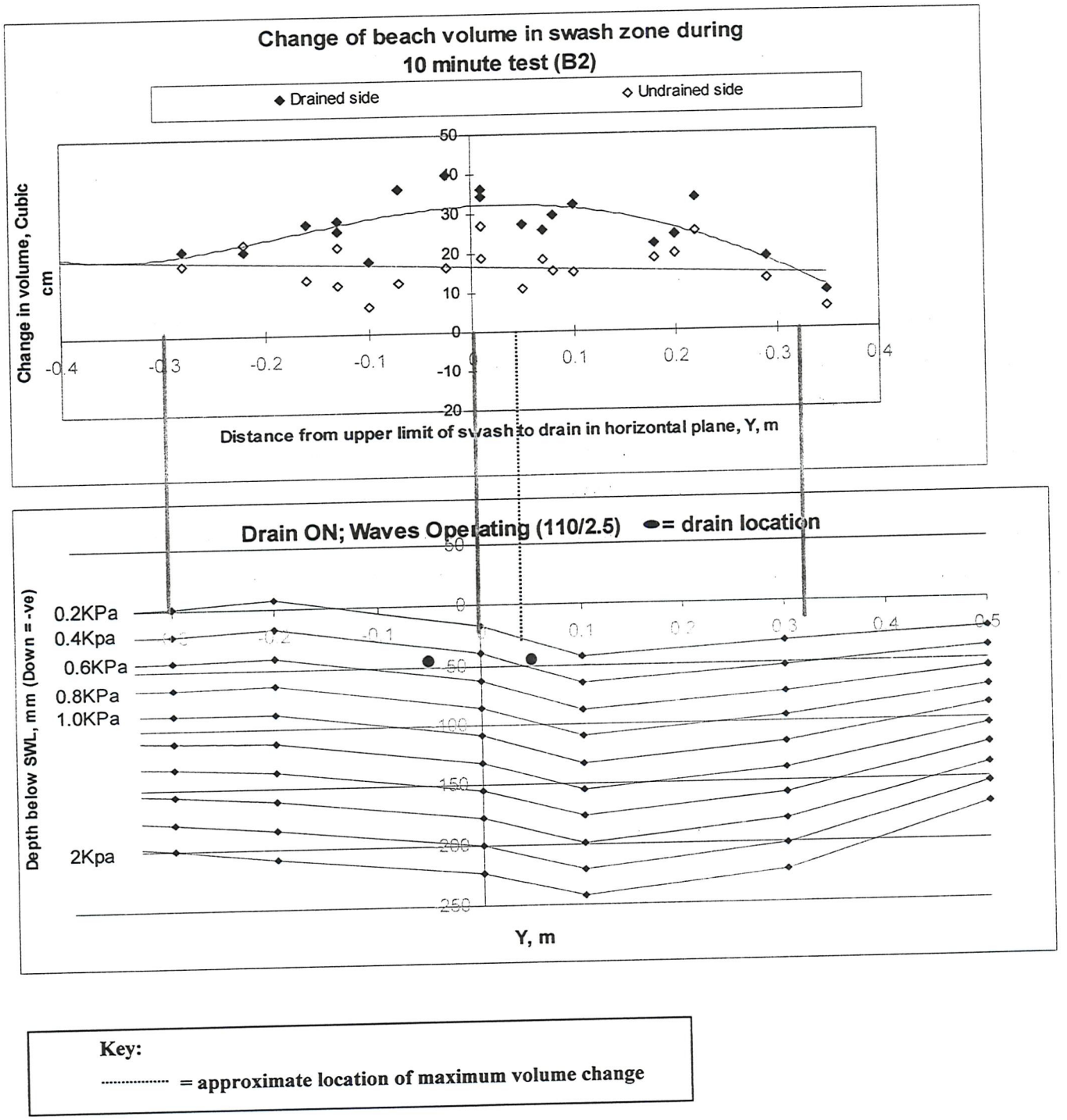

Figure 8.9: Comparison of chart in Figure 8.8 with pore water pressure reduction diagram

Estimate of relative energy removal

The aim of the analysis below is to estimate the relative energy reduction required for effective beach drainage. Relative energy removal is the quantity of energy removed by the drainage system at a certain point on the beach surface in relation to the total energy of the surge at that point.

The data in Figure 8.8 suggest that the greatest volume of sand is being accreted when the upper limit of the swash is located at $y_o = 0.05$m. During the set B experiment the depth, D, of the surge over the centreline of the drainage system when the upper limit of the swash is located at $y_o = 0.05$m was measured through the glass side of the wave tank, and was approximately 2 to 3 mm. As discussed in Chapter 4 (section 4.4), at the upper limit of the swash a short phase of laminar flow occurs, during which rapid sediment deposition occurs (Grant, 1948). Using the Reynolds criteria for laminar flow it was estimated that laminar flow conditions would occur when the wave velocity and depth were less than approximately 0.2m/s and 3mm respectively.

The discharge recorded when the upper limit of the swash was located at $y_o = 0.05$ (as illustrated in Figure 8.10) was approximately 6l/min per m width of system. To gain an estimate the discharge as an equivalent reduction in wave depth, the following assumptions have been made:

1) The drain is most effective in the area directly above the system. The two model drains are 0.1m apart, therefore the length of the effective zone is assumed to be equal to 0.1m (see Figure 8.10).
2) Since the drawdown is non-linear, and increases the nearer to the drain it is measured, it could be assumed that a larger proportion of the discharge measured at the outlet is derived from the effective zone: let it be assumed that approximately 2/3 of the discharge is derived from the effective zone. Therefore a flow rate of 4 l/min per m emanates from the effective zone, which is 0.1m wide.

Hence the 4l/min per m $= 6.67\times10^{-5}$ m^3 per second per m length of drainage system is removed from the effective zone which is 0.1m long (measured in the shore-normal plane). If the velocity of the flow within the upper run-up zone is taken to be approximately 0.2m/s (estimated visually through side of wave tank), then the time taken to travel 0.1m across the effective zone is 0.5 seconds. Therefore water soaks into the beach in the effective zone for a total of approximately 0.5 seconds, thus the volume of water taken into the beach face is 6.67×10^{-5} m^3 per second (per m length of drainage system) $\div 2$. Hence the total volume of water removed from the effective zone during the 0.5 second period is 3.3×10^{-5} m^3/m.

Since the width of the effective zone is assumed to be 0.1m, then the depth of water removed = 3.3×10^{-5} $m^3/m \div 0.1 = 3.3 \times 10^{-4}$ m the 0.1m length of the effective zone. Thus the depth of water removed, Δd, is 0.33mm.

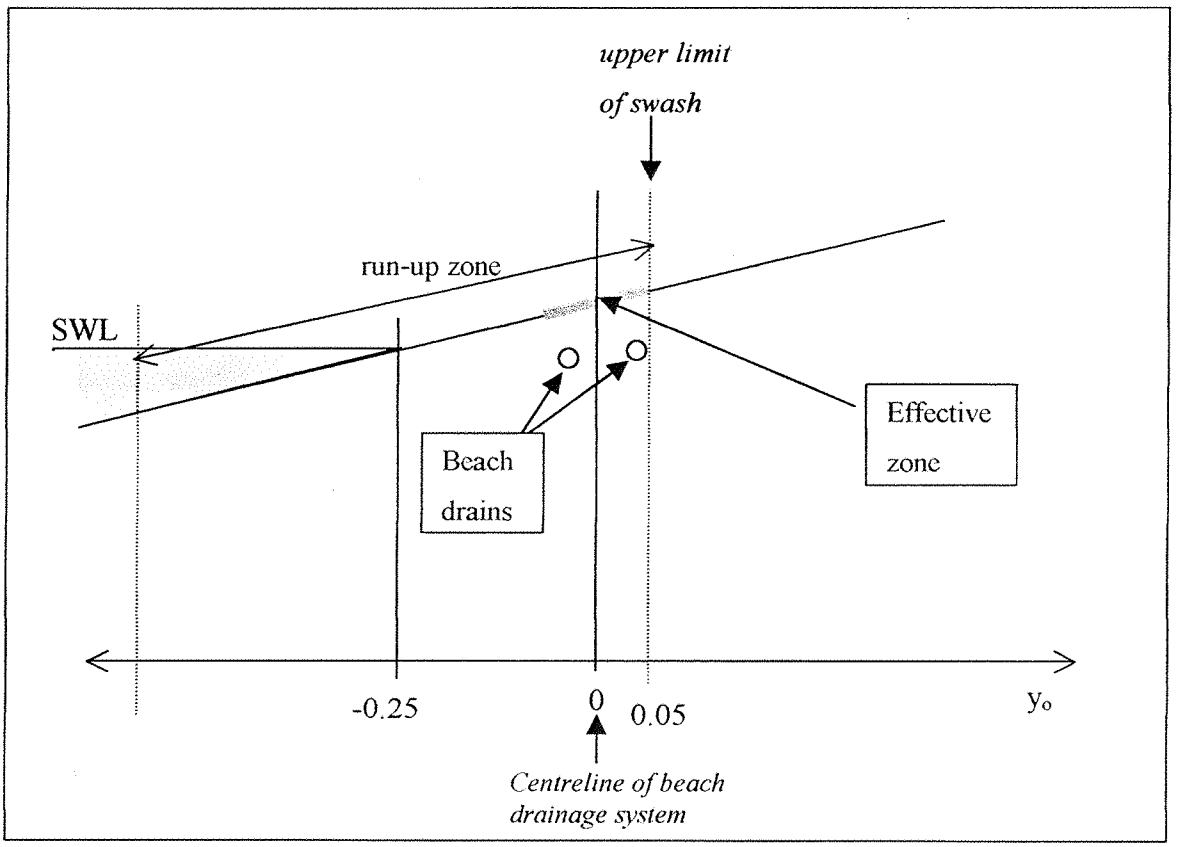

Figure 8.10: Schematic diagram to show position of upper limit of swash when drain system is considered to be most effective.

Hence:

$D \approx 2.5$mm

$\Delta d \approx = 0.33$mm,

$\rightarrow \Delta d/D = 0.33/2.5 = 0.0132 = 13\%$.

Given the assumptions this value is likely to be a conservative estimate, and future work is recommended to determine a more accurate estimate of %energy removal. It is recommended that the actual length and wave velocity in the deposition zone are measured so that these values are known and not estimated. It is thought that this is a conservative estimate, since deposition is not limited to just the laminar flow phase, and is instead determined by the Shields parameter as discussed in Chapter 4. It is difficult at this time to calculate the actual length of the deposition zone without improved instrumentation and model measurements.

Calculation of minimum Δd/D

The data for test set B suggest that, when the overlap y_o <0.05, as the SWL increases the drainage system becomes less effective. According to the results in Figure 8.8, the system is considered to be no longer effective at y_o = +0.3m The drainage system and the difference between the drain on and drain off change in beach volume decreases (Fig. 8.8). Assuming that the drain on and drain off data sets converge when the upper limit of the swash is located at approximately y_o = +0.3m.

The depth of water at y_o = 0 when the upper limit of the swash is at y_o = 0.3m is approximately 15mm (measured). In this case the amount of water removed from the effective zone is a little higher, because the head of water over the drain and hence the discharge are higher than when the upper limit of the swash is located further seaward. When the SWL is at y = 0, the discharge is approximately 7.8l/min per m width of beach (see Figure 8.10). Hence the change of depth in the effective zone (Fig. 8.11) during 0.5 seconds is 0.65mm/2 = 0.33mm. Although the energy removal in the effective zone is higher, the depth of the wave above this effective zone is also higher. Hence the relative energy removal is 0.33/15 = 0.022 or approximately 2%. In this case the energy removed by the drainage system is not sufficient to cause sediment to be deposited, and the change in beach volume for the drained and un-drained tests is approximately the same (Fig. 8.8).

8.3.4 Conclusions

Although the data are subject to scatter, results support the theory proposed in Chapter 4 that relative energy removal is important, and because of this the relationship between SWL position and drain location is non-linear (an optimum and limits exist).
The set B data suggested that optimum performance occurred when the upper limit of the swash was located over the zone of maximum influence of the beach drain.

For the beach drainage model optimum performance occurred when the relative energy removal was approximately 13%, and the system is apparently ineffective when the relative energy is below approximately 2%.

8.4 Relationship between wave climate and beach volume change (test set E)

8.4.1 Introduction

The objective of test set E was to measure the change in beach volume for different wave climates, and compare the drain off and drain on profile responses. The aims were to:

- identify the criterion for erosion and accretion (i.e. which ratio of wave height to period that separates erosion from accretion);
- ascertain whether this boundary is the same for the drain on and drain off tests;
- investigate how the performance of a beach drainage system is affected by wave climate; and
- to compare the experimental data obtained in this study with published data for fine and coarse sand to demonstrate that the drained beach exhibits the behaviour typical of a coarser material beach.

Theory

Seelig (1983) developed an empirical model to predict the beach volume change for a coarse and a fine sand beach under different wave climates (Figure 8.11). For both the coarse and fine material the beach volume change increases with increasing wave energy, reaches a maximum, then begins to decrease as the wave climate becomes more erosive. Eventually the change in beach volume falls below zero, and a net loss of beach material occurs.

As discussed in Chapter 4, the presence of a beach drainage system results in a higher percolation rate into the beach. This is similar to the beach consisting of larger particles, because the flowrate through the beach is greater. When the beach permeability is increased, the amount of energy removed from the surge by water infiltrating into the beach increases. If the percolation rate is increased because the particles are larger, then not only is more energy removed from the surge, but the particles are heavier and require more energy for incipient motion. Therefore, the material is more readily deposited if suspended in the surge, and less readily entrained if lying on the bed and

subject to a shear force. Hence for the same wave climate, a greater change in beach volume would occur. The sediments in the Seelig diagram are characterised by the fall velocity (w). It is assumed that the particle densities are the same.

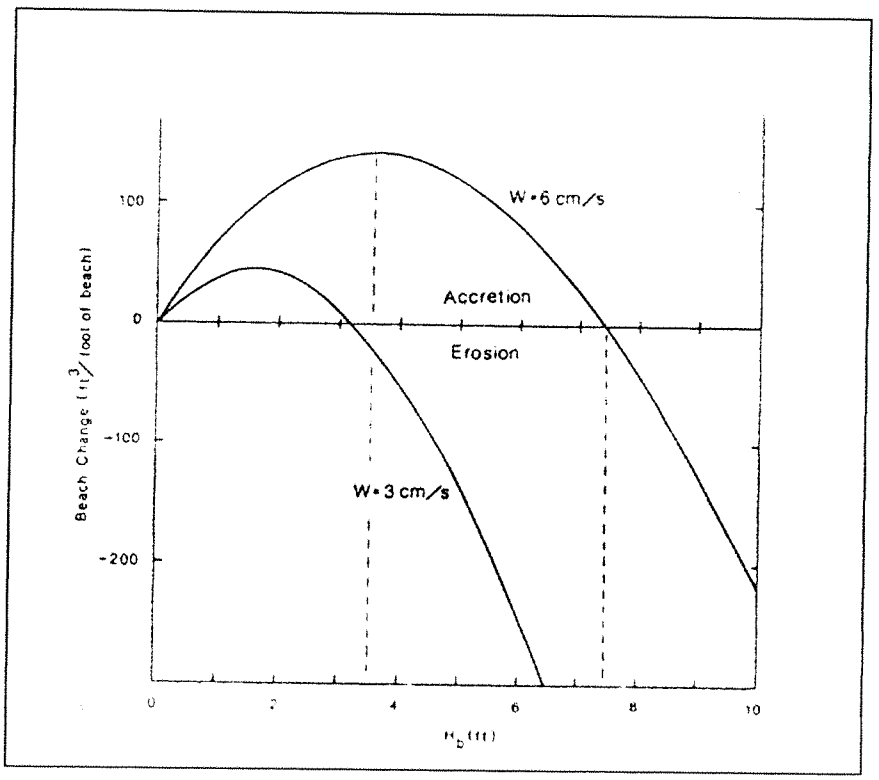

w = fall velocity

Figure 8.11: Predicted beach volume changes (initial beach slope = 1/15 and wave period = 10 seconds). Reproduced with permission (Seelig, 1983).

Installation of a beach drainage system does not affect the size of the sediment particles, but if it is operating it will increase the amount of water taken into the beach face from the overlying surge. This reduces the amount of wave energy available for sediment transport, promoting the same effect described above, but without the added factor of heavier particles. This means that the same relative trend shown in Figure 8.11 is likely to be observed for the drain on and drain off conditions.

8.4.2 Data Collection and Results

The test procedure was similar to that of test set C. The initial profile was prepared and measured, the wave paddle was run for two hours, and the profile was then re-measured. Test set C showed that the beach volume change was affected by the system discharge. Hence to compare the beach volume change from one wave climate to another the discharge was held constant. It was not possible to 'preset' a discharge using the available apparatus; therefore a range of beach volume changes for different discharge values were recorded. Ideally, a full data set would have been obtained for each wave climate (as in the set C tests), from which a volume change/discharge relationship could have been obtained. However owing to the pressures of time only a limited number of data points were collected for each wave climate. When these data points were plotted on a volume change vs discharge graph, a visual comparison was made between this gradient and those of the graphs obtained in test set C (Figure 8.3 and 8.4). This gave an indication as to whether one of the limited number of data points is likely to be an anomaly. All suspect points were re-measured.

Figure 8.12 shows the beach profiles after a two hour test for two different wave climates. The dashed lines show the end profiles when the drain was on, while the solid lines show the undrained beach profiles. The plane grey line shows the initial beach profile. The vertical exaggeration is approximately ×3, and the swash zone is from y = ± 0.05m to y = -0.5. The still water level mark is located at y = -0.25m

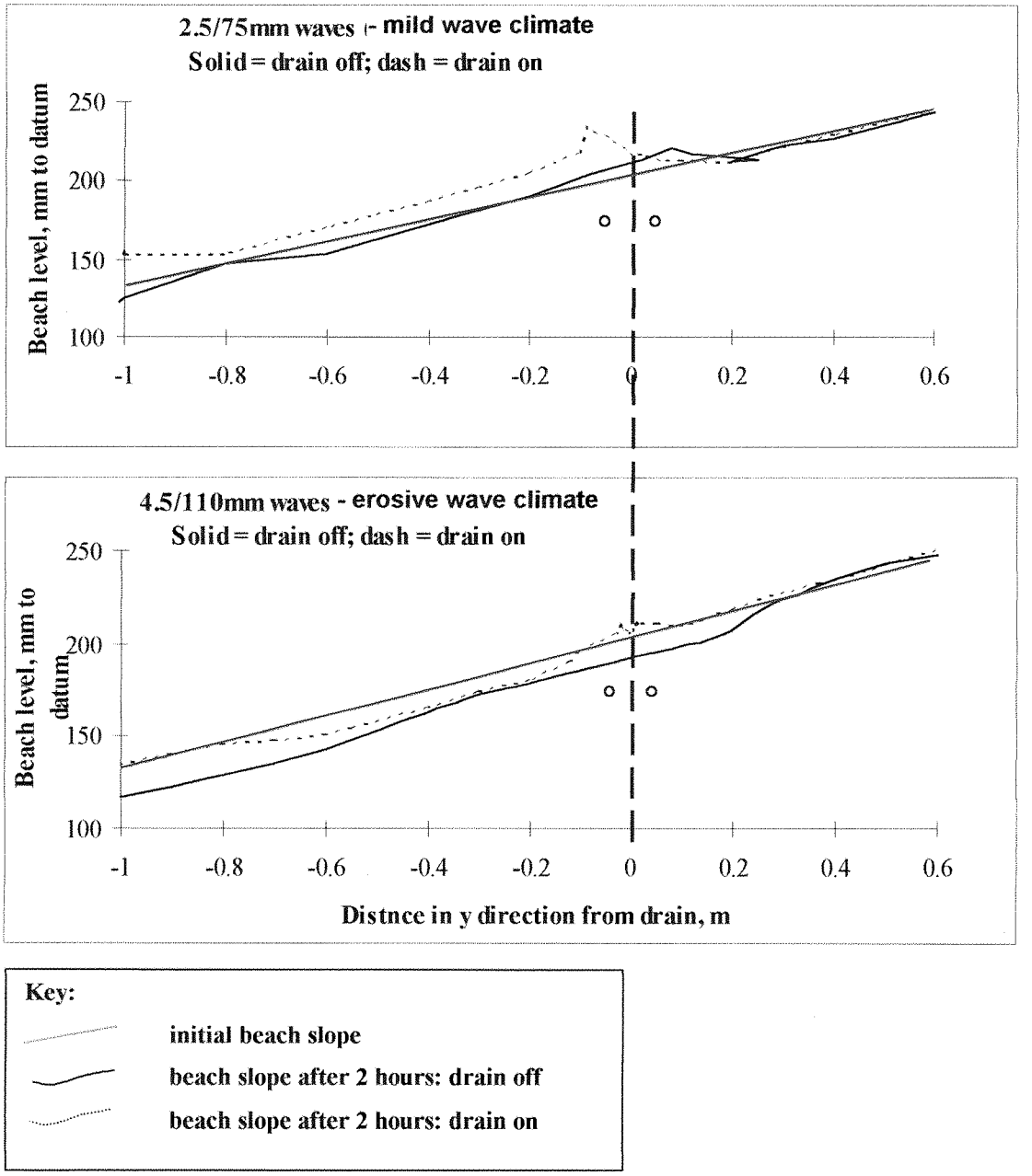

Figure 8.12: Comparison of profile formation under different wave climates.

For both wave climates, the drained beach profile is higher than the undrained profile for the entire length of beach measured. Therefore the drainage system promotes beach stability both within and seaward of the swash zone. For both wave climates, the seaward face of the berm on the drained beach is steeper than that of the undrained beach. Both the drained and undrained beach berms are larger for the milder wave climate.

This test was repeated for several different wave climates, and the change in beach volume for the drain off and drain on tests were calculated with the aid of a spreadsheet (as discussed earlier). Figure 8.13 shows the change in volume for different wave climates for the drain on and drain off tests. The wave energy is expressed in terms of the Dean number, Dn, which was discussed in Chapter 5. (Dn = H/wT, where H = wave height, w = fall velocity and T = wave period). Wave climates were also discussed previously in Chapter 5.

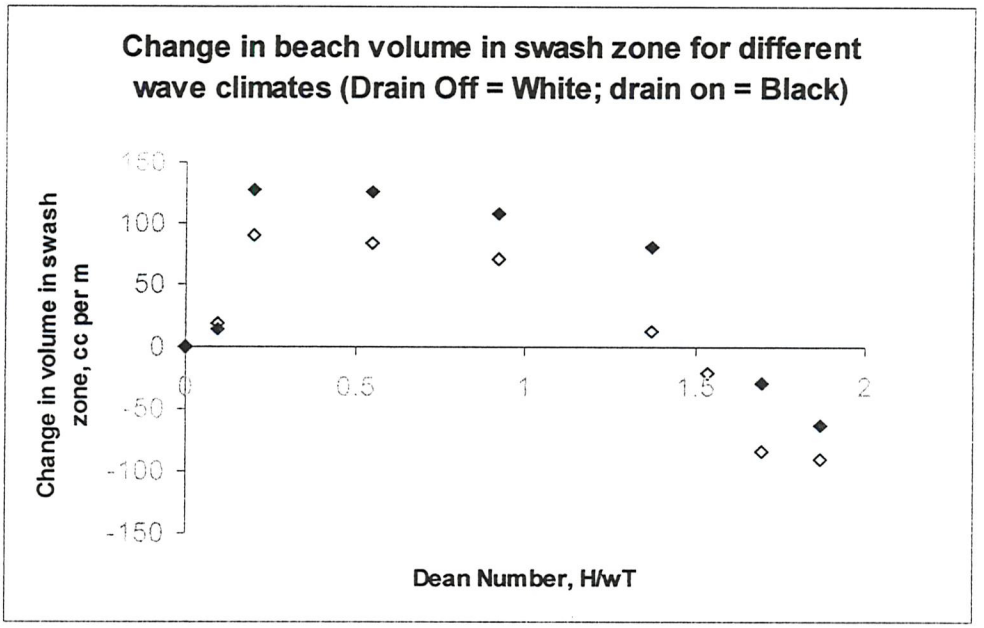

Figure 8.13: Relationship between change in beach volume and wave climate. (Horizontal axis shows the Dean number, indicating increasing wave energy)

8.4.3 Discussion and conclusions

When the wave climate is very mild (the Dean number is approximately 0.1), there is relatively little difference between the change in beach volume when the drain is on and off. There is a steep increase in beach volume change with increasing wave energy from Dn = 0.1 to approximately Dn = 0.2, during which the drain off and drain on data points diverge, and a difference of approximately 35cubic centimetres per m width of beach over the two hour period can be observed between the two data points.

To highlight the trend described above, a polynomial trendline has been fitted to the Figure 8.13 graph, as shown in Figure 8.14. Both curves reach a peak at approximately Dn = 0.6. After this point there is a negative relationship between the change in volume and wave climate: as the wave energy increases, the amount of material deposited on the beach decreases until the volume change = 0. This point is the Dean number that separates erosion from accretion (the threshold Dean number as discussed in Chapter 5), and from Figure 8.14 it can be seen that this value is different depending on whether the drain is on or off.

The beach drain also causes a shift in the value of Dn at which the trendline crosses the horizontal axis. For the data with no drain, the Dean number at which the beach volume change is zero is approximately 1.4, but when the drain is on, this threshold Dean number is increased to 1.65.

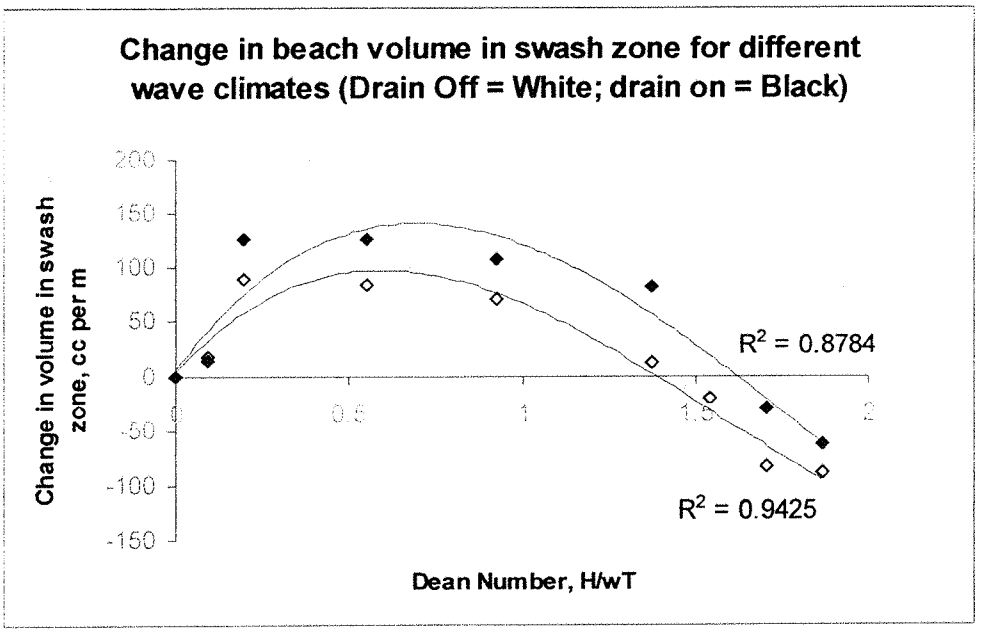

Figure 8.14: Trendline fitted to change is volume vs Dean number data points

The data points suggest that as the wave energy increases above approximately Dn = 1, the change in volume for the drain off and drain on data gradually converge, indicating that the beach drainage system is less effective during more erosive wave climates. Even when the wave climate is sufficient to cause a net loss of beach material, there is still a difference between the drain off and drain on data (within the

experimental range), and less material is lost with the drain on than would be lost without drainage.

The experimental and theoretical discussions suggest that the beach drainage system causes the beach material to exhibit at least in part the effects of a coarser material (as in Figures 8.11 and 8.14). Both a coarser particle size and beach drainage result in a greater volume of surge water infiltrating into the beach face during the surge cycle, leading to a greater energy loss and reducing the ability of the surge to transport sediment.

At Dn = 1.5, the beach drainage system can clearly be seen to cause an accretion of beach material, while when the system is off erosion occurs.

8.5 Change in beach volume with time under successive erosive and accretive wave climates (test set F)

8.5.1 Introduction

The full scale system at Branksome Chine was subjected to a range of conditions, and beach levels were found to fluctuate considerably between consecutive surveys. The system was damaged during erosive conditions, and the resulting loss of beach material caused parts of the drainage pipes to become uncovered and damaged further.

The aim of test set F was to simulate a series of alternate mild and erosive wave conditions, and monitor the change in the beach profile at given intervals in order to observe the beach recovery after storm events both with and without the drainage system operating. This test set was carried out in collaboration with a researcher from the University of Barcelona.

Method

The profile was prepared to an initial slope of 10%. This is slightly steeper than the initial profile used for previous tests, however, since each test was run for several hours (6 hours), there was ample time for the profile to reform to an approximate equilibrium profile for the given conditions.

The beach profile was prepared, and the wave paddle was set to the required settings and switched on for approximately 60 minutes. At the end of this period the profile was re-measured (the wave paddle was stopped for profile measurement). The paddle was then altered to the new setting and the test was restarted . This process was repeated 6 times with the drain off for intermittent mild then erosive wave conditions (see Table 8.1). Then the beach was returned to the original 10% profile, and the steps repeated, but this time with the drain on. The wave climates and times of operation are summarised in Table 8.1.

Profile measurement number	Time period	Wave setting during time period (from previous time period to current total time elapsed).	Wave climate description	Dean Number
0	Start of test	-	-	-
1	0-52	2.5/40mm	low energy	0.55
2	52-103	2.5/40mm	low energy	0.55
3	103-157	2.5/110mm	high energy	1.15
4	157-209	2.5/40mm	low energy	0.55
5	209-262	2.5/40mm	low energy	0.55
6	262-312	2.5/110mm	high energy	1.15
7	312-364	2.5/110mm	high energy	1.15

Table 8.1: Summary of test set F

8.5.2 Results

The change in beach volume was calculated by subtracting the beach levels for a given time from the initial beach levels. Therefore, at stage 6 for example, the change in volume will be the beach profile measured at t = 312 minutes, minus the original beach profile. Figure 8.15 shows the change in beach volume with time for the tests outlined in Table 8.1 (drain off and drain on data are shown on the same graph).

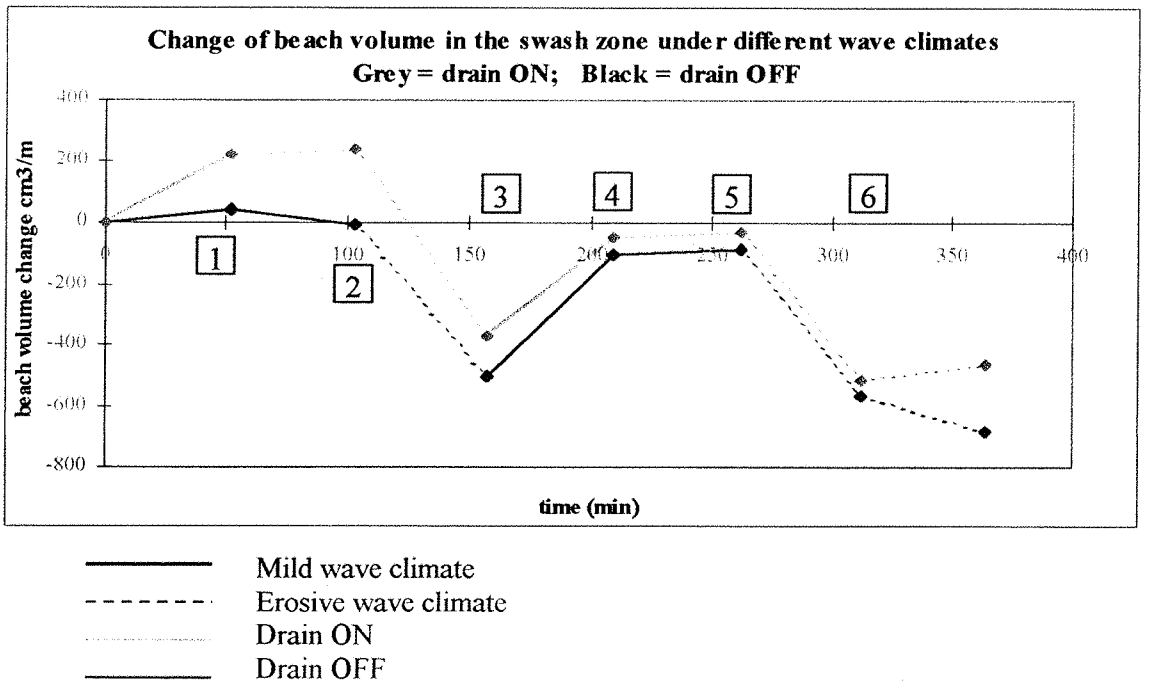

Figure 8.15: Change in beach volume with time for drain on and drain off tests.

8.5.3 Discussion and conclusions

The initial profile was prepared with a 10% slope. During the first stage of the test the wave climate was mild, and there was initially a period of significant accretion when the drain was on, and a smaller amount of accretion when the drain was off. During the second stage there was a further, but smaller increase in volume for the drain on test, while there was a loss of material for the drain off test rendering the total change in volume approximately zero (point 2 in Figure 8.15).

At point 2 the wave generator was altered to produce an erosive climate. During the stage from 2 to 3 the beach experienced back cutting and material was lost for both the drain on and drain off tests. In fact, a greater volume of material was lost from 2 to 3 (Fig. 8.15) for the drain on test. However, the total volume change measured at point 2 was greater for the drain on test.

When the wave climate returned to mild conditions (from 3 to 5) the beach recovered during both tests. More material was present on the drained beach , but the rate of recovery from 3 to 4 was slightly greater for the drain off test. From 4 to 5 there was relatively little change in beach volume for both conditions.

From the beginning of the test to point 5 the net volume for the drained beach was greater than that of the undrained beach.

The real benefit of the beach drainage system becomes apparent from point 5 to the end of the test. This section represented a prolonged period of erosive conditions, and initially a considerable (and equal) amount of material was lost from both beaches. However, during the second consecutive period of higher energy waves the drained beach began to accrete, while the undrained beach continued to experience material loss.

The results indicate that the protection afforded by the drainage system is not instantaneous, and if conditions change suddenly, the drained beach will initially follow the trend of an un-drained beach, and there is a lag time before the beach begins to recover under the influence of the drainage system. If the system is installed

so as to avoid damage during stormy conditions, the beach drainage system will eventually promote accretion.

The beach drainage system is still a useful means of coastal defence, because where a larger amount of material had been accreted during prolonged mild conditions (from t = 0 to point 2), the beach volume was always higher than that of the undrained beach test (i.e. the level of the drained beach was always higher that the undrained beach for the same conditions).

The results suggest that if the Branksome Chine system had been installed deep enough, and had not been damaged during the September storms, then the beach profile would have begun to recover.

In summary, the principal conclusions from this experiment are:

- The drainage system had the greatest effect during the initial period of mild waves
- Even when the drain was on, a net loss of material occurred during erosive wave climates
- The beach drain was able to reduce the amount of erosion that would otherwise have occurred during a period of prolonged erosive conditions.

These three events are akin to the events of the Branksome Chine trial: the system was effective for an initial period of calm weather, after which erosive conditions lead to reduced beach levels on all the beaches (drained and control beaches). The main difference between the results of the mode sequence and the full scale trial is that the model system was able to stabilise the beach from stage 5 to the end of the test and beach levels recovered despite the continued erosive conditions. Unfortunately, the full scale system was not robust enough to withstand the prolonged storms, and the system was damaged, hence beach levels did not recover.

8.6 Conclusions

The model tests have demonstrated that discharge, drain location (relative to SWL), and wave climate can each have a significant effect on beach profile change.

System discharge (test set C)

The results from test C1 show that beach volume change is proportional to the system discharge, and that drainage can induce beach accretion in the swash zone. This result is interesting, since not only can beach drainage retain material that exists on the beach, but is can also promote the deposition of particles. This suggests that increased beach shear strength due to pore water pressure reduction (investigated in Chapter 7) cannot fully explain the mechanism of beach drainage: increased beach strength induced by the drainage system may prevent particles from being moved by the shear force of the surge, but a second phenomenon must exist to explain why beach accretion occurs when the drain is in operation. Data support the theory that the second mechanism is back wash volume reduction leading to laminar flow phase extension and drainage induced deposition.

Still water level location (test set B)

The performance of the beach drainage system varied with the still water level location relative to the drain. The effect of the drainage system was significant between y_o = -0.2m and y_o = +0.2m.

The results of test set B show that the drain is most effective when the upper part of the swash (where the wave is thinnest) is located over the zone of maximum influence of the drainage system. This result also supports deposition phase extension theory (see discussion in Chapter 4) because the maximum amount of material was deposited when the highest volume of water was being removed from the thinnest part of the wave.

The optimum effect was obtained when the relative energy removal was estimated to be 13%, and the drainage system was ineffective when the relative energy was estimated to be less that 2%.

It is important that the upper limit of the swash is located over the zone of influence of the drain. For a full scale system that is subject to a tidal cycle this is not always the case

because the run-up moves relative to the fixed, linear, location of the drainage system. Hence there may be periods during the tide cycle when the system is operating inefficiently. This will be discussed further in Chapter 9.

Similarity to fine/coarse material behaviour

The results of test set E show that the relationships between wave climate and beach volume change with the drain off and drain on mimic those observed with fine and coarse material respectively. This is thought to be because both drainage and coarser material result in increased percolation.

9. Alternative drainage system designs

9.1 Introduction

In Chapter 4 it was argued that the performance of the drainage system depends on the position of the run-up in relation to the zone of influence of the beach drain. Results from the set B experiments detailed in Chapter 8 support this argument, and data suggested that optimum performance occurs when the upper section of the swash is located above the zone of maximum influence of the drainage system.

In tidal conditions, the run-up zone moves in relation to the drainage system. If a single, linear drain is installed, the zone of influence of the drain is limited to a relatively small proportion of the total swash zone. In Chapter 8 (section 8.3) it was shown that the model drainage system (which consisted of two drains 100mm apart) was effective within the zone y_o= -0.2m to y_o = +0.2m. If the tidal range is large, then the run-up zone will be outside of the zone of influence of the drain for a significant portion of the tide cycle. Even with a relatively small tidal range, the distance between the high water and low water marks may be significant due to the gentle slope of a sandy beach.

Beach mat

Beach drainage may be optimised by increasing the area of the beach covered by the system, so that the zone of influence extends throughout the entire swash zone, taking tidal fluctuations into consideration.

A corrugated plastic drainage layer sandwiched between two layers of felt geotextile filter material (geocomposite) was used to construct a drainage mat. The objective was to provide a permeable layer within the beach, feeding water to a collector pipe. A slot was cut down the side of a plastic pipe, and the geotextile sandwich was inserted into the slot. This is shown in Figures 9.1 and 9.2.

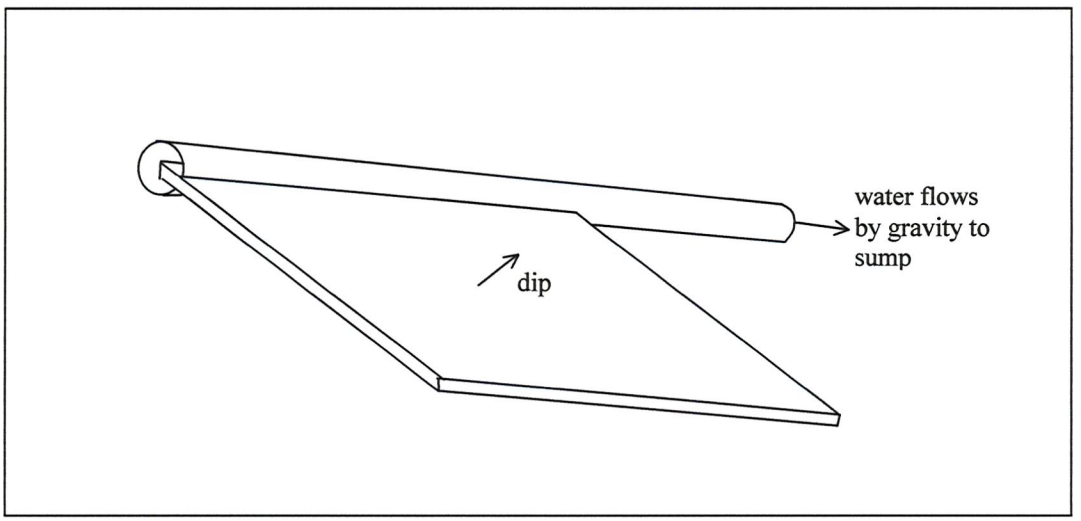

Figure 9.1: Sketch to show beach mat components

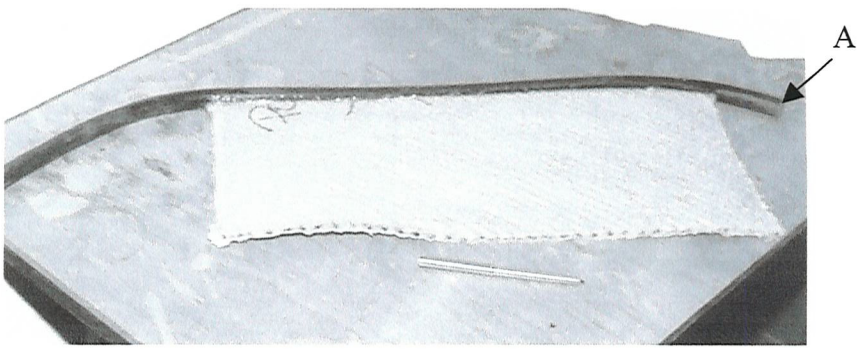

Figure 9.2: Photograph of beach mat

The edges of the geotextile and end of the collector pipe (A in Figure 9.2) were sealed with silicone sealant. Figure 9.3 shows a diagram of a beach drainage mat within a beach. It is recognised that such an installation may prove to be impractical, so the success of such a system would rely upon the development of appropriate installation techniques. This drainage method may be more suited to beaches with a high tidal range where the beach is accessible for a longer portion of the tide cycle.
The design is shown in Figure 9.2.

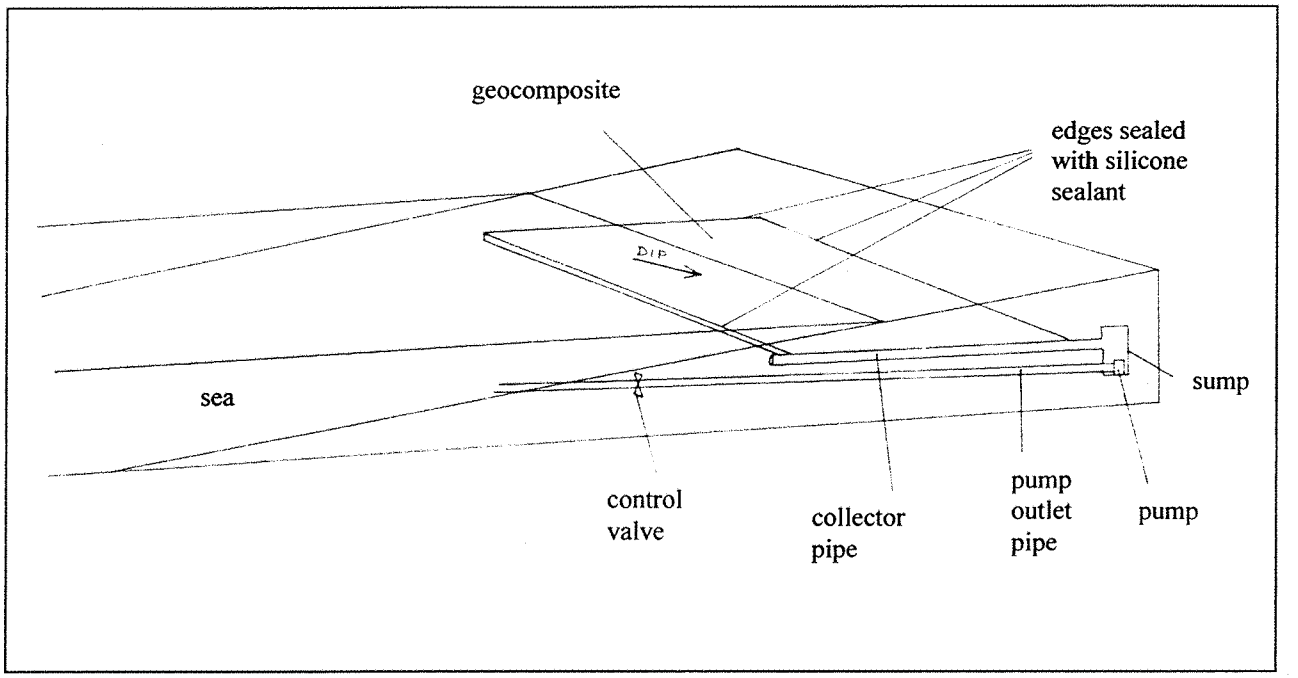

Figure 9.3: Drainage mat located in beach

9.2 Preliminary experiments

A test was carried out to determine whether the beach mat drainage system would be an effective means of beach stabilisation. The apparatus described in Chapter 5 was used, but a screen was installed down the centre of the wave tank to divide the beach in half as shown in Figure 9.4. The mat dimensions were 220mm × 100mm × 7mm. The model beach mat was installed approximately 50mm below the surface of the beach. The test was run for 1 hour, with an accretive wave climate operating (1.5/50mm). The initial beach profile was 1:10 and the centre of the beach mat was located at y = 0.

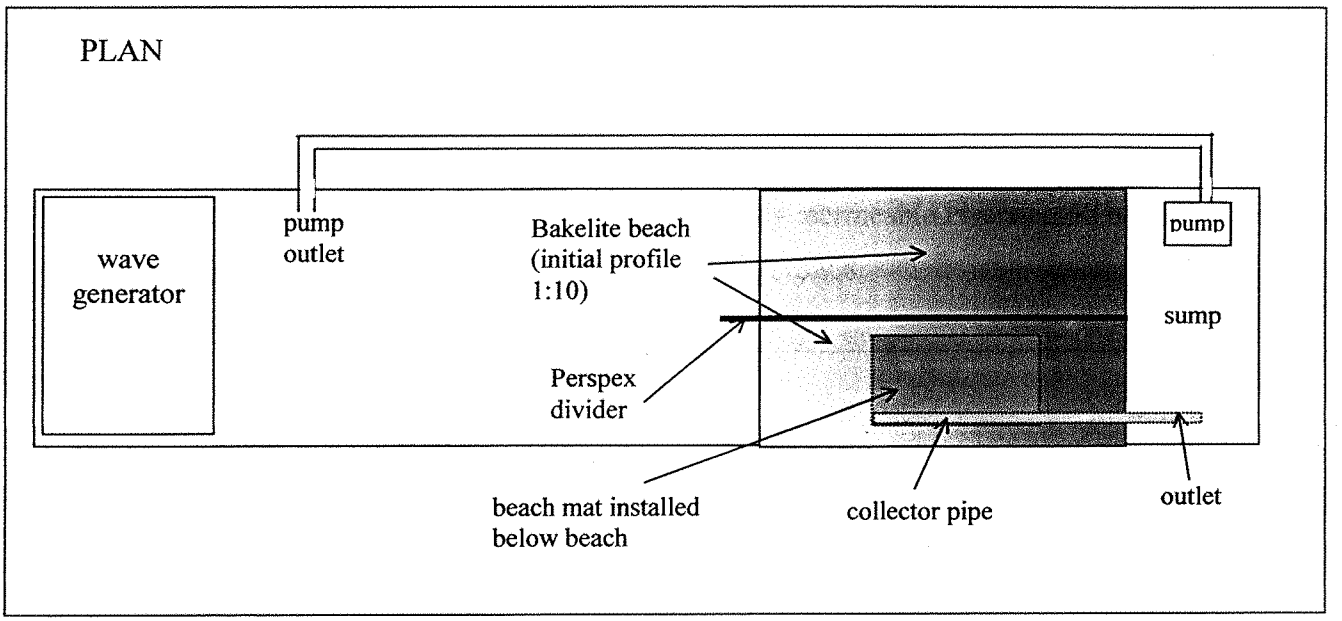

Figure 9.4: Schematic diagram of wave tank with Perspex divider

Results

Figure 9.5 shows the beach profiles either side of the Perspex screen after a 1 hour test. Results show that with an accretive wave climate the beach drainage system resulted in a significantly higher and broader berm than for natural (undrained) conditions. The beach drainage mat also resulted in higher beach levels for some distance seaward of the drain.

The photograph in Figure 9.6 shows the position of the beach berm for test 1 (see Figure 9.5). The crest of the berm was located further seaward when the beach mat drain was in operation.

The measured discharge was 9.5 l/min per m length of system when the still water level was located at y = 0. Figure 8.6 in Chapter 8 showed that for a drainage system constructed from PVC pipes wrapped in a geotextile filter the discharge was 6.5l/min per m when the SWL was at y = 0. The beach mat system discharge was higher possibly due to few losses, or simply due to a larger collection area.

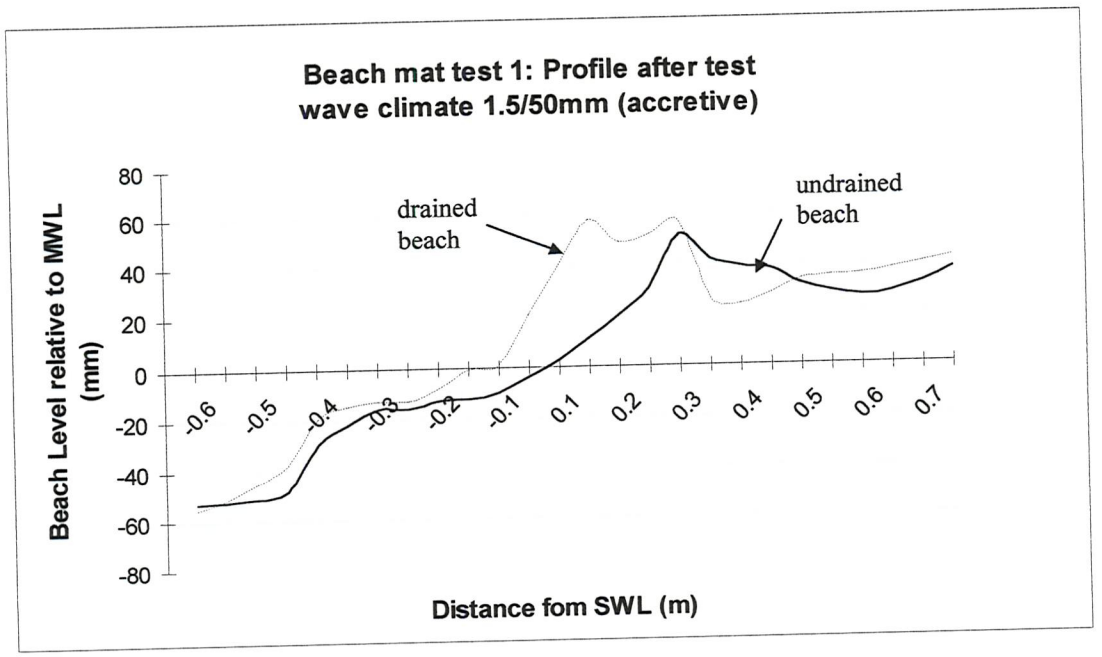

Figure 9.5: Beach profiles after a 1 hour test.

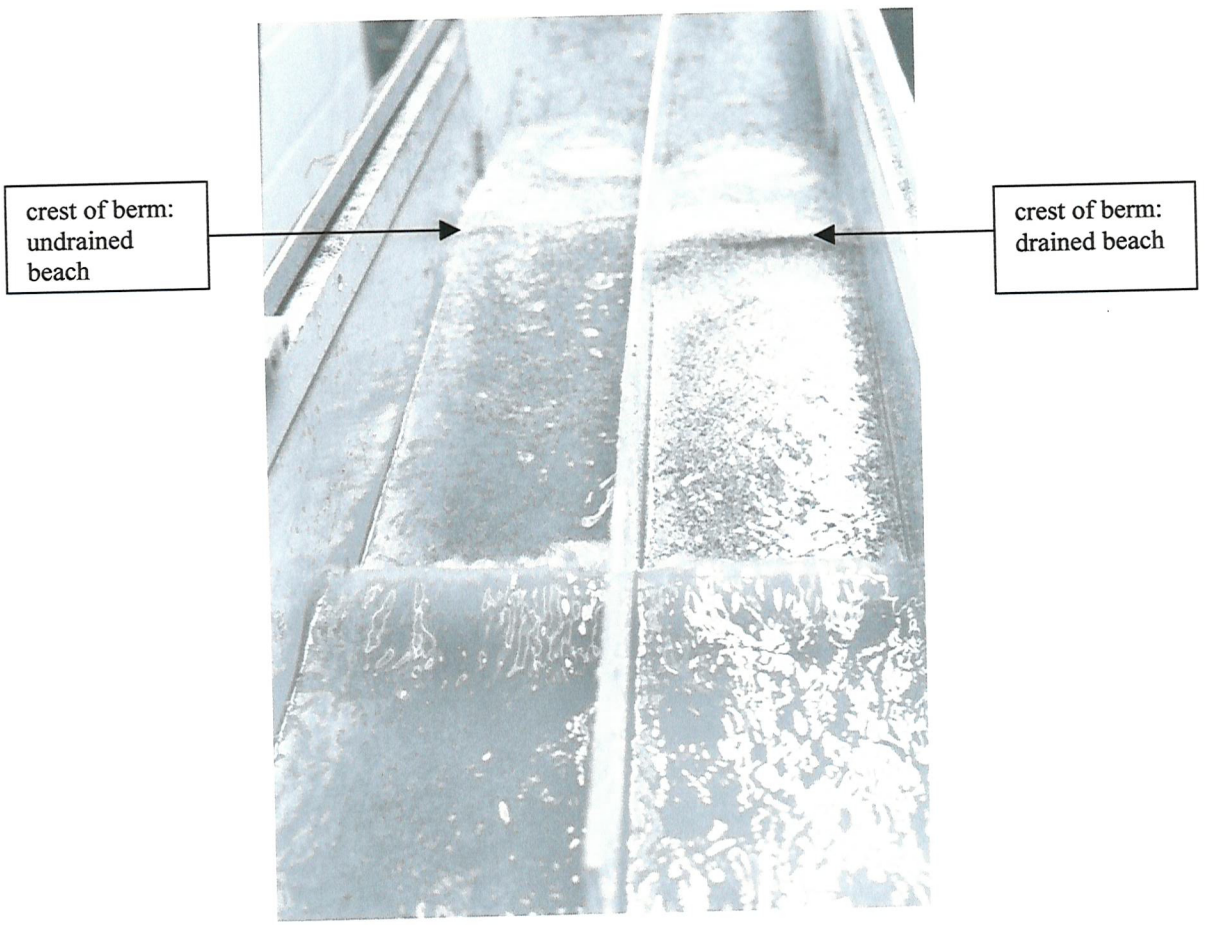

Figure 9.6: Photograph of beach profile during test 1.

9.3 Alternative beach mat configurations

The above experiment was carried out for a pump assisted drainage system. It may be possible to achieve beach stabilisation using a gravity drainage beach mat as shown in Figure 9.7. Alternatively, permeable layers could be used to enhance a linear drainage system as shown in Figure 9.8.

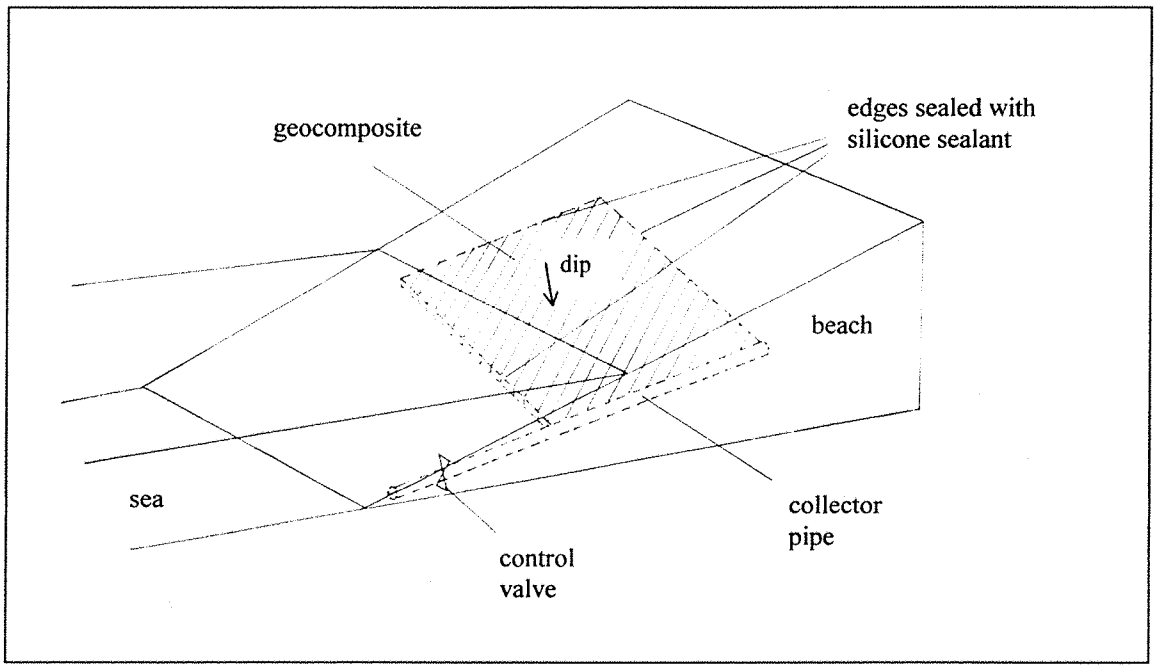

Figure 9.7: gravity drainage beach mat

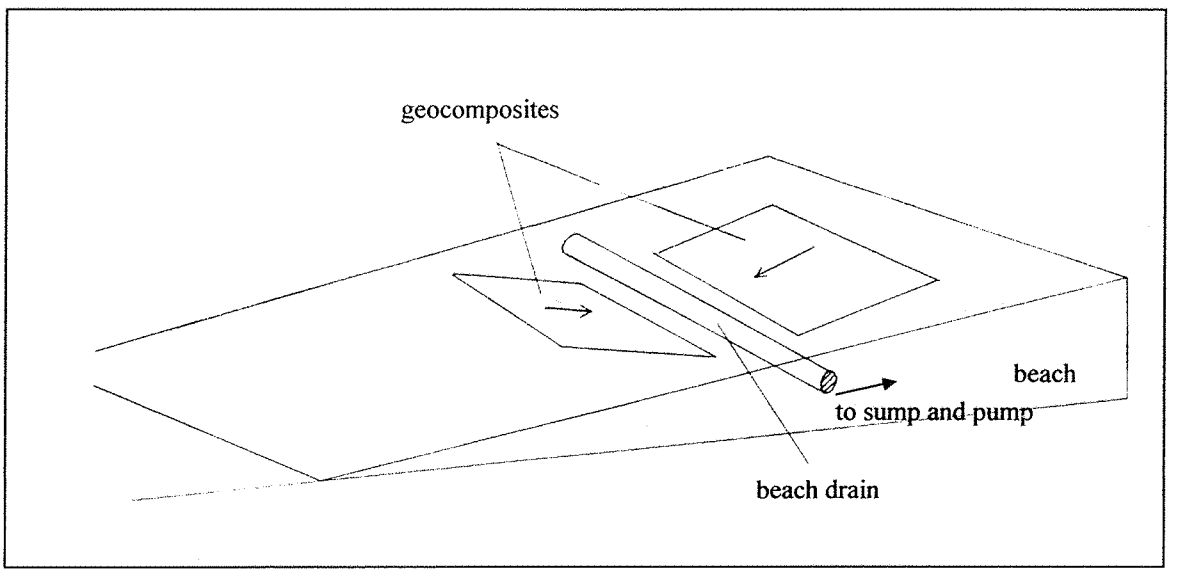

Figure 9.8: beach mat appendage for linear drainage system

9.4 Conclusions

In previous chapters it was shown that the zone of influence of a beach drain is a limiting factor for performance, and that optimum performance occurs when the upper limit of the swash was located over the zone of maximum influence of the drainage systems. In light of these findings, a new beach drainage system was designed to provide a broader zone of influence than a conventional drainage system.

Preliminary experiments have shown that a geocomposite drainage system can stabilise a beach, promoting a broader, and higher berm than would otherwise occur. The geocomposite drain was found to be more effective than the pipes used for the experiments described in Chapters 5-8 because the discharge was higher for the same head and beach material. It was shown in Chapter 8 that drainage system performance is proportional to system discharge (other factors being equal), hence the beach mat is likely to be more effective than the conventional system.

In reality, there are likely to be practical problems associated with the installation of a geocomposite beach drain, and the development of suitable installation techniques is a recommendation for future work.

The use of a geocomposite drain is likely to be advantageous for sites with a high tidal range because:

1) the zone of influence is spread to cover a larger width of beach (therefore the run-up zone will be over the zone of influence of the drain for a longer portion of the tide cycle)
2) a high tidal range affords better beach access for installation

This chapter details a preliminary experiment only, and further study into the use of beach composites for stabilisation is recommended. Improved performance through the broadening of the drainage system zone of influence may alternatively be achieved using several linear drain pipes located parallel to each other in the swash zone: this is also recommended for further study.

10. CONCLUSIONS

10.1 Summary of conclusions

Aims

The main aims of the PhD research project were to

- gain an understanding of the application and practical limitations of beach drainage,
- investigate the mechanisms of beach stabilisation through drainage, and
- investigate the factors affecting beach drainage system performance.

Mechanisms of beach drainage

Three feasible mechanisms for beach stabilisation through drainage were identified to be:

- surge energy reduction (leading to laminar flow phase extension),
- seepage cut-off, and
- effective stress increase.

Prior to this study, little work had been carried out to take these concepts further and provide evidence to support the theories. In this PhD study, the understanding of the above mechanisms has been developed through theoretical discussion. The feasibility of deposition phase extension and increased beach strength through pore water pressure reduction was explored through the advancement of theoretical concepts, and the conclusions were supported with experimental results. In particular it was shown that:

- Beach drainage increases the shear strength of the beach material
- Beach drainage results in a reduction of surge energy due to backwash volume reduction, and this promotes the deposition of sediment.

Surge energy reduction was discussed in terms of relative energy removal, which is the energy removed by the drainage system in relation to the total energy of the overlying wave (for a given point in time). It was argued that optimum performance occurs when the upper limit of the swash is located over the zone of maximum influence of the drain, and experimental data were obtained to support this theory.

Pore water pressure reduction

The drainage system causes a reduction in pore water pressure within the beach, and the following general equation was derived using empirical data:

$$P_w = \rho g d + m(y - y_h) - f(q)$$

Where ρ = density of water; g = acceleration due to gravity; d = depth of water (hydrostatic); q = system discharge; y = distance from the still water level mark to the drainage system in the horizontal plane; m is the set up gradient; and y_h is the distance from the drain to the point at which the pore water pressure is equal to hydrostatic.

The beach drainage system was shown to reduce the effective stress of the beach material from y = -0.4m to y = 0.3m. The calculated effective stress indicates that liquefaction (that would otherwise occur) was completely eliminated between y = 0 and y = 0.3m (from directly over the drain to 0.3m landward of the drain). Liquefaction is believed to be overestimated in the model due to the use of a lightweight sediment.

The influence of the model drain is thought to be skewed landward due to the close proximity of the impermeable boundary at the rear of the tank, and due to wave inundation on the seaward side of the drain.

Factors affecting performance: results of model tests

Model experiments have shown that the system performance, as defined by the beach volume change in the swash zone, is approximately proportional to the system discharge.

The performance also varied with still water level (SWL) location relative to the drain. However this relationship was not linear, and the data suggest that an optimum performance may be identified. The optimum performance occurred when the upper limit of the swash was 0.05m landward of the drain (i.e. when the thinnest part of the wave was over the zone of maximum influence of the beach drain). The effect of the drain was significant when the upper limit of the swash was between y = -0.2m and y =

+0.2m, (i.e. when the upper limit of the swash was located within the zone of influence of the drain).

The drainage system performance varied with wave climate. For extremely mild wave climates, there was relatively little difference between the drain off and drain on beach profiles. For moderately accretive and erosive wave climates the drainage system was effective, and for very erosive wave climates the effect of the drainage system was reduced, although the system did remain effective within the range tested.

Results support the theory that the beach drainage system causes the beach to display the characteristics of a beach consisting of coarser material due to the increase in percolation.

Scaling

Although the model attempted to address the beach face wetness scaling problem noted by Weisman *et al.* (1995),), the model design over-compensated for this effect, and it transpired that in fact the model beach was *drier* than that of the prototype, causing the results to *overestimate* the prototype. This was advantageous since the purpose of the model was to identify the trends between the data sets.

The beach face wetness effect was quantified using the beach face wetness number, W:

$$W = \frac{kTS_o}{8H}$$

where k = beach permeability, T = wave period, S_o = beach slope and H = wave height.

Although quantitatively the model results are unrepresentative of a full scale system, qualitatively, the model findings have important implications for full scale beach drainage, and the trends identified in the model are likely to apply to the prototype, since geometrically the model and full scale systems are similar, wave climates are representative of those observed in the field. Geometric similarity is also assured since the model and full scale equilibrium profiles are the same.

In terms of sediment transport the model and prototype do not satisfy conditions for similitude, and the limitations of using a Bakelite sediment have bee identified. The important point to note is that results pertaining to the magnitude of variables such as beach volume change, discharge, pore water pressure reduction, and liquefaction depth are likely to be an overestimate in the model.

Full scale trial

The full scale trial carried out at Branksome Chine provided a valuable insight into the practical problems likely to be encountered in the field. These were:

- insufficient pipe cover depth resulting in the uncovering and damage of drainage pipes during storms,
- sump damage resulting in sump siltation, and
- pump durability problems.

The drainage system discharge was lower than the discharge calculated by theory and estimated from previous trials. Despite this, however, the system was effective during the first two months of operation (Summer 1998), and an increase in the level of the beach was noted on the drained section that was not apparent on the control beaches.

In September 1998, prolonged storms resulted in the loss of beach material and significant system damage, after which the berm on the drained section disappeared. The system was repaired in December 1998, but subsequent storm damage resulted in discharge rates that were substantially lower than those recorded the previous summer. During this time the system had a negligible effect on the beach profile. The ineffective period caused by system damage was an important control period. This supports the conclusion that the berm noted on the drained section during the previous summer had indeed been caused by the drainage system and was not a local effect.

It is recommended that historical records (of storm events and corresponding beach loss) are taken into consideration during the design stage, and that the system is designed and constructed to withstand storm events likely to recur during the required design life (e.g. 1 in 20 year storm).

10.2 Project appraisal

Novel experiments have been carried out to obtain the results discussed above. Evidence has been provided to support previously unsupported theories of beach stabilisation through drainage.

Experiments were successfully carried out to determine the effect of beach drainage on the liquefaction boundary, and results were obtained to demonstrate the effect of a beach drain on pore water pressure during wave action.

Important information was gained regarding the factors influencing drainage system performance, and some new drainage system designs using geotextile mats have been suggested on the basis of some of these findings.

10.3 Future work

The results indicate that one of the principal mechanisms of beach accretion through drainage is deposition phase extension, but experimental data (for test set B in particular) were scattered, and data for test set C2 were inconclusive. The results from this project are sufficient to confirm the likely mechanisms of beach drainage, but further work is needed to quantify important processes, such as laminar flow phase extension and relative energy removal (although an estimate of these quantities has been derived as part of this study).

The beach drainage model was simplified so that the basic processes and mechanisms could be understood, and that individual parameters could be investigated in isolation. Now that this understanding has been developed, it is necessary to design a more complex representation of a full scale system, so that quantified model data can be scaled up to predict full scale performance for a range of conditions (including tide, land flux and irregular waves). Ideally this should be carried out in conjunction with a controlled full scale experiment from which data may be obtained for model validation.

A future full scale experiment should aim to install the beach drains sufficiently deep to avoid damage during prolonged storms, and must be designed to minimise losses. It is recommended that piezometers are installed in the full scale beach so that the impact of

the drainage system on full scale pore water pressure dynamics can be compared to the findings for the physical model presented in this thesis.

Full scale results suggest that a robust, efficient drainage system would provide an effective beach stabilisation option for Branksome Chine. A recommended future study is an investigation into the feasibility of a combined beach nourishment/beach drainage project for Poole Bay, with the possible removal of groynes. A long term aim is to develop design guidelines for the application of beach drainage systems for use by local authorities such as the Borough of Poole.

Future projects also include further investigation into alternative system designs, in particular researching their performance, practical limitations and developing appropriate installation techniques.

During the course of this project international links have been established between interested parties. Future work is aimed at consolidating these links, and establishing international collaboration for the advancement of beach drainage practice. An international workshop is planned for the near future, and as a result of this PhD project collaboration is continuing between Texas A&M University and the University of Southampton.

APPENDIX A: Global warming and extreme weather conditions media articles

Global warming: it's with us now

Six dead as storms bring chaos throughout the country

Paul Brown
Environment correspondent

The worst storm for a decade, which caused road and rail chaos across the country, killed six people and left hundreds of millions of pounds worth of damage in its wake, last night prompted warnings that Britain is now beginning to pay the price of unchecked global warming.

Torrential rain and winds up to 90mph uprooted trees, blocked roads, and cut electricity supplies across southern England and Wales.

A tornado ripped through a caravan park in Selsey in West Sussex less than 48 hours after a similar twister devastated parts of Bognor Regis, and thousands of ferry passengers were stranded in mid-channel, unable to dock in Dover.

Last night a tanker began leaking chemicals into the English Channel after it was overcome by high seas. The 14-strong crew of the Italian ship Ievoli Sun was airlifted to safety.

Shops, banks and schools were closed as people failed to get to work, and the environment agency issued 25 severe flood warnings across Wales, south-east and south-west England. Dozens of rivers broke their banks, flooding hundreds of homes, and lifeboats rescued stranded people 30 miles inland. In Yorkshire, the first blizzards of the winter coincided with flash floods.

The severe weather followed record rainfall in south-east England in October and an exceptionally wet September. It is exactly the recipe for disastrous flooding predicted by scientists two years ago when studying the potential effects of global warming on Britain.

Yesterday Marilyn McKenzie Hedger, head of the UK Climate Impacts Programme based at Oxford, said: "These events should be a wake-up call to everyone to discover how we are going to cope with climate change.

"We have had a 0.6C rise in average temperature in the last century, and extreme events have started to happen with greater frequency. How are we going to cope when it goes up 2C?"

The government, alarmed at the increase in flooding of property, is expected to issue an order before Christmas banning new building on flood plains. Even before yesterday's events there had been 30 serious instances of flooding of property in the last two years.

The Met Office said that October's rainfall in East Sussex, one of the driest parts of the country, had been nearly three times normal at 226 millimetres (9 inches).

There had also been a number of unusual and record breaking "weather events" this year — for example an exceptionally warm winter and the wettest April since records began in 1766 — but this still did not mean global warming was here, it said. "It is the sort of weather we can come to expect, but we cannot know until this pattern is constantly repeated."

A spokesman for the environment agency said Britain could not wait to find out. "We want a very strong presumption against building on flood plains," he said. "But if it goes ahead in exceptional circumstances the developer, not the public purse, should be responsible for the flood defence — and that should not simply be building walls to shift the problem further downstream."

The government has also altered regulations so that high-rise structures can withstand stronger winds. Flood defences round the coast are now built to withstand rises in sea levels and tidal surges, but in some areas low-value farmland is being abandoned because the cost is prohibitive.

In two weeks, governments of the world meet at the Hague to try to reach agreement on reducing greenhouse gas emissions from the developed countries by an average of 5%, although scientists say 60% reductions are required to keep the climate stable.

With more global warming inevitable because of the extra carbon dioxide already in the atmosphere, the EU is launching a report tomorrow on how it proposes Europe should adapt. It says that Britain and the rest of northern Europe can expect far more flooding, and it will use East Sussex and the recent devastation in the Italian Alps as examples.

Michael Meacher, the environment minister, writing in today's Guardian, says: "It would be foolish to pretend that every time extreme weather conditions occur, it is due to global warming. But the increasing frequency and intensity of extreme climate phenomena suggest that ▸ **Page 2**

The Guardian, 31/10/00

The Independent, 23/12/99

Climate chiefs issue severe weather warning to world

GLOBAL WARMING is now changing the world's climate rapidly, and humanity faces a "critical" position because of it, the chief meteorologists of Britain and the US warn today in a remarkable joint statement.

Peter Ewins, head of the UK Meteorological Office, and James Baker, his US counterpart, confront climate-change sceptics head on with their assertion in a letter to newspapers, including *The Independent*, that the world is warming rapidly and human actions are responsible.

The statement from such senior figures breaks a tradition of caution by scientists involved in climate research, who have been providing evidence for a decade of global warming, but have left the conclusions to politicians. Today's statement will be seen in the context of recent climate-related catastrophes, from the devastation

BY MICHAEL MCCARTHY
Environment Correspondent

of Hurricane Mitch last year to this month's disastrous mudslides in Venezuela brought about by extreme weather conditions consistent with predictions of what global warming may cause.

The two meteorologists attack the sceptical view, still prevalent in the American business community, that fears of global warming are exaggerated. They say in their letter that data on global temperatures over the last year "confirms that our climate is now changing rapidly". And they add: "These new observations, when combined with our improving understanding of the climate system, increasingly point to human influences as the cause of these climate changes.

"The rapid rate of warming since 1976, approximately 0.2 degrees per decade, is consistent with the projected rate of warming based on human-induced effects," the meteorologists say. "Scientists now say that they cannot explain this unusual warmth without including the effects of human-generated greenhouse gases and aerosols." Global warming is believed to be caused by the increased emissions of industrial gases such as carbon dioxide from motor vehicles and power stations. The international community agreed on an outline plan to cut back on "greenhouse gas" emissions at Kyoto, Japan, in 1997, but progress on implementing it has been slow.

The letter from Mr Ewins and Mr Baker is the most definitive statement yet by senior scientists on global warming.

Letters, Review, page 2;
Leading article, Review, page 3

THE THURSDAY REVIEW: LETTERS 2, LEADERS & COMMENT 3-5, RADIO & TV 15-16

The Daily Telegraph, 23/12/99

Stormy prospect for Millennium

By Sandra Laville

A BAND of stormy weather is forecast to bring heavy rain and strong winds on Millennium eve.

Although the wet and windy weather is due to subside over the next couple of days, forecasters said it would return by Friday.

A spokesman for the Meteorological Office said: "We are expecting heavy rain and strong winds — it is too early to say whether it will be as bad as Christmas."

Much of the South and South West remained on red flood alert yesterday and in Scotland and the North ice made driving treacherous.

But the bad weather did not deter bargain hunters at the start of the sales.

Despite predictions that the nation was suffering a "Millennium hangover" after heavy spending at Christmas, stores across the country reported a successful day.

At Europe's largest shopping complex, Bluewater, near Dartford, Kent, queues formed at 4am and stores recorded their busiest day of the year. In Bristol bargain hunters camped out overnight and a one-in one-out policy was operated by some stores for safety.

Flooding left many families in the South homeless over Christmas and yesterday hundreds of homes were still at risk.

Almost 48 hours of continuous rain left rivers in Kent and Sussex flowing dangerously fast. Red warnings were still in place on the Ouse and Cuckmere in East Sussex.

A spokesman for the Met Office warned that more stormy weather was hovering over the West Country.

Snow affected the A83 at Arrochar, close to a section already blocked by a landslip, while the A82 was affected by ice at the Arden roundabout, near Loch Lomond.

Shoppers defy gloom: Page 5
Editorial Comment: Page 25

APPENDIX B: Overview of Beach Management System projects

Overview of BMS Projects 2000-08-15

Project	Year Installed	Period of operation	Length of system	Drain material	Drain diameter & Invert El. (MSL)	Installation method	Tide range	Beach slope Initial / Final	Pump arrangement	d_{50}/U Sand Grain Size	Pump capacity instal	Flow rate $m^3/h/m$ Initial / Final	Appr. drawdown C drain	Littoral conditions	Comments
Hirtshals W, Denmark	1981	Since 9/81	200 m 656'	1)	315 mm 185/200 -2.5m	Backhoe W.pts.	~1.5 m	1:20/1:20	2)	0.26/1.7	400 m^3/h	2.0/1.0			25,000 m^3 sand harvested each year to renourish other beaches
Hirtshals E, Denmark	1983	8 months 1983	200 m 656'	1)	200 mm -2.0 m	Backhoe W.pts.	~1.0 m	1:25/1:20	2)	0.2/1.3	100 m^3/h	0.4/0.15			Width maintained. Erosion rate: 7 m/year
Thorsminde, Denmark	1985	1/85 – 4/91	500 m 1640'	1)	200 mm -2.0/-2.5	Backhoe W.pts.	1.5 m	1:25/1:30	2)	0.35/1.7	700 m^3/h	1.7/1.1			Experimental system, width increased 25 m
Sailfish Point Stuart, Fl. USA	1988	7/88 – 8/96	177 m 580'	3)	50/450 mm -2.4 m	Backhoe W.pts.	0.8 m	1:25/1:15	2)	0.3/3	340 m^3/h	1.5/0.60	0.8 m	4)	Width increased 20-25 m during operation
Enoe Strand, Denmark	1994	Since 7/94	600 m 1969'	5)	113 mm -1.8 m	Plough	0.5-1.0 m	1:15/	2)	0.25/2.3	300 m^3/h	0.4/0.1	1.0 m		Width increased 3 m August 1996. Maintained
Towan Bay, U.K.	1994	Since 9/94	180 m 591'	6)	300 mm	Backhoe W.pts.	7 m	1:45/	2)	0.2/1.7	290 m^3/h	1.27/1.0			General accretionary trend Exposed seawall footing safeguarded
Codfish Park Nantucket I, MA, USA	1994	Since 1/95	357 m 1170'	7)	300 mm -2.1 m	Trench machine	1.0-1.5 m	1:45/	Low vac. wet well (3-5'HG)	1.5/4.2	700 m^3/h	1.7/	0.3 m	8)	Decreases in shoreline width due to storm events. Shoreline erosion rate in the treated areas has been reduced compared to untreated areas
Lighthouse S Nantucket I, MA , USA	1994	Since 1/95	309 m 1015'	7)	300 mm -2.1 m	Trench machine	1.0-1.5 m	1:6/	2)	0.8/3.2	1400 m^3/h	1.8/	0.3 to 1.3 m	8)	
Lighthouse N Nantucket I, MA, USA	1994	Since 1/95	405 m 1330'	7)	300 mm -2.1 m	Trench machine	1.0-1.5 m	1:6/	2)	0.4/3.7	1400 m^3/h	3.2/	0.9 to 1.8 m	9)	
Chigasaki-Naka Beach Japan	1996	5/96 – 9/96 7/97 -	180 m 600'	10)	300 mm -2.3 m	Trench machine Sheet wall	1.6 m	1:10/	2)	0.5/4	500 m^3/h	2.8/			Temporary shut down due to typhone damage. Repaired and reactivated. Shore-line stabilized. Beach level increased.
Riumar I, Ebro Delta Spain	1996	Since 10/96	300 m 985'	11)	160 mm -2.3 m	Backhoe W.pts.	0.2-0.4 m	1:20/	2)	0.2/1.4	290 m^3/h	0.5/	1.0		Width maintained after severe storm event Oct. 97

HV/MAN

Project	Year Installed	Period of operation	Length of system	Drain material	Drain diameter & Invert El. (MSL)	Installation method	Tide range	Beach slope Initial / Final	Pump arrangement	d_{50}/U Sand Grain Size	Pump capacity instal	Flow rate $m^3/h/m$ Initial / Final	Appr. drawdown C drain	Littoral conditions	Comments
Hornbaek W Danmark	1996	Since 12/96	450 m 1410'	11)	160 mm -0.8 m	Plough	0.2-0.4 m	1:10/	2)	0.3/2	170 m^3/h	0.1/	0.5		Width increased 0-5 m, May 1997. Continued accreation
Hornbaek E Denmark	1996	Since 12/96	530 m 1650'	11)	160 mm -1.5 m	Plough	0.2-0.4 m	1:20/	2)	0.3/2	325 m^3/h	0.3/	1.0		
Ystad Sweden	1998	Since 3/98	200 m 656'	11)	160 mm -1.5 m	Plough	~ 1.0 m	1:15/	2)	0.3/3	240 m^3/h	0.8/	1.0		Beach restored on the lea side of the 90 metres long groyne.
Hitotsumatsu Beach Japan	1998	Since 6/98	800 m 2490'	11)	300 mm -2.4	Trench machine	~ 2.0 m	1:20/	2) 2 separate wet wells	0.25/2	2 x 300 m^3/h				Accretionary trend. Beach level increased. 200 metres foreshore treated by 4 drain structures in parallel.
Les Sables d'Olonne France	1999	Since 4/99	300 m 985'	11)	160 – 215 – 280 – 355 – 470 mm -1.2	Trench machine	3.4 m mean	1:70/	2)	0.25/3	250 m^3/h	0.6/			Accretionary trend and substantial foreshore dry up in the drain zone.
Riumar II, Ebro Delta Spain	1999	Since 12/99	300 m 985'	11)	160 mm -2.0 m	Backhoe W.pts.	0.2-0.4 m	1:20/	2)	0.25/1.6	400 m^3h				Width increased 6-8 m March 2000
Markgrafenheide, Germany	2000	Since 8/00	300 m 985'	11)	200 mm -1.4 m	Trench machine	~ 0.3 m	1:30/	2)	0.7/2.6	300 m^3h	0.9/			No measurements at present

[1] Epoxy cemented filter sand around PVC perforated pipe
[2] Gravity wet well with pressure discharge pipe
[3] Horizontal wellpoints with epoxy cemented sand filter attached to PVC pipe
[4] Inlet/mole south of system can add 1 knot to littoral current
[5] Flexible perforated corrugated pipe with filter sand and geotextile cover (at bottom side)
[6] Perforated PVC pipe with gravel wrapped in geotextile
[7] Flexible PE perforated corrugated pipe with geotextile stocking
[8] Tide induced littoral current less severe to 3 knots max.
[9] Tide induced littoral current less severe to 1-2 knots max.
[10] Flexible perforated corrugated pipe with filter gravel 90 m and without filter gravel 90 m
[11] Flexible perforated corrugated pipe with geotextile stocking and filter gravel

HV/MAN

APPENDIX C: Branksome Chine beach survey information

The y-axis runs from (0,0) down the length of the concrete groyne to a metal pole ('beacon') at the end. Note that the x-axis is not parallel to the promenade, since the frontage curves along the length of the control beaches (shown schematically in Figure 3.24).

The surveying instrument was mounted on a tripod over a location of known level and position relative to (0,0). The horizontal angle was zeroed onto the beacon at the end of the concrete groyne, which was selected as the reference object (RO) for this survey. The beacon can be seen in Figures 3.4, 3.24, and 3.25.

At each sample point the horizontal angle (or bearing relative to the RO), horizontal distance (from the instrument to the sample point) and level difference (between the instrument to the sample point) were recorded.

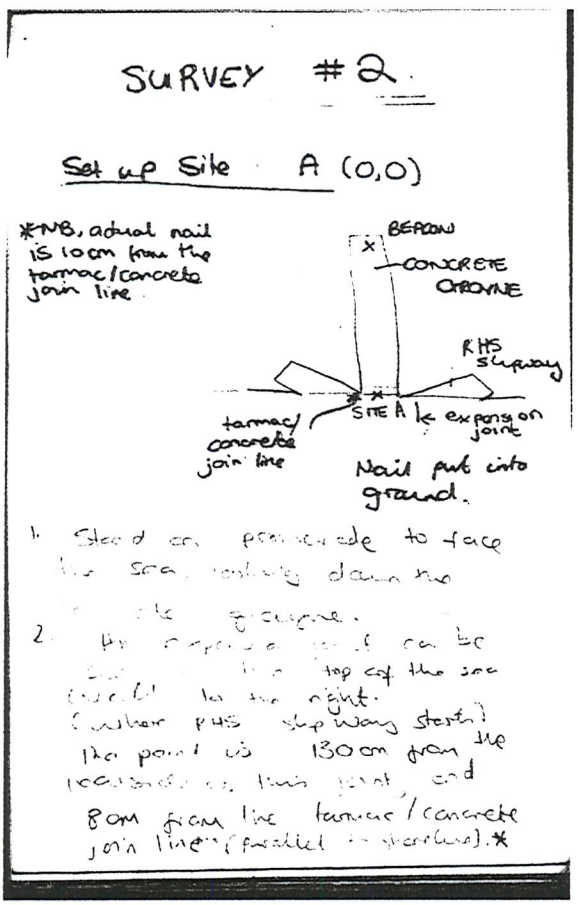

Field book extract

A sample Matlab commend sequence is shown below:

```
» clc
» load example.mat
» x = [1,2,3];
» y = [-1, 5, 8];
» z = [-1.3, -1.6, -1.7];
» xs = 0 : 0.5 : 4;
» ys = -1 : 0.5 : 9;
» [xi,yi] = meshgrid(xs,ys);
» zi = griddata(x,y,z,xi,yi);
» mesh(xi,yi,zi);
» whitebg
» xlabel('x, m'); ylabel('y, m');
» zlabel('Level, mCD');
» title('Example')
```

The variables x, y and z are entered
(x, y) are the co-ordinates of the data points on the local grid.
z is the level at the given data point in metres above chart datum

These steps set up a regular grid on which the random data points can be interpolated.

The field data are interpolated onto the grid using the command 'griddata'.
The command 'mesh' is used to produce a plot of the interpolated levels, zi on the regular grid xi, yi.
This plot is shown below in figure6.5.

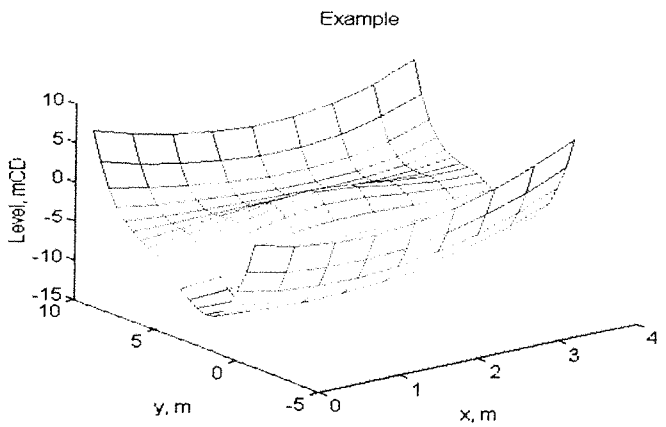

Example Matlab command sequence and 3D plot.

Sample survey data collection sheet

RVEY # 17

TE 15-3-99

FROM B

GHT OF INSTRUMENT = HEIGHT OF PRISM = 1.669 m

HORIZONTAL ANGLE			HORIZONTAL DISTANCE	VERTICAL DISTANCE
eg	Min	Sec	(m)	(m)
5	34	10	93·682	-4·102
4	38	20	103·650	-3·685
1	56	20	104·662	-3·985
7	41	15	106·046	-4·174
3	14	20	105·086	-3·540
3	05	40	106·280	-4·111
2	02	35	103·700	-3·156
4	10	50	103·535	-2·422
8	20	05	101·287	-2·105
9	00	05	88·799	-2·327
2	11	20	84·763	-2·485
5	10	05	81·820	-2·526
0	31	15	76·443	-3·195
9	33	25	71·144	-3·505
6	32	45	71·198	-3·943
2	20	50	70·997	-3·747
3	35	15	60345	-3·773
9	01	15	52·922	-3·531
0	56	25	45·259	-3·296
2	38	30	38·962	-2·514
2	46	35	34·385	-2·275
2	55	20	46·945	-3·865
5	48	40	46·783	-3·696
8	26	35	38·598	-3 892
0	37	05	27·228	-3·673
2	35	30	15677	-3·279
5	49	55	6·616	-2·534
3	08	35	26·423	-2·833
3	04	15	32·880	-3·432
7	31	05	45·106	-4·248
2	33	45	52·583	-3·658
1	53	05	85·290	-3·703
4	08	35	84·264	-3·871
1	55	05	81·011	-3·659
5	01	30	72·868	-3·128
5	31	50	70·228	-2·730
1	18	05	79·019	-3·308
1	09	50	90·615	-3·050

HORIZONTAL ANGLE			HORIZONTAL DISTANCE	VERTICAL DISTANCE
Deg	Min	Sec	(m)	(m)
351	23	20	113·998	-3·663
358	26	45	114·582	-3·240
3	16	50	116·137	-3·100
6	38	25	121·718	-2·405
8	02	50	136·808	-2·285
3	52	30	135·982	-3·162
1	59	10	136·274	-3·231

APPENDIX D: Survey Data

Plan view of beach levels from June- November 1998
Colour bar on right hand side denotes the beach level in metres.
(x, y) co-ordinates are in metres from (0,0).

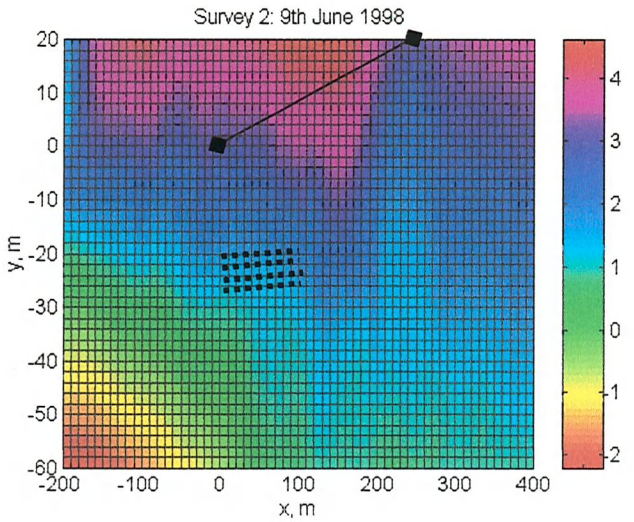

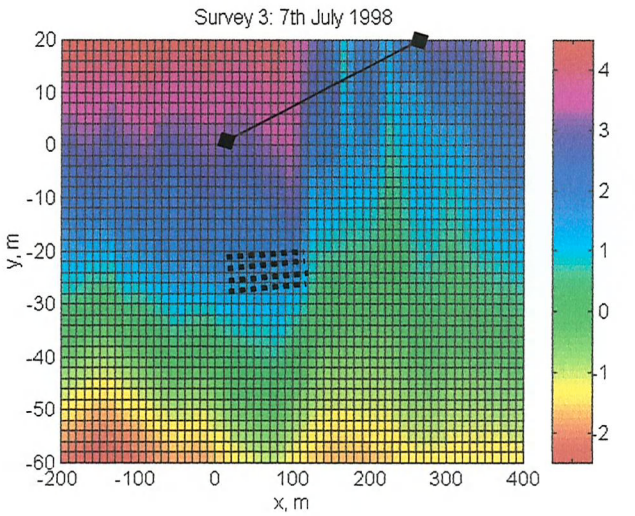

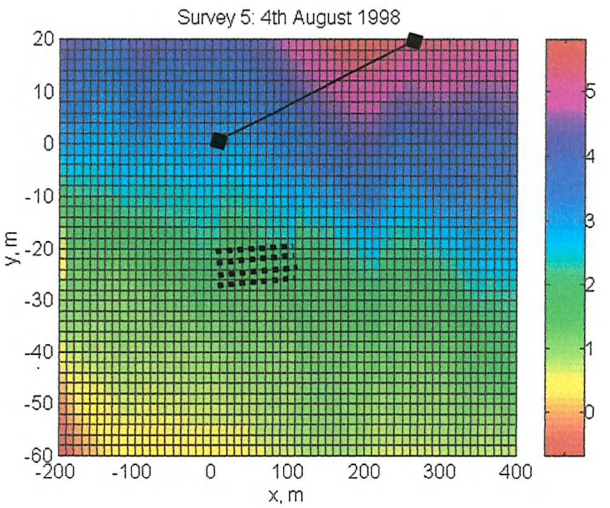

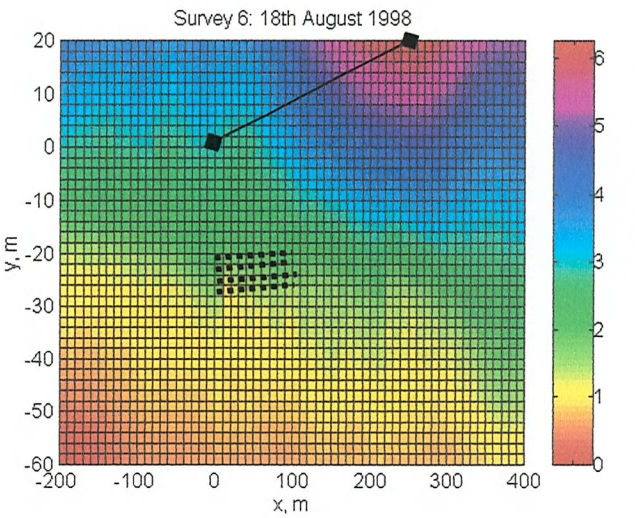

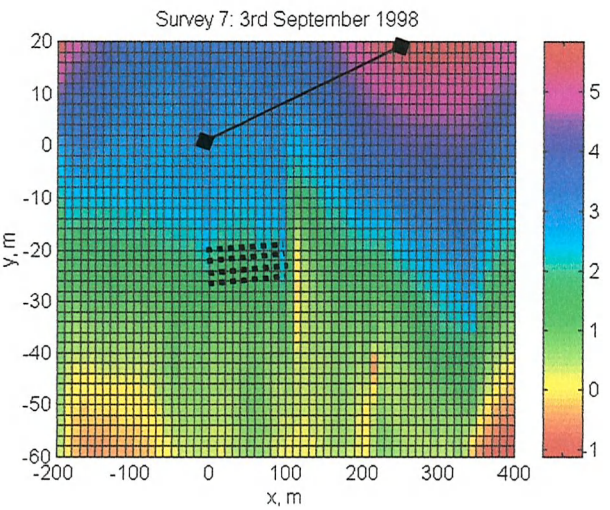

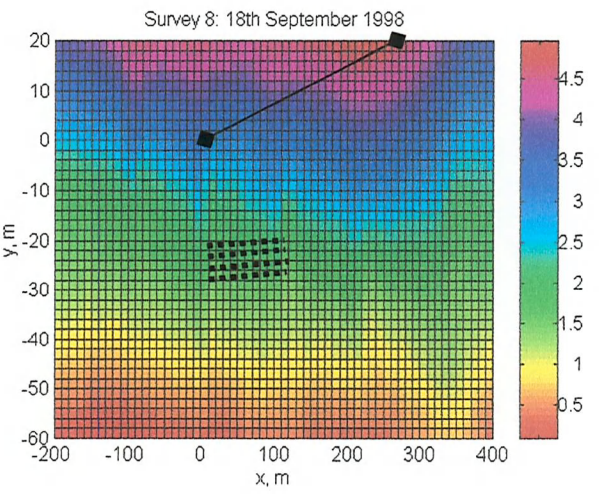

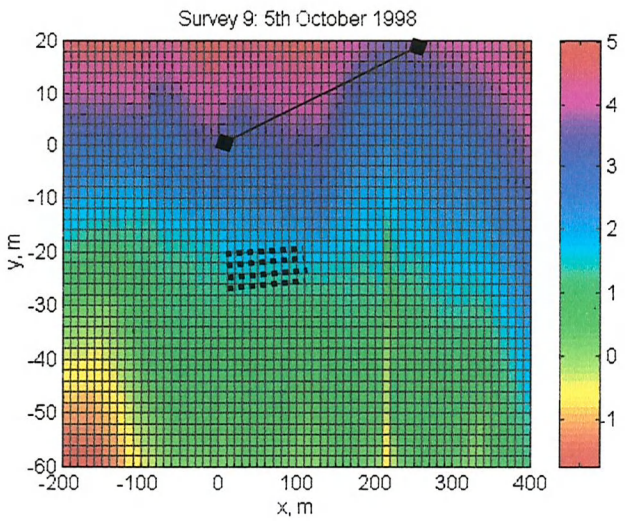

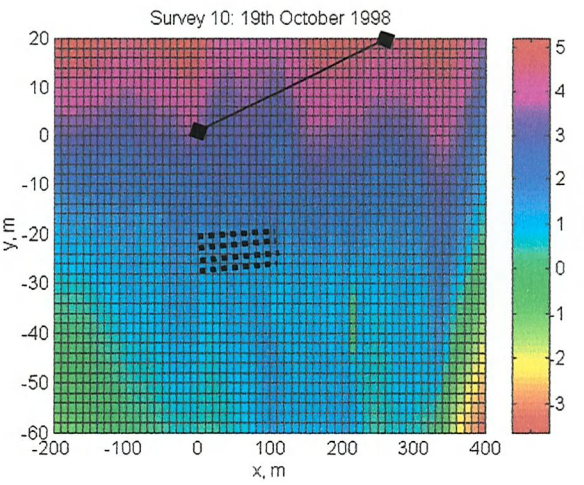

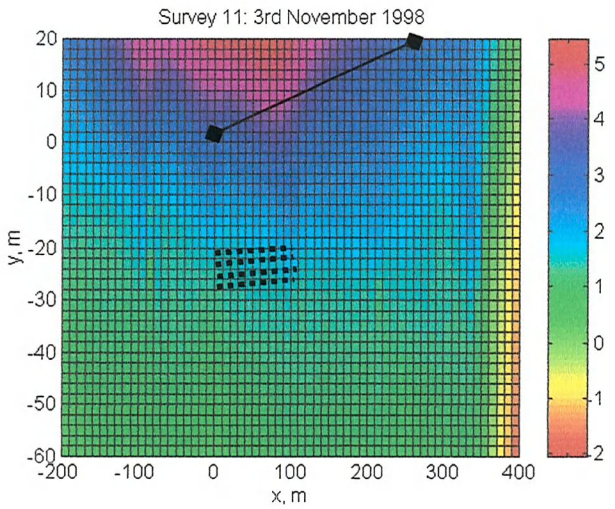

KEY

Approximate location of beach drains

Location of survey stations (with line adjoining two stations). Station A is on the left hand side (0,0), and B is on the right hand side (250,-20)

APPENDIX E: Raw weather data and sample data collection sheet

WEATHER DATA		(RAW)		
Date	Days	Wind Direction	Windspeed (Force)	Wave Height (m)
16/07/98	1	SW	1.5	0.3
16/07/98	1.5	SW	2.5	0.5
17/07/98	2	S	1.5	0.1
17/07/98	2.5	S	1.45	0.1
18/07/98	3	SW	10	1.4
18/07/98	3.5	SW	10	1.6
19/07/98	4	SW	3	0.7
19/07/98	4.5	SW	2	0.5
20/07/98	5	SW	6	0.6
20/07/98	5.5	SW	5	0.5
21/07/98	6	W	3	0.4
21/07/98	6.5	W	3	0.5
22/07/98	7	SW	3.5	0.4
22/07/98	7.5	SW	3.5	0.4
23/07/87	8	SW	5	0.8
24/07/98	9	SE	3	0.8
25/07/98	10	SE	5	1.2
26/07/98	11	SE	6	1.2
27/07/98	12	S	4	0.6
28/07/98	13	SW	4	0.6
29/07/98	14	SW	3	0.4
30/07/98	15	SW	2	0.4
31/07/98	16	SW	3	0.4
01/08/98	17	S	1	0.4
01/08/98	17.5	SW	3	0.6
02/08/98	18	SW	3	0.2
03/08/98	19	SW	1	0.2
04/08/98	20	SW	3	0.4
05/08/98	21	S	4	0.3
06/08/98	22	S	4	0.3
07/08/98	23	S	1	0.3
08/08/98	24	S	1.5	0.4
09/08/98	25	SE	3	1.3
10/08/98	26	SE	3	0
11/08/98	27	NW	2	0.4
12/08/98	28	NW	2	0.3
13/08/98	29	SW	2	0.6
14/08/98	30	NW	3	0.3
15/08/98	31	NW	3	0.8
16/08/98	32	NE	1	0.1
17/08/98	33	NW	2	0.3
18/08/98	34	NW	2	0.3
19/08/98	35	SW	2	0.4
20/08/98	36	SW	1	0.1

21/08/98	37	S	0.5	0.1
22/08/98	38	SE	2	0.3
23/08/98	39	SE	3	0.5
24/08/98	40	SE	3	0.6
25/08/98	41	SE	2	0.4
26/08/98	42	S	3	0.6
27/08/98	43	SW	1	0.2
28/08/98	44	SW	2	0.5
29/08/98	45	SW	4	0.8
30/08/98	46	SW	5	1.3
31/08/98	47	S	6	1.6
01/09/98	48	SE	6.5	1.6
02/09/98	49	SE	6	1.3
03/09/98	50	SE	7	1.4
04/09/98	51	SE	7	1.6
05/09/98	52	SE	7	1.6
06/09/98	53	SE	6.5	1.5
07/09/98	54	SW	6	1.6
08/09/98	55	SW	4	0.9
09/09/98	56	SW	4	0.6
10/09/98	57	SW	3	0.4
11/09/98	58	SW	3	0.3
12/09/98	59	SW	4	0.5
13/09/98	60	SW	2	0.2
14/09/98	61	SW	2	0.1
15/09/98	62	SW	1	0
16/09/98	63	SW	2	0
17/09/98	64	SW	1	0
18/09/98	65	SW	0.5	0.2

Note: No data for 19th -29th September

30/09/98	77	SE	5	0.9
01/10/98	78	S	5	1.5
02/10/98	79	N	2	0.3
03/10/98	80	NE	3	0.3
04/10/98	81	NE	2	0.3
05/10/98	82	NE	2	0.1
06/10/98	83	NE	3	0.5
07/10/98	84	NE	2	0.5
08/10/98	85	N	3	0.25
09/10/98	86	N	2	0.25
10/10/98	87	N	2	0.2
11/10/98	88	S	3	0.2
12/10/98	89	N	2	0.2
13/10/98	90	N	2	0.2
14/10/98	91	NE	3	0.4
15/10/98	92	SW	0.5	0.1
16/10/98	93	SW	3	0.4

17/10/98	94	*SW*	*5*	*0.72*
18/10/98	95	*SE*	*3*	*0.5*
19/10/98	96	*W*	*4*	*0.25*
20/10/98	97	*SE*	*4*	*0.3*
21/10/98	98	*NE*	*6*	*0.6*
22/10/98	99	*NE*	*6*	*0.3*
23/10/98	100	*SW*	*5*	*0.4*
24/10/98	101	*SW*	*7*	*1.5*
25/10/98	102	*SW*	*5*	*1.2*
26/10/09	103	*SW*	*4*	*1.2*
27/10/98	104	*NE*	*5*	*1.3*
28/10/98	105	*SE*	*6*	*1.2*
29/10/98	106	*SW*	*5*	*1.3*
30/10/98	107	*SE*	*4*	*1.4*
31/10/98	108	*NE*	*6*	*1.5*
01/11/98	109	*NE*	*6*	*1.5*
02/11/98	110	*NE*	*5*	*1.6*
03/11/98	111	*SW*	*5*	*1.4*
04/11/98	112	*SE*	*4*	*1.5*
05/11/98	113	*SE*	*4*	*1.6*
06/11/98	114	*SE*	*4*	*1.2*
07/11/98	115	*SW*	*3*	*0.2*
08/11/98	116	*SW*	*3*	*0.2*
09/11/98	117	*SW*	*2*	*0.15*
10/11/98	118	*SW*	*3*	*0.3*
11/11/98	119	*SW*	*2*	*0.25*
12/11/98	120	*SW*	*3*	*0.2*
13/11/98	121	*SW*	*3*	*0.2*
14/11/98	122	*SW*	*3*	*0.25*
15/11/98	123	*SW*	*2*	*0.15*
16/11/98	124	*SW*	*2*	*0.1*
17/11/98	125	*SW*	*2*	*0.1*
18/11/98	126	*SW*	*2*	*0.15*
19/11/98	127	*SW*	*2*	*0.1*
20/11/98	128	*SW*	*3*	*0.1*
21/11/98	129	*SW*	*2*	*0.1*
22/11/98	130	*SW*	*2*	*0.15*
23/11/98	131	*SW*	*3*	*0.1*
24/11/98	132	*SW*	*2*	*0.1*
25/11/98	133	*SE*	*1*	*0.1*
26/11/98	134	*SE*	*1*	*0.05*
27/11/98	135	*S*	*3*	*0.1*
28/11/98	136	*S*	*2*	*0.1*
29/11/98	137	*S*	*2*	*0.2*
30/11/98	138	*SW*	*3*	*0.3*
01/12/98	139	*SW*	*3*	*0.2*
02/12/98	140	*S*	*2*	*0.2*
03/12/98	141	*S*	*2*	*0.2*
04/12/98	142	*SW*	*2*	*0.3*
05/12/98	143	*SW*	*3*	*0.2*

06/12/98	144	W	3	0.1
07/12/98	145	W	4	0.3
08/12/98	146	W	4.5	0.6
09/12/98	147	NW	2	0.2
10/12/98	148	NW	2	0.2
11/12/98	149	W	3	0.3
12/12/98	150	S	2	0.2
13/12/98	151	NW	3	0.3
14/12/98	152	W	4	0.3
15/12/98	153	W	3	0.3
16/12/98	154	E	1	0
17/12/98	155	NW	2	0.2
18/12/98	156	NW	3	0.3
19/12/98	157	SW	3	0.7
20/12/98	158	SW	2	0.5
21/12/98	159	SW	2	0.2
22/12/98	160	SW	2	0.7
23/12/98	161	SW	1	0.2
24/12/98	162	SW	2	0.2
25/12/98	163	SW	2	0.3
26/12/98	164	SW	3	0.5
27/12/98	165	SW	3	0.5
28/12/98	166	SW	3	0.8
29/12/98	167	SW	5	2
30/12/98	168	SW	4	1.2
31/12/98	169	S	2	0.8
01/01/99	170	S	3	1
02/01/99	171	S	5	1
03/01/99	172	SW	5	1.8
04/01/99	173	SE	3	0.3
05/01/99	174	S	2	0.3
06/01/99	175	NW	2	0.3
07/01/99	176	NW	2	0.3
08/01/99	177	NW	2	0.35
09/01/99	178	SW	2	0.2
10/01/99	179	S	3	0.15
11/01/99	180	SW	2	0.1
12/01/99	181	SW	4	0.3
13/01/99	182	SW	2	0.2
14/01/99	183	NE	2	0.2
15/01/99	184	NW	4	0.3
16/01/99	185	NW	3	0.2
17/01/99	186	NW	2	0.2
18/01/99	187	NE	2	0.2
19/01/99	188	NW	3	0.2
20/01/99	189	NW	2	0.3
21/01/99	190	NW	1	0.3
22/01/99	191	NW	2	0.2
23/01/99	192	NW	3	0.3
24/01/99	193	NW	2	0.2

25/01/99	194	NW	3	0.1
26/01/99	195	NW	2	0.1
27/01/99	196	NW	2	0.1
28/01/99	197	NW	2	0.1
29/01/99	198	NW	2	0.1
30/01/99	199	NW	2	0.6
31/01/99	200	SW	1	0.8
01/02/99	201	SW	2	0.5
02/02/99	202	NONE	0	0
03/02/99	203	W	2	0.2
04/02/99	204	S	1.5	0.1
05/02/99	205	SW	1	0.05
06/02/99	206	W	3	0.3
07/02/99	207	W	2	0.3
08/02/99	208	S	3	0.1
09/02/99	209	SW	3	0.1
10/02/99	210	S	3	0.15
11/02/99	211	SW	2	0.1
12/02/99	212	SW	2	0.1
13/02/99	213	SW	3	0.1
14/02/99	214	S	2	0.05
15/02/99	215	SE	1	0.1
16/02/99	216	SE	1	0.15
17/02/99	217	SE	2	0.1
18/02/99	218	SW	1	0.05
19/02/99	219	S	2	0.1
20/02/99	220	SW	3	0.1
21/02/99	221	SW	3	0.1
22/02/99	222	SW	2	0.15
23/02/99	223	SW	1	0.2
24/02/99	224	S	2	3
25/02/99	225	SE	3	0.25
26/02/99	226	SE	2	0.3
27/02/99	227	SW	3	0.2
28/02/99	228	SW	2	0.2
01/03/99	229	SW	3	0.3
02/03/99	230	SW	4	0.3
03/03/99	231	SW	4	0.3
04/03/99	232	SW	2	0.1
05/03/99	233	SW	2	0.1
06/03/99	234	S	2	0.05
07/03/99	235	S	1	0.01
08/03/99	236	SE	2	0.2
09/03/99	237	S	1	0
10/03/99	238	S	1	0.1
11/03/99	239	SE	3.5	0.4
12/03/99	240	S	1	0.05

University of Southampton

INFORMATION REQUIRED

1. Wind speed: an estimate of the Force is sufficient -usually indicated by the sea state

2. Wind direction: direction the wind is coming from (N, E, S, W etc..)

3. Wave height: may be estimated by comparing incoming waves to body height (not literally!). Feet or metres, but please note which.

4. Wave Direction: direction the waves are coming from (N, E, S, W etc..)

RECORDED DATA

DATE	TIME	WIND SPEED (FORCE)	WIND DIRECTION (N, NE, E etc..)	WAVE HEIGHT (METRES/~~FEET~~)	WAVE DIRECTION (N, NE, E etc..)
16.7.98	10 00	1-2	SW	0.3m	SW
16.7.98	1500	2-3	SW	0.5m	SW
17.7.98	1000	1-2	S	0.1m	SW.
17.7.98	1500	1-2	S	0.1m	S
18.7.98	10.00	10 (GUSTING)	SW	1.4m	SW
18.7.98	1500	— " —	SW	1.6m	SW
19.7.98	10.00	3	SW	0.7m	SW
19.7.98	1500	2	SW	0.5m	SW
20.7.98	1000	6	SW	0.6m	S
20.7.98	1500	5	SW	0.5m	SW
21.7.98	1000	3	W	0.4m	SW
21.7.98	1500	3	W	0.5m	SW
22.7.98	1000	3-4	S	0.4m.	S
22.7.98	1400	3.4	S	0.4m	S.
23.7.98	1000	5	SW	0.9m	SW
24.7.98	0940	3	S.E.	0.8	S.E.
25.7.98	1000	5	S.E.	1.2	S.E.
26.7.98	1000	6	S.E.	1.2	S.E.
28.7.	0900	4	S	0.6m	S

Thank you for your help!

References

Publications

Bagnold, R. A. (1940) 'Beach Formation by Waves: Some Model Experiments in a Wave Tank'. *Journal of the Institute of Civil Engineers, Vol. 15, 27-54.*

Baird, A. J., and Horn, D. P. (1996) Monitoring and Modelling Groundwater Behaviour in Sandy Beaches *Journal of Coastal Research, 12(3), 630 - 640*

Briere, C. (1999) Etude de l'evolution d'un profil de plage en modele physique reduit sedimentologique. Etude de prefaisabilite d'un systeme gravitaire de drainage des plages'. *Option Genie Cotier. Rapport de stage. DEA de Genie Civil 1999, Centre de Geomorphologie du CNRS. France. July 1999*

Bowen, Inman and Simmons (1968) 'Wave set-down and wave set-up' *Journal of Geophysical Research 73: 2569-2577*

Buckingham E. (1914) On physically similar systems: Illustrating the use of dimensional analysis. *Phys. Rev. 4, 345-376*

Chappell, J. *et al.*, (1979) 'Experimental Control of Beach face Dynamics by Water Table Pumping.' *Engineering Geology 14 (1979) p. 29 - 41*

Dalrymple, R. A. (1989) Physical Modelling of Littoral Processes', *Recent Advances in Physical Modelling, Edited by R. Martins, Kluwer academic publishers, Dordrecht, The Netherlands, pp 567-588.*

Darcy, H (1856) Les Fontaines Publiques de la ville de Dijon, *Dalmont, Paris.*

Davis, G. A. *et al.*, (1992) 'Gravity Drainage: A New Method of Beach Stabilisation.' *Coastal Engineering Journal 1992, P. 1129 - 1141*

Dean, R. G. (1973) 'Heuristic Models of Sand Transport in the Surf Zone' *Proceedings of the 1st Australian Conference on Coastal Engineering: Engineering Dynamics in the Surf Zone, Sydney pp.209-214.*

Dean, R. G. (1985) 'Physical Modelling of Littoral Processes' *Physical Modelling in Coastal Engineering. Edited by R. A. Dalrymple., A. A. Balkema, Rotterdam, The Netherlands, pp119-139*

Dean, R. G. (1987) 'Coastal sediment processes: Towards engineering solutions'. *Coastal Sediments 1987 ASCE P. 1-24.*

Darbyshire, M. and Draper, L. (1963) 'Forecasting wind-generated sea waves'. *Engineering 195 (April).*

Duncan, J. R., (1964). 'The Effects of Water Table and Tide Cycle in Swash-Backwash Distribution and Beach Profile Development.' *Marine Geology, 2 (1964) 186-197.*

Emery, K. O. and Foster J. F. (1948) 'Water Tables in Marine Beaches. ' *Journal of Marine Research IIV, 3 P. 655 - 6607*

Gourlay, M. R., (1992). 'Wave set-up, run-up and beach water table: Interaction between surf zone hydraulics and groundwater hydraulics.' *Coastal Engineering, 17 (1992) 93-144.*

Grant, U. S. (1948) 'Influence of the Water Table on Beach Aggradation and Degradation' *Journal of Marine Research (VII, 3, 1948)*

Hamer *et al.*, (1999) 'The Benefits of a Strategic Approach to Decision making'. *Proceedings of the 34th MAFF Conference of River and Coastal Engineers*

Hazen, A. (1892) 'Physical properties of sands and gravels with reference to their use in filtration'. *Report of the Massachussetts State Board of Health*

Hudson, R. Y., and Keulegan, G. H. 'Principals of Similarity, Dimensional Analysis, and Scale Models'. *Coastal Hydraulic Models, U. S. Army Corps of Engineers Coastal Engineering Research Centre, Special Report No. 5, May 1979*

Kamphuis, J. W. (1975) 'Coastal Mobile Bed Model – Does it Work?' Proceedings of the 2nd Symposium on Modelling Techniques, ASCE, Vol. 2, pp 993-1009

Kamphuis J. W. (1985) 'On Understanding the Scale Effect in Coastal Mobile Bed Models' *Physical Modelling in Coastal Engineering. Edited by R. A. Dalrymple., A. A. Balkema, Rotterdam, The Netherlands, pp119-139*

Kamphuis J. W. (1991) 'Physical Modelling' *Handbook of Coastal and Ocean Engineering. Edited by J. B. Herbich, Vol. 2, Gulf Publishing Company, Houston, Texas.*

Kamphuis (1995) 'Comparison of Two-dimensional and Three-dimensional Beach Profiles'. *Journal of Waterway, Port, Coastal and Ocean Engineering , May/June 1995*

Kraus, N. C., Larson, M. and Kriebel, D. L. (1991) 'Evaluation of beach erosion and accretion predictors, *Proc. Coastal Sediments '91, ASCE, 572-587*

Machemehl, J. L. *et al* (1975) 'New Method for Beach Erosion Control.' *Engineering in the Oceans: ASCE Speciality Conference, ASCE, New York, NY., 142 - 160*

Mogridge, G. R. and Kamphuis, J. W. (1972) 'Experiments on Ripple Formation Under Wave Action' *Proceedings of the 13th conference on Coastal Engineering, Vancouver, pp 1123-1142*

Nielsen, P (1992) 'Coastal Bottom Boundary Layers and Sediment Transport' *World Scientific Co Pte. Ltd: Advanced Series on Coastal Engineering – Volume 4 324p*

Ovesen, N. K., and Schuldt, J. C., (1992). *'Beach Management System. Documentation. Job No. 300 0141. Danish Geotechnical Institute, Lyngby, Denmark*

Preene, M. and Powrie, W. (1993) Steady-state performance of construction dewatering systems in fine soils' . *Geotechnique, 43, No. 2, 191-205*

Seelig, W. N. (1983), *'Understanding Beach Erosion and Accretion.' Journal of Port, Coastal and Ocean Engineering Vol 109 No.1 Feb 1983 490-494.*

Shields, A. (1936) Anwendung der Ahnlichkeitsmechanik und der Turbulenzforschung auf die Geschiebebewegung, *Heft 26. Preuss. Vers. für Wasserbau und Schiffbau, Berlin*

Smith, A. W. *et al.* (1989) 'An Estimate of the Value of a Beach in Terms of Beach Users', *Shore and Beach. April 1989.*

Terzaghi, K (1936) 'The shearing resistance of saturated soils'. *Proceedings of the First International Conference on Soil Mechanics, 1, 54-56.*

Turcotte, D. L. (1960) 'A sub-layer theory for fluid injection into the incompressible turbulent boundary layer'. *Journal of Aerospace Sciences 27(9) 675-678*

Turner (1993) 'Water Table Outcropping on Macro-Tidal Beaches: A Simulation Model'. *International Journal of Marine Geology, Geochemistry and Geophysics, 115:227-238. Elsevier.*

Turner (1995) 'Simulating the influence of Groundwater Seepage on sediment transported by the sweep of the swash zone across macro-tidal beaches. *Marine Geology 125 (1995) 153-174*

Turner and Nielsen (1997) 'Rapid Water Table Fluctuations within the Beach Face: Implications for Swash Zone Sediment Mobility?' *Coastal Engineering 32 (1997) 45-59*

Turner, I. L. and Leatherman, S. P. (1997). 'Beach Dewatering as a 'Soft' Engineering Solution to Coastal Erosion – History and Critical Review'. *Journal of Coastal Research, Vol 13 No. 4 p. 1050-1063, Fall, 1997.*

Vesterby, H. (1997) 'Beach Drainage - State of the Art.' *Wallingford Training - Seminar on Shoreline Management Techniques, 18th April1996*

Vesterby (2000) 'Modelling Groundwater Flow in Beach Profiles for Optimising Stabilisation Measures'. *International Coastal Symposium 2000, Rotoruna, New Zealand, April 2000*

Wagner, A. A. (1957) 'Unified Soil Classification System' *Proceedings of the Fourth International Conference SMFE. London, Volume 1.*

Weisman, R. N., Seidel, S., and Ogden, M. R., (1995). 'Effect of Water-Table Manipulation on Beach Profiles.' *Journal of Port, Coastal, and Ocean Engineering Vol. 121, No. 2, Mar/Apr, 1995 134-142.*

Bibliography

Barratt, (1992) 'Coastal Zone Planning and Management'. *Imprint – London; Thomas Telford, 1992*

Chadwick, A. J. and Morfett, J. C. (1998) 'Hydraulics in Civil and Environmental Engineering' (3rd Edition) *Published by E & FN Spon.*

Chow, V. T. (1973) 'Open Channel Hydraulics' *Published by McGraw-Hill International Editions Civil Engineering Series.*

Craig, R. F. (1995) 'Soil Mechanics'. *Fifth edition published by Chapman and Hall, reprinted 1995*

'Paperback Atlas of the World', *published by HarperCollins, 1993*

Dyer, K. R. (1990) 'Coastal and Estuarine Sediment Dynamics'. *Published by John Wiley & Sons Ltd.*

Hamill, L. (1995) 'Understanding Hydraulics'. *Published by MacMillan Press Ltd.*

Head, K. H. (1986) 'Soil Laboratory Testing'. *Volume II, p.431-449*

Hughes, S. A. (1993) 'Physical Models and Laboratory Techniques in Coastal Engineering'. *Advanced Series on Ocean Engineering- Volume 7. World Scientific.*

Kiely, G (1997) 'Environmental Engineering'. *Published by McGraw-Hill, ISBN 0-07-709127-2 p.44.*

King, C. A. M. (1966) 'Beaches and Coasts'. *Published by Edward Arnold Ltd.*

Komar, P. D. (1998) 'Beach Processes and Sedimentation', Second Edition, *Published by Prentice-Hall Inc. ISBN 0-13-754938-5*

Morton, R. A. *et al.*,(1983) 'Living with the Texas Shore', *Duke University Press, Durham, North Carolina*

Muir-Wood (1969) 'Coastal Hydraulics'. *MacMillan Press, 1969.*

Powrie, W. (1997) 'Soil Mechanics Concepts and Applications'. *Published by E & FN Spon (An imprint of Chapman and Hall)*

Summerfield, M. A. (1993). 'Global Geomorphology' *Published by Longman Scientific and Technical ISBN 0-582-30156-4, Chapters 13 and 17.*

Non-publications referenced in text

BBC 1 'South Today' programme, 28/8/00

Belfield (1999) 'Tide Plotter 1999'. *Available via internet purchase.*

Burstow, S. (1996) 'The affordable alternative: Beach drainage system, Newquay'. *Borough of Restormel Report, 1996.*

Marin, P., McGee, N., and Shaw, R. (1998) 'An Investigation into Beach Drainage' *Part IV Group Design Project, University of Southampton, Department of Civil and Environmental Engineering*

Moore, B. D. (1982) 'Beach profile evolution in response to changes in water level and wave height'. *Masters Thesis, Dept. Civil Engineering University of Delaware, Newark.*

Mulvaney, H. S. (1997) 'An Investigation into the Development of Beach Drainage: A New Method of Coastal Protection' *Part III Project, University of Southampton, Department of Civil and Environmental Engineering*

Vesterby, H. (1999), Overview of Beach Management System Projects, Document supplied by the Danish Geotechnical Institute, Lyngby, Denmark